Imperial College London

CIRCULATING MICROVESICLES AS MEDIATORS OF ACUTE PULMONARY VASCULAR INFLAMMATION

Ying Ying Tan

(College ID: 00729060)

Supervisors:

Dr. Kieran P. O'Dea (Senior Lecturer)

Prof. Masao Takata (Magill Chair in Anaesthetics)

Section of Anaesthetics, Pain Medicine and Intensive Care (APMIC)

Department of Surgery & Cancer

Faculty of Medicine

Imperial College London

Submitted in partial fulfilment of the requirements for the award of

Doctor of Philosophy (PhD) in Clinical Medicine Research

Date of submission: 4th December 2020

Funded by Imperial College London President's PhD Scholarship

Abstract

Acute lung injury (ALI) resulting from remote 'indirect' causes is a major problem in sepsis and systemic inflammatory response syndrome (SIRS) but the underlying mechanisms are poorly understood. Circulating microvesicles (MVs) have been implicated as long-range mediators of vascular inflammation and their role as biomarkers in sepsis and SIRS has been widely investigated in clinical studies in recent years. However, the *in vivo* functional roles of MVs in sepsis and ALI have received less attention. Specifically, the role of *in vivo* MVs in the development of sepsis/SIRS-induced indirect ALI has not been previously evaluated.

We hypothesised that circulating microvesicles (MVs) play a crucial role in propagating inflammation to the lungs, contributing to the development of pulmonary vascular inflammation in indirect ALI. The overall aims of this project were to: 1) evaluate MV uptake by pulmonary vascular cells and the mechanisms involved, 2) characterise the intravascular production of MVs in animal models of sepsis and sterile extrapulmonary organ injury, and 3) identify the contribution of *in vivo*-derived circulating MVs to the development of indirect ALI.

The major findings of this work were that during sub-clinical endotoxaemia in mice, lung-marginated $Ly6C^{high}$ monocytes become a major target for circulating MV uptake via a phosphatidylserine receptor mechanism[1]. In mouse models of sepsis and extrapulmonary organ injury, neutrophil- and monocyte-derived MVs were the predominant MV subtypes being produced during endotoxaemia, while platelet- and endothelial-derived MVs were predominant during kidney ischaemia reperfusion injury. When MVs obtained from plasmas of endotoxaemic mice were adoptively transferred to isolated perfused lungs (IPLs), they induced significant increases in lung oedema. Depletion of intravascular lung monocytes by treatment with clodronate liposomes resulted in the reversal of the oedema, demonstrating the role of monocytes in MV-induced ALI. To investigate the contribution of different circulating MV subtypes, we immunoaffinity isolated myeloid (CD11b+) and platelet (CD41+) MVs from endotoxaemic mouse plasmas and transferred these to the IPL. We found that myeloid-MVs induced significant lung oedema and potent release of soluble mediators, whereas platelet-MVs produced a statistically significant, but much lower level of oedema and negligible release of soluble mediators.

In summary, these findings indicate an important role of myeloid-derived MVs, particularly those derived from neutrophils and/or monocytes, and their interaction with lung-marginated monocytes in the pathogenesis of pulmonary vascular inflammation in indirect ALI. Further work to elucidate the specific MV molecular effectors mechanism involved will facilitate an enhanced understanding of ALI pathobiology.

Dedications

This thesis is dedicated to my parents, I would not be where I am and who I am today without your unconditional love and support. Thank you for your emphasis on education despite not attending universities yourselves. I hope this PhD could somehow compensate a little for all that you have sacrificed to raise all six of us.

I also dedicate this thesis to my partner Nathanael. I would not have been able finish the PhD without your immense support, love and encouragement throughout. Thank you for being my personal mentor, the best audience to all my scientific presentations and for being the best shoulder to cry on through tough times.

Acknowledgement

I would like to first thank and acknowledge my supervisors. Dr Kieran O'Dea and Professor Masao Takata, for their trust, patience, time and effort in moulding me into a scientist through those years I have been in the lab. I thank Kieran, for being both a good friend and supervisor. My PhD would not have been as colourful and exciting without you. Thank you for being the most understanding and accommodating supervisor, through all my stubbornness. I am glad to be able to witness your promotion to Senior Lecturer during this time and I wish you nothing but the best in your future endeavours. I thank Prof Takata for taking me on as your student and for seeing the potential in me. Thank you for teaching me how to be a meticulous scientist and for keeping an open door whenever I need guidance and directions. I am immensely grateful to have grown under your supervision, both academically and personally.

I would also like to acknowledge and thank Dr Sanooj Soni for talent-spotting me as my MRes supervisor, without whom I would not have considered doing a PhD. Special thanks to Marissa Koh, for being the best friend and colleague. PhD would not have been as survivable and enjoyable without you. Thank you for being the best listener (and brownies provider) to all my IPL-fails and for the memories we shared in the physiology lab, may this remain our fondest memory of our PhDs.

My appreciation also goes to:

- Dr Brijesh Patel for teaching me the pulmonary perfusion technique.
- Dr Sneh Shah for laying the groundwork for *in vivo* MV uptake and for the amazing step-by-step guide in how to use the IPL system.
- Dr Kate Tatham and Dr Kenji Wakabayashi for their guidance and advice with the IPL.
- Dr Hailin Zhao and Prof Daqing Ma for their kind support and guidance with the kidney ischaemia reperfusion model.
- Imperial Facility for Imaging by Light Microscopy (FILM) for helping with confocal microscopy.
- Hera Tsiridou for the great collaboration that expanded this work into human *in vitro* model.
- All other past and current members of the Critical Care group, all of whom have helped me significantly in one way or another along the way: Faruq, Mike, Rosalba, Roger, Hideta, Justin, Aurelie, Virginia, Rhianna and Eirini.

Statement of originality

I certify that this thesis, and the research to which it refers, are the product of my own work conducted during the course of my PhD registration period at Imperial College London. Those that have been assisted by others have been fully acknowledged and referenced herein.

Declaration of copyright

Table of Contents

Index of figures

Index of tables

Index of equations

Abbreviations

AKI	Acute kidney injury
ALI	Acute lung injury
ARDS	Acute respiratory distress syndrome
ARF	Acute renal failure
ATP	Adenosine triphosphate
BALF	Bronchoalveolar lavage fluid
BSA	Bovine serum albumin
C-S	Chondroitin sulfate
CLP	Caecal ligation and puncture
COX	Cyclooxygenase
D-S	Dextran sulfate
DAMPs	Damage-associated molecular pattern
DIC	Disseminated intravascular coagulation
DMEM	Dulbecco's modified eagle medium
ELISA	Enzyme-linked immunosorbent assay
FCS	Foetal calf serum
FU	Fluorescence Unit
FWB	FACS Wash Buffer
HAS	Human Albumin Solution
HMGB-1	High mobility group box 1
HSP	Heat shock protein
I.P.	Intraperitoneal
I.V.	Intravenous
ICAM-1	Intercellular adhesion molecule 1
ICU	Intensive care unit
IFN	Interferon
IL	Interleukin
ILVs	Intraluminal vesicles
IPL	Isolated perfused lung
IRI	Ischaemia reperfusion injury
IVC	Inferior vena cava
LOX	Lipoxygenase
LPS	Lipopolysaccharide
LT	Leukotriene
MAP	Mean arterial pressure
MMPs	Matrix metalloproteinases
MOF	Multiple organ failure

MSCs	Mesenchymal stem cells
MVBs	Multi-vesicular bodies
MVs	Microvesicles
NO	Nitric oxide
NOS	Nitric oxide synthase
PAF	Platelet activating factor
PAMPs	Pathogen-associated molecular pattern
PaO_2/FiO_2	Partial pressure of oxygen to fraction of inspired oxygen ratio
PBS	Phosphate Buffered Saline
PC	Phosphatidylcholine
PEEP	Positive end expiratory pressure
PG	Prostaglandin
PIMs	Pulmonary intravascular macrophages
PMNs	Polymorphonuclear cells
Poly-C	Polycytidylic acid
Poly-I	Polyinosinic acid
PRRs	Pattern recognition receptor
PS	Phosphatidylserine
PSG	Penicillin streptomycin glutamine
PSGL-1	P-selectin glycoprotein ligand-1
RAGE	Advanced glycation end products
RES	Reticuloendothelial system
RPMI	Roswell Park Memorial Institute medium
SIRS	Systemic inflammatory response syndrome
SOFA	Sequential Organ Failure Assessment
SR-A	Scavenger receptor A (CD204)
SR-B	Scavenger receptor B (CD36)
TNF-α	Tumour necrosis factor alpha
VCAM-1	Vascular adhesion molecule 1
VEGF	Vascular endothelial growth factor
vWF	Von Willebrand factor

Chapter 1

Introduction

Chapter 1 Introduction

1.1 Acute Lung Injury (ALI) and Acute Respiratory Distress Syndrome (ARDS)

1.1.1 Definition, diagnosis and epidemiology

Acute Respiratory Distress Syndrome (ARDS) is a clinical syndrome first described by David Ashbaugh in 1967 based on 12 cases over 2 years in the intensive care unit (ICU)[2,3]. These patients developed symptoms that included severe dyspnea, tachypnea, cyanosis that is refractory to oxygen therapy, loss of lung compliance and diffuse alveolar infiltration seen on chest X-ray[4]. Due to the heterogeneity of underlying causes and the lack of uniform definitions for ARDS over the years, the American European Consensus Conference (AECC) defined ARDS in 1994 as "acute onset of respiratory failure", characterised by bilateral opacities on chest imaging and partial pressure of oxygen to fraction of inspired oxygen ratio, $PaO_2/FiO_2 \leq 200$mmHg, in the absence of left arterial hypertension[5]. Acute Lung Injury (ALI) was also described by the AECC at the same time, using similar criteria but with less severe hypoxaemia ($PaO_2/FiO_2 \leq 300$ mmHg). In 2013, the Berlin definition proposed three categories of ARDS based on degree of hypoxaemia: mild ($PaO_2/FiO_2 \leq 300$ mm Hg), moderate ($PaO_2/FiO_2 \leq 200$ mmHg), and severe ($PaO_2/FiO_2 \leq 100$ mmHg). Severe ARDS can be identified with 4 ancillary variables: radiographic severity, respiratory system compliance (≤ 40mL/cmH_2O), positive end-expiratory pressure (PEEP ≥ 10cmH_2O), and corrected expired volume per minute (≥ 10L/min)[6]. Since then, ALI and ARDS have been used interchangeably in clinical settings to encompass both syndromes. Despite the wide disparity in the literature due to changes in ALI/ARDS definition, population based prospective epidemiology studies have reported that the incidence of ALI in units of cases per 100,000 person-years, is around 79 in the US[7], 15-34 in Europe[8], 34 in Australia[9] and 18 in Scandinavia[10]. Across these studies, mortality of ALI patients is reported to be in the range of 32-50%[11,12]. Whilst most epidemiologic studies have focussed on patients in the ICU requiring mechanical ventilations, studies have shown that cases of ALI also occurs in non-ICU settings, suggesting a general underestimation of ALI incidence[13].

1.1.2 Pathophysiology

Pathological features of ARDS are often characterised based on histological evidence of ultrastructural differences, categorised into three main phases: acute, subacute and chronic phases, alternatively referred to as the exudative, proliferative and fibrotic phases, respectively. In the first week of disease onset during the acute/exudative phase, there is evidence of interstitial and alveolar oedema alongside with accumulation of inflammatory cells in the alveoli such as neutrophils, monocytes, red blood cells and platelets. In second week, it progresses into the subacute/proliferative phase where prominent hyaline membranes are observed, with some oedema resorbed. This phase is called the proliferative phase based on evidence of alveolar type II epithelial cells proliferation in an attempt to repair the tissue damages. Fibroblasts also become apparent in the interstitial space and alveolar lumen, facilitating the build-up of collagen fibrils and fibrosis. Finally, the lung enters the chronic, fibrotic phase where resolution of neutrophil infiltrates happens and there is an increased number of lymphocytes and macrophages in the lung. Depending on the degree of lung fibrosis and collagen build-up, which reduces lung compliance and predicts a poor outcome, patients may progress through these phases without significant degree of fibrosis and eventually oedema and inflammation of the lung is resolved[14,15]. However, if there is a secondary complication to the lung such as sepsis, persistence and progression of injury often occurs, leading to fatal complications such as multiple organ failure (MOF), pulmonary fibrosis and pulmonary vascular destruction without progressing through the repair and resolution phase. Overall, the main characteristics of ALI/ARDS includes the formation of protein-rich edema fluid in the alveolar space and interstitium, associated with the loss of alveolar-capillary integrity, excessive transepithelial neutrophil migration and release of pro-inflammatory, cytotoxic mediators[14,16,17].

1.1.3 Biomarkers, prevention and treatment

Despite a wide range of biomarkers having been investigated in plasma and bronchoalveolar lavage fluid (BALF) to define different phases of disease progression, currently there is no single biomarker available to predict or identify ALI with high accuracy[18]. Fremont et al. have shown the use of a panel of biomarkers including receptor for advanced glycation end products (RAGE), procollagen peptide III, brain natriuretic peptide, angiopoietin-2, interleukin (IL)-10, tumour necrosis factor alpha (TNF-α),

and CXCL8, to be effective in differentiating trauma patients with or without ALI[19]. Plasma levels of protein C, CXCL8 and intercellular adhesion molecule-1 (ICAM)-1 were also found to predict mortality in ALI patients[20].

Despite efforts in identifying biomarkers, there is no effective treatment available to prevent the development of ALI. Both statins and anti-platelet therapy have been investigated for their efficacy in preventing the incidence of ALI without success[21,22]. Despite implementation of revised definitions of ALI/ARDS to aid research and treatment options, there is no specific 'gold standard' therapy for ARDS to date. Diagnosis remains reliant on clinicians' ability to identify an intricate pattern of clinical findings in critically ill patients who often have multiple underlying diseases and current available treatment is limited to fluid management, lung-protective mechanical ventilation in the ICU and treatment of the underlying causes, if known. Recently, following the increasing trend in personalised medicine, a personalised time-controlled adaptive ventilation was suggested as prevention and treatment for the development of ALI[23]. Anti-inflammatory and anti-oxidant pharmacologic agents such as inhaled nitric oxide, corticosteroids, antiproteases and ketoconazole have been investigated in search for an effective therapy over the past decade without major success[24–26]. More recently, targeted drug delivery using nanoparticles and cell therapy using mesenchymal stem cells (MSCs) for the treatment of ALI/ARDS have been gaining more attention[27,28]. However, given the biological complexity and our limited understanding of the disease pathogenesis, these novel approaches may require more time to realise an actual new treatment option in ALI.

1.1.4 Indirect and direct forms of ALI

Traditionally, it has been thought that insults applied to the lungs, either through airways or via the circulation, results in similar pathophysiology which precedes diffused alveolar damage[17]. However, as ALI is a multifactorial disease with multiple aetiologies, the underlying pathophysiology leading to failure of the lung can be quite different despite a common end state being present. Thus, AECC has divided ALI into two categories based on the inciting causes: direct (pulmonary) and indirect (extrapulmonary) ALI. Direct ALI is caused by pulmonary insults causing injury mainly to the alveolar epithelial cells, whereas indirect ALI is caused by extrapulmonary insults in the settings of systemic

inflammation where pulmonary vascular endothelial injury is more prominent[29]. It is now well appreciated that crucial pathophysiological differences exist between direct and indirect forms of ALI. Based on pathophysiologically oriented views and taking into account where the underlying condition is anatomically located, clinical disorders associated with the development of ALI are summarised below (Table 1.1), adapted from Bernard[5], Ware[17], Doi[30] and Shaver[29]. This subgrouping of ALI/ARDS based on the underlying causes has significantly affected basic research, clinical progression and patients' response to therapies[29,31,32].

Direct lung injury	Indirect lung injury
Pneumonia (bacterial, viral, fungal)	Sepsis/SIRS
Aspiration of gastric content	Severe trauma
Mechanical ventilation (barotrauma, volutrauma)	Blood transfusion
Pulmonary contusion	Cardiopulmonary bypass
Near-drowning	Severe burns injury
Fat embolism	Acute kidney injury/ renal dysfunction
Inhalation injury	Acute pancreatitis
Reperfusion injury (Lung transplant/ pulmonary embolism)	Drug overdose

Table 1.1 Underlying conditions associated with the development of ALI/ARDS.
(Adapted from Bernard[5], Ware[17], Doi[30] and Shaver[29])

Despite exhibiting some common features, several clinical studies have demonstrated that direct and indirect ALI are truly different pathophysiologically. Pelosi et al. described several pathophysiological differences between direct and indirect ALI, highlighting prevalent damage of direct ALI as intra-alveolar oedema and accumulation of fibrin, collagen and neutrophil aggregates, whereas indirect ALI is mainly represented by microvascular congestion and interstitial oedema, with relative sparing of the intra-alveolar spaces, as summarised (Table 1.2)[31,33,34].

	Direct ALI (Pulmonary ARDS)	Indirect ALI (Extrapulmonary ARDS)
Alveoli		
Alveolar epithelium	++	+
Altered type I & II cells	++	-
Alveolar neutrophils	++	-
Apoptotic neutrophils	++	-
Fibrinous exudates	++	-
Alveolar collapse	++	+
Local Interleukin	++	-
Interstitial space		
Interstitial oedema	-	++
Collagen fibres	++	+
Capillary endothelium	-	++
Blood		
Interleukin (IL)	+	++
TNF-α	+	++

Table 1.2 Histological and biochemical alterations in pulmonary and extrapulmonary ARDS. *(Adapted from Pelosi[31])*

Despite indirect ALI causing less pronounced oedema, Sequential Organ Failure Assessment (SOFA) score, which is a mortality prediction scoring system, was found to be significantly higher in indirect ALI patients than direct ALI patients, whereas mortality, mechanical ventilation days and hospital length of stay were found to be similar between direct and indirect ALI[35]. When respiratory mechanics of patients with indirect ALI and direct ALI were compared, it has been demonstrated that the lungs of patients with direct and indirect ALI respond differently to positive end-expiratory pressure (PEEP), prone position and recruitment manoeuvres, where direct ALI patients were shown to have stiffer lungs and indirect ALI patients have stiffer thoracoabdominal cage and more compliant lungs[32,36]. However, when long-term (6 months) functional recovery was compared between patients with direct or indirect ALI, no difference between two groups were found, despite higher ventilatory requirements of direct ALI patients[37]. In recent years, retrospective cohort studies have demonstrated that despite comparable mortality rates between patients with direct and indirect ALI, some predictors of mortality may be distinct between these two forms of ALI, highlighting their fundamental differences. For

example, age and lung injury score were only associated with mortality of direct ALI patients but not indirect ALI, whereas number of organ failures, disseminated intravascular coagulation (DIC) score and high-resolution computed tomography score are a common predictor of mortality between these two forms of ALI[38,39].

However, it is important to note that the differentiation between these two forms of ALI is not simple or clear-cut. It can be difficult to discriminate direct and indirect ALI in clinical setting as both of them may coexist in the same patient. Thille et al. demonstrated that PEEP and alveolar recruitment does not differ between patients classified as direct or indirect ALI, whereas physicians were unable to classify the rest of the patients, which comprised of more than one third of the total patients examined[40]. Inter-organs crosstalk, both from lung-to-periphery and periphery-to-lung, is a complex process that may take days to develop and thus the precise origin of the initial insult may be difficult to identify, which is essential in the classification of direct or indirect ALI. For example, pneumonia may be limited to one lung producing a direct ALI, while the other non-infected lung is subsequently injured indirectly hours or days later via the systemic dissemination of inflammation due to loss of compartmentalisation in the infected lung[33]. However, as there was no difference found in mortality between direct and indirect ALI[41], it is still under debate whether the aetiology-based differentiation between direct and indirect ALI is factual or "just a concept"[42]. Nonetheless, the recognition of ALI/ARDS subtypes is essential in relation to the understanding of the underlying biology and the associated patients' response to therapy, which may have contributed to the heterogeneous and inconclusive outcomes observed in clinical trials so far.

With the recent emergence of COVID-19 outbreak, caused by severe acute respiratory syndrome coronavirus-2 (SARS-CoV-2), phenotypes of ARDS has been more widely discussed and recognised to be a heterogenous mix of different diseases leading to common end-state of lung injury and failure. COVID-19 patients were often presented with profound hypoxaemia despite very compliant lungs and significant pulmonary interstitial oedema/angiopathy, which is suggestive of significant endothelial injury[43,44] and is more consistent with indirect ALI pathophysiology. Additionally, lung injury and multiple organ failure (MOF) could progress with or without diffuse alveolar damage or compromised

lung compliance in these patients, causing a critical “paradigm shift” in the research of ARDS[45–47]. Recently, Calfee and colleagues have proposed a more thorough subphenotyping strategy to futher categorise ARDS patients via biomarker-based (focal vs. diffuse; hypoinflammatory vs. hyperinflammatory) and clinical-based subgroups (direct vs. indirect; early vs. late)[48–50]. Despite the rapidly changing views on the characterisation and categorisation of ALI/ARDS, it is important to “find the signal in the noise”, as the recognition of differences in the subphenotypes of ALI/ARDS could help deepen our understanding of the pathogenesis that has been on a standstill for decades, in hope of advancement in the development of new therapeutic interventions.

1.2 Systemic inflammatory response syndrome (SIRS) and sepsis

Systemic inflammatory response syndrome (SIRS), is a clinical syndrome following inflammation that can be attributed to an infection (which is termed “sepsis”) or to a non-infectious sterile insult such as polytrauma, surgery, pancreatitis, or major burns. Both non-infectious SIRS and sepsis often result in deleterious, overwhelming inflammatory host response in the bloodstream. Amongst all other risk factors, sepsis is the most common underlying condition in the development of ALI/ARDS, amounting to approximately 75-80% of ARDS patients with severe sepsis of both suspected direct origin with accompanying SIRS (pulmonary infection) or indirect (extrapulmonary sepsis) sources[7,51]. In parallel, it has been found that of 7,000 sepsis patients examined, the site of infection was most commonly the lungs (64%), followed by abdomen (20%), bloodstream (15%) and renal or genitourinary tract (14%)[52]. Overall, sepsis-induced ARDS has higher case fatality rate than patients with other risk factors of ARDS[53]. Whilst sepsis-induced direct ALI often results from infection in the respiratory system, the mechanisms underlying non-pulmonary sepsis/non-infectious SIRS-induced indirect ALI is not well understood[54].

1.2.1 Sepsis definition, diagnosis and epidemiology

Like ARDS, sepsis is a term used to describe patients with clinical symptoms of a systemic response to infection, including bacterial, viral, fungal and parasitic organisms. A consensus conference held in 1991 by the American College of Chest Physicians and the Society of Critical Care Medicine (Sepsis-1) defined sepsis as the host’s systemic inflammatory response syndrome (SIRS) to infection, if more than one of the following SIRS criteria are met: 1) body temperature >38°C or <36°C. 2) heart rate >90/min, 3) respiratory rate >20/min or $PaCO_2$ <32 mmHg, 4) white blood cell count >12,000/mm^3 or <4,000/mm^3 or 5) immature neutrophil bands of >10%[55]. Overall, the consensus suggested that when “SIRS” is a result of suspected infectious process, it is termed “sepsis”, whereas “severe sepsis” is used when sepsis is associated with organ dysfunction, hypoperfusion or hypotension, and if sepsis-induced hypotension persists despite adequate fluid resuscitation, it is termed “septic shock”. Although the definition of sepsis was revaluated and modified to expand the list of diagnostic criteria in 2001 (Sepsis-2), SIRS criteria continues to be widely used for diagnosing sepsis in various clinical settings. However, SIRS criteria was later deemed unspecific and limit the diagnosis accuracy in

clinical setting, where a significant fraction of patients who developed organ dysfunction without fulfilling the SIRS criteria were omitted from diagnosis[56]. In an effort to standardise the multiple definitions and terminologies being used, the 2016 Sepsis-3 conference defined sepsis as "life-threatening organ dysfunction caused by dysregulated host response to infection", and the Sequential Organ Failure Assessment (SOFA) scoring system was incorporated to increase diagnostic accuracy and to replace the use of SIRS criteria[57,58]. A higher SOFA score is associated with increased probability of mortality, whilst organ dysfunction can be identified as an acute change in total SOFA score of ≥2 points consequent to the infection, via the scoring of severity from 0-4 in PaO_2/FiO_2 ratio, platelet count, bilirubin level, mean arterial pressure (MAP), mental status, creatinine level and urine output. As organ dysfunction has become essential incorporated within the sepsis definition, the term "severe sepsis" is now redundant, whereas "septic shock" was redefined as a subset of sepsis in which there is an "underlying circulatory and cellular/metabolic abnormalities associated with greater risk of mortality than sepsis alone", identified by persisting hypotension requiring vasopressors to maintain a MAP >65mmHg and a serum lactate level >2mmol/L (>18mg/dL) despite adequate volume resuscitation. These drastic changes in the definition of sepsis has not only imposed a significant shift in clinical practice, but also the viewpoint and approach in basic research[56,59,60]. The most recent global epidemiology study has reported an estimated total sepsis incidence of 48.9 million cases, with age-standardised incidence of 677.5 cases per 100,000 person-years in 2017[61]. The age-standardised mortality of sepsis is reported to be 148.1 per 100,000 person-years. Overall, sepsis-related deaths represent 19.7% of all global deaths, significantly highlighting it as a major global health problem[61].

1.2.2 Non-infectious SIRS

Despite much attention placed in sepsis definition and the elimination of SIRS criteria in clinical diagnosis, non-infectious or 'sterile' SIRS remains an important clinical condition, separate from sepsis but with similar pathophysiology, including development of indirect ALI/ARDS. In hospital, many SIRS patients are presented without an identifiable infection upon admission but subsequently develop evidence of infection after, leading to shock, MOF and death. There are several theories regarding the inflammatory response to sterile insults leading to SIRS. One of the most widely

accepted theory at that time was the translocation of bacteria from the gut or intestines following haemorrhage or shock as the cause of “sepsis syndrome” without an obvious source of infection[62,63].

Traditionally, it was thought that operation of the innate immune response was primarily based on recognising and responding to invasive microorganisms and their antigens, thereby distinguishing non-self from self. In the late 1990s, a different theory was put forward by immunologist Polly Matzinger who proposed “the danger model”, suggesting that the host immune surveillance is concerned primarily with the identification of danger signals released from damaged cells or tissues, irrespective of whether these were a result of sterile injury or infection[64]. Since then, sepsis/SIRS studies have recognised the significance of sterile inflammation in eliciting the same clinical features as sepsis, in the absence of an obvious source of infection. Sterile inflammation or non-infectious SIRS can result from the acute inflammatory systemic response to non-infectious insults, including severe non-penetrating polytrauma (bone fracture and soft tissue injury), ischaemia reperfusion injury (IRI), major burns injuries and haemorrhagic shock[65]. Similar to infection-induced inflammation in sepsis, sterile inflammation in SIRS is marked by the presence of fever, tachycardia, tachypnoea, or leucocytosis. Like ARDS, the recognition of differences between bacterial sepsis and sterile SIRS in relation to the biological triggers and inflammatory pathways would facilitate our understanding of the disease pathogenesis and future development of novel therapeutics.

1.2.3 Pathophysiology

In 1996, Roger Bone first described that the balance between pro-inflammatory and anti-inflammatory responses is essential in maintaining or restoring homeostasis during health and disease. He described that in sepsis/SIRS, an excessive and destructive pro-inflammatory reaction (which he termed systemic inflammatory response syndrome, SIRS) is opposed by a severe, anergic anti-inflammatory reaction (termed compensatory anti-inflammatory response syndrome, CARS)[66]. This concept has been widely accepted and further developed and characterised since, where SIRS is ascribed to the excessive release of pro-inflammatory cytokines including TNF-α, IL-6 and IL-1β, whereas CARS is attributed to excessive anti-inflammatory cytokines such as TGF-β and IL-10. Subsequently, Hotchkiss et al. described a two-phase model of sepsis, where early pro-inflammatory

response of SIRS precedes the immunosuppression state of CARS, where there is an increased risk of secondary infection associated with higher morbidity and mortality[67]. Although this SIRS/CARS model has been widely accepted, it remains debatable whether septic patients are hyperinflammatory or immunocompromised at any given time frame[68]. A recent cytokine profiling study has also shown that both pro- and anti-inflammatory mediators are upregulated in the early period of sepsis and are both reliable predictors of mortality, questioning the relevance of this two-phase SIRS/CARS hypothesis[69]. Interestingly, Cavaillon et al. proposed a compartmentalisation model, where instead of a generalised whole body response, SIRS conditions predominate in the inflamed tissues which are hyper-responsive to *ex vivo* stimuli, whereas CARS predominates in the blood where leukocytes derived from the hematopoietic compartment are hypo-responsive during sepsis[70,71].

Other than the aberrant release of cytokines and numerous inflammatory mediators described in SIRS/CARS model, microcirculatory dysfunction is commonly observed during early stages of sepsis/SIRS, where decreased functional capillary density and increased blood flow heterogeneity is observed in patients. The dysregulated perfusion of the microvasculature in sepsis/SIRS is a cumulative result of nitric oxide (NO) dysregulation and functional impairment of several vascular cell types including the endothelial cells, smooth muscle cells, red blood cells, platelets and leukocytes[72]. If the reduction in perfusion is not corrected in a timely manner by clinical interventions to restore blood flow and oxygenation, circulatory shock and tissue hypoxia follows. As a result of mitochondrial dysfunction and metabolite accumulation during tissue hypoxia, parenchymal cells undergo respiratory distress, triggering a cascade of pathogenic mechanisms, leading to MOF and death[73,74]. Other immunopathologic alterations were also suggested to account for the morbidity and mortality of sepsis, including dysregulated coagulation, cellular dysfunction, metabolic alterations, mitochondrial dysfunction and dysregulated apoptosis[68,72]. Overall, pathophysiology of sepsis/SIRS is heterogeneous and multifactorial, possibly due to the wide variety of possible sources of infection, triggers of inflammation and the reactivity and response of the immune system, dependent on various genetics and environmental factors.

1.2.4 Biomarkers, current treatments and clinical trials

Several inflammatory biomarkers of sepsis/SIRS have been identified over the years for diagnosis and monitoring of treatment, including markers of neutrophil and monocyte activation, pro- and anti-inflammatory cytokines and chemokines, reviewed by James Faix[75]. Markers of the hyperinflammatory phase of sepsis/SIRS include pro-inflammatory cytokines TNF-α, IL-1β and IL-6, whereas markers of immunosuppressive phase include anti-inflammatory cytokines IL-10 and TGF-β. Markers of neutrophil and monocyte activation, such as decreased expression of HLA-DR on monocytes[76,77], soluble CD14[78] and soluble RAGE[79] released by monocytes, and increased surface expression of CD64, CD11b and TREM-1 on neutrophils[80,81] are commonly measured and were shown to have prognostic value in sepsis/SIRS. Clinically, serum levels of C-reactive protein (CRP) and procalcitonin (PCT) are commonly used in the diagnosis of sepsis/SIRS, where PCT was found to have higher diagnostic accuracy than CRP in patients with suspected bacterial infections compared to those with non-infectious causes of inflammation[82]. Overall, further identification of biomarkers that can distinguish between sepsis and sterile SIRS is of considerable importance for guiding towards more effective patient treatment.

As discussed above, treatment of ALI mainly relies on identifying the underlying cause. In the case of sepsis/SIRS-induced ALI, more attention is required as treatments such as inhaled agents may be of little help in resolving pulmonary vascular inflammation originating from an extrapulmonary source. It is abundantly clear from the literature to date, that no single mediator or pathway drives the pathophysiology of sepsis[68]. As with ALI patients, current treatments available for sepsis/SIRS are mainly supportive measures such as blood or plasma replacement, infusion of resuscitative electrolyte or glucose containing fluids, ventilation and vasopressor support. Much focus has been placed on anti-cytokines and other inflammatory mediator-based therapies in the last 30 years in an effort to treat the underlying trigger of septic responses, but to no avail. More than 100 clinical trials aiming to modulate these septic responses by targeting endogenous pro-inflammatory mediators have all failed, with none of these leading to any new treatment[83]. For instance, trials of anti-TNF-α[84] and anti-IL-1 receptor antagonist[85] both failed to reduce mortality in patients with septic shock and severe sepsis. Aside from targeting these major players of inflammation, other trials targeting the deleterious effect

of bacterial-derived endotoxin activity including Toll-like receptor 4 (TLR4) antagonists[86] and recombinant bactericidal permeability increasing (BPI) protein[87] have also failed to demonstrate any difference in sepsis mortality. Even the previously approved drugs for the treatment of sepsis such as Xigris (recombinant activated protein C) and Eritoran (TLR4 inhibitor), were withdrawn from the market due to lack of clinical efficacy[88]. As sepsis is a heterogeneous syndrome where a variety of different pathogens and sites of infection affects a diverse patients population, it is therefore unlikely that modulating the level of only one of these targets in a non-patient specific manner would have a significant effect on outcome[89]. The complexity of cell biology and redundancy of inflammatory cascades involved in sepsis/SIRS that became evident since the advent of these single-mediator targeted trials has questioned/undermined these approaches and implies a need to redirect basic and pre-clinical research to develop alternative strategies.

1.3 Innate immunity and inflammation

1.3.1 An overview of the innate and adaptive immune response to infection

The pathophysiology of sepsis and associated organ dysfunction is a result of failure in homeostasis, which can be define as "the inability to maintain internal equilibrium by adjusting its physiological processes under fluctuating environmental conditions in response to infection or injury"[90]. The body's response to infection or injury is a normal physiological process, where the activation of the innate immune system and the subsequent signalling cascades are intended to eliminate infection or to repair damage without causing damage to tissues, organs or other systems. However, when the host response to infection and injury is dysregulated, uncontrolled inflammatory responses lead to sepsis/SIRS.

The immune system responds to an encounter of initial infection in three phases: 1) the innate phase (0-4h), 2) the early induced innate response (4-96h) and 3) the adaptive immune response (>96h)[91]. In the first innate phase, soluble molecules present in the blood including antimicrobial enzymes such as lysozymes, antimicrobial peptides such as defensins and a system of plasma proteins known as the complement system, targets the foreign pathogens to either kill, weaken or signal phagocytic cells to the site of infection and promote inflammation or phagocytosis. If the removal of infectious agent is incomplete during this initial phase, the second phase of the immune system develops, where cells of the innate immune system consisting mainly of macrophages, monocytes, neutrophils, dendritic cells and natural killer (NK) cells sense the presence of pathogens by recognising molecules typical of a microbe that is not shared by host cells, termed pathogen associated molecular pattern (PAMPs). The recognition of PAMPs by pattern recognition receptor (PRRs) on these innate immune cells initiates a cascade of inflammatory mechanisms in an effort to eliminate the infection. Activated macrophages and dendritic cells release cytokines and chemokines such as TNF-α, IL-1β, IL-6, IL-12, CXCL8 and CCL2, to induce local inflammatory response by activating vascular endothelium or to further recruit leukocytes to the site of infection.

If the infectious organism survives these first two lines of defence, the final adaptive immune response is engaged, where naïve T and B cells undergo clonal expansion, differentiate into effector cells and

migrate to the site of infection for further removal of infection. In T cell mediated immunity, whilst CD8 T cells are specialised to kill infected cells, CD4 T cells can differentiate into several subclasses such as helper T cell-1 (Th1), -2 (Th2), -17 (Th17) and regulatory T cells (T_{reg}). Each of these subclasses of CD4 T cells are specialised to provide help via different functions. For example, Th1 cells release interferon-gamma (IFN-γ) to activate macrophages, Th2 cells release interleukin (IL)-4. IL-5, IL-13 to recruit eosinophils, basophils and mast cells, Th17 release IL-17 for downstream neutrophil recruitment, and T_{reg} suppress T-cell activity to prevent the development of autoimmune response.

1.3.2 PAMPs and DAMPs

PAMPs is a term used to describe conserved motifs expressed by microbial pathogens which are recognised by the innate immune system. PAMPs such as lipopolysaccharide (LPS), peptidoglycan, lipopeptides, lipoteichoic acid, flagellin and bacterial DNA, are invariant due to their essential structural roles and biological functions in bacteria as constituents of bacterial cell wall, proteins and nucleic acids. As all microbes, not just pathogenic microbes possess PAMPs, they are sometimes referred to as microbes-associated molecular pattern (MAMPs). PAMPs are recognised by the innate immune cells through pattern recognition receptor (PRRs) that are located either on the cell surface, including toll-like receptors (TLRs) and C-type lectin receptors (CLRs), or in the cytosol, including nucleotide-binding oligomerisation domain (NOD)-like receptors (NLRs) and retinoic acid-inducible gene-I (RIG-I)-like receptors (RLRs)[92]. The binding of PAMPs to PRRs expressed on the innate myeloid cells initiate the signalling cascades that triggers the recruitment of intracellular signalling proteins that serve to amplify the inflammatory signal, resulting in transcriptional release of cytokines, chemokines and cell death pathways in order to achieve rapid elimination of pathogens and injured cells[93].

Since the description of the danger model[64], it has been shown that PRRs can initiate the same inflammatory response cascades via the recognition of endogenous danger molecules, termed the damage-associated molecular pattern (DAMPs). In contrast to PAMPs expressed by microbes/pathogens, DAMPs can be released from damaged or dying host cells during inflammation and injury without infection. The number of endogenous molecules considered DAMPs is

considerable but some of the most studied include adenosine triphosphate (ATP), high mobility group box 1 (HMGB-1), heat shock proteins (HSPs), defensins, lactoferrin, DNA, histones, hyaluronans and heparin sulphate. Similar to PAMPs, DAMPs are able to initiate the activation of the innate immune system and trigger the production of pro-inflammatory cytokines, chemokines, activated complement and other mediators as first line defence response[65,94]. Matzinger proposed that pathogens also trigger inflammation through eliciting injury in cells/tissue, suggesting that DAMPs release is an important signal of danger during infection, distinct from an infection elicited by non-invasive commensals colonising the exterior surfaces and tracts of the body without producing damage or stress.

The initiation of inflammatory responses by PAMPs and DAMPs in the context of sepsis and SIRS, respectively, can both result in similar mechanisms of multiple organ dysfunction that do not distinguish between infectious or non-infectious origin[95]. In patients, elevated levels of various DAMPs such as cell-free DNA, HMGB-1 and histones were found to associate with the severity of sepsis/SIRS and were predictors of the development of organ injury and MOF[96–98]. Increased levels of HMGB-1 were also observed *in vivo* after trauma-induced haemorrhagic shock and were positively correlated with severity, whereas decreased level of HSP70 was observed[99]. Administration of histone *in vivo* was also shown to cause a dose-dependent death after development of multiple organ injury[100]. Interestingly, the deletion of HSP70 gene were shown to increase the development of ARDS and mortality of septic mice[101], showing direct evidence of DAMP-mediated sepsis-induced ALI pathogenesis. Significantly, in non-human primate models, bacterial sepsis has been shown to progress to organ failure and death long after control of the initial inciting infection, suggesting that persistence of inflammation and ultimately, organ injury, could be driven by endogenous DAMPs release secondary to the initial infection[102,103]. These studies highlight the importance of DAMPs in the pathogenesis of sepsis/SIRS in the clinical setting and ICU, where despite antibiotic control of infection, the patient fails to resolve their condition.

Lipopolysaccharide (LPS)

The recognition of LPS, a component of the gram-negative bacterial cell wall by the TLR4 is the most widely researched and best-characterised mechanism of inflammation. TLR4 is one member of the ten TLRs currently characterised in human (TLR1-10) and of the twelve in mouse (TLR1–TLR9, TLR11–TLR13)[104]. TLRs are localised either to the cell surface or to intracellular compartments such as the endoplasmic reticulum, endosome, lysosome, or endolysosome, each of which binds to a specific class of ligand. TLRs located on the cell surface such as TLR1, TLR2, TLR4, TLR5, TLR6, and TLR10, mainly recognise membrane components of microbes such as lipids, lipoproteins and protein, whereas TLRs located intracellularly such as TLR3, TLR7, TLR8, TLR9, TLR11, TLR12, and TLR13, recognize nucleic acids components of bacteria or viruses[104].

In mammalian cells, LPS signalling requires the “LPS receptor complex”, which includes LPS-binding proteins that transfer LPS to CD14 and the extracellular accessory protein MD-2 present on host cell for its recognition by TLR4. CD14 is an essential part of the LPS receptor complex that is expressed on cell membranes of the myelomonocytic lineage including monocytes, macrophages and to a lesser extent on neutrophils. In certain cell types such as endothelial cells where membrane CD14 is absent, soluble form of CD14 serves as the accessory molecule for the surface recognition of LPS. The TLR4-mediated response is divided into 2 categories: an early MyD88-dependent response and a delayed MyD88-independent response[105]. Depending on the pathway activated, after the binding of LPS receptor complex to TLR4, they associate with different adaptor proteins such as myeloid differentiation factor 88 (MyD88), Toll/IL-1 receptor homology domain-containing adapter protein (TIRAP), TIR domain-containing adaptor-inducing interferon-β (TRIF) or TRIF-related adaptor molecule (TRAM). The MyD88-dependent response is better characterised, where the ligation of LPS with its receptor complex LPS-binding protein, CD14, MD-2 and TLR4 results in the recruitment of TIRAP and MyD88 to the receptor complex. This leads to the association of interleukin-1 receptor associated kinases (IRAK)-1 and -4, which form a scaffold with tumour necrosis factor receptor (TNFR)-associated factor 6 (TRAF6). This causes activation of TAK1 protein kinase complex and the activation of two different downstream pathways: the Mitogen Activated Protein Kinase (MAPK) and the IκB kinase (IKK) complex cascades. The activation of MAPK family members such as p38,

extracellular signal-regulated kinase (ERK1/2), and c-Jun N-terminal kinase (JNK), and the phosphorylation of IκB leading to translocation of NF-κB to the nucleus, cause downstream gene transcription and protein expression of various pro-inflammatory cytokines and chemokines, including TNF-α, IL1-β, IL-6, CXCL8, IFN-γ, MCP-1, RANTES[106–109], cell adhesion molecules (CAMs), selectins and costimulatory molecules that further enhance the recruitment of leukocytes and their interaction with endothelial cells. The LPS signalling pathway is summarised in Figure 1.1 below.

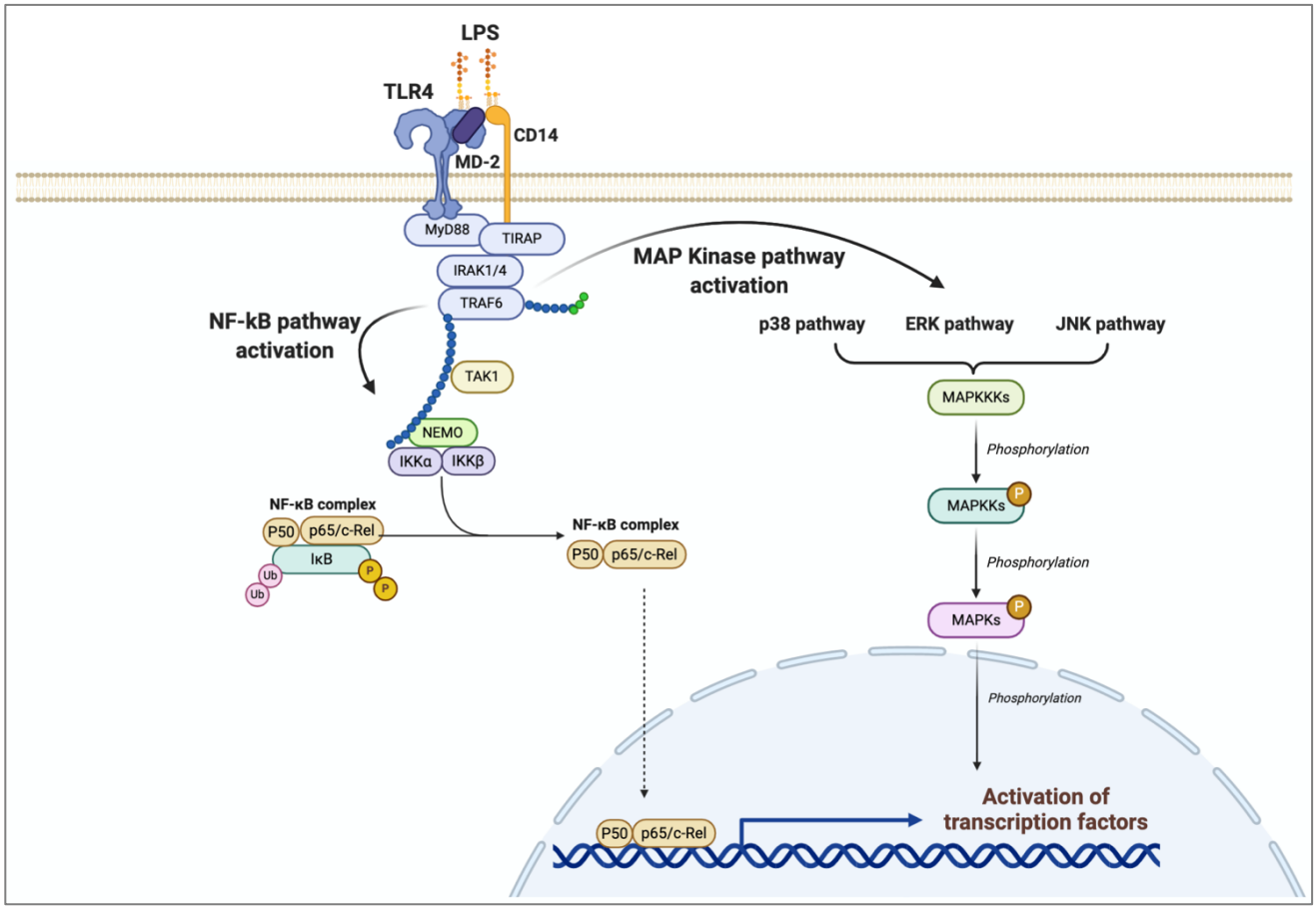

Figure 1.1 LPS signalling and its downstream activation of the MAPK and the NFκB pathways. *Binding of LPS to its receptor complex CD14, MD-2 and TLR4 causes recruitment of TIRAP and MyD88 to the receptor complex and the association of IRAK1/4 and TRAF6. This activates downstream MAPK and the IκB kinase pathways, leading to the activation of transcription factors and protein expression of various pro-inflammatory cytokines and chemokines. (Made with BioRender)*

Ischaemia reperfusion injury (IRI) and tissue hypoxia

In the context of non-infectious SIRS, various sterile inflammation such as ischaemia reperfusion injury (IRI) can also elicit a systemic inflammation response similar to that observed during microbial infection[65]. IRI occurs when tissue suffers from hypoxia as a result of severely decreased or

completely arrested blood flow, and when blood flow is reintroduced (termed reperfusion), tissue damage is further enhanced as a result of inflammatory responses. The degree of cellular and tissue injury varies in extent with the magnitude and duration of decrease in blood supply. During ischaemia, the lack of oxygen supply (hypoxia) causes a prevalence of anaerobic metabolism, resulting in drop in cellular pH, increased influx of sodium ions, depletes cellular ATP and decrease in calcium efflux. These series of molecular events lead to an eventual calcium overload in cells, oxidative and nitrosative stress, endoplasmic reticulum and mitochondrial dysfunction. Upon restoration of blood supply during reperfusion after ischaemic period, despite necessary reestablishment of oxygenation, metabolism and removal of potential toxic by-products produced during ischaemia, sudden flux of oxygen and ATP production fuels the formation of reactive oxygen species (ROS) and reactive nitrogen species (RNS). The release of these oxidative stress-induced mediators promote further downstream cascades of inflammatory mediator and cytokine release and promote leukocyte-endothelial interaction, exacerbating injury both locally and in remote organs[110,111].

Oxidative stress and ROS

Oxidative stress associated with generation of ROS as a result of cellular injury as described above, is well recognised in recent years to associate with pathogenesis of various inflammatory disease processes other than IRI. In the context of sepsis and non-infectious SIRS, tissue hypoxia as a result of sepsis-induced circulatory shock contribute to similar mechanism of oxidative stress-associated cellular and tissue injury[112–114]. In addition to hypoxia and ischaemia, recruitment of innate immune cells during infection such as PMNs was also found to contribute to oxidative stress due to their ability to generate ROS for microbicidal activity. ROS were historically thought to be a toxic mediator but are now recognised to be produced as normal by-product of mitochondrial respiration during energy production. ROS is a collective term to include all oxygen-containing reactive species that are unstable due to its unpaired electron in the outer orbital, causing them to react avidly with surrounding molecules in an indiscriminate fashion. Therefore, their production must be tightly regulated and balanced by antioxidant defence system to scavenge these radicals. ROS can be generated through various enzymatic and non-enzymatic pathways, each producing a different species of ROS. Endogenous enzymes such as NADPH oxidase reduces extracellular O_2 to superoxide $O_2^{\bullet-}$, which is

utilised by phagocytic cells such as PMNs and macrophages to kill microbes, nitric oxide synthase (NOS) generates superoxide $O_2^{\bullet-}$ instead of $^{\bullet}NO$ under tissue acidosis from hypoxia or ischaemia, and xanthine oxidase generate hydrogen peroxide H_2O_2 during reoxygenation of hypoxic tissues[115–117]. Non-enzymatic sources of ROS includes the mitochondria electron transport chain, cytochrome P450 of endoplasmic reticulum and from accumulation of free iron during tissue hypoxia[118–120].

ROS are now known to mediate various signalling pathways including the MAPK cascade and the NF-κB transcription cascade. In particular, ROS regulate MAPK activity by both activating the MAPK phosphorylation and by inactivating the dephosphorylating enzyme MAPK phosphatase, thereby activating downstream kinases p38, ERK and JNK, whereas ROS can also lead to phosphorylation of IκB kinase, allowing the translocation of NF-κB to the nucleus for transcriptional activities[121,122]. The activation of these pathways by dysregulated ROS have a profound effect on the process of inflammation, where the gene transcription and protein expression of various downstream cytokines and chemokines are activated non-specifically and excessively during inflammation.

1.3.3 Soluble mediators of inflammation

Following tissue injury, the innate immune cells release a wide variety of soluble mediators extracellularly to help combat the invading pathogen by facilitating the amplification of inflammatory response, including cytokines, chemokines, ROS/RNS and lipid mediators (eicosanoids and platelet activating factors). Other than soluble mediators released by cells, the complement system consisting a large number of plasma proteins, also plays a vital role in the innate immunity. As sepsis/SIRS is a heterogeneous syndrome that entails a hyper-responsive immune state, most, if not all, of these soluble mediators involved in normal inflammatory responses are implicated in the pathogenesis of sepsis in one way or the other[123–127]. However, as mentioned above, clinical trials targeting these mediators have not shown any success to date, possibly due to the substantial overlap and functional redundancy of these soluble mediators in immunity.

Cytokines

Cytokines are a series of small proteins released by cells that facilitate the interaction and communication between cells, capable of acting in an autocrine, endocrine and paracrine manner. In response to PAMPs and DAMPs, effector cells of the immune system including macrophages, mast cells, neutrophils, monocytes, basophils, eosinophils, B cells and T cells can secrete a wide range of cytokines that are categorised into two broad classes: the pro-inflammatory cytokines and anti-inflammatory cytokines, which exert either a net amplification or inhibition of the inflammatory response of their target cells. Cytokines encompass the tumour necrosis factor (TNF) family, interleukin (IL) family, interferon (IFN) family, chemokine family, colony stimulating factors (CSFs) and transforming growth factor beta (TGF-β) family. Each of which can interact in pleiotropic (single cytokine exert different effect on different target cell), redundant (similar functions can be stimulated by different cytokines), synergic (multiple cytokines acting cooperatively), antagonistic (opposing effects that inhibits one another) and cascade induction (feedforward amplification) manner, forming an interconnected network that is often difficult to dissect[128].

The coordinated release of pro-inflammatory cytokines, including TNF-α, IL-1, IL-6 and IFN, results in vasodilation and adhesion molecule upregulation to facilitate recruitment of more leukocytes to the site of infection/injury, as well as the enhancement of leukocyte actions in microbicidal activity. Mononuclear phagocytes including macrophages and monocytes are main producers of TNF-α and the most widely known member of the IL-1 family, IL-1β, but other sources include neutrophils and mast cells. The binding of TNF-α and IL-1β to their respective receptors TNF receptors (TNFR1/TNFR2) and IL-1 receptor (IL-1R) stimulate the downstream intracellular activation of MAPK and transcription factor NF-κB cascades, leading to further amplification of inflammatory responses and leukocyte-endothelial interaction[129]. IL-6 is released by a wide variety of cell types including activated mononuclear phagocytes, endothelial cells, fibroblasts and lymphocytes, and are involved in promotion of coagulation by stimulating tissue factor formation and the maturation and activation of lymphocytes. IFN is released specifically by lymphocytes such as natural killer cells, helper T cells and cytotoxic T cells to facilitate anti-viral functions by inducing the expression of major histocompatibility complex (MHC) for antigen presentation in antigen presenting cells.

The main functions of anti-inflammatory cytokines including IL-4, IL-10, IL-13 and TGF-β, are to antagonise the activity of pro-inflammatory cytokines and to inhibit further pro-inflammatory responses. T cells and macrophages release IL-10 to inhibit cytokine production by mononuclear phagocytes and promote B cell proliferation, whereas IL-4 and IL-13 are released by T cells, basophils, eosinophils, mast cells, and NK cells to inhibit pro-inflammatory cytokine responses and release in monocytes and macrophages, and to promote Th2 lymphocyte response. TGF-β is released by macrophages, T cells and B cells to inhibit lymphocytes proliferation and promote wound healing, as well as to antagonise the action of both TNF-α and IL-1β through inhibition of their secretion[130,131].

Another class of cytokines, the colony stimulating factors (CSFs) such as granulocyte-CSF (G-CSF), granulocyte/macrophage (GM-CSF) and macrophage-CSF (M-CSF), are released by several cell types, including fibroblasts, endothelial cells, stromal cells, macrophages, smooth muscle cells and osteoblasts. Due to their potent activity in promoting the survival, growth, differentiation and function of effector cells including mononuclear phagocytes (monocytes and macrophages), neutrophils and eosinophils, the excessive production of CFSs can have detrimental effects in inflammatory conditions[132].

Chemokines

Chemokines are small proteins secreted into the extracellular space by innate immune cells, which has a main function of recruiting and guiding innate immune effector cells (monocytes, neutrophils, eosinophils, basophils, mast cells, dendritic cells, NK cells) from the circulation to the site of infection/injury in tissue, as well as plays a vital role in coordinating the interaction between cells. They also control the release of monocytes and neutrophils from the bone marrow into the circulation during homeostasis as well as in response to infection and inflammation. Secreted chemokines by activated cells are bound to extracellular matrix components, forming a chemotactic gradient to guide cells which express their specific chemokine receptor along their concentration gradient. Chemokines

are categorised into four groups based on the positioning of their initial cysteine residue: CC, CXC, XC and CX_3C[133,134].

1. CC chemokine is the largest chemokine family consisting of twenty-eight members: CCL1-28. They have various functions such as inflammatory monocyte homing and trafficking (CCL2/MCP-1), macrophage and NK cell migration (CCL3/MIP-1α), modulating Th2 responses (CCL8, CCL13, CCL17, CCL18, CCL22), and homing and migration of effector and memory T cells (CCL5/RANTES).
2. CXC chemokine family consist of sixteen members: CXCL1-16. They have a main function of promoting neutrophils homing from bone marrow and its trafficking (CXCL1/mouse KC, CXCL8/human IL-8, CXCL2/MIP-2, CXCL5/ENA-78, CXCL12/SDF-1).
3. XC chemokine family only consists two members: XCL1 and 2, or lymphotactin α and β. They are mainly responsible for CD8+ T cell and NK cell recruitment.
4. CX_3C chemokine family only consist of one member: CXCL1 or Fractalkine. Its soluble form has a major function of inducing NK cell, monocyte and T cell migration, whereas its membrane-bound form induces adhesion of leukocytes[135].

Overall, increased levels of various pro- and anti-inflammatory cytokines and chemokines have been found in septic patients, including IL-6, CXCL8, IL-10, IL-18 (IFN-γ-inducing factor) and TNF-α[127]. However, the blood level of cytokines (and other mediators) may only reflect the saturation of the interstitial and cellular compartments, representing only the "tip of the iceberg"[136]. In parallel with this theory, various extracorporeal cytokine removal therapies have failed to demonstrate any significant outcome in improving organ injury and mortality in septic patients[137,138].

Eicosanoids and platelet activating factor (PAF)

Other than cytokines and chemokines, innate immune cells also release lipid-derived mediators such as eicosanoids and platelet-activating factor (PAF), which are crucial in initiating the leukocyte trafficking required in host defence. Eicosanoids are mainly derived from arachidonic acid (AA) cleaved from membrane phospholipids by phospholipase A_2 as a result of cell activation, which are

then converted into different derivatives of eicosanoids by two enzymes cyclooxygenase (COX) and lipoxygenase (LOX). COX produces prostaglandins (PGD_2, PGE_2, PGF_2, PGI_2) and thromboxanes (TxA_2), whereas LOX produces leukotrienes (LTA_4, LTB_4, LTC_4, LTD_4, LTE_4). Eicosanoids are produced mainly by myeloid cells in response to PRR activation by PAMPs and DAMPs, whereas PAF is produced by leukocytes, endothelial cells and platelets. During inflammation, PGD_2, PGE_2 and PGI_2 are potent vasodilators, inhibit platelet aggregation and mediate leukocyte trafficking and recruitment, whereas PGF_2 and TXA_2 mediates vasoconstriction, promote platelet adhesion and aggregation, smooth muscle contraction and proliferation as well as activation of endothelial inflammatory responses[139,140]. LTB_4 and PAF are also important chemotactic agents for monocytes and neutrophils, and PAF plays a vital role in facilitating leukocytes adhesion to endothelium for subsequent transmigration process[141–143]. Significantly, higher levels of plasma $PGF_{2\alpha}$ were found in sepsis non-survivors compared to survivors and was associated with the development of ARDS in sepsis patients[144]. However, COX and PAF inhibition therapies in sepsis clinical trials using non-steroidal anti-inflammatory drugs (NSAIDs) and PAF receptor antagonist respectively, has not shown any significant impact on disease severity and mortality[145–148].

Nitric oxide (NO)

Nitric oxide (NO) is one of the most researched vasoactive molecules known to regulate vasomotor tone in the systemic vascular bed, produced by nitrox oxide synthase (NOS). NOS has three isoforms: inducible NOS (iNOS), endothelial NOS (eNOS) and neuronal NOS (nNOS), all of which has a general function of converting L-arginine to L-citrulline and NO. nNOS and eNOS are both constitutive enzyme isoforms present in neurons and endothelial cells, respectively, that are activated by calcium/calmodulin binding and are responsible for a constant low production of NO in maintaining vascular integrity and blood flow. Conversely, iNOS are present mainly in leukocytes and vascular smooth muscles, and are regulated transcriptionally upon stimulation by PAMPs, DAMPs and cytokines, resulting in NO production at a higher concentration compared to constitutive NO release[149]. The role of NO as a vital mediator of vascular motor tone has drawn attention to its implication in the systemic vasodilation, hypoperfusion and shock seen in sepsis patients[150]. Interestingly, *ex vivo* studies have shown that PAF induced pulmonary oedema by

decreasing endothelial NO production, whereas in extrapulmonary tissues, PAF induced oedema by increasing endothelial NO levels[151], suggesting a dual role of NO in the body and non-specific inhibition may lead to unfavourable outcomes. Clinical trials in the inhibition of NOS to reduce levels of NO in sepsis patients was stopped early due to its effect in increased mortality[152].

The complement system

The complement system consists of a group of plasma proteins involved in the control of inflammation, sensing the presence of pathogens and the removal of immune complexes or cells opsonised by antibody. The ability of the complement system to recognise features of microbial surfaces and marks them for destruction with or without the presence of antibodies makes them part of the plasma component of the PRRs, as well as acting as an effector arm of the antibody response. Complement can be activated via three different pathways: Classical, Alternative and Mannose-Binding Lectin pathway. In brief, all three pathways generate a C3 convertase and C5 convertase. C3 convertase cleaves C3, leaving C3b bound on the microbial surface and release C3a, whereas C5 convertase cleaves C5 into C5b, which triggers late event of the complement pathway and release C5a. Whilst C3b is a major opsonin and C5b forms part of the membrane attack complex that facilitate cell lysis, C3a and C5a are anaphylatoxin and act as chemotactic factors that recruit phagocytic cells to the site of infection and cause inflammation. The ability of C5a to promote the production of various cytokines and chemokines[153] and its association with increased mortality in sepsis patients[154] has made it an attractive therapeutic target in sepsis[155]. A phase II clinical trial targeting against C5a using monoclonal antibody was performed in septic patients (SCIENS; NCT02246595), though the results of these trials have not been published so far.

1.3.4 Cellular mediators of inflammation

Cells of the innate immune system perform a multitude of functions, where each cell type is unique but has overlapping and cooperative functions with one another. Cells of myeloid origin, mononuclear phagocyte system cells (macrophages, monocytes, dendritic cells) and granulocytes (mast cells, neutrophils, eosinophils and basophils), are the main subpopulations in innate immunity that are activated rapidly upon the encounter and recognition of PAMPs and DAMPs. Other non-myeloid cell types such as lymphocytes, natural killer cells and platelets also play important roles in orchestrating the body response to infection and inflammation. During local inflammation/injury, tissue-resident macrophages and mast cells can become activated following microbial challenge and release cytokines and chemokines such as histamine, TNF-α, CXCL1 (KC) and CCL2 (MCP-1) to recruit neutrophils and monocytes. Following recruitment of neutrophils, different monocyte subsets are subsequently recruited by chemotactic signals sent out by neutrophils, such as cathepsin G and azurocidin, creating a feed-forward loop of amplified inflammatory processes[156–158]. Recruited neutrophils typically act in concert with monocytes/macrophages, which release various growth factors (GM-CSF and G-CSF) and pro-inflammatory cytokines (TNF-α), that can activate and prolong neutrophil survival to enhance the strength and duration of the anti-microbial effects[159,160]. However, despite evidence showing factors released by neutrophils to recruit inflammatory monocytes, some studies have shown that monocyte recruitment is independent of prior neutrophils migration[161]. Due to their potent bactericidal and inflammatory properties, if the interaction between recruited neutrophils and monocytes is not tightly regulated, it can be detrimental to the host and contributes significantly to the pathogenesis of various inflammatory diseases[159]. During the acute phase of inflammation, macrophage, monocytes and neutrophils play major role in the orchestration of immune response within hours of infection/injury onset.

Macrophages

Macrophages are considered terminally differentiated mononuclear phagocytes, retaining a high degree of phenotypic and functional plasticity adapted to the local tissue environment but still have the ability to change in response to stress. Therefore, there is a substantial degree of heterogeneity among each resident macrophage population in each tissue according to their specific function

required within the organ. For example, in the lung, there are several subsets of macrophages residing at each compartment, such as alveolar macrophages and three subsets of interstitial macrophages[162], whereas in other organs, the major resident macrophages take different names such as liver (Kupffer cells), spleen (splenic macrophages), bone (osteoclasts), skin (Langerhans cells) and brain (microglial). Alongside mast cells, macrophages act as sentinels and a first line of defence against infection, playing important roles in safe-guarding of the local tissues via their ability to phagocytose pathogens and secrete chemokines to recruit other immune cells such as neutrophils and monocytes to further enhance the local inflammatory responses[163]. After the successful clearance of the invading pathogen, macrophages also play an important role in the clearance of cells and cell debris that were infected or damaged at the site of infection. Macrophages are also a member of a heterogeneous group of professional antigen-presenting cells, including dendritic cells and B cells, that could process and present antigens for the recognition by T cells, playing a vital role in the connection between innate and adaptive immune response.

Monocytes

Monocytes are characterised by their functional plasticity and primary roles in orchestrating the development and resolution of inflammation. Monocytes are derived from a bone marrow reservoir of pluripotent haematopoietic stem cells which undergo sequential differentiation through the common myeloid-progenitor, granulocyte-macrophage progenitor, the common macrophage and dendritic cell precursor and finally the committed monocyte progenitor before being released into the blood. In the blood, there are 2 main monocyte subsets in human and mice[164–170]: 1) 'inflammatory' monocytes (human 'classical' subset $CD14^{high}$ $CD16^{-}$ $CCR2^{high}$ $CX3CR1^{low}$; murine equivalent $CD11b^{+}$ $Ly6C^{high}$ $CCR2^{high}$ $CX3CR1^{low}$), 2) patrolling monocytes (human 'non-classical' subset $CD14^{low}$ $CD16^{++}$ $CCR2^{low}$ $CX3CR1^{high}$; murine equivalent $CD11b^{+}$ $Ly6C^{low}$ $CCR2^{low}$ $CX3CR1^{high}$). There is a third subset of monocytes in human that are less defined and are not present in mice, termed the intermediate subset (human $CD14^{int}$ $CD16^{+}$ $CCR2^{low}$ $CX3CR1^{high}$). Upon maturation, monocytes are produced and released continuously from the bone marrow and circulate in the bloodstream, in which each monocyte subset exhibit different lifespans. Classical monocytes circulate in the bloodstream for a day, intermediate monocytes circulate for about 4 days and non-classical monocytes for 7 days[171].

The inflammatory subset of monocytes are recruited to the inflamed tissues during infection/injury and are able to differentiate into dendritic cells or resident macrophages after resolution of inflammation, whereas the patrolling monocytes are perceived as 'resident monocytes' that carries out immunosurveillance, found in both resting and inflamed tissues[164,166,172,173]. However, these classification may be oversimplistic as monocyte subsets are heterogeneous and different sub-phenotypes of monocytes are continually being discovered, both in the bone marrow and in the blood[174,175].

Neutrophils

Neutrophils, the most abundant cell type of granulocytes, are an indispensable member of the innate immune system for the defence against intruding pathogens during infection. Neutrophils are being produced extensively in steady state within the bone marrow in large numbers, around 10^{11} cells per day[176,177]. They are released continuously into the bloodstream in a circadian regulated fashion to patrol the tissues for any infections or danger signals[178,179]. During local inflammation, a series of aggressive responses are initiated, where neutrophils are rapidly deployed from the blood and from the bone marrow reservoir to the site of infection or inflammation for effective containment of pathogens and initiation of the tissue remodelling process. As the major role of neutrophils is to contain infection or inflammation, they are equipped with defensive capabilities such as phagocytosis to ingest microbes, degranulation to release the content of their granules such as elastase, myeloperoxidase (MPO), defensins and matrix metalloproteinases (MMPs) to destroy pathogens and carry out NETosis to produce extracellular traps (NETs) that snare and degrade microbes via similar mechanisms as degranulation[177,180,181]. Due to their large armoury of anti-microbial and bactericidal mediators, enzymes and oxidative capacity, neutrophils have the potential to cause significant tissue damage when activated. To minimise these collateral effects on host tissues, neutrophils normally reside within the blood with a short half-life (4-18 hours)[182] before undergoing pre-programmed apoptotic cell death and clearance by the reticuloendothelial system (RES)[183–185].

1.3.5 Priming & Tolerance

Other than the recognition of PAMPs and DAMPs, the innate immune system is a dynamic and multifaceted system and is far from one-dimensional response to any one particular insult/injury, especially in the context of sepsis/SIRS. It has been found that members of the innate immune system, particularly monocytes and macrophages, exhibit an enhanced responsiveness to a secondary stimulus if previously exposed to low-grade stimulus, a phenomenon termed priming[186,187]. Through priming, the activation and subsequent responses of innate immune cells can be regulated in a way so that a continuum of activation states is achieved, to prepare the host response in case of a secondary infection. Experimentally, *in vivo* exposure to subclinical low-dose of LPS (<100pg/ml) heightened the activation states of monocytes and macrophages and create a more robust expression of pro-inflammatory mediator release in response to a second LPS challenge[188,189], including TNF-α - , IL-12 and IFN[190]. Other than a direct response to PAMPs, the adherence of leukocytes to endothelial cells may also represent another form of interaction-dependent priming, whereby cells become more responsive once in contact with the vascular endothelium. This process plays a key role in neutrophil/monocyte-mediated ALI, where neutrophils and monocytes remain in the pulmonary capillaries in a latent activation state but not migrating across the endothelium, a phenomenon termed margination/sequestration. Leukocytes margination and priming in the lungs will be discussed in more detail in Section 1.4.2.

Conversely to priming response after exposure to low-grade endotoxin, monocytes can tolerate refractorily to a second endotoxin challenge shortly after the first encounter in a high-grade sublethal dose, a phenomenon termed endotoxin tolerance[70]. Experimentally, after an initial exposure to high dose LPS challenge, monocytes exhibit a reduced expression of HLA-DR and TNF-α production in response to a secondary LPS challenge[191,192]. In the context of non-infectious injury, ischaemic pre-conditioning, where transient brief episodes of ischaemia before a subsequent prolonged ischaemia reperfusion injury has also been shown to induce tolerance, reducing the extent of subsequent organ damage[193]. Interestingly, cross-tolerance between infectious and non-infectious injury was also observed, where LPS pre-conditioning protected animals against secondary IRI in the brain via monocyte deactivation and reduced neutrophil infiltration[194]. Overall, both priming and tolerance

phenomenon observed in monocytes were shown to operate via the regulation of the MAPK and NFκB pathways[192,195–197], further highlighting the redundancy of the immune system during infection and inflammation. Interestingly, when monocytes were isolated from septic patients' blood, they showed responses of endotoxin tolerance when stimulated with LPS *ex vivo* via down-regulation of NFκB, causing reduced pro-inflammatory cytokines production[198–200], in line with Cavaillon's compartmentalisation model of sepsis described previously.

1.3.6 Immunity and the nervous system

Tracey and colleagues discussed how the nervous system is involved in the regulation of inflammatory responses in sepsis and inflammation, such that the stimulation of the efferent vagus nerve could suppress inflammation[90,201]. They described the interconnected neurological and immunological feedback systems, detailing how the nervous system could directly influence the capacity of the immune system to produce TNF-α and the host sensitivity and tolerance to LPS. These findings add yet another dimension to the ever multifaceted and complex nature of immune response during infection and injury and have expanded our perception of immunology beyond the blood.

1.3.7 The endothelium in sepsis and SIRS

The vascular endothelium is a truly pervasive tissue, where they cover a surface area of more than 3000m^2 throughout the whole body[202]. Endothelial cells were once considered a metabolically inactive cell lining and were described as merely a simple nucleated membrane. However, it has now been recognised that endothelial cells are highly dynamic and metabolically active in the regulation of vascular motor tone and are key determinants of many active physiological functions such as blood cell trafficking, coagulation, homeostasis, functional permeability barrier, angiogenesis and innate and adaptive immunity. While endothelial cells line all vascular structures, significant structural and functional heterogeneity exists amongst these cells in different organs. Thickness of endothelial cells can vary from less than 0.1μm in capillaries to 1μm in the aorta. Endothelial cells in various sizes, shapes and orientations relative to blood flow have been described in various parts of tissues such as the aorta, inferior vena cava, arterioles, capillaries, postcapillary venules and pulmonary artery and vein[203].

During inflammation in the systemic circulation, neutrophils recruitment occur in post-capillary venules and this process requires their capture, rolling and firm adhesion on activated endothelial cells to facilitate their subsequent transmigration into tissues. Various selectins, adhesion molecules, integrins, cytokines and chemokines have been identified for their participation in this process, characterised mainly in human umbilical vein endothelial cells (HUVECs) *in vitro*, as a great representation of endothelium in systemic blood vessels[204,205]. These early studies led to the evolution of the "multistep paradigm" concept of leukocyte interaction with the systemic endothelium[206,207]. In brief, the multistep cascade of leukocyte interaction with systemic endothelium involved activation of endothelial cells by various inflammatory mediators or haemostatic signalling molecules, such as cytokines, chemokines, eicosanoids, NO and complement, triggering the first step of enhanced tethering of leukocytes to the vascular wall. The leukocytes then tether and roll along the endothelium mediated by selectins (P- and E-selectins) expressed on endothelial cell binds to P-selectin glycoprotein ligand-1 (PSGL-1), on neutrophils, as well as flow or shear forces exerted by the blood flow. In activated leukocytes, integrins such as $\alpha_4\beta_1$ (VLA-4), $\alpha_L\beta_2$ (LFA-1 or CD11a/CD18), $\alpha_m\beta_2$ (Mac-1 or CD11b/CD18) on the surface change their conformation from 'bent' to 'extended' shapes, adopting a high-affinity and avidity conformation for their subsequent binding to their respective ligand receptors[208]. Binding of integrins to adhesion molecules such as intercellular adhesion molecule-1 (ICAM-1) or vascular adhesion molecule-1 (VCAM-1) on endothelium facilitate firm adhesion and subsequent arrest of leukocytes on the vessel wall[209,210]. Eventually, this cascade of events leads to transmigration or diapedesis of leukocytes across the endothelium barrier to extravascular sites by disrupting the adherens and tight junctions of the endothelium.

Despite characterisation of the molecules and mechanisms involved in the multistep cascade of leukocyte interaction with systemic endothelium, each organ contain a highly specialised and heterogenous group of endothelial cells for different vascular functions[211], resulting in their differences in sensitivity and response to inflammation. Therefore, the interactions of leukocytes with endothelium in different organ vasculatures are distinct, with potential important consequences for local inflammation and development of organ injury. For the scope of this study, the mechanism of

pulmonary vascular endothelial inflammation and leukocytes interaction in the lung will be discussed more specifically in detail in section 1.4.

There are many indications that suggest a hyperinflammatory state of endothelial cells during sepsis/SIRS, mainly demonstrated through measurements of biomarkers in human clinical trials and animal models of sepsis. For example, plasma level of endothelial activation/injury markers such as angiopoietin-2, von Willebrand factor (vWF), vascular endothelial growth factor (VEGF), soluble FMS-like tyrosine kinase-1 (sFlt-1), and E-/P-selectin, have been implicated to associate with increased mortality and poor outcome in septic patients[175,212–214]. In caecal ligation and puncture (CLP), the 'gold standard' animal model of sepsis, increased expression of adhesion molecules ICAM-1 and VCAM-1 on endothelial cells were observed in various organs, including lung, kidney, liver and heart[215,216]. ICAM-1 and VCAM-1 are important molecules involved in neutrophil adherence and transmigration, as well as adhesion of monocytes and lymphocytes during inflammation, both of which are highly implicated in the increased permeability of the endothelium and their subsequent dysfunction during disease progression. Serum levels of ICAM-1 and VCAM-1 have been found to associate with multiple organs dysfunction and mortality in septic patients[217], indicating the detrimental effects of endothelial dysfunction during sepsis.

1.4 Inflammatory mechanisms and models of sepsis-induced indirect ALI

The lung is a unique organ consisting of three major compartments: the airways, vasculature and interstitium. The airway interface is made up of mainly alveolar epithelial cells and alveolar macrophages, which is constantly exposed to a large number of airborne pathogens through every breath, whereas the vasculature which is made up of mainly endothelium, smooth muscles and fibroblasts has a vast surface area of 120m^2 and is constantly exposed to the entire cardiac output that passes through the lung with every heartbeat[218]. While maintaining low blood pressure, the pulmonary vasculature interacts with vast variety of vasoactive mediators, circulating cells and potential pathogens. The hallmarks of ALI/ARDS are increased capillary permeability leading to interstitial and alveolar oedema and influx of circulating inflammatory cells from circulation to the lung. Therefore, it is essential to understand the mechanism of vascular inflammation and permeability regulation in the lung for better understanding of the disease pathogenesis.

1.4.1 The pulmonary endothelium

The pulmonary endothelium is a continuous, squamous monolayer of cells that lines the blood vessels, which together with alveolar epithelial cells forms a thin 0.1μm layer called the alveolar-capillary membrane. However, similarly to the systemic vasculature, endothelial cells in the lungs exhibit heterogeneity in size, shape and orientation. Notably, in a study of rat blood vessels where the pulmonary endothelial pavement patterns were compared across pulmonary artery, veins, aorta and vena cava, endothelial cells in the pulmonary artery were found to be smaller in rectangular shape, whereas endothelial cells in pulmonary vein were larger and more rounded[219].

Permeability

In addition to morphological/structural heterogeneity, recent research has shown functional heterogeneity within the lung vascular beds, where calcium handling, regulation of permeability, proliferative potential, as well as physiological and biological responses to diseases, could differ significantly between macro- and micro-vascular endothelial cells of different vessels within the lung. Unlike other organs, the lung needs to maintain a relatively dry interstitial and alveolar gas space to facilitate efficient gas exchange. Similarly to the relatively impermeable blood-brain barrier, the

regulation of vascular permeability by the pulmonary endothelium is crucial in preventing detrimental oedema and to maintain normal lung function[220]. However, endothelial permeability varies between different vessels within the lung. The pulmonary microvascular endothelium is much more impermeable to fluid and protein flux than pulmonary arteriole or venular endothelium[221,222], whereas the pulmonary venules has greater permeability for diffusion of macromolecules compare to pulmonary arterioles[223–226].

In the pulmonary endothelium, increase in vascular permeability is characterised by both disruption of paracellular junction between endothelial cells and the enhancement of transcellular protein transport. The paracellular permeability is regulated by inter-endothelial junctional complexes consisting of tight junctions (occludins, claudins and zonula occludins), adherens junctions (VE-cadherin and the associated catenins) and focal adhesions (direct interaction of junctional protein complexes with cytoskeleton). Overall, the destabilisation of these junctional complexes promotes leukocyte transmigration and formation of oedema via intercellular gaps[227,228]. Transcellular permeability on the other hand, is mainly dependent upon the transport of plasma proteins (e.g. albumin), mediated mainly by caveolae. Although the mechanism(s) by which endothelial cell transcytoses albumin is not completely understood, we know that upon binding of albumin to gp60, caveolin-1 interaction with the gp60 clusters induces Src tyrosine kinase signalling, which in turn phosphorylates dynamin-2 and caveolin-1, initiating endocytosis, transcytosis and exocytosis of the protein albumin to the other side of the endothelial barrier[229].

Although *in vitro* lung endothelial cultures have been used widely to study permeability change, some stimulatory agents found to increase permeability change *in vitro* does not necessarily represent the response of the lungs *in situ*, suggesting phenotypic differences between endothelial cells in culture and *in situ*[230]. Specifically, *in vitro* pulmonary endothelial cells exhibit strong permeability change in response to thrombin, LPS and TNF-α in a Rho-kinase dependent manner (and subsequent actin stress fibre formation)[231–235], but none of these agents increases vascular permeability by direct interaction with endothelial cells in isolated perfused lungs (IPL)[236–239]. Notably, LPS and TNF-α were able to induce oedema when leukocytes are present in IPL, suggesting that these agents acted

primarily on immune cells rather than directly on endothelial cells[236,240–242]. Conversely, PAF and bradykinin trigger significant oedema formation in the IPL but not *in vitro*[243–246].

Protein expression and mediator release by pulmonary endothelial cells

The constitutive function of pulmonary endothelial cells includes regulation of coagulation and thrombolysis, promotion of blood flow, as well as the synthesis and metabolism of vasoactive compounds such as angiotensin II, prostacyclin, thromboxane A_2, nitric oxide (NO), endothelin-1, and angiotensin converting enzyme (ACE)[247]. Upon activation by exposure to inflammatory stimuli (PAMPs or DAMPs) or in contact with activated leukocytes, the pulmonary endothelium expresses leukocyte adhesion molecules and cytokines, become procoagulant and induce changes in vascular permeability and tone via alteration in their synthesis of vasoactive compounds. Endothelial-derived vasoactive compounds such as NO and endothelin-1 are implicated in calcium sensitisation in smooth muscle of the lungs in response to vasoconstriction during hypoxia[248]. Endothelin-1 level was also found to be potential predictor of lung function during *ex vivo* lung perfusion and after lung transplantation[249], and is correlated with pulmonary hypertension[250].

In comparison to other organs, the lung expresses the highest levels of VEGF, ICAM-1, VCAM-1 and P-selectin[251–253]. Although VEGF is mainly produced by alveolar type II epithelial cells, its diffusion from the neighbouring cells to bind to VEGF receptors on pulmonary vascular endothelium, and in orchestration with angiopoietin-1 and angiopoietin-2 via Tie-2 receptor signalling, plays a critical role in the regulation of pulmonary vascular permeability[253,254]. Increased level of VEGF was consistently found in various *ex vivo* models of lung injury including cystic fibrosis, lung transplant and cardiopulmonary bypass[255–257]. Importantly, VEGF was found to be higher in the plasma of ARDS non-surviving patients compared to control subjects[258]. In parallel, increased plasma levels of angiopoietin-2 were found to exacerbate pulmonary inflammation *in vivo*[259] and were correlated with pulmonary oedema and mortality in patients with ARDS[121,260]. Increased expression of ICAM-1, VCAM-1 and P-/E-selectin on the surface of pulmonary endothelial cells was also known to promote vascular leakiness via increased neutrophil adherence *in vivo* and *in vitro*[261,262], which may potentially contribute to endothelial inflammation and injury observed in ALI/ARDS.

1.4.2 Leukocytes margination and sequestration in the pulmonary circulation

In 1960s, Athens et al. demonstrated that almost 50% of the infused granulocytes were distributed to 'circulating' pool within the bloodstream, whereas the other 50% were marginated away from the luminal flow to the venule walls, forming the 'marginal' pool[263–265]. In the same series of studies, the marginal (or marginated) pool were shown to be able to mobilise back into the circulating pool by infusion of adrenaline, whereas endotoxin infusion increased the size of both pools by mobilising new cells from bone marrow. Apart from large venules, granulocytes margination can also happen in the narrow capillaries of various organs including spleen, liver, kidney and the lung. In the pulmonary microcirculation, leukocytes such as neutrophils with diameters of 12-14μm must undergo deformation to squeeze through the narrow pulmonary capillaries, which has an average diameter of 6μm[266]. Along with the low blood flow velocity in the pulmonary circulation, this increased transit time of leukocytes through the pulmonary capillaries thus leads to an overall higher concentration of leukocytes in the lung microvasculature compared to large vessels in the macrocirculation. Doerschuk described the term 'margination' to define the increased concentration of leukocytes in normal, uninflamed lungs, and 'sequestration' to refer to leukocytes trapped in the lung capillaries during inflammation via enhanced adherence to the endothelium and are prepared to 'transmigrate' across the endothelial barrier[266]. As described above, various adhesion molecules, integrins and selectins are required for the sequestration of leukocytes in the post-capillary venules in extrapulmonary macrocirculation. In the lungs, it has been shown that the principal site of leukocyte migration is the capillary bed rather than post-capillary venules, and the sequestration of leukocytes in the pulmonary capillaries are independent of selectins or adhesion molecules[267]. However, selectin-mediated rolling was demonstrated in pulmonary arterioles and venules[268,269], and for neutrophils to remain retained/sequestered within the pulmonary capillaries for longer period, binding of L-selectin to PSGL-1, and CD11/CD18 ($\alpha_M\beta_2$ integrin) to ICAM-1 on endothelial cells in pulmonary capillaries remains a critical process[270,271].

In addition to neutrophils, large proportions of monocytes also marginate in the lungs[272]. Although monocytes and neutrophils are of similar diameter, monocytes were found to be less deformable than

neutrophils, which may contribute to a more prolonged transit time across the pulmonary capillaries as compared to neutrophils[273]. During endotoxaemia, LPS was found to increase monocyte stiffness (decreased deformability) via F-actin reorganisation, whereas the expression of CD18 (β_2 integrin) on monocytes was found to be essential in their prolonged retention in the lungs by enhancing their adhesion to the endothelium[274], similarly to neutrophils. Under steady state in mice, low levels of both $Ly6C^{high}$ and $Ly6C^{low}$ monocytes were found to patrol within large vessels of the lung and between capillaries[173], whereas during endotoxaemia, significant proportion of $Ly6C^{high}$ monocytes mobilised from the bone marrow reservoir marginate to the lungs in a functional primed state by exhibiting enhanced phagocytic capacity and potentially predisposes the lung towards injury[187,275,276].

1.4.3 Neutrophil-mediated lung injury

In the lungs, marginated neutrophils may take on primary role in host defense during blood-borne infection, in contrast to the spleen and liver where intravascular resident macrophages are dominant in immobilisation of circulating pathogens[277,278]. Neutrophil-associated organ injury is a well characterised phenomenon in ALI/ARDS, especially during direct lung insults[279]. During direct ALI/ARDS, cytokines such as TNF-α and IL-1β released by activated alveolar macrophages activate the lung endothelium via upregulation of selectins and adhesion molecules[280], and neutrophils are recruited to the lung by chemokines such as CXCL1/CXCL8 and CXCL2[281]. After firm adherence to the endothelium by binding to adhesion molecules via selectin and integrin expression as described above, neutrophils can transmigrate across the endothelial barrier and epithelial barrier into the alveolar space, where they release various cytokines, chemokines, proteolytic enzymes, peptides and cytotoxic mediators such as azurocidin, defensins, proteinase 3, MMPs, MPO, ROS and RNS[279]. Neutrophil-mediated lung injury is often discussed as a two-step process, where tissue damage induced by neutrophil degranulation and respiratory burst that requires an initial ‘priming’ step, is followed by a second ‘activation’ step[282,283]. Recently, it has been considered that the primed neutrophils sequestered in the pulmonary vasculature can de-prime and be mobilised back into the circulation in the absence of a second insult, but when there is a second lung-directed insult, transmigration of the primed neutrophils occurs, leading to their full activation and eliciting tissue damage[284]. Overall, the activation and transmigration of neutrophils into the alveolar space causes

increased permeability in the lung due to the disturbed endothelial and epithelial barriers in the alveolar space, leading to formation of lung oedema and accumulation of protein-rich oedema fluid in the alveolar space. The release of cytotoxic and immune cell-activating agents in the alveolar space by neutrophils causes further alveolar damage via inactivation of surfactant, formation of hyaline membranes and apoptosis and necroptosis of epithelial cells. Although recruitment of neutrophils into the alveolar space is a hallmark of direct ALI, several indirect models of ALI have also shown neutrophil-dependent injuries[285], where neutrophil margination and sequestration in the pulmonary capillaries is followed by microvascular congestion and oedema formation, mainly in the interstitial space[34].

1.4.4 Monocyte-mediated lung injury

It has been demonstrated that circulating monocytes are also important in the pathogenesis of sepsis-induced ALI, as septic lung injury can occur even in neutropenic patients[286–288]. However, their role in the pathogenesis of ALI/ARDS has been large overlooked. In livestock animal such as pigs and sheep, the resident pulmonary intravascular macrophages (PIMs) were thought to be responsible for their unique susceptibility to experimental ALI[289,290]. In species that lacks PIMs such as human and mice, monocytes are rapidly mobilised from bone marrow into the circulation during inflammation, and rapidly marginate to microcirculation of various organs, where they contribute to local inflammation and innate immune response[187,266,291]. Therefore, it has been proposed that the lung-marginated monocytes may resemble characteristics of PIMs during inflammation and contribute to the development of lung injury and inflammation[292,293]. Various studies have shown that marginated intravascular monocytes plays a key role in the pathogenesis of ALI, where their depletion in the lung attenuated pulmonary vascular inflammation and oedema both *in vivo* and *ex vivo*[294–299]. Several studies carried out in our group has shown that intravascular monocytes were able to exert pro-inflammatory and pro-injurious effects locally within the pulmonary vasculature, suggesting their role in the development of ALI[187,291,294,297]. The monocyte-derived effectors that induce tissue damage or injury are unclear, but role for TNF-α during indirect ALI[291] and VEGF during direct ventilator-induced ALI[300,301], both secreted by Ly6C^{high} monocytes, were shown to play a crucial role in the pathogenesis of ALI.

1.4.5 Animal models of ALI

There is a wide array of *in vivo* animal models for both direct and indirect ALI that reproduces the physiological and pathological characteristics of human ALI to varying degrees. These features include the acute onset, diffuse bilateral alveolar injury, severe hypoxemia, decreased lung compliance, increase endothelial-epithelial permeability, increased lung cytokines and neutrophilic alveolar infiltrates[285]. It is now recognised that no single animal model for ALI is ideal, as none of them can completely reproduce all features of human ALI/ARDS. Instead, the choice of model will depend on the pathophysiological mechanism to be addressed, which should be tailored to the purpose of individual hypothesis. In the official American Thoracic Society workshop report, animal models were suggested to include at least three of the four main features of clinical ALI: histological evidence of tissue injury; alteration of the alveolar capillary barrier; presence of an inflammatory response; and evidence of physiological dysfunction[302]. In aid of these guidelines, Aeffner et al. has also provided methodologic guidance on how to approach the measurements of these features[303]. However, as different animal models have shown significant differences between direct and indirect injury in all four of these pathophysiologic features, a variety of different animal models are used across different research groups. For example, Menezes et al. compared animal models of direct and indirect ALI and showed that intratracheal LPS model induced more pronounced injury to the alveolar epithelium and apoptotic neutrophils, whereas intraperitoneal LPS model presented interstitial oedema[304]. Moreover, Bhargava et al. shown that intratracheal IL-6 exerted anti-inflammatory effects in animal model of direct ALI (intratrachael endotoxin), but not in indirect model of ALI (intraperitoneal endotoxin), highlighting the fundamental differences in the pathogenesis and response to treatment between these two forms of ALI[305]. Some of the most commonly used experimental models of direct and indirect ALI is tabulated as below (Table 1.3), adapted from Shaver[29] and Matute-Bello[285].

Direct lung injury	Indirect lung injury
Intratracheal LPS/bacteria	Intravenous LPS/bacteria
Acid aspiration	Peritonitis/Intraperitoneal LPS
Surfactant depletion (saline lavage)	Cecal ligation and puncture (CLP)
Mechanical ventilation	Haemorrhage
Infectious organisms	Non-pulmonary ischaemia reperfusion
Bleomycin	Intravenous oleic acid injection
Hyperoxia	Femur fracture with hemorrhage
	Ischaemic renal injury

Table 1.3 Experimental animal models of direct and indirect lung injury.

Common models used to simulate direct (left column) and indirect (right column) lung injury in small experimental animals. Intra-alveolar injury induced by pulmonary challenges such as intratracheal LPS, acid aspiration, surfactant depletion and injurious mechanical ventilation are commonly used to induce direct lung injury, whereas extra-pulmonary injury induced by intravenous or intraperitoneal LPS, CLP and haemorrhage are commonly used to induce indirect lung injury. (Adapted from Shaver[29] and Matute-Bello[285])

In addition to these standalone single insult models, "two-hit" injury models, which combines different insults have been developed in an attempt to better capture the multifactorial nature of ALI/ARDS. For example, intratracheal instillation of LPS or hydrochloric acid followed by ventilator-induced lung injury (VILI) was used to better simulate the severity of direct ALI[306], whereas haemorrhage followed by caecal ligation and puncture (CLP) was used to induce features of indirect ALI. In some cases, direct and indirect lung insults are used in combination, such as CLP followed by VILI[307]. Overall, research efforts have been placed largely on reproducing clinical features of ALI *in vivo*. Despite their use as pre-clinical models for potential therapeutic targets and treatments, overwhelming inflammatory insults to recreate respiratory failure in animal models does not necessarily aid our understanding of the basic inflammatory mechanism in ALI pathogenesis. In order to gain a deeper and more precise understanding of the cellular and molecular components of ALI pathogenesis, it is preferable to utilise models designed to resolve specific research question.

Animal models of sepsis/SIRS-induced indirect ALI

Amongst the animal models used to study indirect ALI, the general biological aims coincide with the modelling of sepsis or non-infectious SIRS, which are to recreate an overwhelming inflammatory

response in the systemic circulation. For example, administration of LPS or bacteria (either intravenously or intraperitoneally) and CLP, are aimed towards the recognition of bacterial products, or PAMPs, by the innate immune system. On the other hand, other models such as haemmorrhage/bone fracture, ischaemia reperfusion injury (IRI) and oleic acid injection are aimed towards recreating the production of DAMPs by dying or damaged cells through processes/procedures that induce excessive cellular damage. Although *in vivo* polymicrobial sepsis models such as CLP may be considered more appropriate when studying the overall clinical picture of sepsis-induced ALI, it is now appreciated that CLP produces only a very mild degree of ALI before mice die due to sepsis itself. Overall, as indirect ALI often result from insults carried via the bloodstream to the pulmonary circulation, the study of mediators released into the circulation during sepsis/SIRS is important.

Ex vivo isolated perfused lung models

In addition to *in vivo* animal models, *ex vivo* isolated perfused lungs (IPL) of laboratory animals has been widely used in the study of lung function and inflammation[308–310]. IPL has several advantages for the study ALI as it provides intact standalone organ preparation without the systemic influence of other organ systems and the ability to modify several parameters with precision such as ventilation protocols and gas content, perfusate constituents and pulmonary vascular flow. The IPL system has commonly been used in the investigation of direct lung injuries such as pneumonia[311], ventilator-induced lung injury (VILI)[295,312], lung ischaemia-reperfusion injury (IRI)[294,313], with the advantages of measuring cytokines and chemokines released into the pulmonary perfusate[294,310,311]. In the context of pulmonary vascular injury, IPL serves as a useful model for the measurement of vascular reactivity and permeability in response to various biological or pharmacological mediators, including PAF, thrombin, TNF-α, LPS and sphingosine-1-phospohate (S1P)[236–239,314–316].

Despite its advantages over *in vivo* models, IPLs are underused for the study of indirect ALI, potentially owing to the difficulty in maintaining IPL for prolonged period of time for measurement of transcriptional responses, or its limitation in recreating significant oedema with standalone indirect insults as described above (1.4.1). For example, the infusion of LPS and TNF-α, two components well

known to be involved in the pathophysiology of sepsis, into the perfusion circuit of IPL failed to elicit oedema formation in the lung in the absence of leukocytes or blood components[230]. Interestingly, IPL obtained from LPS-treated, but not untreated rats, exhibited significant increase in pulmonary perfusion pressure in presence of blood components in IPL perfusate, suggesting *in vivo* responses to LPS are critical[317]. These findings are consistent with the essential role for 'primed' lung-marginated leukocytes in development of indirect ALI and suggest the suitability of IPL for this investigation. Indeed, several studies have reported the retention of marginated leukocytes following relatively long perfusion periods, specifically in the lung transplant setting, suggesting they are retained in an active state[294,318–320]. Additionally, IPL serves as a useful tool to investigate the interaction of pulmonary vascular cells with circulating mediators produced during sepsis in isolation, allowing precise assessment of the mechanism involved in lung injury during sepsis-induced indirect ALI.

1.5 Extracellular vesicles (EVs)

Extracellular vesicles (EVs) is the collective name of a heterogeneous family of small membranous vesicles originating from the endosome or plasma membrane are released by virtually all cell types. Their biological function was unclear for some time as they were first described in 1976 by Peter Wolf as platelet dust. Thus, EVs were initially regarded as debris for disposal of cellular waste without any biological significance[321]. However, with improved research tools over the years for the isolation, measurement and imaging of EVs, much has been revealed regarding their biological function in intercellular communication and their pathological significance in health and diseases. Currently, there are 3 main sub-groups of EVs characterised on the basis of size, content and mechanism of formation: 1) exosomes; 2) microvesicles (MVs) or microparticles (MPs) or sometimes referred to as ectosomes or shedding vesicles; and 3) apoptotic bodies.

1.5.1 Biogenesis and markers of EVs

Exosomes are the smallest EVs, sized between 30-100nm, whereas MVs are generally between 100nm-1μm and apoptotic bodies are 1-5μm in size[322]. However, these size ranges are not an absolute indicator of EV subgroups, as considerable overlap exist between each subgroup[323]. Therefore, basic differences in biogenesis and surface markers serve as crucial additional information for identification of EVs. Exosomes are thought to be released by living cells through an active endosomal pathway both under resting and activated conditions. They are initially formed by inward bulging and pinching off from the plasma membrane to form early endosomes. The inward budding of endosomes then forms intraluminal vesicles (ILVs) in internal complexes known as multi-vesicular bodies (MVBs) evolved from the late endosome. These MVBs can then either undergo fusion with lysosomes for the degradation or recycling of the ILVs, or fuse with the plasma membrane to release the ILVs into the extracellular environment as exosomes.

MVs on the other hand, are released following cell activation or apoptosis via direct budding from the plasma membrane, carrying surface markers from their precursor cells. However, there are differences between the parent cell and daughter MV surface molecules due to phospholipid membrane rearrangement associated with the blebbing process and MV formation. Due to differences

in biogenesis, exosomes are thought to carry distinct surface markers from those seen on the surface of MVs. Overall, the outward budding of MVs results in their 'right-side-out' membrane orientation, which guarantees the surface expression of their parental cell markers[324]. However, the initial inward budding of plasma membrane in the formation of exosomes may lead to the transfer of plasma membrane markers of the parental cells to the inner membrane of endosomes during this process, which could then flip inside-out through endosomal budding[325]. This process could lead to the occasional surface expression of parental cell markers in some exosomes[326,327].

Components of the endosomal sorting complex responsible for transport (ESCRT) complex and tetraspanins such as CD9, CD63, CD81 were previously considered to be specific markers of exosomes, but it is now recognised that MVs and apoptotic bodies can also carry them[328]. A recent position statement by the International Society of Extracellular Vesicles (ISEV) has clarified the common expression of ESCRT components in both exosomes and MVs, including TSG101, VPS4 and Alix, suggesting the use of "small EVs" in general instead of specifically naming certain preparation as exosomes or MVs[329]. This highlights the challenge in the field of EV research, where there is significant overlap in size and markers between exosomes and MVs, making them difficult to be distinguished from each other. So far, a consensus has yet to be established on specific markers to differentiate exosomes from MVs[329]. For simplicity, here we chose to refer to EVs that express their parental cell marker as MVs, rather than exosomes in this study, based on their 'right-side-out' membrane orientation characteristics during formation.

Phosphatidylserine (PS) expression in MVs

Under resting conditions, phospholipids are asymmetrically distributed in the plasma membrane, where positively charged phosphatidylcholine (PC) and sphingomyelin are aligned on the outer leaflet, whereas the negatively charged phosphatidylserine (PS) and the neutrally charged phosphatidylethanolamine are aligned on the inner leaflet. Such asymmetric distribution is tightly regulated by aminophospholipid translocases including "flippases" which govern the normal resting phospholipid distribution, "floppases" which are responsible for the translocation of PS from the inner to outer leaflet of plasma membrane, and "scramblases" which favours randomisation of

phospholipids distribution in a bi-directional manner[330,331]. When cells are activated, increased intracellular calcium causes the activation of calpain, cytoskeletal contraction and dysregulation of aminophospholipid translocases, resulting in the externalisation of PS to the outer leaflet, followed by membrane budding and the shedding of MVs into the extracellular space[324,332–334]. The externalisation of PS has been widely described as an essential process in the biogenesis of MVs and their identification has served as a general marker of MVs for decades.

Annexin V, a calcium-dependent phospholipid-binding protein that has a high affinity for the anionic phospholipid PS, is often used as an identification marker for MVs. Annexin V positive MVs were traditionally referred as procoagulant MVs[335–337] after Thiagarajan et al. first demonstrated the expression of anionic phospholipids on platelets and platelet-derived MVs, and their involvement in binding to factor Va[338], demonstrating their procoagulant properties. However, we have progressed to understand that MVs can be released by a variety of other cell types and the procoagulant properties of non-platelet-derived MVs remains unclear[339]. In contrast, platelet MVs were shown to also carry anti-coagulant properties, implicating that their procoagulant role is not definite[340]. It has been suggested that the MVs produced from cell activation and apoptosis may exhibit distinctive phenotypes in size, composition and marker, including PS expression[341,342]. Two distinct populations of MVs with or without surface PS expression have been widely described in various *in vitro* and *in vivo* models, though this may be dependent on the conditions/stimulation upon cell activation[343–348]. Additionally, the exposure of PS by necroptotic MVs[349–351] and exosomes[352] have recently been described, suggesting the heterogeneity and the lack of a specific marker for the identification of MVs. Therefore, the use of annexin V as a generic marker for MVs remains controversial to date. Some believe it helps to distinguish cell debris and precipitates that lack PS expression from the MVs[353], whereas some define MVs only by size and surface antigen staining without testing for Annexin V positivity[344,354–356] and some categorise MVs into annexin V positive and negative populations[345,357].

Other than Annexin V staining for PS, alternative generic MV detection methods were recently investigated, including calcein, CFSE, lactadherin (a PS-binding protein) and Di-8-ANEPPS, but none were found to provide absolute sensitivity and exclusivity in the detection of EVs by flow cytometry[358].

Other alternative labelling of EVs using lipophilic dyes such as PKH67, DiD, DiL, or bio-maleimide such as BODIPY were also commonly used, but none of these provide any specificity to vesicular membrane as they readily stain any lipid structure (in the case of lipophilic dyes) and cysteine residues and thiol groups on cell membranes (in the case of bio-maleimide)[359,360].

1.5.2 Isolation and detection of EVs

Several isolation techniques have been developed to purify EVs from non-vesicular components such as cell debris, protein aggregates, as well as to separate EV subgroups from each other. Separation techniques are based on EV characteristics such as by size, density surface proteins, sugar, lipid composition or charge[329], and these techniques include filtration, differential centrifugation, density gradient, precipitation and immunoaffinity[361]. As each technique carries its own limitation, there is no single isolation technique available to date that could isolate EVs with high yield and purity, but a combination of several techniques is often required to improve the yield and purity of EV preparation.

Several technologies have been utilised for detection and quantification of EVs, based on individual particle number and size, or quantification of crude EV content such as protein or lipid. Quantification based on particle number, employs technologies such as flow cytometry, nanoparticle tracking analysis, dynamic light scattering and resistive pulse sensing. Flow cytometry is the most preferable technique used to detect and quantify EVs, as it allows precise enumeration and characterisation of EVs based on surface marker expression and size. However, as smaller EVs fall below the size threshold of standard flow cytometer, high resolution flow cytometry is the most preferable[362], though this newer technology is costly and is often not readily available in every laboratory setting. There is thus an ongoing effort in the optimisation and standardisation of standard flow cytometry platforms to facilitate EVs research[363]. Morphology and purity of EVs can also be visualised by electron microscopy, atomic force microscopy, fluorescence and confocal microscopy.

1.5.3 MV production

Disease-state related EVs (biomarkers and propagator) has largely been attributed to MVs with a more defined cell source/origin, rather than exosomes, thus MV production during health and disease

is of major interest. MVs are produced by most, if not all, cell types including vascular cells (endothelial and vascular smooth muscle cells), blood components (leukocytes, erythrocytes, platelets), cardiomyocytes, podocytes and cancer cells[364]. Depending on the cell source location, MVs produced can be release into all bodily fluids including the circulating blood, lymph, cerebrospinal fluid, amniotic fluid, urine, saliva and others. Similar to the production of soluble mediators, the production of MVs from immune cells can be activated upon encounter of various stimuli including PAMPs, DAMPs, cytokines, chemokines, lipid mediators, complement, ROS, hormones, fatty acids, as well as increased intracellular calcium[365]. Several stimuli have been identified in the production of MVs, largely from *in vitro* studies. Physiological stimuli in MV generation/production are typical to the cell type and function[366–369], e.g. platelets release MVs in response coagulation factors (thrombin, ADP, collagen), neutrophils in response to inflammatory cytokines and chemoattractants (TNF-α, fMLP, CXCL8) and monocytes in response to ATP and LPS. Chemical agonists are also used in *in vitro* studies, primarily the calcium ionophore A23187, but also phorbol myristate acetate (PMA), a protein kinase C activator.

1.5.4 MVs in intercellular communication

Intercellular communication is known to occur via two main mechanisms: 1) soluble mediators released from cells and binding to the same cell (autocrine), or to other cells locally (paracrine) or remotely via fluids (endocrine), and 2) cell-to cell-contact (juxtracrine). It is now increasingly clear that MVs provide a third pathway of intercellular communication by carrying bioactive mediators such as membrane receptors and adhesion molecules, cytokines, chemokines, enzymes, eicosanoids and RNAs. In contrast to soluble mediator, the membrane-bound and lipid-encapsulated forms of these mediators carried by MVs offer additional advantage of molecular stability, allowing them to signal over long distances in an endocrine fashion. The content of MVs are derived from the parental cell, therefore each MV subtype carries content typical to their respective precursor cells, with the potential for modification of content depending on factors such as cell-activating stimulus[370].

In sepsis/SIRS, MVs produced by vascular cells such as monocyte, neutrophils, platelet, endothelial cells and erythrocytes found in the circulating blood, and the bioactive mediators of which are of major

interest as biomarkers and potential propagators of systemic inflammation[371]. Multiple and distinct molecules have been attributed to vascular cell-derived MVs, reviewed in brief here. Monocyte MVs can initiate extrinsic coagulation cascade via tissue factor (TF)[372] and were found to carry pro-inflammatory cytokines TNF-α and IL-1β[373–376]. Neutrophil MVs can carry cytotoxic mediators such as ROS, leukotriene, and various neutrophil enzymes including MPO, elastase, proteinase 3 and matrix metalloproteinases (MMPs)[377–381]. Platelet MVs are mainly involved in the regulation of coagulation via expression of procoagulant phospholipid PS, factor X, and prothrombin[382–386]. Endothelial MVs mainly carry markers of endothelial activation such as ICAM-1, VCAM-1, E-selectin, vWF, bioactive enzymes such as MMP-2, MMP-9 and endothelial protein C receptor known involved in coagulation[387–390]. Erythrocyte MVs were mainly shown to be released during *ex vivo* storage of erythrocytes and carry procoagulant activity via expression of PS[391,392]. However, these findings are largely derived from *in vitro* studies, and the molecular content of MVs derived from each cell type may differ significantly depending on the nature of the stimulation upon cell activation, subsequently affecting their interaction with target cells and its associated outcome.

1.5.5 Biodistribution, clearance and uptake of MVs

In a post-ISEV workshop survey in 2018, experts have agreed strongly on the statement that, as I quote, “most cell types, sooner or later, internalise at least a proportion of stained EVs, seemingly regardless of the cell of origin”, with many agreed on the common mechanism of MVs interaction with cells via endosomal uptake and acidification[393]. In brief, MV uptake by target recipient cells were found to involve a variety of endocytic pathways including phagocytosis, micropinocytosis, caveolin-mediated uptake or clathrin-dependent or independent endocytosis, as reviewed by Mulcahy et al[394]. MVs can also interact with target cells via membrane fusion and induce surface receptor activation by contact[371]. In addition, factors of the microenvironmental conditions such as pH appear to modulate MV interactions with target cells, such that the acidic environment at the site of ischaemic reperfusion injury could facilitate fusion of MVs with recipient cells[395]. Overall, the way in which MVs interact with target cell may significantly affect the associated outcome, as the delivery of different bioactive cargoes to their recipient cell depends largely on whether they are endocytosed by, fused with, or presented/lysed on the outside of the target cell[396].

The *in vivo* activity of MVs is determined by their target cell/tissue interactions. *In vivo* trafficking studies involving injection of *in vitro*-labelled MVs, indicated that the liver and spleen are major organs for MV uptake under resting conditions[397–399]. Organ-resident macrophages appeared to be primarily responsible for uptake of MV from the blood and were shown to be very efficient, with MVs shown to be removed rapidly from the circulation within 10min of injection[397,400]. However, the majority of *in vivo* trafficking studies with injected EVs in small rodents are focused on the targeted therapeutics/drug delivery[401,402], utilising either MSCs-derived, or drug-loaded engineered exosomes, in normal recipients or in cancer models for therapeutic purposes[403–411]. Therefore, little is known of the fate of endogenously produced, circulating MVs during systemic inflammation or organ injury. Regarding EV uptake in the lungs, it was found that the lung is not a major site of EV uptake under normal conditions in mice[397], though there is some evidence that it is a significant target for instance in lung tumour exosome homing or uptake of platelet MVs by endothelial cells[398]. However, in sheep and pigs, the lung-resident PIMs were shown to play a major role in clearance of systemically-injected tracer particles[412]. In animals without PIMs, lung-marginated monocytes were also found to exhibit enhanced phagocytic capacity[275]. Therefore, the contribution of these lung-marginated monocytes to the development of lung injury could potentially be attributed to their enhanced phagocytic uptake or interaction with disease-propagating MVs from the circulation during inflammation.

As described above, PS is a ubiquitous membrane phospholipid, which when newly exposed on the cell surface plays a crucial role in initiating the engulfment of PS-expressing apoptotic cells by phagocytes such as monocytes and macrophages[413]. Concurrently, PS recognition was shown to also play a major role in MV uptake by mononuclear phagocytes via various PS receptors including Del-1, MFG-E8/lactadherin, integrin, TIM4, Gas6[398,414–419]. However, more specific MV-cell recognition mechanism involving adhesion molecules could also play a critical role, particularly where PS expression is low on MVs, or during inflammation when adhesion molecule expression is upregulated on vascular cells, including myeloid leukocytes and the vascular endothelium.

1.5.6 MVs in sepsis/SIRS and the development of ALI/ARDS

Despite substantive advances in our understanding of MVs in the last decade, there are still a large number of major unanswered questions in the field of MVs research[396]. In particular, definite proofs of how MVs alter cell physiology using *in vivo* systems are scarce, and hence it is unclear whether disease-associated MVs are merely a cell activation by-product and convenient biomarker, or they play an active role in disease pathogenesis, or both[365]. Several clinical studies have measured the level of plasma MVs, often in an effort to characterise their potential as biomarker in sepsis, reviewed by Raeven et al.[371]. Elevated levels of platelet-, granulocyte-, and endothelial-derived MVs were first reported in patients with meningococcal sepsis[420]. Since then, amongst the relatively large number of clinical studies measuring level of circulating MVs in septic patients, MVs derived from platelets[421–424], leukocytes[380,425–428] and endothelial cells[429–431], were most commonly detected. In another study where a comprehensive panel of MV cell sources were investigated in septic patients, increased level of circulating MVs across all MV subtypes was observed, including platelet- (CD41a+), endothelial- (CD31+ CD41a-), erythrocyte- (CD235a+), leukocyte- (CD45+), neutrophil- (CD66b+), monocyte- (CD14+), T cell- (CD3+) and B cell-derived (CD19+)[432].

However, the heterogeneous nature of septic patients renders inconsistency in the findings of MVs and its association with clinical outcomes. Of the vascular MV subtypes evaluated, endothelial-derived MVs appear to be consistent in showing a relationship with vascular dysfunction in sepsis. Indeed, it was demonstrated recently that the increased level of endothelial-derived, ACE-positive MVs serve as an predictor of ARDS development in septic patients[431]. Our group has recently demonstrated that neutrophil-MVs are markedly elevated in the plasma of both sepsis and burns patients, and the acute levels were highly correlated with clinical severity/mortality in patients with severe burns injury[427]. Others have also reported that neutrophil-derived MVs are associated with mortality in critically-ill patients admitted to ICU[377]. In contrast, among studies where MVs were found to be elevated in clinical studies on sepsis or ARDS patients, an inverse correlation were consistently found between circulating MV levels with organ dysfunction, disease severity or mortality[433–437].

Despite recognised role of MV in transcellular exchange of messages and their increased level were observed in septic patients, functional data derived from patient plasma MVs are scarce, most of which focussed solely on their pro-coagulation activity. MVs from patients with meningococcal sepsis were shown to have procoagulant activity via thrombin generation *in vivo* and *in vitro*[420,421], whereas in a human endotoxaemia model, TF+ monocyte-derived MVs were also shown to carry procoagulant activity[438]. In another study, MVs (mainly platelet-derived) from septic patients were shown to induce apoptosis on vascular endothelial cells *in vitro* via NADPH oxidase activity[439]. In animal studies, when MVs (mainly leukocyte-derived) obtained from septic rats that underwent CLP were infused into naïve recipient rats, it induced systemic vasodilation via increased iNOS expression and NO overproduction[440]. Conversely, MVs from patients with septic shock, mainly platelet- and endothelial-derived, exerted protective effects in mice by enhancing vascular reactivity in aorta of LPS-treated mice via thromboxane A_2, but not NO overproduction[429]. In another study, intratracheal and intravenous administration of MVs isolated from blood of intratracheal LPS-treated rats (mainly leukocyte- and endothelial-derived) were shown to induce lung injury in naïve recipient rats, where neutrophils infiltration was observed via lung histology[441]. Although systemic administration of *in vitro*-generated MVs from erythrocytes[391,442] and human endothelial cells[443,444] have also been shown to produce some features of indirect ALI in mice *in vivo*, it remains unclear whether *in vitro* generated MVs are representative of the *in vivo* endogenously produced MVs, as MV phenotype (content, mode of uptake and signalling outcome) may differ significantly according to the nature of the stimulation in which they were produced in, as described above.

1.6 Hypothesis

Our laboratory has recently begun investigating the *in vivo* trafficking of circulating MVs, addressing the effects of systemic inflammation on MV uptake within the pulmonary vasculature. We demonstrated that under resting conditions, MVs were predominantly cleared by liver Kupffer cells, and to lesser degree by liver endothelial cells. During LPS-induced subclinical endotoxaemia, Ly6C^{high} monocytes show a several-fold increase in MV uptake, which together with their increased margination in pulmonary vasculature equated to a substantially increased clearance by the lungs. These results suggested the uptake of MVs by the pulmonary-marginated Ly6C^{high} monocyte during subclinical endotoxaemia could play a critical role in sepsis-related pulmonary vascular inflammation and indirect ALI.

Therefore, I hypothesised that MV uptake in the pulmonary vasculature would play a crucial role in the propagation of systemic inflammation or remote organ injury to the lung, leading to the development of indirect ALI. To address this question, the strategy was first to evaluate the uptake mechanism of *in vitro* generated MVs by lung-marginated monocytes and then to explore the potential roles of *in vivo* generated MVs in mouse models of sepsis and organ injury. As we had recently demonstrated an association between the acute increases in neutrophil- and monocyte-derived MVs with clinical severity/mortality in ICU-admitted severe burns injury patients[427], I further hypothesised these MV subtypes may drive pulmonary inflammation and injury during sepsis/SIRS.

1.7 Aims & objectives

The aim of this project is to assess the role of MVs as mediator of acute pulmonary vascular inflammation in sepsis/SIRS-induced ALI, with three central objectives:

1. To determine MV uptake by pulmonary vascular cells using *in vitro* and *ex vivo* models.
2. To determine MV production in *in vivo* models of systemic inflammation and extrapulmonary organ injury.
3. To identify the contribution of *in vivo*-derived circulating MVs and lung-marginated monocytes to the pathogenesis of indirect ALI.

Chapter 2

Materials & Methods

Chapter 2 Materials & methods

2.1 Materials

Table 2.1 Equipment

Equipment	Applications	Supplier
CyAn ADP analyser	Flow cytometry	Beckman-Coulter
EL_x800 microplate colourimetric reader	ELISA	Biotek instruments
FL_x800 microplate fluorescence reader	MV DiD-fluorescence quantification	Biotek instruments
Accument pH tester (AET 15)	IPL buffer pH measurement	Fisher Scientific
IPL-1 system	IPL perfusion	Harvard Apparatus
Custom-made ventilator	IPL ventilation	Harvard Apparatus
Physiosuite Righttemp	Kidney IRI procedure	Kent Scientific Cooperation
Tissue dissociator	Mechanical tissue dissociation	GentleMACS, Miltenyi Biotec
Dissociation tubes (C or M)	Mechanical tissue dissociation	GentleMACS, Miltenyi Biotec

Table 2.2 Software

Software	Applications	Supplier
FIJI	Confocal image analysis	ImageJ
Summit	Flow cytometry data acquisition	Beckman-Coulter
FlowJo 10.5.3	Flow cytometry analysis	FlowJo
Labchart reader	Physiology data analysis	AD instruments
Powerlab	Physiology data acquisition	AD instruments
SPSS statistics	Statistical analysis	IBM
Graphpad Prism	Statistical analysis	GraphPad software LLC

Table 2.3 In-house buffer

In-house buffers	Applications	Constituents
FACS wash buffer	Flow cytometry	• 1x PBS • 2% (v/v) Foetal calf serum (FCS) • 0.1% (w/v) Sodium Azide • 5mM EDTA
IPL perfusate	IPL perfusion	• RPMI-1640 • 100Units penicillin+10µg/ml streptomycin • 4% (v/v) BSA • 136.2mM NaCl (0.98g per 500ml) • 28.8mM $NaHCO_3$ (0.21g per 500ml)

Table 2.4 Reagents, buffers & pharmacological agents

Inhibitors/Reagents	Applications	Supplier
Heparin sodium	Blood anticoagulant	Wockhardt
Intracellular (IC) fixative buffer	Cells/tissue fixation	Invitrogen
Lipopolysaccharide (LPS) (Ultrapure *Escherichia coli* O111:B4)	*In vivo* studies	Autogen Bioclear
RPMI media (No phenol red)	IPL buffer	ThermoFisher Scientific
Bovine Serum Albumin (30% (v/v), sterile-filtered)	IPL buffer additive	Sigma Aldrich
Sodium Bicarbonate	IPL buffer additive	Sigma Aldrich
Sodium Chloride	IPL buffer additive	Sigma Aldrich
DMEM media	J774A.1 cell culture	Sigma Aldrich
Clodronate liposome	Macrophage depletion	FormuMax Scientific Inc.
Penicillin-streptomycin	Media antibiotics	Sigma Aldrich
Annexin V binding buffer	MV labelling	Biolegend
DiD dye	MV labelling	Life technologies
Diluent C	MV labelling	Sigma Aldrich
Antimycin A	MV uptake inhibition	Sigma Aldrich
Chondroitin sulfate (C-S)	MV uptake inhibition	Sigma Aldrich
Cytochalasin D	MV uptake inhibition	Sigma Aldrich
Dextran Sulfate(D-S)	MV uptake inhibition	Sigma Aldrich
Dynasore	MV uptake inhibition	Sigma Aldrich
Phosphatidylcholine (PC)-liposomes	MV uptake inhibition	Encapsula NanoSciences
Phosphatidylserine (PS)-liposomes	MV uptake inhibition	Encapsula NanoSciences
Polycytidylic acid (Poly-I)	MV uptake inhibition	Sigma Aldrich
Polyinosinic acid (Poly-C)	MV uptake inhibition	Sigma Aldrich
RGDS peptide	MV uptake inhibition	Sigma Aldrich
RGES peptide	MV uptake inhibition	Sigma Aldrich
Sodium Azide (NaN_3)	MV uptake inhibition	Alfa Aesar
Sodium Fluoride (NaF)	MV uptake inhibition	Sigma Aldrich
BD Phosflow Lyse/Fix buffer	RBC lysis	BD Biosciences

Table 2.5 Mouse antibodies

Antibodies	Conjugate	Clone	Supplier
ICAM-2	AlexaFluor 488	3C4	eBioscience
Streptavidin	AlexaFluor 488	-	Biolegend
Annexin V	FITC	-	Biolegend
F4/80	FITC	BM8	Biolegend
Anti-integrin β_5	PE	KN52	eBioscience
CD106	PE	105713	Biolegend
CD11b	PE	M1/70	Biolegend
CD162	PE	2PH1	BD Bioscience
CD204	PE	REA148	Miltenyi
CD31	PE	MEC13.3	Biolegend
CD45	PE	30-F11	eBioscience
CD45	PE	30-F11	eBioscience
CD51	PE	RMV-7	Biolegend
CD61	PE	2C9.G2 (HMβ_3-1)	Biolegend
CD62E	PE	10E9.6	BD Bioscience
CD62L	PE	MEL-14	Biolegend
CD86	PE	GL1	eBioscience
E-selectin	PE	10E9.6	BD Bioscience
ICAM-1	PE	YN1/1.7.4	Biolegend
Ly-6G	PE	1A8	BD Bioscience
MerTK	PE	2B10C42	Biolegend
TER-119	PE	TER-119	Biolegend
TIM-4	PE	RMT4	Biolegend
MHC-2	PerCP	M5/114.15.2	Biolegend
CD11b	PE-CF594	M1/70	BD Bioscience
CD41	PE-Cy7	MWReg30	Biolegend
Ly-6C	PE-Cy7	HK1.4	Biolegend
CD31	APC	MEC13.3	Biolegend
CD36	APC	HM36	Biolegend
VCAM-1	APC	429	Biolegend
Ly-6G	APC-Cy7	1A8	Biolegend
CD11b	Biotin	M1/70	Biolegend
CD31	Biotin	MEC13.3	Biolegend
CD41	Biotin	MWReg30	Biolegend
CD45	Biotin	30-F11	Biolegend
F4/80	Biotin	BM8	Biolegend
Ly-6C	Biotin	HK1.4	Biolegend
Ly-6G	Biotin	1A8	Biolegend
TER-119	Biotin	TER-119	Biolegend
Anti MFG-E8	Hamster IgG	D161-3	MBL CO. LTD
Anti-CD162	Unconjugated	4RA10	BD Bioscience
Anti-CD62L	Unconjugated	MEL-14	eBioscience
Purified CD16/32	Unconjugated	93	Biolegend

2.2 Animals

All protocols were reviewed and approved by the U.K. Home Office in accordance with the Animals (Scientific Procedures) Act 1986, U.K. Experiments were performed using male C57BL/6 mice (Charles River) ages 8–12 weeks (22–26 g) under project licences PPL70/7585 & P8E434E5B for sepsis and isolated perfused lung models and PPL70/8496 for kidney ischaemia reperfusion injury model. All procedures were performed under personal licence ICDB43F39. All animals were kept in 12:12h light-dark cycle with access to food and water *ad libitum*.

2.3 Induction of subclinical endotoxaemia

LPS challenge doses were based on a previous study in monocyte margination and priming of the lungs to secondary challenges[187]. To produce subclinical endotoxaemia and lung priming, C57BL/6 mice received a single intravenous (i.v., via tail vein) injection of 20ng LPS for 2 hours. After 2 hours, mice were euthanized via anaesthetic overdose and femoral artery exsanguination for collection of pulmonary vascular-marginated cells, or mice were anaesthetised for the IPL procedure.

2.4 Induction of endotoxaemia for *in vivo* production of MVs

A moderate dose of 2μg LPS/mouse was administered i.v. via tail vein to produce endotoxaemia with only mild or undetectable clinical symptoms (e.g. huddling, prolonged inactivity). Animals were anaesthetised with intraperitoneal (i.p.) xylazine (13mg/kg) & ketamine (130mg/kg) at set time points (1, 2 or 4h) post-LPS challenge. Abdominal laparotomy was conducted to expose inferior vena cava (IVC) and the animal was sacrificed via exsanguination, where 20UI heparin was injected via the IVC to circulate for 1min and 1ml of venous blood was collected in a syringe with 23G needle.

2.5 Kidney ischaemia reperfusion injury (IRI)

Mouse core temperature was stabilised to 37°C on warming pad (PhysioSuite, Kent Scientific Corporation) with a feedback rectal probe during induction of general anaesthesia with i.p. xylazine (13mg/kg) & ketamine (130mg/kg). Sterile, pre-warmed saline (200μl) was injected subcutaneously above neck to replace body fluids lost during surgery. Abdominal laparotomy was conducted to

expose the left kidney. The surrounding connective tissue of the left renal artery and vein were bluntly separated from the left renal blood vessels and blood supply was occluded using a non-traumatic vascular clamp (S&T ZV vascular clamp size B-2, Fine Science Tools) with clip applying forceps (S&T CAF-4, Fine Science Tools) to induce unilateral renal ischaemia. Unilateral left kidney ischaemia was induced for 20-45min, depending on experiment. Occlusion of blood flow was confirmed by visualisation of renal cyanosis, after which the abdomen was temporarily closed with a pre-warmed sterile gauze during ischaemia induction period. After the ischaemic period, the kidney was reperfused for 1h by visualisation of cyanosis disappearance (colour of kidney changes from dark red/purple to bright red/pink). Sham-operated control mice underwent anaesthesia and abdominal laparotomy without the application of the kidney ischaemia vascular clamp. The animal was sacrificed via exsanguination, where 20UI heparin was injected via the IVC to circulate for 1min and 1ml of venous blood was collected in a syringe with 23G needle. The blood, both kidneys and the lungs were harvested for further processing.

2.6 Harvest of pulmonary-marginated vascular cells

Lung-marginated cells were collected by *ex vivo* perfusion of pulmonary vessels via the pulmonary artery for analysis and *in vitro* experimentation. At 2h post-induction of subclinical endotoxaemia, mice were sacrificed via anaesthetics overdose with i.p. pentobarbitone. Mice were thoracotomised to expose the chest cavity and 20IU of heparin was injected into the right ventricle, followed by cannulation of the pulmonary artery and left atrium. Once the cannulations were established, mice were tracheotomised, and lungs were inflated with 15ml/kg body weight of air to maintain optimal opening of pulmonary microvasculature for perfusion. The lungs were perfused with Hank's Balanced Salt Solution (HBSS without calcium and magnesium) supplemented with 4% (v/v) clinical-grade human albumin solution (HAS) using a syringe pump at 10ml/h, gradually increased to a constant flow of 50ml/h over 12min when the lungs became a translucent white. A total of 10ml perfusate was collected on ice and centrifuged at 300 x g for 10min and the resulting cell pellet was washed in HBSS ($+Ca^{2+}/Mg^{2+}$) to restore calcium and then re-suspended in 0.5% (v/v) HAS-HBSS and penicillin(100Units/ml)-streptomycin(10µg/ml) for *in vitro* experimentation.

2.7 *Ex vivo* isolated perfused lungs (IPL)

2.7.1 IPL buffer osmolality & pH

For *ex vivo* organ perfusion, especially the lung, higher osmolality of buffer is needed to maintain normal physiology. As organs are usually perfused with whole blood which contains much higher osmolality and experience higher osmotic pressure, it is important to adjust the osmolality of perfusion buffer to match to that of *in vivo*. Osmolality of the basal RPMI-1640 buffer was adjusted from the commonly used 300mOsm/kg[313,445,446] to around 350mOsm/kg[310] to match the blood osmolality of mice, which falls in the range of 300-350mOsm/kg[447] depending mouse strains. RPMI-1640 basal media contains nutrients, vitamins and other inorganic salts including 103.44mM (6000mg/L) sodium chloride that makes up osmolality of around 276mOsm/kg. An additional of 1900mg/L sodium chloride and 420mg/L sodium bicarbonate were added to the basal medium to adjust osmolality to 350mOsm/kg and pH 7.4[448] (Table 2.6). After all additional components were dissolved in the pre-warmed (37 ºC) bottle of 500ml media, the media was sterile-filtered with 0.22µm syringe filter unit (Merck, Millipore), supplemented with penicillin(100Units)-streptomycin(10µg/ml) and stored at 4ºC for further use (see Table 2.3 for ingredients).

	Mass (g) added per 500ml	Molecular weight	mg/L	mmol/L	mOsm/kg
RPMI-1640					276.0
NaCl	0.95	58	1900	32.76	65.5
$NaHCO_3$	0.21	84	420	5.00	10.0
Final					**± 351.5**

Table 2.6 IPL buffer osmolality and pH adjustment.

To adjust osmolality of IPL buffer from basic basal media to physiological range of 350mOsm/kg and to maintain physiological pH of 7.4 during IPL procedure when lung is ventilated with 5%CO_2, 0.95g of sodium chloride (NaCl) and 0.21g of sodium bicarbonate ($NaHCO_3$) is added to a bottle of 500ml RPMI-1640 media, supplemented with 5ml penicillin (100Units)-streptomycin (10µg/ml).

In replacement of the low-endotoxin bovine serum albumin (BSA)[295] or human albumin solution (HAS)[1,294] previously used in our lab, the use of sterile-grade BSA in perfusion buffer has greatly enhanced the lifetime of our IPL preparation. Prior to IPL set up for experimentation, 15ml of 4% (v/v) BSA-RPMI was prepared in a 50ml conical tube and left in a 37ºC 5% CO_2 incubator overnight with

loosened lid to restore the acid-base buffering equilibrium (Equation 1). Similarly, to maintain physiological pH 7.4 of buffer during experimentation, the IPL was ventilated with 5% CO_2.

$$NaHCO_3 + H_2O \Leftrightarrow NaOH + H_2CO_3 \Leftrightarrow NaOH + H_2O + CO_2(g)$$

Equation 1 Acid base equilibrium equation for IPL perfusate buffer.

2.7.2 IPL maintenance and sterility

Running the IPL system under sterile and endotoxin-free conditions is essential, particularly for evaluation of sterile inflammatory insults. Therefore, an optimal cleaning routine of the circuit tubing and connectors was established in this study. After each experiment, all perfusate buffers were drained and tubing was first filled with sterile grade water to rinse out all remaining buffer. After which, water was drained, and tubing was filled with high quality detergent (Mucasol™, 10% (v/v), Thermo Fisher Scientific, U.K.) overnight. The next day, the circuit was drained, and tubing rinsed several times with sterile grade double-distilled water. Before experimentation, tubing was last washed with sterile PBS supplemented with penicillin(100Units)-streptomycin(10µg/ml) and then replaced with perfusate buffer, also containing these antibiotics (see below).

2.7.3 IPL mounting and experimentation

LPS-treated (20ng, i.v., 2h) or untreated C57BL/6 mice were anaesthetised with intraperitoneal (i.p.) xylazine (13mg/kg) & ketamine (130mg/kg). Anaesthesia was confirmed by loss of reflex by toe pinch and the mouse was injected with 20IU of heparin i.v. via tail vein. Tracheostomy was carried out and lungs were given two sustained inflation breaths (5s, 25cmH_2O) and ventilation was commenced at a tidal volume of 6-7ml/kg, at respiratory rate of 80 breaths/min, positive end expiratory pressure (PEEP) of 5cmH_2O, with 21% FiO_2. Abdominal laparotomy was carried out in the IPL chamber and the mouse was then exsanguinated via the IVC. The sub-hepatic portion of lower abdomen was removed, and the upper body remain was rinsed with sterile saline. Lungs were maintained at continuous positive airway pressure (CPAP) of 5cmH_2O to prevent accidental injury during thoracotomy and ventilation gas was switched from 21% FiO_2 to 5%CO_2/21%O_2 to ensure normocapnia.

Midline thoracotomy was performed, and the pulmonary artery and left atrium were cannulated. Using the perfusate buffer prepared as described above, perfusion was initially commenced via an open circuit (non-recirculating) at a rate of 0.1ml/min and gradually increased to 25ml/kg/min (=0.625ml/min for a 25g mouse), during which 3ml of perfusate containing non-adherent blood cells was flushed out via point A sampling port (Figure 2.1). Perfusion was then switched from a non-recirculating to recirculating circuit, and the preparation allowed to stabilise for 15min at 25ml/kg/min perfusion flow rate before experimentation. To maintain humidity in the IPL chamber and prevent lung tissue drying, 3ml of sterile saline was added to the bottom of chamber without direct contact with the lung preparation and a cover lid placed on the chamber throughout the experimentation period. At 15min intervals, the respiratory and vascular mechanics of the IPL preparation were measured using an end inspiratory pause technique and 25cmH_2O deep inflation was applied twice for 5 seconds to recruit the lung, preventing atelectasis. These respiratory parameters remained stable throughout the timeframe investigated (up to 4h), regardless of the treatments used. At the end of experimentation, different lobes of lungs were collected and processed for analysis (Figure 2.8).

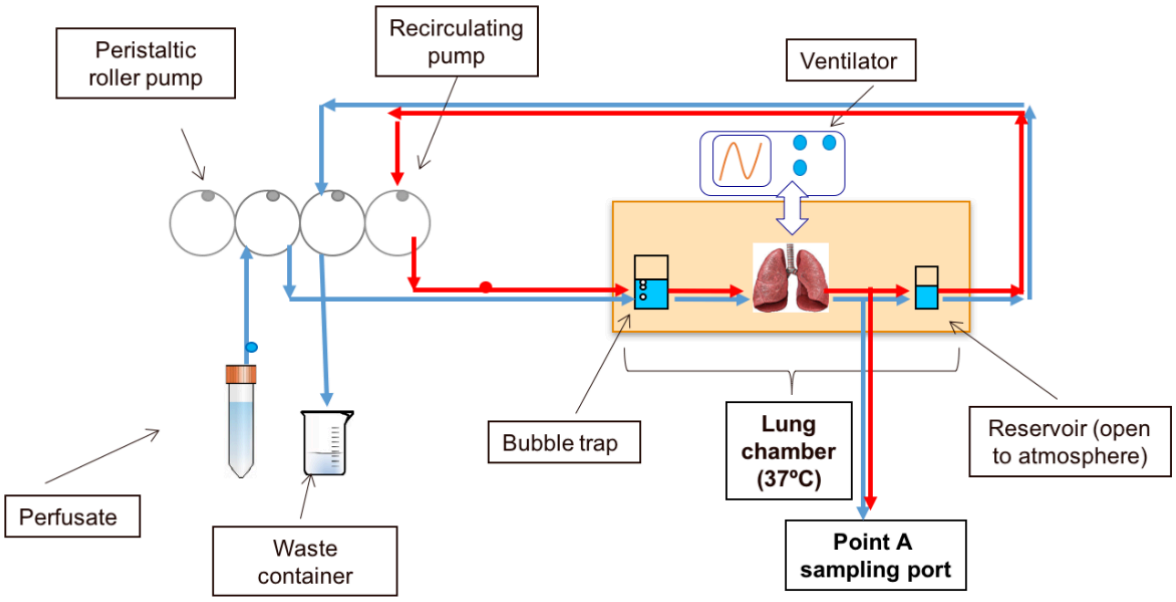

Figure 2.1 Isolated perfused lung (IPL) perfusion circuit.

Open, non-recirculating circuit (Blue) and closed, recirculating circuit (Red). During washing steps, solutions were filled into and disposed-off via the non-recirculating circuit. During experimentation, IPL buffer was filled via the non-recirculating circuit and subsequently closed off via the recirculating circuit for experimentation up to 4h. (Adapted from Dr. Kate Tatham's PhD thesis)

2.7.4 IPL respiratory and vascular mechanics

When the perfusion flow stabilised at 25ml/kg/min, pulmonary arterial pressure (PAP) recorded by pressure transducers (PowerLab, AD instruments) fell within the range of 4-8mmHg for both untreated and LPS-pretreated mice (Figure 2.2). Left atrial pressure (LAP) was maintained at 2.5mmHg by altering the reservoir positioning throughout the perfusion period (Figure 2.3), enabling maintenance of optimum blood flow within pulmonary capillaries during perfusion. Pulmonary vascular resistance (PVR) was calculated as the difference between PAP and LAP, as a reversed function of perfusion flow rate (ml/min) (Equation 2).

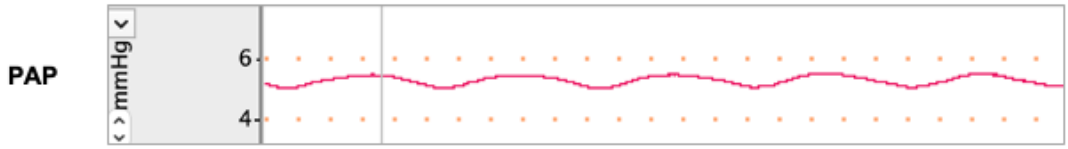

Figure 2.2 Pulmonary arterial pressure (PAP).

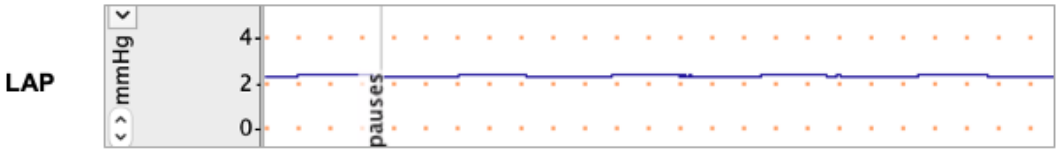

Figure 2.3 Left atrial pressure (LAP).

$$PVR\ (mmHg\ \min ml^{-1}) = \frac{PAP\ (mmHg) - LAP\ (mmHg)}{Perfusion\ flow\ rate\ (ml\ min^{-1})}$$

Equation 2 Calculation for pulmonary vascular resistance.

Respiratory mechanics were recorded automatically (PowerLab, AD instruments) during inspiratory pauses at 15min intervals before and after lung recruitment (two sustained inflation breaths for 5 seconds at 25 cmH_2O). To calculate lung respiratory mechanics, including respiratory elastance (Ers) **(Equation 3**) and resistance (Rrs) (**Equation 4**), mean of each measurement were calculated from 3 different data points during inspiratory pauses (Figure 2.4, highlighted in yellow box). Measurements taken included airway pressures: peak inspiratory pressure (PIP), plateau airway pressure (Pplat), end expiratory airway pressure (PEEP) (Figure 2.5), and airway flow: tidal volume (V_T) (Figure 2.6) and steady-state airway flow, (Q_{aw}) (Figure 2.7).

$$Ers\ (cmH_2O\ kg\ ml^{-1}) = \frac{P_{plat}(cmH_2O) - PEEP\ (cmH_2O)}{V_T\ (ml\ kg^{-1})}$$

Equation 3 Calculation for respiratory elastance.

$$Rrs\ (cmH_2O\ ml\ sec^{-1}) = \frac{PIP\ (cmH_2O) - P_{plat}\ (cmH_2O)}{Q_{aw}\ ((ml\ sec^{-1})}$$

Equation 4 Calculation for respiratory resistance.

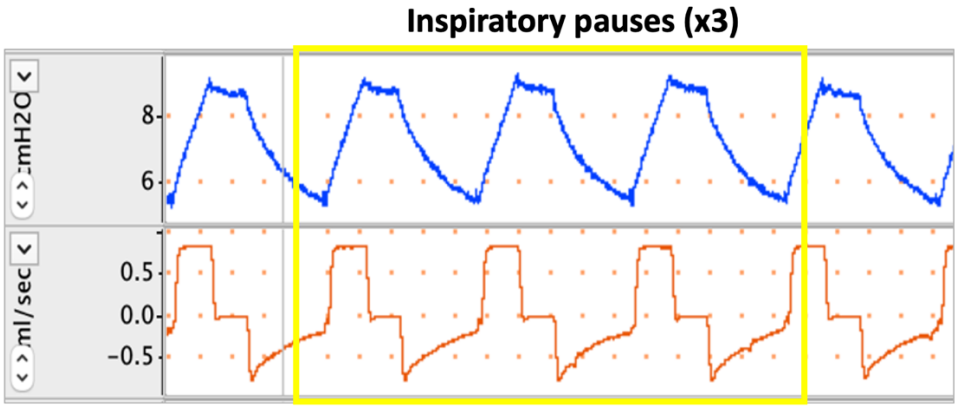

Figure 2.4 Inspiratory pauses to identify airway pressure (blue trace) and airway flow (orange trace).

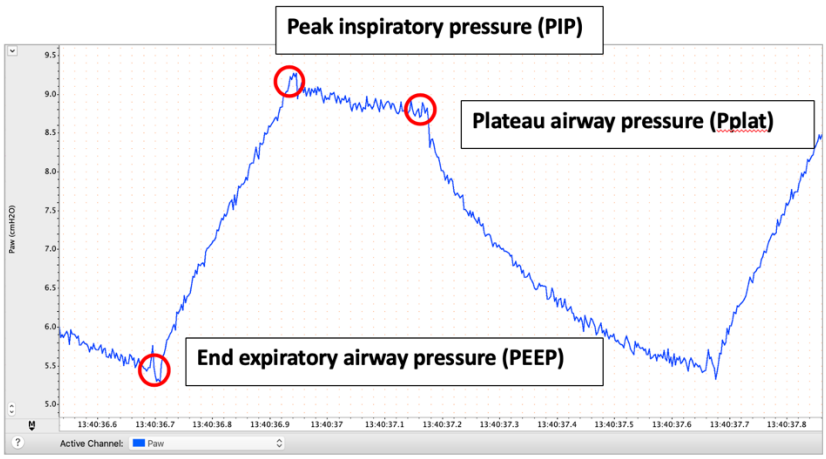

Figure 2.5 Airway pressure trace during an inspiratory pause.

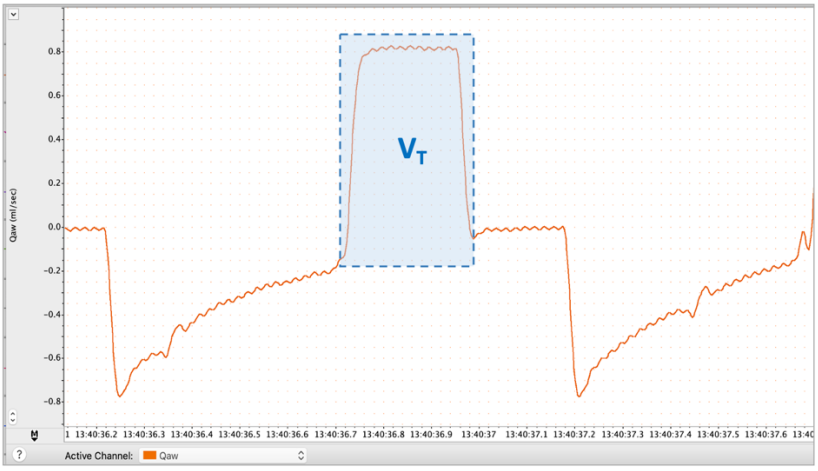

Figure 2.6 Tidal volume (V_T) highlighted, during an inspiratory pause.

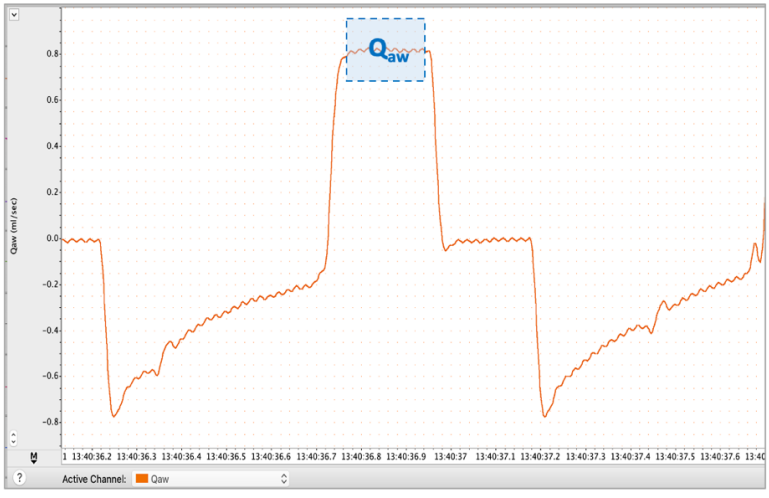

Figure 2.7 Steady-state airway flow (Q_{aw}), highlighted, during an inspiratory pause.

2.7.5 IPL perfusate sampling and processing

At the end of the IPL run, the total circuit perfusate (~2.5ml) was collected via Point A sampling port (Figure 2.1). The perfusate was then centrifuged at 300 x g for 10min at 4ºC to sediment cells, followed by 20,000 x g for 30min to remove MVs and any cell debris. Supernatant was aliquoted and stored at -80°C for future analysis by Enzyme-Linked Immunosorbent Assay (ELISA).

2.7.6 IPL bronchoalveolar lavage fluid (BALF) sampling and processing

After perfusate collection, perfusion and ventilation was ceased and a silk 2/0 suture was placed around the lower right lobe and tied off at the hilum. 0.65ml of saline was slowly injected into the lung via the tracheal tube and lung was lavaged gently for 3 times. Resulting BALF was collected and centrifuged at 300 x g for 10min to remove alveolar cells and the supernatant aliquoted and stored at -80°C for future protein quantification by Qubit assay or cytokines analysis by ELISA.

2.7.7 Lung injury measurement by wet-to-dry weight ratio

The tied-off right lower lobe was lightly blotted on tissue and weighed immediately for wet weight. After which, it was placed in a 60°C oven overnight (24h). Dry weight of the lung was measured the next day for wet-to-dry weight ratio analysis as a lung injury indicator.

2.7.8 Snap freezing lung tissue

Following bronchoalveolar lavage, the left lung was snap frozen in a microcentrifuge tube submerged in pre-chilled 2-methylbutane on dry ice. The snap frozen lung was stored at -80°C for future protein analysis by western blot.

2.7.9 Preparation of single cell suspension

The left lung was excised and process directly or after brief storage on ice. Single cells suspensions were prepared by mechanical disaggregation and fixation, or enzymatic digestion, as described below (2.9.1).

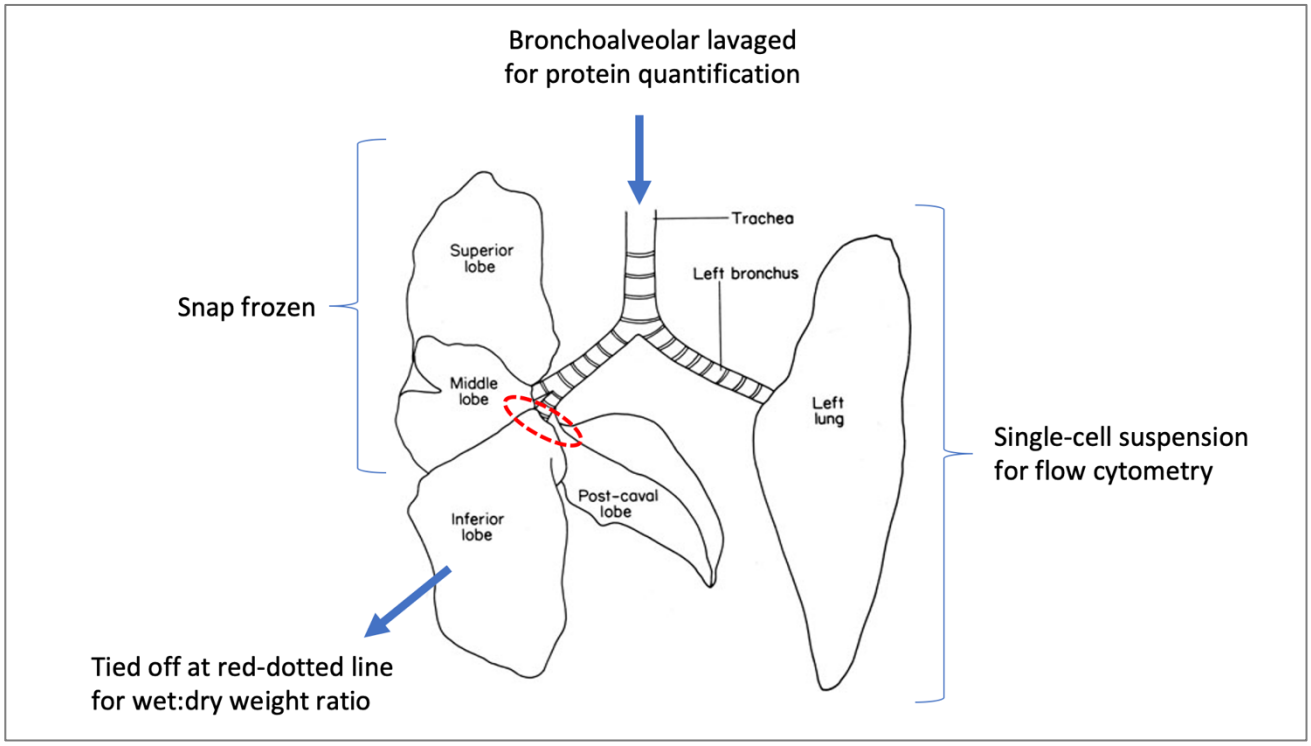

Figure 2.8 Lung sample collection for analysis.

After IPL experimentation, the right lower lobe was tied off for wet-to-dry weight ratio analysis, and the remaining lung was lavaged with 0.65ml saline for collection of BALF. The left lung was processed to form single cell suspension for flow cytometry analysis and the remaining right lung was snap frozen for western blotting.

2.8 Microvesicles (MVs)

2.8.1 *In vitro* MV production by J774A.1 macrophages

J774A.1 macrophage cell line (ATCC, UK) was maintained in Dulbecco's Modified Eagle's Medium (DMEM) (Sigma-Aldrich, UK) supplemented with 10% (v/v) heat-inactivated foetal calf serum (FCS) (Sigma-Aldrich, UK) and 1x penicillin-streptomycin-glutamine (PSG) (Gibco, UK), at 37°C in a humidified 5% CO_2 incubator. Cells were seeded at a density of $6x10^6$ cells in 6mm petri dishes and maintained in medium overnight for adherence prior to experimentation. Adherent cells were rinsed 4x with PBS ($-Ca^{2+}/Mg^{2+}$) to remove cellular debris and EVs. Cells were then stimulated with ATP (3mM) in PBS ($+Ca^{2+}/Mg^{2+}$) for 30min to produce MVs through activation of the $P2X_7$ receptor[449]. Following ATP treatment, cells and media were triturated gently, to ensure consistent recoveries and centrifuged in fixed angle rotor at 300 x g for 10min to remove cells, followed by 20,000 x g for 15min at 4°C to pellet MVs.

2.8.2 DiD-labelling of J774A.1 MVs and fluorescent quantification

DiD solid (1,1'-Dioctadecyl-3,3,3',3'-Tetramethylindodicarbocyanine, 4-Chlorobenzenesulfonate Salt) (Life technologies, UK) was dissolved in ethanol to prepare a 1mM stock, from which an intermediate stock of 30μM DiD was prepared in diluent C (Sigma, UK). MV pellet was resuspended in PBS and incubated with final concentration of 5μM of DiD, at RT for 7min in dark. DiD-labelled MVs were pelleted by centrifugation at 20,000 x g for 15min and re-suspended in 0.5% (v/v) HAS-HBSS. 10ul of MVs were stained with fluorophore-conjugated anti-CD45 and/or anti-CD11b at 1 in 100 final concentration in filtered PBS (with 0.22μm syringe filter) for flow cytometric analysis and counts were determined using counting beads (see section 2.9.3 on flow cytometry analysis).

For total DiD-labelled MV fluorescence measurement, DiD-labelled MVs were treated with final concentration of 1% (v/v) Triton X-100 in PBS to enhance the fluorescence signal, which was measured using fluorescent plate reader (Biotech FLx800) at 635nm and 680nm absorption and emission wavelengths. MV dose was adjusted according to fluorescence reading depending on experiments, based on a MVs dose-response curve and linear calibration of MVs fluorescence against number of MVs, obtained at initial stage of experiments.

2.8.3 Plasma preparation for MV analysis

Blood was centrifuged at 1,000 x *g* for 10min to remove cells and majority of platelets and the plasma supernatant was centrifuged for a further 5min at 1,000 x *g* to obtain platelet-poor plasma (PPP). These centrifugation steps yielded high quality of PPP with minimal loss of MV content. MVs in PPP were then processed for flow cytometry analysis and for experimentation.

2.8.4 Immuno-affinity isolation of *in vivo* MV subtypes

PPP was centrifuged at 20,000 x g for 30min to pellet MVs. MVs were resuspended in filtered PBS and stained with the microbead-conjugated antibody/biotin-conjugated antibody at 1µl per 10^6 MVs concentration for 30min on ice. For positive selection or depletion of a single MV population, MVs were incubated either directly with conjugated microbeads (CD11b-microbeads for myeloid-MVs) (Miltenyi Biotec) or biotinylated antibodies (CD41-Biotin for platelet-MVs) (Miltenyi Biotec) combined with anti-biotin microbeads (Miltenyi Biotec). For depletion of other MV populations, MVs were incubated with a mixed cocktail of pre-titrated biotinylated antibodies (anti-TER119 for RBC-, anti-CD31 for endothelial-, anti-CD41 for platelet-, and anti-CD11b for myeloid-derived MVs) (Biolegend) for 15min, followed by anti-biotin magnetic beads, for 30min on ice.

Labelled MVs were passed through a magnetised column, either the medium-size (MS) or large-size (LS), depending on the amount of MVs: MS columns for less than 10^7 target MVs and LS columns for more than 10^7 target MVs. 'Positively-selected' bead-bound MVs were captured within the column with the flow-through contained the 'negatively-selected' bead-free MV fraction. Column-bound positively-selected MVs were eluted by removing the column from the magnet and flushed through with filtered PBS for 3 times (3 x 1ml for MS, 3 x 3ml for LS). Eluted or flow-through fractions were centrifuged at 20,000 x g for 30min and resuspended in either IPL buffer for experimentation or in filtered PBS for flow cytometric analysis.

2.9 Flow cytometry

2.9.1 Preparation of single-cell suspensions for flow cytometry analysis

Single cell suspensions were prepared from tissues (lung, kidney, spleen or liver) by mechanical disaggregation using a gentleMACS™ Tissue Dissociator (Miltenyi Biotec) suspended in 2ml formaldehyde fixative (Cellfix, eBioscience) in MACS C tubes, as described previously[450]. After a brief fixation period (1-5min – dependent on the procedure), fixation reaction was stopped via addition of cold FACS Wash Buffer (FWB) (see Table 2.3 for ingredients). Cell suspensions were then passed through a 40μm nylon filter (BD Falcon) and dispersed further with a syringe plunger and flushed through with FWB. The cell suspension was centrifuged at 400 x g for 10min at 4°C to obtain cell pellet. To remove red blood cells in the single cell preparation, cell pellet was resuspended in 1-step Fix/Lyse Solution (1X) (eBioscience, UK) for 1min and washed twice with FWB prior to antibody staining. Cells were resuspended in 1ml FWB, from which 50μl were stained at 4°C for 30min in dark with fluorophore-conjugated anti-mouse Abs (Table 2.7).

Channel	Myeloid leukocytes panel (Final conc.)	Endothelial cells panel (Final conc.)
FITC	F4/80 (1/400)	ICAM-2 (1/400)
PE	ICAM-1/CD86/TNF/L-selectin (1/200)	ICAM-1/E-selectin (1/200)
PE-Texas Red	CD11b (1/400)	CD31 (1/400)
PerCP	MHC-2 (1/400)	CD45(1/400)
PE-Cy7	Ly6C (1/400)	CD41(1/400)
APC	-	VCAM-1(1/200)
APC-Cy7	Ly6G (1/400)	-

Table 2.7 Fluorophores-conjugated anti-mouse antibody panel for single cell suspensions for flow cytometry.

After antibodies staining, samples were washed and centrifuged at 400 x g for 5min at 4°C and resuspended in FWB for flow cytometric analysis (CyAn™ ADP Analyser, Beckman Coulter). Data were analysed with FlowJo software (Tree Star). Absolute cell counts in samples were assessed using Accucheck counting beads (ThermoFisher Scientific, UK).

2.9.2 Flow cytometry gating strategy for lung myeloid leukocytes and endothelial cells

Single cell suspension was prepared from IPL by mechanical disaggregation and fixation of lung tissue. Singlet events were gated and lung endothelial cells were identified as CD45-, CD41-, ICAM2+ and CD31+ populations (Figure 2.9), whereas myeloid CD11b+ cell subpopulation were identified as: Ly6C^{high}, F4/80+ monocytes; Ly6C^{med}, F4/80- neutrophils; Ly6C^{low} F4/80+ cells were Ly6C^{low} monocytes (MHCII-) and interstitial macrophages (MHCII+) (Figure 2.10).

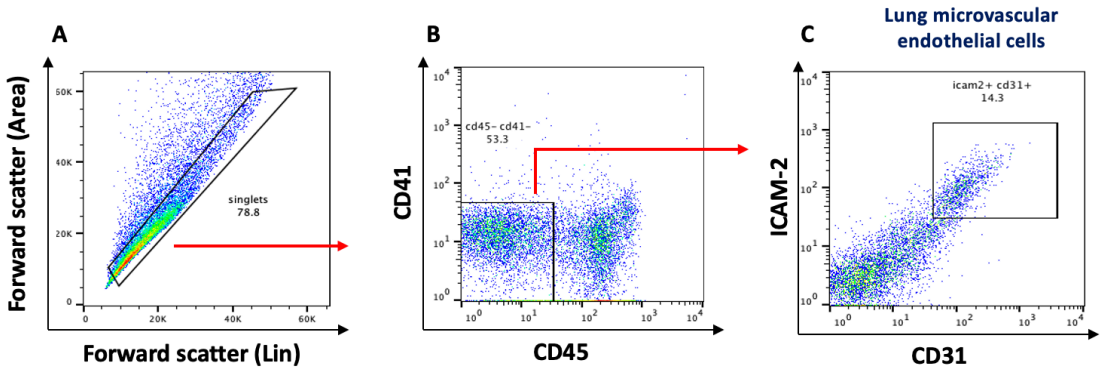

Figure 2.9 Flow cytometry gating strategy of lung endothelial cells.

(A) Singlet events were identified by the linear correlation between FS Area and FS Lin. (B) leukocytes and platelets identified as CD45+ and CD41+, respectively, were excluded. (C) Lung endothelial cells were identified as CD45-, CD41-, ICAM-2+ and CD31+ population.

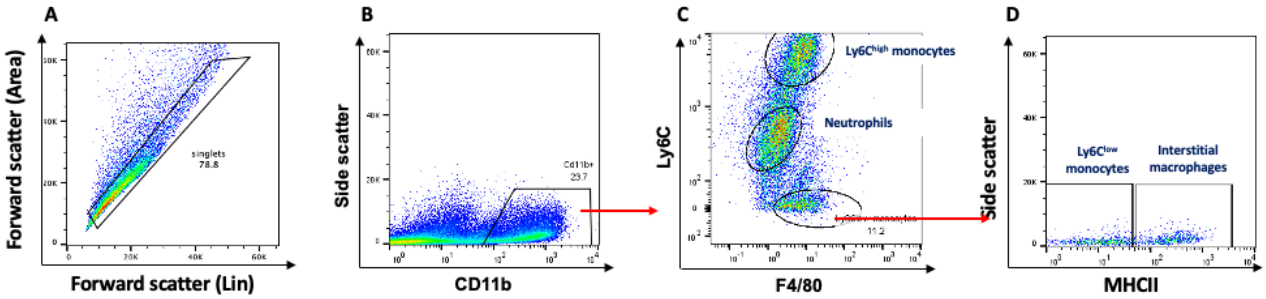

Figure 2.10 Flow cytometry gating strategy of lung myeloid leukocytes.

(A) Singlet events were identified by the linear correlation between FS Area and FS Lin. (B) CD11b was used to identify myeloid cells. (C) Ly6C^{high} monocytes were identified by their expression of F4/80 and high level of Ly6C. Neutrophils were identified by their lack of F4/80 expression but intermediate Ly6C expression. (D) F4/80 positive, but low Ly6C population was further identified as MHCII positive, interstitial macrophages or MHCII negative, Ly6C^{low} monocytes.

2.9.3 Flow cytometry staining and analysis of MVs

For identification of MVs by flow cytometry, 3 separate criteria had to be satisfied: 1) size less than 1μm; 2) positive for specific precursor cell surface markers; and 3) sensitivity to detergent lysis. MVs were resuspended in 0.22μm filtered PBS, from which 10μl samples were stained for 30min at 4°C in dark with fluorophore-conjugated anti-mouse Abs at 1 in 100 concentrations. Fluorophores-conjugated antibodies used for each MV preparations were as summarised in Table 2.8 (for *in vitro*-derived J774A.1 MVs), Table 2.9 (for *in vivo*-derived kidney IRI MVs), and Table 2.10 (for *in vivo*-derived endotoxaemia MVs). After antibody staining, MV samples were resuspended in 1ml filtered PBS with 5μl AccuCheck 6μm counting beads (Invitrogen, Paisley, UK) for MV quantification by flow cytometry with side scatter trigger threshold, where the 1μm gate was calibrated with fluorescent sizing calibration beads (Sperotech, UK) (Figure 2.11). Where annexin V staining was carried out, annexin V binding buffer (Biolegend, UK) was used in replacement of PBS.

Channel	Antibody
FITC	Annexin V
PE	CD45
APC	DiD

Table 2.8 Fluorophore-conjugated anti-mouse antibody panel for identification of *in vitro*-derived J774A.1 MVs.

Sample / Channel	1	2	3
FITC	Annexin V		
PE	CD11b	CD11b	CD31
APC	Ly6G	Ly6C	CD41

Table 2.9 Fluorophore-conjugated anti-mouse antibody panel for identification of *in vivo*-derived kidney IRI MVs.

Sample / Channel	1	2	3	4
FITC	Annexin V			
PE	CD11b	CD11b	CD31	TER119
PE-Cy7	CD45	Ly6C	CD41	CD41
APC	F4/80	Ly6G	CD11b	CD11b

Table 2.10 Fluorophore-conjugated anti-mouse antibody panel for identification of *in vivo*-derived endotoxaemia MVs.

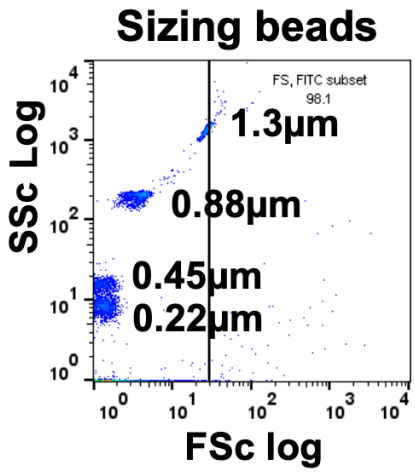

Figure 2.11 Flow cytometry gating for MVs was determined by fluorescent sizing calibration beads.

2.10 Confocal microscopy

Cytospin poly-lysine slides (Sigma, UK) were prepared from pulmonary perfusate cell suspension by sedimentation of a total of 5 × 10^5 cells (3.4.7). After cytospin, cells were mounted with ProLong™ Gold Antifade Mountant with DAPI (P36931, ThermoFisher Scientific, UK). Zeiss LSM-510 inverted confocal microscope was used to observe the cells with/without immersion oil (10976, Sigma) depending on objective lens magnification. Images were photographed with Zeiss KS-300 imaging software and analysed using FIJI software.

2.11 Protein assays

2.11.1 Qubit protein assay for BALF protein quantification

Qubit working solution was prepared by diluting Qubit protein reagent 1 in 200 in Qubit protein buffer. 10μl of each pre-diluted Qubit protein reagent standards was prepared in 190μl Qubit working solutions, whereas 1-20μl samples (depending on concentration) was diluted in Qubit working solutions to make up a total of 200μl final volume. Prepared standard and samples were vortexed and incubated in PCR tubes for 15min at RT, according to manufacturer's instructions. Protein concentrations contained within each standard was read on Qubit fluorometer on "Protein Assay" setting to calibrate standard curve, followed by reading of each samples to obtain final protein concentration. Detection range of Qubit protein assay was 12.5μg/ml to 5mg/ml.

2.11.2 Bradford protein assay for western blot protein quantification

BSA standards were prepared in PBS at following concentrations with serial dilution: 2mg/ml, 1mg/ml, 0.5mg/ml, 0.25mg/ml, 0.125mg/ml, 0.0625mg/ml, 0.03125mg/ml and a blank. Standards and samples (each at 5μl) were added in duplicate to a 96-well microplate and incubated with 250μl of Coomassie (Bradford) Protein Assay Reagent with continuous mixing on a plate shaker for 5min. The microplate was then read at a wavelength of 595nm on EL_x800 microplate colorimetric reader (Biotek instruments). Sample protein concentrations were determined from the standard curve using Prism software. Detection range of Bradford protein assay was 100μg/ml to 1.5mg/ml.

2.12 Enzyme-Linked Immunosorbent assay (ELISA)

Standard sandwich ELISAs (R&D systems – DuoSet ELISA) were conducted to measure IPL perfusate cytokine concentrations. The capture antibody was diluted to recommended working concentration with PBS according to manufacturer's instructions. Maxisorp™ 96-well microplate (ThermoFisher Scientific, UK) was coated with 50ul of capture antibody and the plate was sealed and incubated overnight at 4°C. Each well was washed 3 times with wash buffer (0.05% (v/v) Tween-20 in PBS) and residual fluid was aspirated, and the plate blotted dry. The plate was blocked with 1% (v/v) BSA for 1h at room temperature. Washing and aspiration steps described above was repeated, followed by addition of 50µl of standards and samples to each well and incubated at RT for 2h. Washing and aspiration steps were repeated and 50µl of biotinylated detection antibodies at recommended working concentrations were added to each well for 2h at room temperature. Washing and aspiration steps were repeated and 50µl of streptavidin-HRP was added to each well and was incubated in dark for 20min. The plate was washed and aspirated again, followed by addition of 50µl substrate solution (tetramethylbenzidine) (Sigma-Aldrich, UK) to each well. The plate was again left in the dark and at RT for 30min. 50ul of stop solution (2M sulphuric acid) was added to terminate substrate reaction. Plate was gently swirled to ensure thorough mixing of solutions and the optical density of each well was read at a wavelength of 450nm using EL_x800 microplate colourimetric reader (Biotek instruments). When ELISA kits were used (e.g., Endothelin-1 and Angiopoietin-2), procedures were carried out according to manufacturer's instructions. Detection range of standard sandwich ELISAs were summarised in Table 2.11.

Target	Detection range
RAGE	125 – 8000pg/ml
KC	15.6 – 1000pg/ml
VEGF	15.6 – 1000pg/ml
IL-6	15.6 – 1000pg/ml
MIP-1α	7.81 – 500pg/ml
MIP-2	15.6 – 1000pg/ml
MCP-1	3.91 – 250pg/ml
TNF-α	31.2 – 2000pg/ml
IL-1ß	15.6 – 1000pg/ml
ACE	93.8 – 6000pg/ml
IL-10	31.2 – 2000pg/ml
TGF-β	31.2 – 2000pg/ml
RANTES	31.2 – 2000pg/ml
GM-CSF	7.81 – 500pg/ml
Angiopoietin-2	39.1 – 2500pg/ml
Endothelin-1	0.4 – 25pg/ml

Table 2.11 ELISA detection range.

2.13 Statistical analysis

All data underwent assessment of normality by Shapiro-Wilk test. Normally distributed data were analysed by t-test, one-way ANOVA with Bonferroni's/Dunnett's multiple comparison, or two-way ANOVA with Sidak's multiple comparison test, following log-transformation where necessary. When data were not normally distributed, Mann-Whitney's U test or Kruskal-Wallis with Dunn's multiple comparisons was used. In cases where normality tests were underpowered due to small n numbers, scatter plots were used to allow graphical inspection of data distribution and analysed by nonparametric tests. Statistical analyses were performed using GraphPad Prism 8, with p-value <0.05 considered significant. Animal numbers were calculated for each experiment, considering required replicates to give enough statistical power based on the estimated effect size. Statistical power of 0.8 (80%) was estimated to be attained at n=4, 6, and 9 for an effect size of 2.5, 2 and 1.5 (respectively), assuming data normality, equal variance, non-paired two-tail tests at $p<0.05$.

Chapter 3

Mechanism of microvesicle uptake by lung-marginated Ly6C^{high} monocytes during endotoxaemia

Parts of the content of this chapter have been published as a conference abstract and a journal publication:

Enhanced Recognition and Internalisation of Microvesicles by Lung-Marginated, Ly-6Chigh Monocytes During Endotoxaemia. *Y. Y. Tan, K. P. O'Dea, S. Soni, S. Shah, B. V. Patel & M. Takata. FASEB Journal (2017) 31 (1): 327.7*

Monocytes mediate homing of circulating microvesicles to the pulmonary vasculature during low-grade systemic inflammation. *K. P. O'Dea, Y. Y. Tan, S. Shah, B. V. Patel, K. C. Tatham, M. R. Wilson, S. Soni & M. Takata. Journal of Extracellular Vesicles (2020), 9:1, 1706708.*

Chapter 3 Mechanism of microvesicle uptake by lung-marginated Ly6C^{high} monocytes during endotoxaemia

3.1 Abstract

Background

Circulating microvesicles (MVs) have been implicated as long-range mediators of vascular inflammation, but their precise role in the pathophysiology of pulmonary vascular inflammation is unclear. MV recognition and uptake by cells within the pulmonary vasculature will be critical in determining their subsequent role in inducing pulmonary injury from systemic inflammation. Our lab has recently demonstrated that during subclinical endotoxaemia in mice, the pulmonary circulation becomes primed as a 'de novo' site for uptake of MVs via increased lung margination of Ly6C^{high} monocytes and their increased capacity for MV uptake. Here, we investigated the mechanism responsible for the preferential MV uptake by Ly6C^{high} monocytes *in vitro* using cells harvested by perfusion from the pulmonary vasculature, as well as in *ex vivo* isolated perfused lungs (IPL).

Methods

Lungs of untreated or low-dose LPS (20ng, i.v. 2h)-pretreated C57BL/6 mice were perfused to obtain lung-marginated vascular cells. MVs derived from J774A.1 macrophage by ATP stimulation were labelled with the fluorescent lipophilic dye, DiD, and then co-incubated with lung perfusate cells for 1h *in vitro*. For IPL experiments, DiD-labelled MVs were infused into the closed, recirculating IPL circuit for 1h. MV uptake was quantified by flow cytometry or confocal microscopy.

Results

As previously found *in vivo*, preferential uptake of MVs was observed *in vitro* in Ly6C^{high} monocytes compared to other vascular cell subpopulations obtained from LPS-pretreated mice. MV uptake in Ly6C^{high} monocytes obtained from LPS-pretreated mice was also substantially higher when compared to those obtained from untreated mice. Inhibition experiments *in vitro* demonstrated that MVs are endocytosed into the cells via phosphatidylserine (PS)-recognition mechanism through scavenger receptor A (SR-A) and integrin. In *ex vivo* IPL, Ly6C^{high} monocytes displayed a higher capacity for MV uptake in IPL obtained from LPS-pretreated, but not from untreated mice.

Conclusion

Preferential uptake of MVs by lung-marginated Ly6C^{high} monocytes was demonstrated *in vitro* and *ex vivo*, suggesting a PS-associated mechanism in MV uptake. Enhanced MV uptake within the pulmonary microvasculature during systemic inflammation by lung-marginated Ly6C^{high} monocytes could have significant implications for pathogenesis of acute lung injury (ALI) during endotoxaemia.

3.2 Background

Despite recognised role of MV in transcellular exchange of messages, their dynamics in sepsis/SIRS-induced organ injury remains unclear. The distribution of MVs in the circulation, their differential clearance by each organ and cell-specific uptake mechanism within the vascular beds are critical for understanding the contribution of MVs to organ injury from systemic inflammation. However, *in vivo* data of organ- and cell-specific uptake of circulating MVs is relatively limited. Among these studies, liver, lung, spleen and kidney were found to be major organs for MV uptake[397–399,451–455]. Under normal resting conditions, systemically administered MVs were found to be rapidly removed (within 10min) from the circulating blood by organ-resident macrophages of the liver and spleen[397,400]. Yet, little is known of circulating MV uptake dynamics during acute systemic inflammation as *in vivo* trafficking studies evaluated MV uptake only in normal non-inflammatory animals or in cancer models[403–410,456], rather than in systemic inflammatory models.

Our laboratory has previously shown that during subclinical endotoxaemia, the Ly6C^{high} subset of monocytes mobilises from the bone marrow reservoir and marginates to the pulmonary microvasculature. These newly marginated monocytes were functionally primed, responding vigorously to secondary microbial challenges and contributing to the development of ALI[187,291,450]. Interestingly, uptake of circulating fluorescence-labelled bacteria by lung-marginated monocytes was increased during the subclinical endotoxaemia[276], consistent with previous findings in endotoxaemic rats showing increased pulmonary uptake of injected bacteria and inset particles, with a concomitant reduction in their uptake by the liver[457]. Based on these observations, it was hypothesised that during systemic inflammation, lung-marginated monocytes develop an important role in MV trafficking and uptake with potential implications for their biological functions with the lungs.

Using flow cytometry to quantify uptake in individual cells, we observed that uptake of MVs (J774.1 macrophage line-derived) in the lung is low under non-inflammatory resting conditions but that it increased dramatically during LPS-induced subclinical endotoxaemia, attributed to increased uptake by lung-marginated monocytes[1]. Under resting conditions, MVs were predominantly cleared by liver Kupffer cells, and to lesser degree by liver endothelial cells. During subclinical endotoxaemia, Ly6C^{high}

monocytes show a several-fold increase in MV uptake, which together with their increased margination in pulmonary vasculature equated to a substantially increased uptake of MVs by the lungs as compared to liver (Figure 3.1)[1]. Despite LPS-induced inflammation, MV uptake in the lung was relatively low in the less abundant Ly6C^{low} monocytes, much lower in neutrophils, and negligible in endothelial cells and alveolar macrophages. These results suggest that the uptake of MVs by the pulmonary-marginated Ly6C^{high} monocyte during subclinical endotoxaemia could play a critical role in sepsis-induced indirect ALI, where clearance of circulating MVs is redirected from the hepatic to the pulmonary circulation for cell type-specific uptake during inflammation.

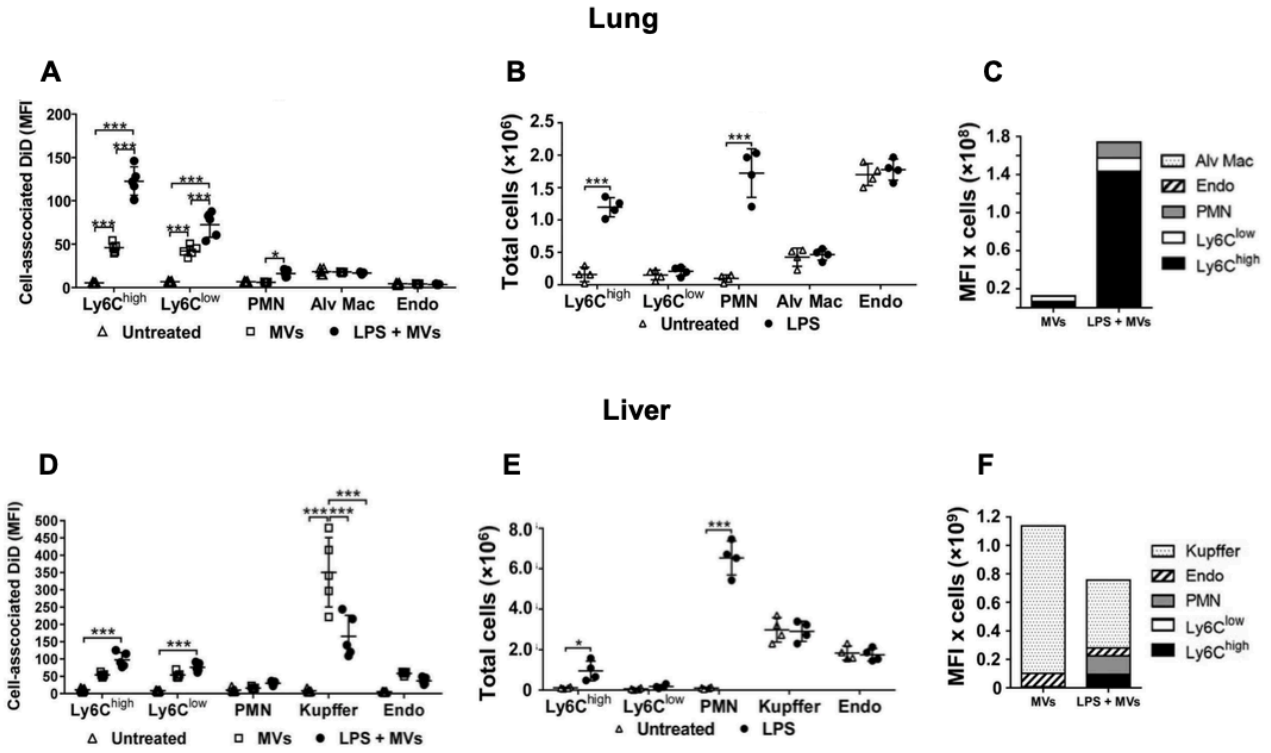

Figure 3.1 Uptake of circulating MVs in the lung (A-C) and liver (D-F) during low-grade systemic inflammation.

DiD-labelled J774A.1 macrophage-derived MVs were injected i.v. via tail vein into untreated or low-dose LPS-treated (20ng, i.v., 2h) mice. At 1h post MV injection, lung and liver were harvested for preparation of fixed single-cell suspension and analysis by flow cytometry. (A, D) Cell-associated DiD fluorescence is indicated (mean fluorescence intensity: MFI) as a measure of MV uptake per cell in each of the cell populations. (B, E) Total number of cells for each cell type investigated in the organ. (C, F) Total uptake of MVs per organ, estimated by calculating the individual cell-associated DiD MFI values (from A or D) × group mean cell counts/organ (from B or E). (Adapted from O'Dea[1])

3.3 Aims

To extend the *in vivo* findings of enhanced MV uptake by lung-marginated monocytes during endotoxaemia, in this study we aimed:

1) To develop an *in vitro* model suitable for determination of the MV uptake dynamics by lung-marginated cells.
2) To identify receptor-dependent mechanisms of MV uptake by lung-marginated Ly6C^{high} monocytes.
3) To evaluate MV uptake by pulmonary vascular cells in an *ex vivo* isolated perfused lung (IPL) model.

3.4 Methods

3.4.1 Induction of subclinical endotoxaemia

For induction of sub-clinical endotoxaemia, C57BL/6 mice received a single i.v. (via tail vein) injection of 20ng LPS for 2h. After 2h, mice were euthanized via anaesthetic overdose and exsanguinated at the femoral artery for confirmation of termination.

3.4.2 Harvesting lung-marginated cells

Untreated or 2h low-dose LPS-treated mice were sacrificed by anaesthetics overdose. Mice were thoracotomised and 20IU of heparin was injected into the right ventricle, followed by cannulation of the pulmonary artery and left atrium. Once the cannulations were established, mice were tracheotomised, and lungs were inflated with 15ml/kg body weight of air to maintain optimal opening of pulmonary microvasculature for perfusion. Lungs were perfused with 4% (v/v) HAS-HBSS at 10ml/h and gradually increased to a constant flow of 50ml/h for 12min until the lungs turn translucently white and 10ml of perfusate was collected. Perfusate cells were washed 3 times with HBSS and resuspended in 0.5% (v/v) HAS-HBSS for experimentation.

3.4.3 MV production *in vitro* and DiD fluorescent-labelling

J774A.1 macrophages were seeded at a density of $6x10^6$ cells in 6mm petri dishes overnight. The next day, adherent cells were washed with PBS and treated with 3mM of ATP for 30min to produce MVs[1]. MVs were isolated by differential centrifugation and resuspended in 0.5% (v/v) HAS-HBSS and labelled with DiD fluorescence for experimentation. DiD-labelled MV fluorescence were quantified for standardisation of MV concentrations in following uptake experiments. See main methods (2.8.1 & 2.8.2) for details.

3.4.4 MV uptake *in vitro*

Washed lung perfusate cells were counted by flow cytometry and each experiment condition is standardised to 50,000 $Ly6C^{high}$ monocytes in 0.5ml ($1x10^5$ $Ly6C^{high}$ monocytes/ml) based on dose-response obtained at initial stage of experimentation. Lung perfusate cells were incubated with standardised amount of fluorescently labelled MVs at 37ºC for up to 1h, with or without pretreatment

of various pharmacological inhibitors or competitive inhibitors (unlabelled MVs or liposomes) on a benchtop rotating wheel (microcentrifuge tube) for continuous mixing. After incubation of perfusate cells with MVs with or without inhibitors, cells were washed and centrifuged at 300 x g for 10min for flow cytometric analysis or processed for confocal imaging.

3.4.5 *In vitro* MV uptake mechanism studies

For energy depletion studies, MVs were either incubated with perfusate cells at 4°C with continuous mixing, or cells were pretreated with energy depletion toxins (10mM Sodium Fluoride (NaF), 0.1% (w/v) Sodium Azide (NaN_3), 1μg/ml Antimycin A) for 15min on ice prior to addition of MVs at 37°C for 1h. For trypsinisation treatment, washed perfusate cells (after MV uptake) were resuspended in 1x trypsin for 5min at 37°C, prior to centrifugation at 300 x g for 10min for flow cytometric analysis. For MV uptake inhibition studies, perfusate cells were pre-incubated with various inhibitors for 15min on ice prior to addition of MVs. Uptake inhibitors used include 2μM Cytochalasin D, 0.25mM Dynasore, 2mM RGDS peptide (or control RGES peptide), 50μg/ml polyinosinic acid (Poly-I) (or control polycytidylic acid (Poly-C)), and 25μg/ml dextran sulphate (D-S) (or control chondroitin sulphate (C-S)). For competitive inhibition experiments, titrated concentration of unlabelled MVs or phosphatidylserine (PS)-liposomes (or control phosphatidylcholine (PC)-liposomes) sized to 100 nm were added simultaneously to perfusate cells at 37°C for 1h. PS-liposomes were formulated with PS and PC at a 1:1 molar ratio and PC liposomes were formulated as PC only using high-pressure argon extrusion (Encapsula NanoSciences, USA).

3.4.6 MV uptake *ex vivo* IPL

MV uptake in IPL was performed with untreated or low-dose LPS-pretreated C57BL/6 mice. In brief, IPL was perfused with 4% (v/v) BSA-RPMI at a rate of 25 ml/kg/min and ventilated with 5%CO_2 at 5cmH_2O PEEP, 6-7ml/kg tidal volume and sustained inflation performed at 25cmH_2O at every 15min interval. Standardised dose of DiD-labelled MVs (240,000FU) were infused into the non-recirculating perfusion circuit of IPL for 1h. Lungs were harvested, and single cell suspension (after 5min fixation to stabilise DiD signal) was prepared for flow cytometric analysis of MV uptake.

3.4.7 Cytospin poly-lysine slides preparation for confocal microscopy

After MV uptake experiment, pulmonary perfusate cells were centrifuged at 300 x g for 10min, resuspended in RBC lysis solution (MACS Miltenyi Biotech, UK) for 10min at RT, washed and fixed in 4% (v/v) paraformaldehyde for 5min at RT. Fixed cells were stained with primary biotin anti-mouse Ly-6C antibodies (HK1.4, BioLegend) at 4°C overnight, followed by Alexa Fluor-488 streptavidin secondary antibodies (BioLegend) for 1h at RT. Cytospin poly-lysine slides (Sigma, UK) were prepared from pulmonary perfusate cell suspension by sedimentation of a total of 5×10^5 cells by cytospin centrifugation at 100 x g for 5min onto poly-lysine slides. Cells were mounted with ProLong™ Gold Antifade Mountant with DAPI (P36931, ThermoFisher Scientific, UK) and analysed by confocal microscopy.

3.5 Results

3.5.1 Production and characterisation of fluorescently-labelled J774A.1 macrophage-derived MVs.

To investigate pulmonary vascular mechanisms of MV uptake, we generated MVs from J774A.1 macrophages by brief stimulation with ATP, a commonly used physiologically-relevant and defined method to generate MVs via activation of the $P2X_7$ receptor inflammatory signalling pathway[449]. After labelling with DiD, MVs were evaluated by flow cytometry. A 1µm upper size gate determined using fluorescent sizing calibration beads (Figure 2.11) and DiD-labelled MVs were identified as APC channel positive events within the 1µm region (R1) (Figure 3.2, A) and sensitive to 0.1% (v/v) Triton X-100 detergent treatment (Figure 3.2, B). MV counts were determined relative to number of AccuCheck 6µm counting beads (R2). As a negative control, mock incubations of DiD in buffer without MVs were performed (PBS-DiD), but this produced relatively insignificant amounts of DiD fluorescence-positive events under the same gating strategy (Figure 3.2, C). The total fluorescence present in DiD-labelled MV preparations was quantified using a fluorescent plate reader and fluorescence unit (FU) was determined (Figure 3.3). Statistical analysis of serially diluted samples showed a linear correlation between MV counts (CD45+, DiD+) by flow cytometry and FU measurement by fluorescent plate reader, indicating a direct relationship between flow cytometry based MV counts and total fluorescence emission of a range of dilutions.

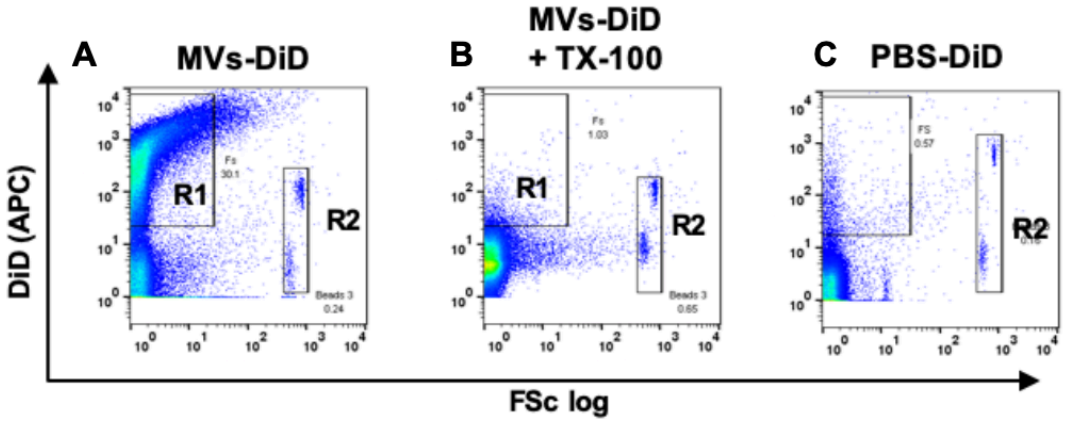

Figure 3.2 Flow cytometric gating of *in vitro*-generated J774A.1 MVs.

J774A.1 macrophages were stimulated with ATP (3 mM, 30min) and the released MVs were labelled with DiD (5μM, 7min, RT) and analysed by flow cytometry. (A) DiD-positive events (R1) was counted using a 1μm gate determined from fluorescent sizing calibration beads and DiD-positive events were all lower than the 6μm diameter Accucheck counting beads (R2). (B) Incubation of samples with non-ionic detergent (0.1% (v/v) Triton X-100) resulted in the disappearance of all DiD-positive events, confirming the dissolvement of their vesicular membrane. (C) As negative control, DiD dye was resuspended in PBS and centrifuged at 20,000 x g for 15min without MVs (PBS-DiD). (Representative figure, n=1)

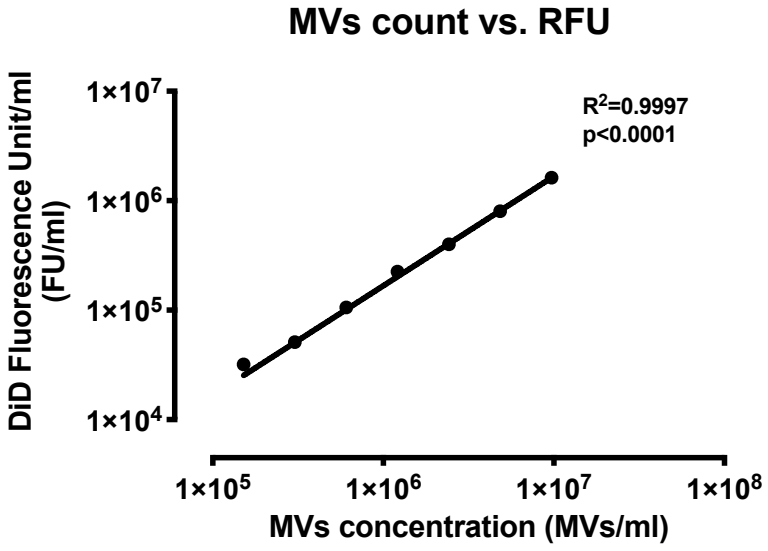

Figure 3.3 Correlation between DiD-labelled MVs count and fluorescence unit (FU).

Total fluorescence of 2-fold serially diluted DiD-labelled MVs were quantified using fluorescence plate reader and number of MVs were counted using flow cytometric analysis. Correlation analysis indicated linearity and correlation (Pearson correlation coefficient) between DiD-labelled MVs fluorescence (FU/ml) and concentrations of DiD-labelled MV determined by flow cytometry (DiD and CD45 double-positive events). (Representative pilot experiment, n=1)

To further characterise the J774A.1-derived MVs, various surface receptor expressions such as CD45 and CD11b were tested for their myeloid origin and annexin V for phosphatidylserine (PS) expression, with their respective isotype controls (Figure 3.4). To differentiate MVs from exosomes, these MVs were also examined for common exosome markers, the tetraspanins such as CD9, CD63, CD81 and the lysosome-associated membrane protein, LAMP2 (Figure 3.4). Although CD9, CD81 and LAMP2 were clearly detectable on EVs, these markers were also expressed at high levels on the plasma membrane of untreated parent J774A.1 cell (Figure 3.4, inset histogram overlays). By contrast, surface CD63 was absent from both MVs and cells. These results suggest the derivation of these MVs from the plasma membrane of their precursor cells, rather than exosomes. Similarities between expression profiles of tetraspanins on MVs and the parental cell membrane have been described previously in other cell lines[458]. Therefore, identity of J774A.1-derived MVs was verified by their size and surface expression of CD45, CD11b and PS for following studies.

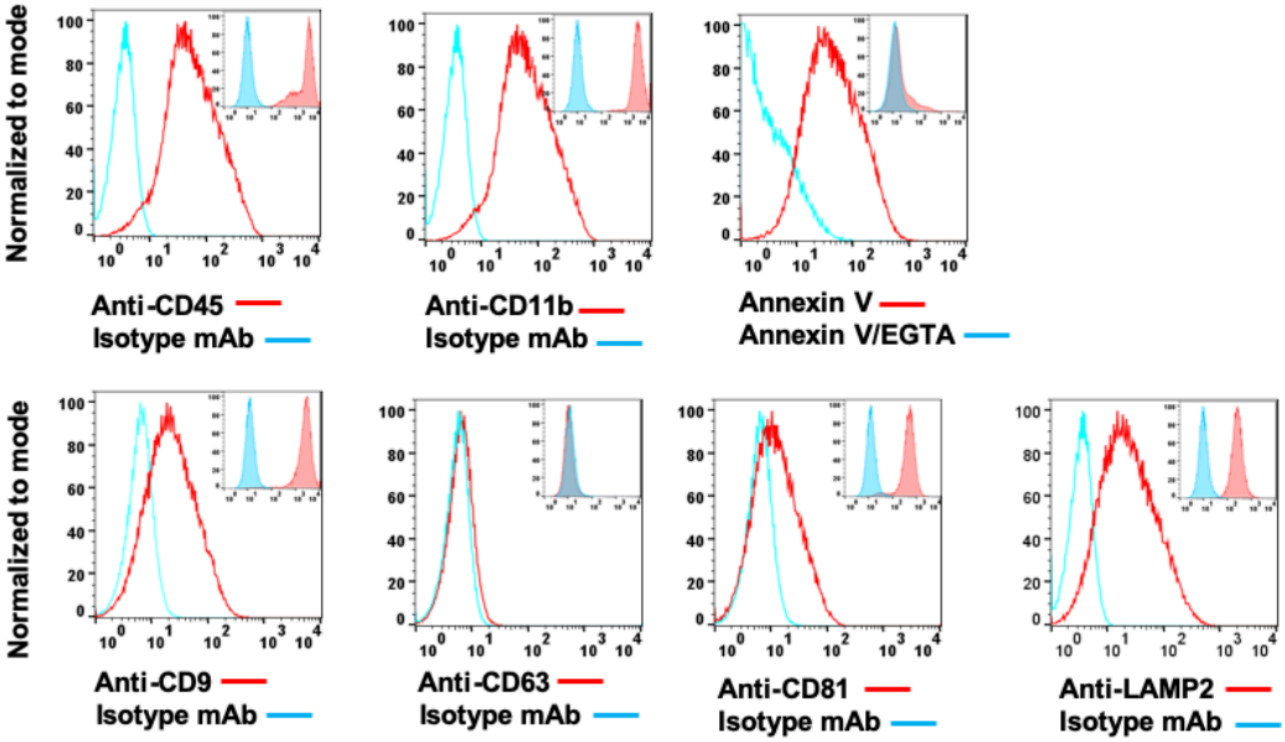

Figure 3.4 Subcellular origin of J774A.1 macrophage-derived MVs.

The subcellular origin of DiD-positive J774A.1 macrophage-derived MVs was assessed by antibody staining against common myeloid cell marker CD45, CD11b and annexin V for phosphatidylserine (PS) expression. The non-exosomal origin of these MVs was also verified by staining against common exosome markers CD9, CD63, CD81 and LAMP2. Expression of these markers on MVs (main histogram overlays) corresponded directly to the expression of these markers on their parental cells (inset histogram overlays), suggesting the derivation of these DiD-labelled MVs from the plasma membrane of their precursor cells. Note that J774A.1 macrophages do express CD9, CD81 and LAMP2, but not CD63 on their surface. (Representative figure, n=1)

3.5.2 Characterisation of pulmonary perfusate cell populations

We investigated the possibility of using pulmonary perfusate preparations harvested from the lung as physiologically relevant and potentially more abundant source than blood. Intravenous injection of low-dose LPS (20ng, 2h) was used to induce subclinical endotoxaemia in mice, which was previously found to induce a maximal recruitment of monocytes to the lungs without inducing obvious clinical symptoms such as lethargy or piloerection[187]. Cellular profiles of pulmonary perfusates obtained from untreated and subclinical endotoxaemic mice were assessed by flow cytometry (Figure 3.5). Compared to untreated mice, the proportions of Gr-1^{high} F4/80- neutrophils and Gr-1^{med} F4/80+ (Ly6C^{high}) monocytes were much higher in perfusates from mice with subclinical endotoxaemia, whereas no difference in the number of Gr-1^{low} F4/80+ (Ly6C^{low}) monocytes in the pulmonary perfusates was observed (Figure 3.6), mirroring previous analysis of using single cell suspension from lung tissue[187]. Numbers of monocytes collected via pulmonary vascular perfusion (enriched for the lung-marginated pool, after IVC exsanguination) in LPS-treated mice was much higher than that obtained via cardiac puncture (i.e. systemic circulating whole blood) (~5x10^5 Ly6C^{high} monocytes in pulmonary perfusate vs. ~1x10^5 Ly6C^{high} monocytes in blood, data not shown), consistent with expansion of the marginated monocyte pool lungs during inflammation[187,291]. Overall, the procedure was successful and could be performed in a rapid and reproducible fashion to recover cells from a physiologically relevant source, with potential to perform multiple assays on MV uptake *in vitro*.

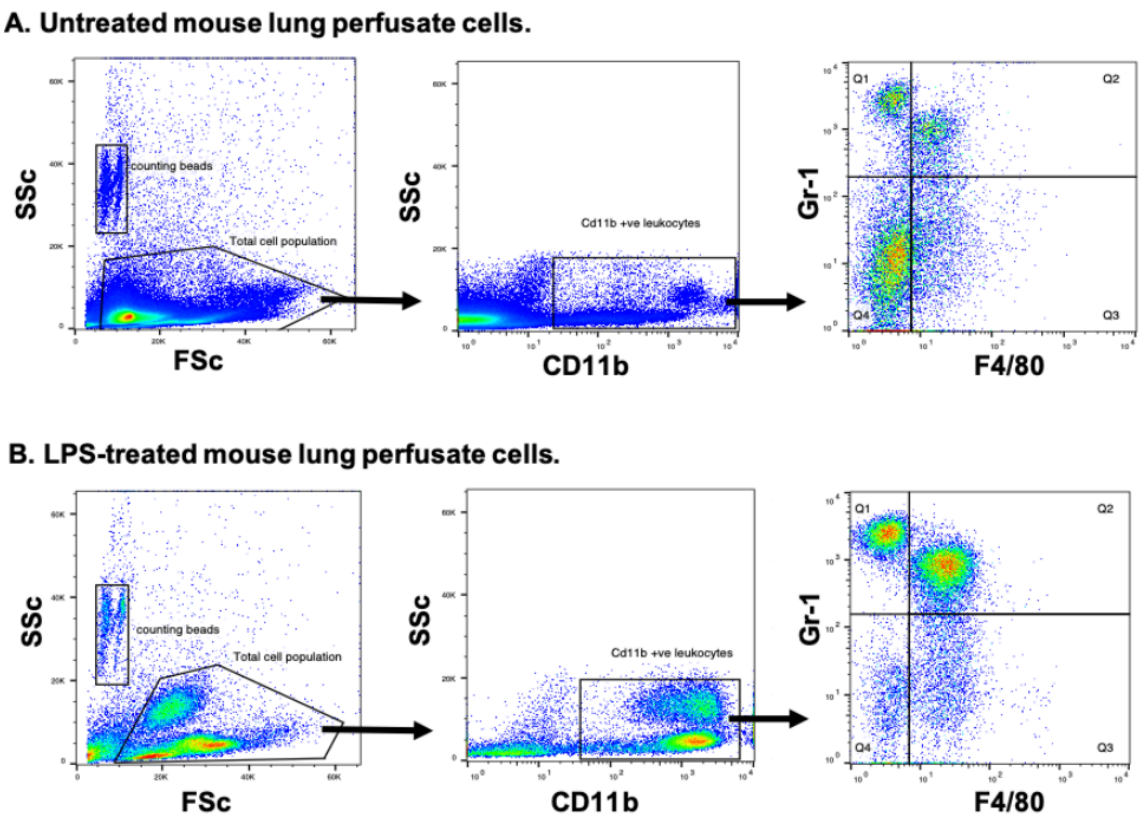

Figure 3.5 Flow cytometric gating of myeloid leukocytes from pulmonary perfusate of untreated and LPS-pretreated mice.

Pulmonary perfusates obtained from untreated and low-dose LPS (20ng, i.v. 2h)-pretreated mice were stained for CD11b, F4/80 and Gr-1 (anti-Ly6C & -Ly6G). Flow cytometry was used to distinguish each cell population based on their surface marker expression: monocytes were identified as CD11b+ and F4/80+ populations and their subsets were gated as Gr1-med (Q2) or Gr1-low (Q3) which differentiates them based on their Ly6C antigen expression. Neutrophils were identified as a CD11b+, F4/80- and Gr-1-high population (Q1). Note: In subsequent experiments, anti-Ly6C and anti-Ly6G Abs were used instead of anti-Gr-1 to differentiate neutrophils more distinctly from monocytes but gating strategies remained similar. (Representative figure, n=1 from each treatment group)

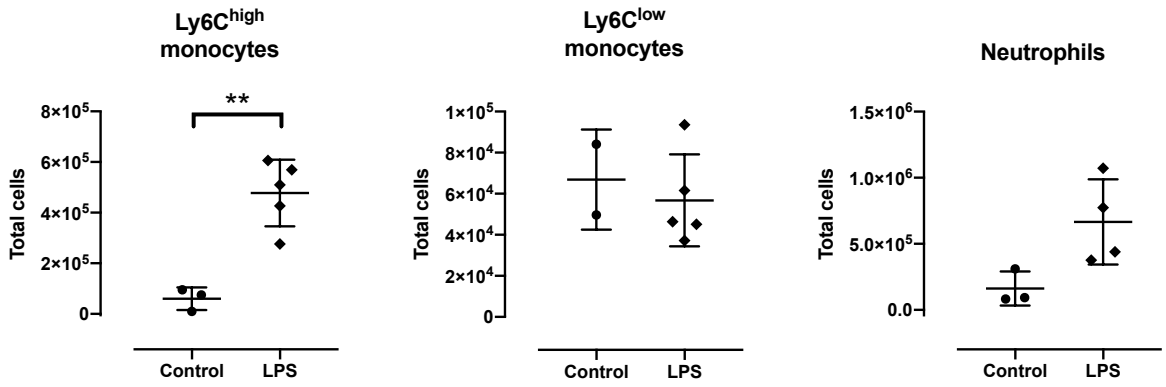

Figure 3.6 Total number of myeloid leukocytes recovered from pulmonary perfusate of untreated and LPS-pretreated mice.

*Ly6C^{high} monocytes, Ly6C^{low} monocytes and neutrophils in the pulmonary perfusates obtained from untreated and low-dose LPS (20ng, i.v. 2h)-pretreated mice were quantified by flow cytometry. Compared to untreated control mice, higher number of Ly6C^{high} monocytes and neutrophils were collected in pulmonary perfusates of low-dose LPS-pretreated mice, whereas no difference in the number of Ly6C^{low} monocytes was observed. (Mean ± SD, n=2-5, *p<0.05, two-tailed unpaired t-tests)*

3.5.3 Characterisation of MV uptake dynamics and kinetics by Ly6C^{high} monocytes *in vitro*

As Ly6C^{high} monocytes were the primary target cell population within the pulmonary vasculature during subclinical endotoxaemia (Figure 3.1), we focussed on their uptake dynamics and kinetics for establishing the *in vitro* uptake model. Pulmonary perfusate from a single subclinical endotoxaemic mice was subdivided into microcentrifuge tube containing standardised number of 5x10^4 Ly6C^{high} monocytes (and other cell types) and co-incubated with different amounts of DiD-labelled J774A.1 macrophage-derived MVs in a final volume of 0.5ml (=1x10^5 Ly6C^{high} monocytes/ml) for 1h (based on *in vivo* method). MV uptake was assessed by measurement of cell-associated DiD MFI using flow cytometry. Ly6C^{high} and Ly6C^{low} monocytes appeared to a reach saturation level at > 2x10^7 MVs/ml), whereas neutrophils uptake of MVs remained relatively negligible up to 1x10^7 MVs/ml (Figure 3.7). Based on this dose response curve, an intermediate concentration of MVs (1x10^6 MVs/ml, or 100,000FU/ml, indicated as dotted line) was chosen for standardisation of all subsequent *in vitro* MV-uptake experiments.

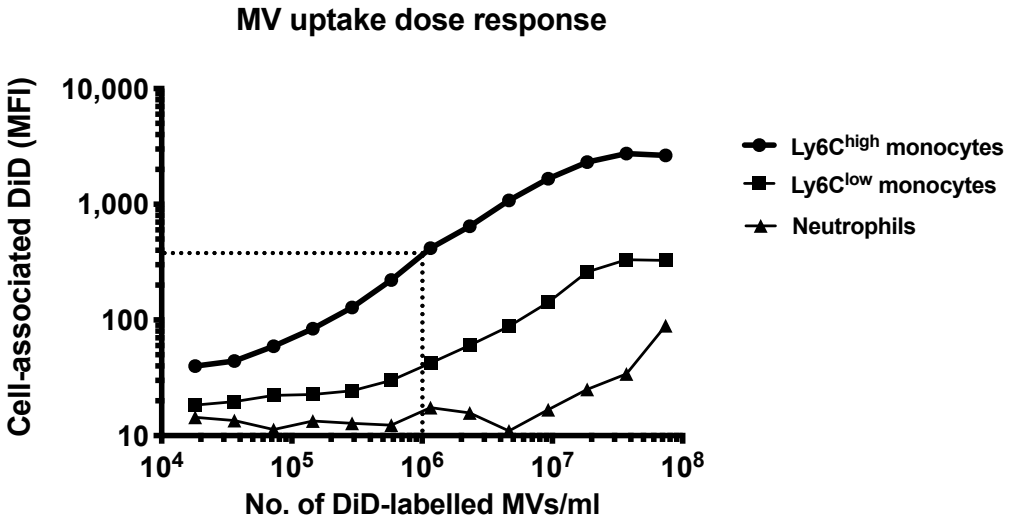

Figure 3.7 Dose response curve of DiD-labelled MV uptake by Ly6C^{high} monocytes.
Pulmonary perfusate cells from subclinical endotoxaemic mice were incubated with increasing concentration of DiD-labelled MVs for 1h. Uptake by Ly6C^{high} and Ly6C^{low} monocytes reached a maximum with 2x10^7 MVs/ml, at ~2500MFI and ~300MFI, respectively. Neutrophils uptake of MVs remained relatively negligible up to 1x10^7 MVs/ml. A moderate concentration of DiD-labelled MVs (1x10^6 MVs/ml, or 100,000FU/ml, indicated as dotted lines) was chosen for all subsequent experiments (Representative pilot experiment, n=1).

Next, we analysed the kinetics of MVs. Pulmonary perfusate from subclinical endotoxaemic mice were incubated with the standardised MV concentration for different intervals up to 1h. MV uptake by Ly6C^{high} monocytes was apparent as early as 20min and reached saturation at 50min and plateaued between after 50min, whereas MV uptake by Ly6C^{low} monocytes and neutrophils remained relatively negligible at this MV concentration throughout 1h incubation (Figure 3.8). Hence, subsequent *in vitro* MV uptake experiments were carried out for 1h using standardised concentration of DiD-labelled MVs (100,000FU/ml), incubated with pulmonary perfusate cells (standardised to contain 1x10^5 Ly6C^{high} monocytes/ml).

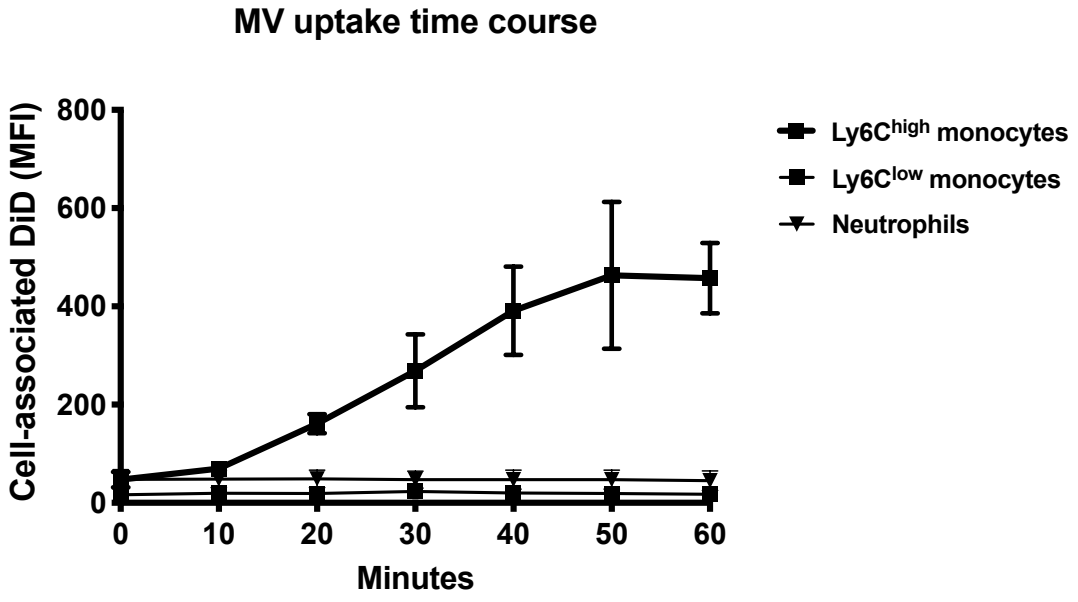

Figure 3.8 Time course of DiD-labelled MV uptake by Ly6C^{high} monocytes.
Pulmonary perfusate obtained from subclinical endotoxaemic mice were incubated with standardised dose of DiD-labelled MVs (100,000FU/ml) for up to 1h. MV uptake by Ly6C^{high} monocytes reached a maximum at 50min and plateaued after. MV uptake by Ly6C^{low} monocytes and neutrophils remained relatively negligible throughout. 1h incubation period was chosen for subsequent experiments. (Mean ± SD, n=3)

To investigate if increased cell-associated DiD fluorescence was a consequence of direct MV-cell interactions rather than transfer of free DiD or DiD dye dissociation from MVs during incubations, competitive inhibition experiments were carried out with unlabelled MVs in increasing concentrations in mixture with the standard concentration of $1x10^6$/ml DiD-labelled MVs (=100,000 FU/ml). Unlabelled and DiD-labelled MVs were added simultaneously to the pulmonary perfusate cells and DiD-labelled MV uptake was assessed in Ly6C^{high} monocytes after 1h. Unlabelled MVs were found to reduce cell-associated DiD levels in a dose-dependent fashion indicating competitive inhibition, where presence of an equivalent amount of unlabelled MVs ($1x10^6$/ml) and DiD-labelled MVs ($1x10^6$/ml) halved the cell-associated DiD-labelled MV uptake from 140MFI to 70MFI, giving rise to a defined half maximal inhibitory concentration (IC_{50}) (Figure 3.9). These results effectively ruled out DiD-associated non-specific artefacts.

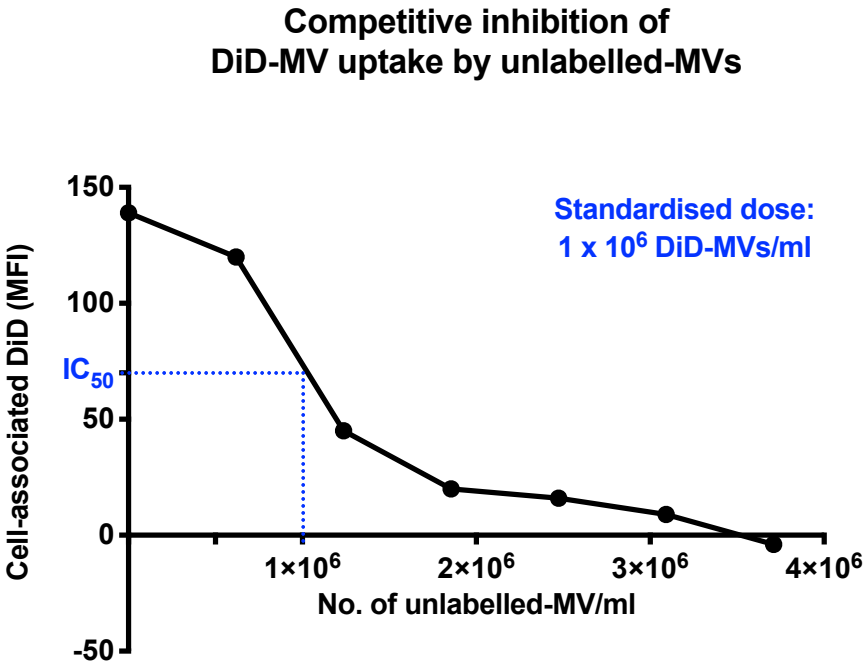

Figure 3.9 Competitive inhibition of DiD-labelled MV uptake in Ly6C^{high} monocytes by unlabelled MVs.

Pulmonary perfusate cells from subclinical endotoxaemic mice were incubated with $1x10^6$/ml DiD-labelled MVs with varying concentrations of non-fluorescently labelled MVs for 1h. DiD-labelled MV uptake by Ly6C^{high} monocytes was halved (from 140 MFI to 70MFI) in presence of $1x10^6$/ml unlabelled MVs (dotted line), suggesting a direct competitive relationship with defined half maximal inhibitory concentration (IC_{50}), negating the possibility of non-specific DiD artefacts (Representative pilot experiment, n=1).

3.5.4 Comparison of MV uptake by pulmonary vascular myeloid leukocyte subpopulations

To further evaluate the specificity and preferential of uptake by Ly6C^{high} monocytes as compared to its counterpart Ly6C^{low} subset during subclinical endotoxaemia, a series of separate experiments were performed. Pulmonary perfusate cells were obtained from either untreated or subclinical endotoxaemic mice and incubated with DiD-labelled MVs for 1h. Low-dose LPS challenge in mice was found to significantly increase uptake capacity of MVs in Ly6C^{high} monocytes (control: 908±574 vs. LPS: 1713±536 MFI), but not in Ly6C^{low} monocytes (control: 572±339.5 vs. 345±445.7 MFI) and neutrophils (control: 63.2±76.61 vs. LPS: 14.2±21.14 MFI) (Figure 3.10). These results with pulmonary vascular cells in isolation suggest that MV uptake capacity of Ly6C^{high} monocytes is enhanced directly by subclinical endotoxaemia, rather than indirect *in vivo*-induced effects such as increased MV availability due to reduced uptake by the liver.

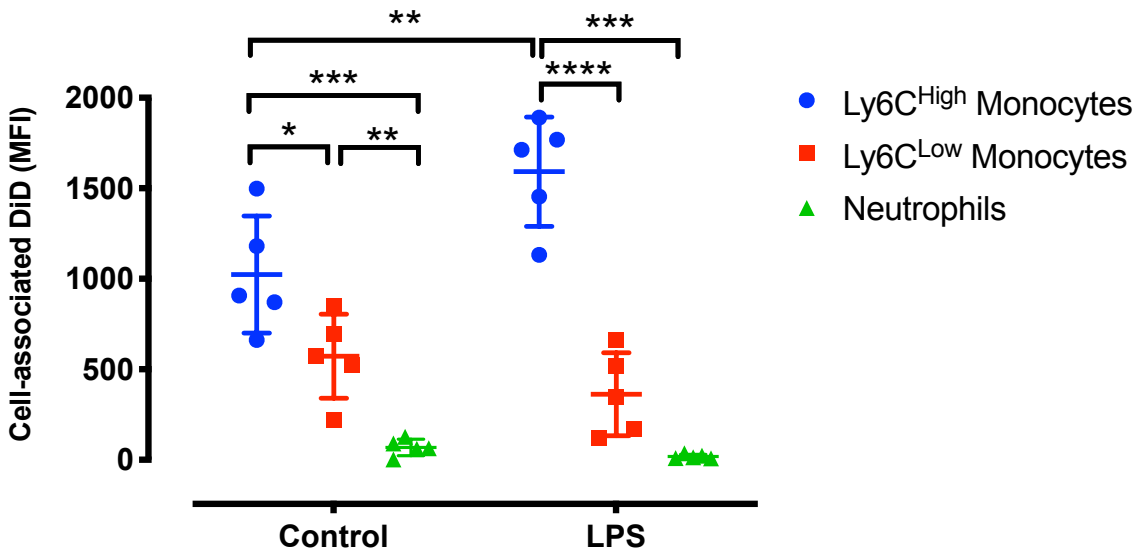

Figure 3.10 Preferential uptake of MVs by lung-marginated Ly6C^{high} monocytes *in vitro*.
*Pulmonary perfusate cells from untreated or subclinical endotoxaemic mice were incubated with standardised dose of DiD-labelled MVs in vitro for 1h. LPS challenge in vivo increased MV uptake capacity of Ly6C^{high} monocytes, but not Ly6C^{low} monocytes and neutrophils. (Mean ± SD, n=5, *p<0.05, **p<0.01, ****p<0.0001, two-way ANOVA with Sidak's multiple comparison test.)*

3.5.5 Mechanisms of MV internalisation by Ly6C^{high} monocytes *in vitro*

The upregulation of MV uptake capacity Ly6^{high} monocytes and expansion of the lung-marginated pool during systemic inflammation indicates the potential for expression of their bioactivity and alternative forms of inflammatory signalling within the pulmonary vasculature. The expression of MVs bioactivity depends on how they interact with and processed by their target cells, with a variety of mechanisms involved, such as surface ligand-receptor interaction, membrane fusion and endocytosis/internalisation[332,371]. Using the *in vitro* pulmonary perfusate model, we investigated MV uptake by confocal microscopy and carried out quantitative analysis of MV uptake in the presence of various inhibitors and treatments by flow cytometry.

For confocal imaging, Ly6C^{high} monocytes were identified by anti-Ly6C antibodies conjugated to green fluorescence, DiD-labelled MV were shown in red fluorescence and the DAPI stained cell nucleus in blue (Figure 3.11). Neutrophils were distinguished from Ly6C^{high} monocytes by their DAPI-stained multi-lobular nucleus and much lower levels of anti-Ly6C antibody staining (data not shown). Clear DiD staining was restricted to Ly6C^{high}-stained monocytes, consistent with flow cytometry data. Monocytes displayed a rounded cell morphology in the absence of MVs incubation, whereas after co-incubation with MVs, plasma membranes of monocytes appear ruffled, suggesting active membrane reorganisation in these cells. Moreover, the DiD signal (red) appear localised within the cytoplasm of monocytes, strongly suggesting that MVs were internalised rather than fused with the plasma membrane. This interpretation was further supported by a 3D reconstruction imaging using z-stack confocal microscopy imaging, where DiD-labelled MVs were shown to be internalised by Ly6C^{high} monocytes in clusters within the cytoplasm (Figure 3.12).

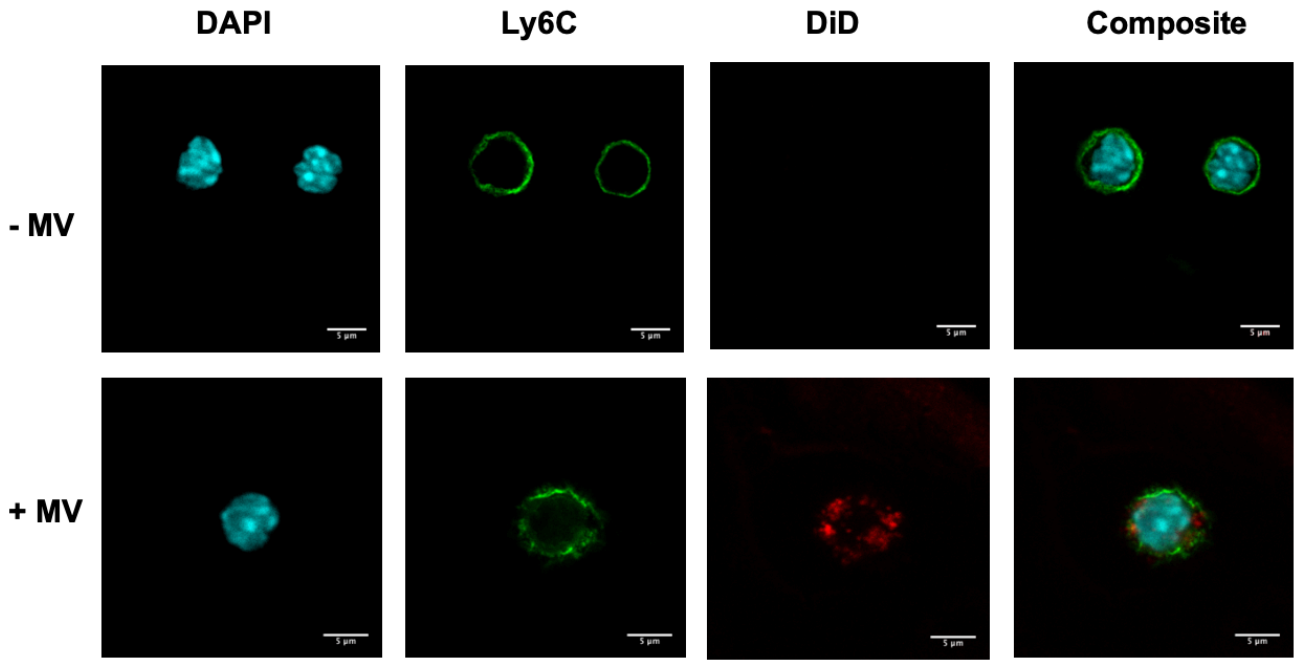

Figure 3.11 Confocal microscopy imaging of MV uptake by Ly6^{high} monocytes

Pulmonary perfusate cells were incubated with DiD-labelled MVs, fixed and stained with DAPI (blue, cell nuclei), and anti-Ly6C Alexa-Fluor 448 antibody (green) was used to identify Ly6C^{high} monocytes. The upper panel shows adjacent Ly6C^{high} monocytes without MV co-incubation as a control, displaying a rounded morphology. The lower panel shows a Ly6C^{high} monocyte after incubation with DiD-labelled MVs (red), where MVs were localised in cell cytoplasm contained within the Ly6C-stained plasma membrane, suggesting internalisation of MVs by Ly6C^{high} monocytes rather than membrane fusion. (Magnification x1000, 5µm scaling bars inset)

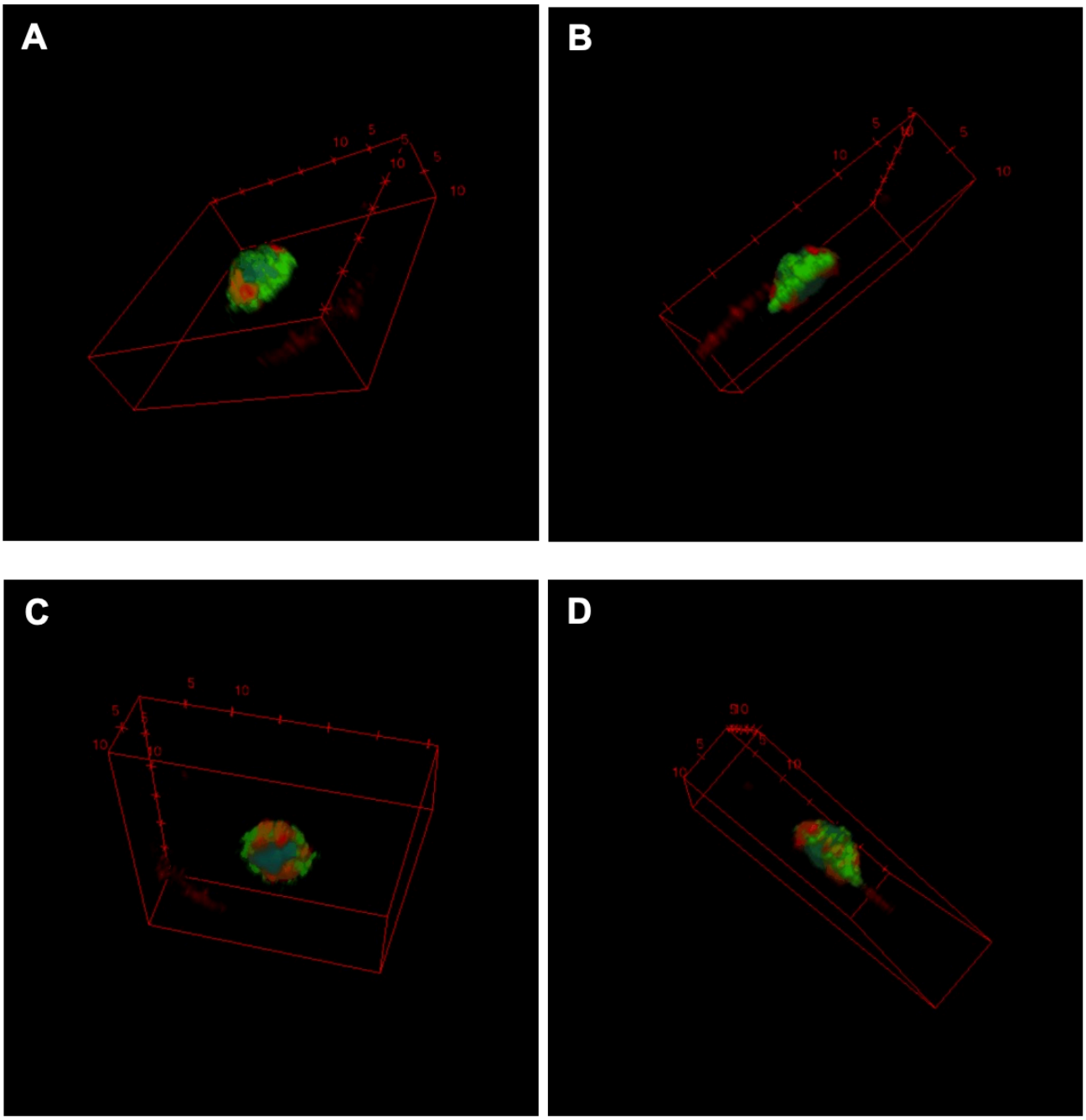

Figure 3.12 3D z-stack confocal microscopy of MV localisation and uptake by Ly6C^{high} monocytes.

Pulmonary perfusate cells were incubated with DiD-labelled MVs, fixed and stained with DAPI (blue, cell nuclei), and anti-Ly6C Alexa-Fluor 448 antibody (green) was used to identify Ly6C^{high} monocytes. 3D Z-stack images were constructed to show 3D localisation of MVs in a single Ly6C^{high} monocyte. (A) view of cell from the front (B) view of cell from the right side (C) view of cell from the back (D) view of cell from the left side. DiD staining (red) shows clusters of MVs localised within the cell cytoplasm, further suggesting internalisation rather than fusion. (Surrounding red box indicates the orientation of the view, as well as for scaling (1 bar = 5µm)) (Magnification x1000)

As an alternative quantitative approach, we investigated MV uptake mechanisms in pulmonary perfusate cells by flow cytometry. Following incubation with MVs, cell were treated with trypsin to remove surface bound MVs as described previously[459], but no effects were observed on levels of Ly6C^{high} monocytes-associated DiD fluorescence, suggesting that majority of MVs were internalised (Figure 3.13), as was evident from confocal imaging shown above. We next investigated whether the uptake of DiD-labelled MVs by Ly6C^{high} monocytes is an active endocytic process, as has been reported for EV uptake in mononuclear phagocytes subpopulations, including monocytes, macrophages and dendritic cells[460–463]. Co-incubation of MVs and perfusate cells at 4ºC reduced MV uptake significantly, suggesting this was an energy-requiring process. This interpretation was further evaluated by measuring MV uptake in the presence of energy-depleting metabolic inhibitors mixture: sodium fluoride (NaF), which inhibits enolase and pyruvate kinase; sodium azide (NaN_3), which inhibits cytochrome c oxidase; and antimycin A, which inhibits cytochrome c reductase. Addition of these inhibitors resulted in complete ablation of MV uptake, indicating that internalisation of MVs by Ly6C^{high} monocytes is an active, energy dependent process, likely to involve endocytic pathways. As endocytosis can occur by various mechanisms, we tested the mechanism of MV uptake with phagocytosis inhibitor Cytochalasin D, which inhibits cytoskeletal function via actin microfilament disruption, and the clathrin-mediated endocytosis inhibitor, Dynasore, which inhibits dynamin GTPase. Both cytochalasin D and Dynasore partially inhibited endocytosis of MVs (~50%). Similar incomplete inhibition has been observed previously in EV uptake studies and can be attributed to the involvement of multiple pathways in MV-cell interaction[461,464–466]. These results together, showed that Ly6C^{high} monocytes internalise MVs via an energy-dependent, active endocytic process, involving both phagocytosis and clathrin-dependent endocytosis pathway.

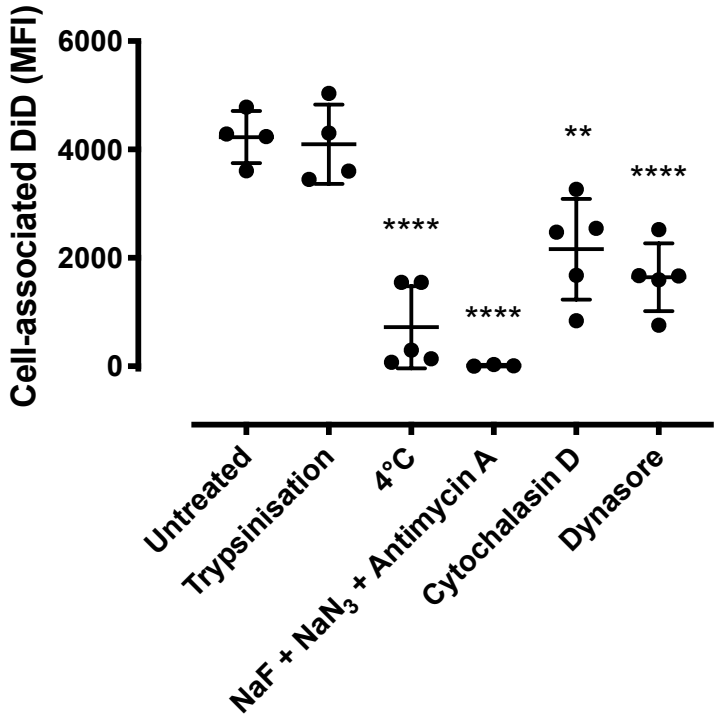

Figure 3.13 Lung-marginated Ly6C^{high} monocytes internalised MVs via active endocytosis.
*Pulmonary perfusate cells from subclinical endotoxaemic mice were incubated with DiD-labelled MV for 1h. The untreated group represents DiD-labelled MV uptake by Ly6C^{high} monocyte without inhibitors at 37°C. Trypsinisation of cells post-incubation with MVs did not reduce Ly6C^{high} monocyte associated DiD fluorescence, indicating that MVs were not cell surface-bound. Incubation of Mvs and cells at 4°C, and in the presence of energy depletion toxin (10mM NaF, 0.1% (w/v) NaN_3, 1μg/ml Antimycin A) at 37°C, significantly reduced MV uptake, indicative of an active energy-dependent process. Pre-incubation of pulmonary perfusate cells with endocytosis pathways inhibitors, Cytochalasin D (2μM) and Dynasore (0.25mM), partially inhibited MV uptake. (Mean ± SD, n=3-5, **p<0.01, ****p<0.0001 vs. untreated, one-way ANOVA with Dunnett's multiple comparison.)*

3.5.6 Receptor-mediated uptake of MVs by Ly6C^{high} monocytes *in vitro*

PS externalisation on the outer plasma membrane leaflet is an essential 'eat me' signal for the phagocytic clearance of apoptotic cells and has also been shown to be a critical determinant of MV uptake by mononuclear phagocytes. As shown by annexin V binding (Figure 3.4), J774A.1-derived MVs have significant levels of exposed membrane PS. Considering the potential role of PS recognition in determining the differences in MV uptake capacity and upregulation between Ly6C^{high} and Ly6C^{low} monocytes during subclinical endotoxaemia (Figure 3.10), we investigated the *in vivo* expression several known PS receptors on lung-marginated monocyte subsets by flow cytometry.

Using lung cell suspensions prepared from either untreated or low-dose LPS (20ng, i.v., 2h) treated subclinical endotoxaemic mice, we measured receptors previously implicated in PS-dependent cell and EV uptake: MerTK, TIM-4, CD51 (α_v integrin), CD61 (β_3 integrin) and β_5 integrin, as well as scavenger receptors including scavenger receptor A (SR-A or CD204), MARCO, SR-B (CD36) and CD68 (Figure 3.14)**.** We found no significant difference in the expression of any of the above listed surface receptors in monocytes between control untreated and low-dose LPS treated mice, however there appeared to be differences between subsets in some cases. Both α_v and β_3 integrin subunits were detected on both monocyte subsets but not β_5 integrin, MerTK and TIM-4. Although α_v integrin subunit was expressed at a similar level on both Ly6C^{high} and Ly6C^{low} monocytes, β_3 integrin subunit was more highly expressed on the Ly6C^{high} subset. For scavenger receptor measurements, higher expression of SR-A (CD204) was detected on Ly6C^{high} monocytes than Ly6C^{low} monocytes, whereas higher expression of SR-B (CD36) was detected on Ly6C^{low} than Ly6C^{high} monocytes. Expression of MARCO and CD68 were below detectable levels in both monocyte subsets.

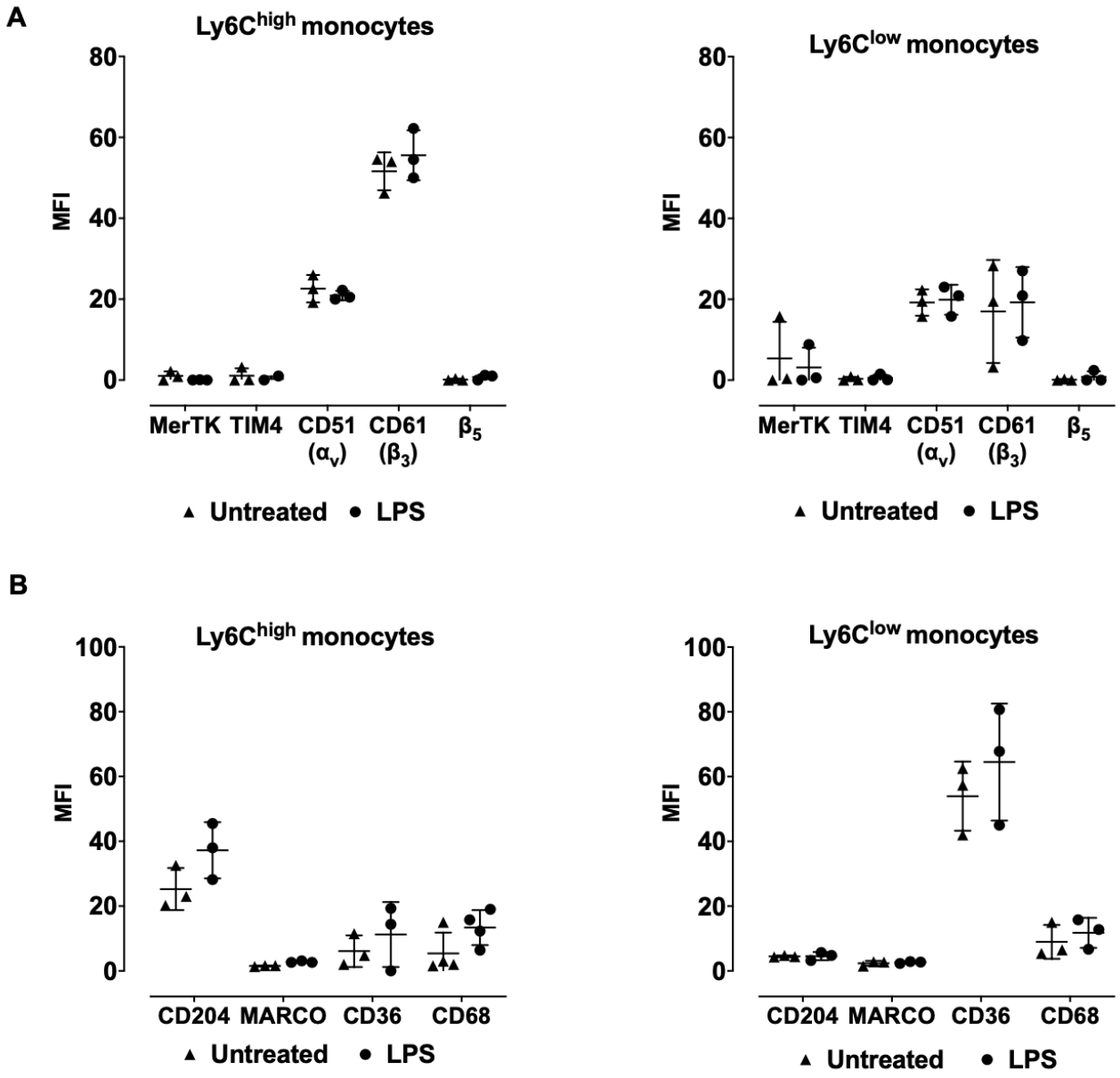

Figure 3.14 Flow cytometric analysis of surface receptor expression on Ly6C^{high} and Ly6C^{low} monocytes.

In vivo expression of PS and scavenger receptors on monocyte subsets were determined in lung single cell suspensions from untreated and subclinical endotoxaemic mice (20 ng, i.v., 2h) by flow cytometry. (A) PS receptor expression. β_3 integrin was expressed at higher levels on Ly6C^{high} than on Ly6C^{low} monocytes, in both untreated and LPS-treated mice. α_v integrin was expressed on both monocyte subset (B) Scavenger receptor expression. Scavenger receptor A (SR-A, CD204) was expressed at higher levels on Ly6C^{high} than on Ly6C^{low} monocytes. SR-B (CD36) was expressed at higher levels on Ly6C^{low} monocytes than Ly6C^{high} monocytes. (n=3).

As Ly6C^{high} monocytes express higher levels of $\alpha_v\beta_3$ integrin and SR-A than Ly6C^{low} monocytes, we considered that PS recognition might be a critical determinant of the differential MV uptake by monocyte subsets. Therefore, we tested the RGD peptidomimetics (integrin blocking peptide) in the MV-cell co-incubation assay to assess the role of the PS-integrin mechanism in MV uptake. We found a substantial reduction in MV uptake by pre-incubation of pulmonary perfusate cells with 2mM RGDS, in comparison to its non-binding control RGES (Figure 3.15). In addition, we found that in the presence of PS-liposomes, MV uptake by Ly6C^{high} monocytes was almost completely inhibited, in contrast to partial but non-significant reductions by PC-liposomes. As Ly6C^{high} monocytes express higher SR-A (CD204) but lower SR-B (CD36) than Ly6C^{low} monocytes, we evaluated MV uptake in the presence of SR-A inhibitors polyinosinic acid (Poly-I) and dextran sulfate (D-S) (Figure 3.16). MV uptake was similarly inhibited by Poly-I and D-S by ~50%, compared to their respective negative control polymers (polycytidylic acid (Poly-C) and chondroitin sulphate (C-S)). These results together suggest that β_3 integrin, possibly in heterodimer with α_v integrin subunit, as well as SR-A, contribute to the mechanism of MV uptake by Ly6C^{high} monocytes via a PS-recognition mechanism, as summarised in schematic below (Figure 3.17).

In addition to integrins and scavenger receptors, there are other adhesion molecules known to be more highly expressed on Ly6C^{high} monocytes, such as L-selectin and PSGL-1, which has been implicated in P-selectin mediated binding of platelets to monocyte-derived MVs[467]. We also found a higher expression of these receptors on Ly6C^{high} monocytes in comparison to Ly6C^{low} monocytes present in lung perfusates from subclinical endotoxaemic mice (data not shown). However, receptor inhibition experiments using unconjugated anti-PSGL-1 and anti-L-selectin blocking antibodies did not alter MV uptake by Ly6C^{high} monocytes, suggesting that this receptor mechanism is not relevant to the MV uptake by lung-marginated monocyte subsets (data not shown).

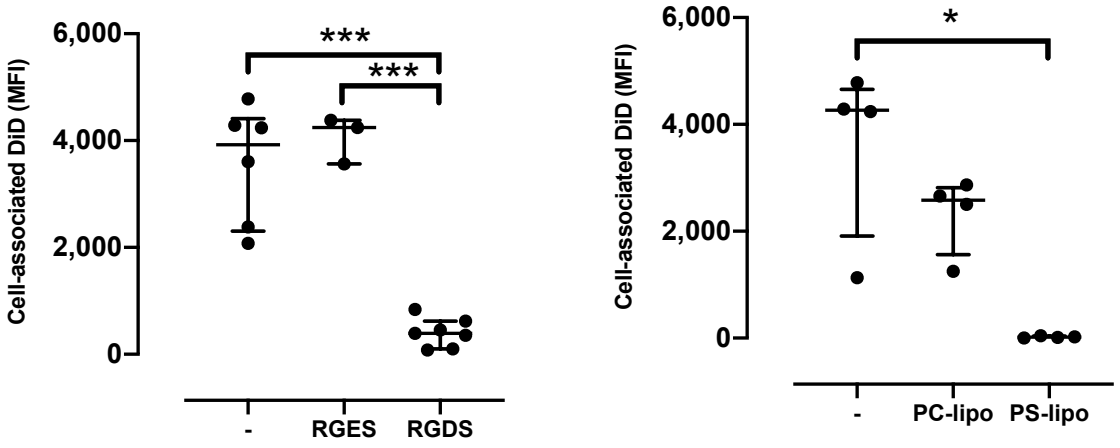

Figure 3.15 MV uptake by Ly6C^{high} monocytes via a phosphatidylserine (PS)-integrin-associated pathway.

*Pulmonary perfusate cells from subclinical endotoxaemic mice incubated with DiD-labelled MV in the presence of either integrin receptor inhibitor RGDS peptide, or competitive PS inhibitor, PS-liposomes (PS-lipo). Uptake of MV by Ly6C^{high} monocytes were partially inhibited by RGDS peptide (2mM), while PS liposomes (0.25mM) abolished MV uptake almost completely, in comparison to controls RGES peptide and phosphatidylcholine-liposomes (PC-lipo), respectively. (Mean ± SD, n=3-7, *p<0.05, **p <0.01, one-way ANOVA with Bonferroni's multiple comparisons test (peptide blocking), Friedman test with Dunn's multiple comparisons tests (Liposomes blocking))*

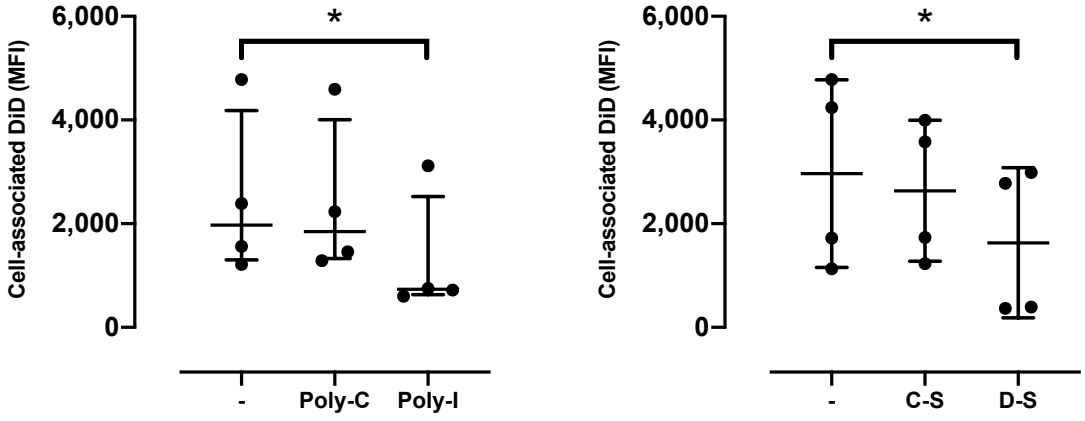

Figure 3.16 MV uptake by Ly6C^{high} monocytes via a scavenger receptor-associated pathway.

*Pulmonary perfusate cells from subclinical endotoxaemic mice incubated with DiD-labelled MV in the presence of two different types of SR-A inhibitors polyinosinic acid (Poly-I) and dextran sulphate (D-S). Uptake of MV by Ly6C^{high} monocytes were partially inhibited by 50μg/ml Poly-I and 25μg/ml D-S, in comparison to their respective controls polycytidylic acid (Poly-C) and chondroitin sulphate (C-S). (Mean ± SD, *p<0.05, n=4, Friedman test with Dunn's multiple comparisons tests.)*

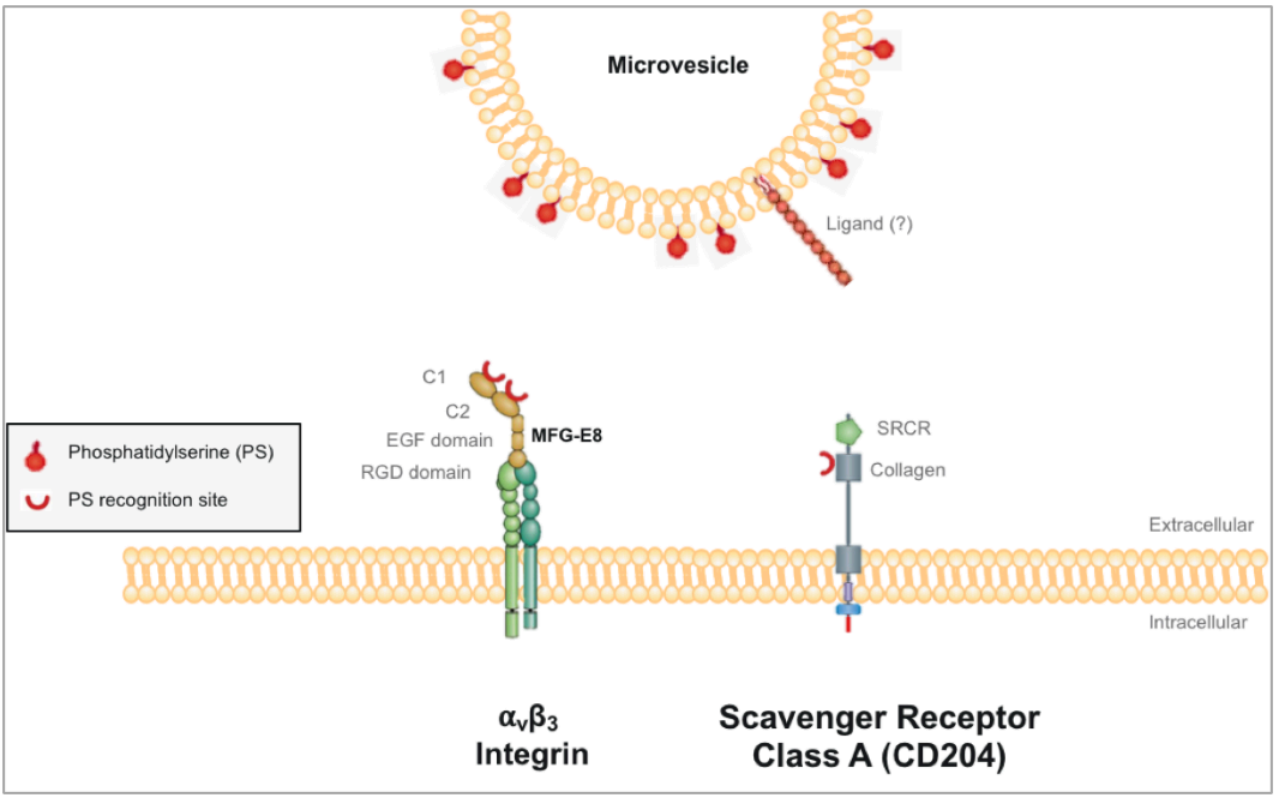

Figure 3.17 Receptor-dependent mechanism implicated in MV uptake by lung-marginated Ly6C^{high} monocytes.

PS-recognition receptor mechanism is involved in the internalisation of MVs by lung-marginated Ly6C^{high} monocytes, implicating the involvement of both $\alpha_v\beta_3$ integrin receptors and scavenger receptor A (SR-A).

3.5.7 MV uptake in the *ex vivo* isolated perfused lung (IPL) model

To further investigate MV uptake within the pulmonary circulation, we used an *ex vivo* isolated perfused lung (IPL) system, to enable the investigation of pulmonary-specific MV interactions by completely eliminating systemic variables. Lungs were isolated from either untreated or subclinical endotoxaemic mice (20ng, i.v., 2h LPS-pretreated) and perfused briefly at slow flow rate for 5min to remove non-marginated cells, mainly residual red blood cells. A standardised dose of DiD-labelled MVs based on DiD fluorescence equivalent to that used in previous *in vivo* studies (240,000 FU), was infused into the closed, recirculating circuit for 1h. Flow cytometric analysis of lung single cell suspensions showed that amongst the pulmonary vascular populations analysed, Ly6C^{high} monocytes were almost the exclusive target of MVs and that uptake, where MV uptake was significantly higher in LPS-pretreated IPL compared to control IPL (Figure 3.18). This increase was substantially higher than the previous *in vivo* studies despite using the same amount of MVs, presumably due to increased MV availability in the absence of systemic clearance by the reticuloendothelial system (RES) in the IPL.

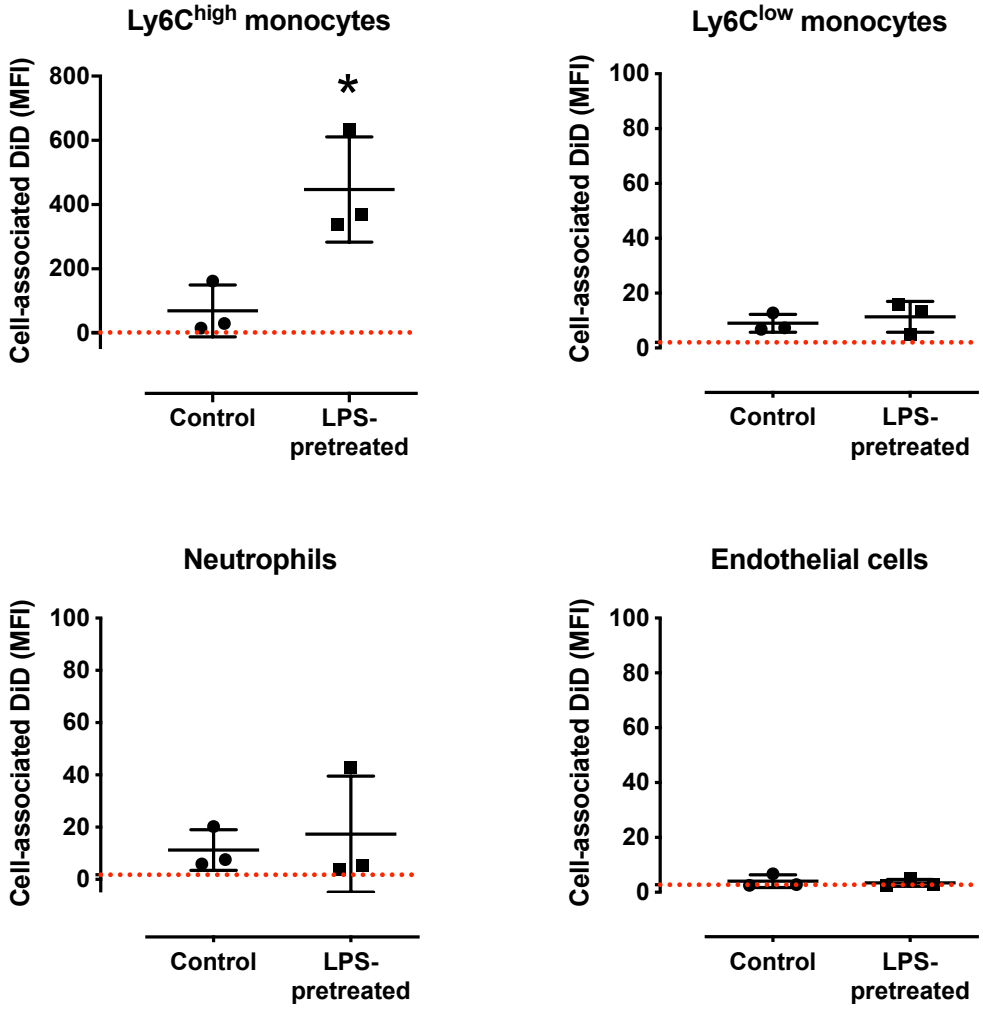

Figure 3.18 MV uptake in the *ex vivo* isolated perfused lung (IPL) model.

*Lungs from normal or low-dose LPS-pretreated (20ng, i.v., 2h) mice were isolated, perfused and mechanically ventilated using the IPL system. After a brief, slow flow-rate flush (5min) to remove non-marginated cells (mainly red blood cells), DiD-labelled MVs (240,000 FU) were infused into the close, non-recirculating IPL circuit for 1h. Lungs were harvested for flow cytometric analysis of cell-associated DiD (MFI), as a quantitative indicator of MV uptake. MV uptake by Ly6C^{high} monocytes was upregulated in the LPS-pretreated IPLs, in comparison to untreated IPLs. MV uptake by other cell types (Ly6C^{low} monocytes, neutrophil and, endothelial cells) were relatively negligible in both untreated and LPS-pretreated conditions. (Mean ± SD, n=3, *p<0.05, two-tailed unpaired t-tests.)*

3.6 Discussion

3.6.1 Summary

This chapter extended our previous *in vivo* findings on monocyte-dependent redistribution of MV uptake from the hepatic to pulmonary circulations under systemic inflammatory conditions. Based on previous in vivo studies (Figure 3.1), we further hypothesised that the decreased uptake of MVs in liver Kupffer cells during subclinical endotoxaemia was due to increased uptake by the expanded population of lung-marginated Ly6C^{high} monocytes. To address this question and to define the uptake process, novel methodologies were developed to harvest the large numbers of lung-marginated Ly6C^{high} monocytes for *in vitro* studies. In addition, I re-established the *ex vivo* IPL system within the research group as a model to assess 'pulmonary-specific' MV uptake. These approaches enabled the investigation of detailed mechanisms involved in MV uptake and opens up a new opportunity to investigate the effect of MVs in lung inflammation/injury during subclinical endotoxaemia using IPL in subsequent follow up studies. The results obtained supported our previous *in vivo* observation of cell type-specific MV uptake by Ly6C^{high} monocytes, and further elucidated the mechanisms involved. Key findings from this chapter include: 1) Lung-marginated Ly6C^{high} monocytes has a subset-specific, preferential increase in its capacity to take up MVs during systemic inflammation, 2) MV uptake by lung-marginated Ly6C^{high} monocytes is an active, energy-dependent endocytic process, 3) MV uptake by lung-marginated Ly6C^{high} monocytes is regulated via a PS-recognition mechanism and involved co-participation between $\alpha_v\beta_3$ integrin receptor and scavenger receptor A, 4) IPL results showed that systemic injection of LPS enhanced MV uptake by lung-marginated Ly6C^{high} monocytes "per se", irrespective of the *in vivo* effect of systemic clearance on the availability of circulating MV.

3.6.2 *In vitro* MVs generation and characterisation

ATP signalling through $P2X_7$ receptor pathway produces rapid translocation of PS from the inner leaflet to the outer leaflet of plasma membrane, which precedes the blebbing and release of MVs from cells[468]. In this study, we generated MVs from an *in vitro* macrophage cell line via extracellular ATP stimulation[449], as a physiologically relevant method for acute, non-apoptotic release of MVs *in vitro*[469]. Our isolated MV preparations were enriched by differential centrifugation method that included an initial low-speed centrifugation step (300 x g, 10min) to remove cells, whilst ensuring maximum

recovery of larger MVs within the whole population, followed by high-speed centrifugation step (20,000 x g, 15min) to remove exosomes. Although initial centrifugation at higher speeds (e.g. 1500–2000 × g) are often used for removal of cell debris, larger EVs (e.g. apoptotic bodies) and platelets, they have been shown to reduce MV recovery substantially (~75%), presumably due to overlapping density and their associated sedimentation rates. To exclude cell debris as well as constitutively released EVs from preparations, multiple rinses of the adherent J774A.1 adherent cultures were carried out, prior to MV generation. Nonetheless, as EVs contain subpopulations of vesicles with overlapping sizes, each EV subpopulations could not be distinctively isolated from each other by differential centrifugation. With MVs being the 'middle-sized' EVs, where their size range falls in between that of their smaller counterpart exosomes and larger counterpart apoptotic bodies, our MV preparation may contain some 'contamination' with exosomes and apoptotic bodies, and, as such, posing an inevitable limitation in studies using isolated MVs.

Traditionally, it has been thought that the difference between exosome and MV biogenesis causes them to carry distinct surface markers from those seen on the surface of MVs[322]. However, the specificity of some exosomes markers were questioned in recent years, as the expression of tetraspanins CD9, CD63, CD81, and ESCRT components TSG101, VPS4 and Alix, were shown to be commonly expressed by both exosomes and MVs[328,329]. In this study, the use of tetraspanins to distinguish exosomes from MVs were further complicated by the expression of these tetraspanins on the parental J774A.1 macrophage cell line, making it less useful in the identification or isolation of an absolute MVs population. Moreover, PS, a marker traditionally used to identify MVs, were also found to be expressed by some exosomes[326,327,352], and in some cases, not expressed by some MVs[343–348]. For these reasons, here we chose to refer to EVs within the size range of <1μm detectable by flow cytometry, which expresses their parental cell marker, in this case CD45 and CD11b, as MVs rather than exosomes, based on their 'right-side-out' membrane orientation characteristics during formation.

3.6.3 Physiological relevance of *in vitro* MV-pulmonary perfusate cell assays

Our strategy to derive large numbers of Ly6C^{high} monocytes from the anatomically appropriate site by pulmonary perfusion represents a novel and robust method to study the intravascular uptake of MVs

by lung-marginated cells *in vitro*. In contrast to the use of circulating blood, cells harvested via pulmonary perfusion are not only more likely to reproduce the *in vivo* biological properties of lung-marginated cells, but with respect to Ly6C^{high} monocytes during endotoxaemia, they are 5 times greater in number than that present in circulating blood (~5x10^5 Ly6C^{high} monocytes from pulmonary perfusate vs. ~1x10^5 Ly6C^{high} monocytes from cardiac puncture)[1,187]. This difference relates to the preferential margination of monocytes to various microvascular beds, particularly the lungs, during inflammation where their numbers in circulating blood are often reduced to very low levels, producing monocytopenia[171,187,266,291].

In contrast to isolated monocytes cultures, pulmonary perfusates comprising of a mixed population of cells including erythrocytes, platelets and leukocytes, preserved the natural *in vivo* cellular profile, allowing a degree of 'competition' in MV uptake experiments *in vitro*. Our initial dose response curve showed that MV uptake by other cell types such as Ly6C^{low} monocytes and neutrophils reached different levels of saturation at a distinct concentration compared to that of Ly6C^{high} monocytes. Although MV uptake by neutrophils remained negligible at relatively lower concentrations of MVs, they were found to start taking up MVs under higher MV concentration, despite reaching saturation at a much lower scale. The use of a standardised, moderate MV concentration for 1h incubation period for the subsequent quantitative studies avoided over-saturation of these *in vitro* MV-cell assays. The rapid uptake kinetics observed here, which was diminished at low temperature and with endocytosis inhibitors, suggested an indispensable active, energy-dependent uptake process. Together, the characterisation of MV uptake using pulmonary perfusate containing mixed cell types, combined with incubation with MV at a relatively physiological level within acute timeframe (<1h) highlighted the significance of our findings on the monocyte-subset specificity in MV uptake. Based on these considerations, the physiological relevance of studies on MV clearance and relating to vascular cells, where a single *in vitro* cell line or primary cell type is used[398,416,470], or with prolonged period of co-incubation[471],should be interpreted with more caution.

3.6.4 Endocytic mechanism of MV uptake

An active endocytic process has been widely reported for EV uptake in mononuclear phagocytes, including monocytes, macrophages and dendritic cells[460–463]. In this study, we demonstrated that Ly6C^{high} monocytes internalise MVs via clathrin- and dynamin-dependent endocytosis. In line with these findings, the uptake of synthetic nanoparticles and microparticles by various cell lines such as tumour epithelial cells, human monocytes and macrophages, were previously shown to be mediated via the same mechanisms[466,472]. Interestingly, the presence of serum was found to significantly reduce the uptake of these particles, potentially due to the formation of protein corona around the surface of these particles, modifying their surface properties and their particle-cell interaction[472,473]. However, compared to synthetic nanoparticles and microparticles, much less is known regarding the formation of protein corona on biological EVs (exosomes and MVs)[474]. As all of our MV uptake experiments were carried out under serum-free conditions, the effect of serum on the uptake of MVs were not explored in this study, potentially posing a limitation in its physiological relevance when compared to *in vivo* where circulating MVs were constantly in contact with serum and other plasma components. Nonetheless, under these serum-free *in vitro* conditions, the relative differences in MV uptake between monocyte subsets and the increases due to subclinical endotoxaemia (Figure 3.10) were similar to those found in vivo previously (Figure 3.1), further consolidating the physiological relevance of these findings.

3.6.5 Receptor-mediated MV uptake by Ly6C^{high} monocytes

Translocation of PS to the outer plasma membrane is a fundamental process to the blebbing of MVs from its parental cell and the recognition of PS is likely to be a key mechanism of MV uptake by various cell types such as macrophages[416], endothelial cells[398] and human monocytes[475]. A subset of RGD motif-binding integrin receptors (i.e. $\alpha_v\beta_3$ and $\alpha_v\beta_5$) have been indicated in the detection and engulfment of apoptotic cells[476] and MVs[405] by tethering PS to their RGD-binding motif via bridging molecules such as MFG-E8 (lactadherin)[416,418,477,478] or developmental endothelial locus-1 (Del-1)[398,479,480]. The higher expression of β_3 integrin detected on Ly6C^{high} monocytes than on Ly6C^{low} monocytes, as well as the partial inhibition of MV uptake by RGDS peptide in this study, implicated

the participation of the PS-integrin associated pathways, via bridging molecules such as lactadherin and Del-1.

Despite previous findings showing higher expression of SR-A (CD204) on Ly6C^{low} monocytes than Ly6C^{high} monocytes[167], our receptor expression data showed the contrary, potentially due to the difference in the activation status of monocytes (systemic circulating pool vs lung-marginated monocytes pool). Although SR-B (CD36) has previously been implicated in the uptake mechanism of endothelial-derived MVs by platelets[481], its expression level on Ly6C^{high} monocytes were much lower than that on Ly6C^{low} monocytes. Interestingly, another class A scavenger receptor, MARCO, was implicated as the primary receptor in the uptake of negatively-charged MVs by Ly6C^{high} monocytes[482], despite its low expression levels detected here in this study and in the literature[472]. Although MARCO could also be a target of polyinosinic acid and dextran sulphate in the MV uptake inhibition study alongside with CD204, its low expression level on Ly6C^{high} monocytes detected here suggested a stronger role for CD204 in this SR-mediated uptake mechanism.

3.6.6 MV uptake by Ly6C^{high} monocytes in the *ex vivo* IPL model

The study of MVs uptake using the IPL model enables the evaluation of MVs uptake by Ly6^{high} monocytes within their *in vivo* physiological environment in the pulmonary circulation, without the systemic clearance effect exerted by the liver and spleen. Using this model, we verified the direct effect of inflammation on the upregulation of MV uptake capacity in Ly6C^{high} monocytes and demonstrated that subclinical endotoxaemia induced a switch in MV uptake to an alternative pathway involving newly-marginated monocytes in the lungs. Direct biological effects of MVs on monocytes were previously demonstrated *in vitro*, where MVs were shown to induce cytokine expression, differentiation patterns and phenotypic polarisation on monocytes[377,449,483–485]. In mice, lung-marginated, Ly6C^{high} monocytes were shown to play a central role in the development of pulmonary vascular inflammation and acute lung injury[187,291,294,295,297]. Therefore, the margination of Ly6C^{high} monocytes during endotoxaemia and its increased ability to take up MVs could potentially have implications in the pathophysiology of sepsis-induced indirect ALI.

3.8 Conclusion

To understand the cellular and molecular biology involved in the uptake of MVs during inflammation, in this chapter we investigated the mechanisms of MV uptake by lung-marginated monocytes *in vitro* and their uptake dynamics in *ex vivo* IPL, using a generic source of MVs generated from J774A.1 macrophage cell line. In this study, we successfully characterised a PS-associated receptor mechanism in the uptake of MV by lung-marginated Ly6C^{high} monocytes. Although this monocyte subset-specific homing of MV uptake to the lung during systemic inflammation may be relevant to the development and evolution of ALI, the use of an *in vitro* cell line-generated MVs may not be representative of the *in vivo* endogenously produced MVs during systemic inflammation. Therefore, further functional studies using a disease-relevant, *in vivo*-derived endogenous MVs are necessary to establish their physiological relevance in ALI.

Chapter 4

Characterisation of MV production in clinically relevant animal models of extrapulmonary inflammation

Parts of the content of this chapter have been presented as a conference abstract:

Investigation into the Roles of Circulating Microvesicles Within the Pulmonary Vasculature Using Ex Vivo Isolated Perfused Lung. *Y. Y. Tan, K. P. O'Dea, A. Pac Soo, M. Takata. American Journal of Respiratory and Critical Care Medicine 2019; 199: A7317.*

Chapter 4 Characterisation of MV production in clinically relevant animal models of extrapulmonary inflammation

4.1 Abstract

Background

Sepsis/SIRS and acute kidney injury (AKI) are two most common extrapulmonary causes of acute lung injury (ALI). Here, we compared the production of circulating MV subtypes between intravenous LPS as a model of endotoxaemia, and kidney ischaemia reperfusion injury (IRI) as a model of AKI. The models were also combined to assess potential modifications of the MV response in a sepsis-related single peripheral organ injury. Our aim was to provide new insights into MVs as long-range signalling messenger in the propagation of systemic inflammation and distant organ injury to the lung, as potential crucial mediator in the development of ALI.

Methods

For kidney IRI, unilateral renal ischaemia was conducted in C57BL/6 mice via application of vascular clamp on left renal artery and vein, or mice was sham operated as control. After 30min ischaemia, the kidney was reperfused for 1h. For endotoxaemia model, mice were injected with moderate 2μg dose of LPS via tail vein for up to 4h. For the combined model, unilateral renal ischaemia was performed on low-dose LPS (20ng, i.v., 2h)-pretreated mice. After each procedure, blood was collected, and the platelet-poor plasma processed for MVs analysis by flow cytometry.

Results

Unilateral renal ischaemia induced a significant increase in the circulating levels of platelet- and endothelial-MVs. Smaller but significant increases were observed in neutrophil- and monocyte-MVs, alongside with significant increased number of neutrophils and Ly6C^{high} monocytes in the ischaemic kidney at 1h post-ischaemia reperfusion. Pretreatment of mice with low-dose LPS prior to kidney IRI increased numbers of marginated neutrophils and Ly6C^{high} monocytes in the ischaemic kidney and the lungs further, but significantly reduced the circulating levels of endothelial- and platelet-MVs. In the endotoxaemia model, systemic LPS injection produced significant increases in circulating neutrophil- and monocyte-MVs at 1h post-LPS and their levels remained sustained up to 4h. In contrast, MVs from other vascular cell types (endothelial-, platelet- and erythrocytes-derived) remained relatively unchanged from normal untreated control levels throughout.

Conclusion

The MV subtype production profiles were distinct between the models of systemic inflammation and sterile local organ injury. Further functional studies investigating the activity of these *in vivo*-generated MVs are warranted in understanding their respective roles during pulmonary vascular inflammation and their involvement in the disease pathogenesis of indirect ALI.

4.2 Background

Experimental modelling of ALI *in vivo* has long been focussed on recreating features of human ARDS in animal models, utilising a variety of overwhelming infectious and injurious insults including caecal ligation puncture (CLP) model of sepsis, acid aspiration and high-volume mechanical ventilation. However, as it is now appreciated that not one animal model of ALI is able to recreate all features of human ARDS, merely aiming to recreate specific end-stage features of ARDS may hinder further understanding of the disease pathogenesis. Especially in recent years, as direct and indirect ALI are widely recognised as two distinctive forms based on their underlying causes, it is more important to utilise relevant animal models representative of their respective underlying pathogenesis. Based on the findings demonstrated in Chapter 3, we developed a central hypothesis that MVs released during extrapulmonary inflammation plays a crucial role in inducing pulmonary inflammation via increased interaction with lung-marginated monocytes, contributing to indirect ALI.

To obtain definitive insights into MV function within the pulmonary vasculature, we included two key criteria in the modelling strategy: (1) provision of *in vivo* generated circulating MVs as an optimal source for functional studies and (2) focus on IPL as a model of ALI to define pulmonary-specific MV effects, eliminating any remotely or systemically generated responses to circulating MVs. Here as the first step of the two-part modelling strategy, we aimed to evaluate two distinctive models of extrapulmonary inflammation, which are clinically relevant to the contribution of indirect ALI, and to characterise the production of circulating MVs therein. As peripheral organ injury and endotoxaemia are common causes of indirect ALI, we chose renal ischaemia reperfusion injury (IRI) and intravenous LPS model, and combination of both, to simulate extrapulmonary inflammation contributing to indirect ALI in this investigation.

4.2.1 Acute kidney injury-induced ALI

Acute kidney injury (AKI) is a severe condition, where secondary injury in the lung is most frequently presented as a common complication amongst other associating distant organ dysfunction[486,487]. The development of lung oedema from AKI can result from either cardiogenic or non-cardiogenic causes, attributed to either elevated left atrial pressure, or increased pulmonary capillary permeability due to

inflammation[488]. Renal IRI is a well-established component in AKI leading to inflammatory cascades, resulting in non-cardiogenic pulmonary oedema and inflammation[489–491]. Despite the implication of soluble cytokine release and apoptotic signalling in the cascade of events leading from AKI to ALI[492–494], the inflammatory mechanism of AKI-induced ALI is not fully understood. *In vivo* studies of AKI-induced ALI often require severe renal failure to induce minor evidence of lung injury, produced mainly via bilateral renal ischaemia for extended periods or bilateral nephrectomy[494–498]. The induction of lung oedema by bilateral nephrectomy indicates that in addition to renal IRI, uraemic toxin accumulation from the loss of renal function is also involved in eliciting pulmonary injury[498]. However, the lung is also susceptible to IRI in other organs such as the liver, intestines, gut and hind limb[499–502], suggesting that the IRI component of AKI is a significant contributor to indirect ALI, independently of secondary renal failure effects.

Interestingly, elevated level of endothelial-derived MVs have been found in renal failure patients[503,504] and the release of inflammatory MVs has been proposed as a pathogenic factor in renal IRI-induced ALI[490]. Whilst the release of MV has been characterised in hepatic[357,505], cardiac[452] and hind limb[335] models of IRI *in vivo*, MV studies in kidney-associated injury have focussed mainly on the role of MSC-derived MVs in renal repair and recovery[506–509]. No supporting studies have demonstrated the pro-inflammatory effect of MVs released during renal IRI in indirect ALI. Despite evidence of inflammatory mediators released in the circulation and leukocytes margination to the lungs after renal IRI[510–512], the inflammatory mechanism involved in the kidney-lung crosstalk remained elusive. Activation and apoptosis of *in vitro* lung endothelial cells were observed when treated with serum of mice that underwent bilateral renal ischaemia procedures[494,513], though it is unclear which component in the serum elicited this response. We hypothesised that MVs are released locally at the site of injury during kidney IRI, enter the pulmonary circulation via the venous return and plays a key role in mediating AKI-induced ALI via interactions with lung-marginated cells or the pulmonary endothelium.

4.2.2 Sepsis-induced ALI

Sepsis is a well-known underlying risk factor in the development of ALI. Experimental models of endotoxaemia induced by CLP or intravenous/intraperitoneal administration of LPS in rodents are

most commonly used to emulate human sepsis as both models cause a hyperinflammatory state that entails the release of a variety of soluble mediators. However, the kinetics and magnitude of cytokine production profiles differ significantly between these two models. In LPS injection model, plasma cytokine release peaked within early timepoints after injection, whereas CLP induced cytokine release that continued over the course of 48h[514,515]. Although it has been suggested that the cytokines production profile in CLP model mimic human sepsis more accurately, it is now appreciated that CLP produces only a very mild degree of ALI before mice die due to sepsis itself. Moreover, the biological complexity of the CLP model makes it unsuitable for studies that require clear distinction between bacterial products and host-derived mediators. In contrast, LPS has been shown as a pivotal trigger of gram-negative sepsis and the associated lung injury, representing a much more feasible and reproducible model of sepsis or endotoxaemia.

In recent years, there has been an increasing focus on the role of MVs as biomarkers of sepsis or SIRS[371], including that derived from platelets[421–424], leukocytes[380,425–428] and endothelial cells[429–431]. Where quantitative comparisons of MV subtypes has been undertaken, myeloid-, and primarily neutrophil-derived MVs were the most acutely increased subtypes in sepsis/SIRS patients[420,421,427,516], suggesting relationships with the disease pathogenesis. However, as MVs are produced rapidly in response to inflammatory stimuli and their effects exerted during early stages of disease development, the characterisation of MVs obtained from substantially ill patients may provide little to no information on their actual biological activities. Yet, data on MV production during the prodromal period in SIRS patients is not available. Although LPS treatment in human volunteers indicated an increase in circulating MV level within hours[438], the functional analysis was focussed on pro-coagulant activity rather than MV characterisation and quantification. In animal models studying circulating MVs, sampling of blood in polymicrobial sepsis was performed relatively late (e.g. 24h) during the onset of clinical symptoms[440,517–519], while in the LPS models of endotoxaemia, kinetic analyses have again been focussed on procoagulant activity of platelet-derived or tissue factor-expressing MVs[520–522]. When the effects of MVs were studied in ALI, systemic administration of *in vitro*-generated erythrocyte-[391,442] and endothelial cell-derived[443,444] MVs were used, showing an exacerbation of ALI in MV-treated mice. However, the physiological relevance of these *in vitro*-generated MVs remained

dubious. Therefore, for provision of MVs, single dose of i.v. LPS will be used in this study to induce endotoxaemia as a non-infectious and physiologically relevant *in vivo* source of pro-inflammatory MVs. This model not only provides precise *in vivo* response kinetics and reproducible levels of MV production, the isolated MV preparation for subsequent functional studies will be free of unwanted microbial products compared to CLP model.

4.2.3 Models development

In contrast to *in vitro* cell line-generated MVs described in the previous chapter, this chapter will focus solely on MVs generated *in vivo*, eliminating various problems inevitable for *in vitro* experiments such as stimulus- and culture condition-dependent MV production, phenotype and function[380,523], which would significantly reduce the physiological relevance of those models. Here, we investigated the production of circulating MVs in 3 different models of extrapulmonary inflammation: 1) kidney IRI, 2) subclinical endotoxaemia with kidney IRI, and 3) clinical endotoxaemia. Our objectives were two-fold: to establish the MV subtype profiles in single organ injury vs. systemic inflammation and to evaluate the suitability of each model for further functional studies via adoptive transfer to recipient IPL in subsequent studies. Our strategy included the avoidance of overwhelming inflammatory responses and limiting the observation periods to acute timepoints to focus on MV production as part of the primary response to each insult rather than as part of later and less defined phases of the *in vivo* responses.

4.3 Aims

To assess the production of MVs from animal models of sepsis and sterile peripheral organ injury, we aimed to:

1) Develop a relevant model of kidney ischaemia reperfusion injury for the assessment of MVs production during sterile inflammation.
2) Characterise the production of MV subtypes during kidney ischaemia reperfusion injury, in combination with subclinical endotoxaemia by i.v. LPS pretreatment.
3) Characterise the production of MV subtypes during clinical endotoxaemia using a single bolus i.v. LPS model.

4.4 Methods

4.4.1 Induction of unilateral kidney ischaemia reperfusion injury (IRI)

Untreated or low-dose LPS (20ng, i.v., 2h)-pretreated mice were anaesthetised and subjected to unilateral left kidney ischaemia for 30min, followed by 1h reperfusion. Sham-operated control mice underwent similar anaesthesia and abdominal laparotomy without the application of the renal vascular clamp. At the end of the procedures, mice were exsanguinated with 20UI heparin via the IVC to collect 1ml of venous blood, and both kidneys and the lungs were harvested to prepare single cell suspensions for flow cytometry analysis.

4.4.2 MV production from untreated or *in vivo* endotoxaemic mice

C57BL/6 mice were untreated or injected i.v. via tail vein with moderate dose of 2μg LPS to induce endotoxaemia. At set time points (1, 2 and 4h) post-LPS challenge, mice were anaesthetised, and blood exsanguinated via the IVC with 20IU heparin to collect 1ml of venous blood.

4.4.3 Blood processing for MV quantification by flow cytometry

Blood was centrifuged at 1,000 x *g* for 10min at 4°C to remove cells and the plasma supernatant centrifuged at 1,000 x *g* for a further 5min to obtain platelet-poor plasma (PPP) with minimal loss of MV content. MVs in PPP were then analysed immediately by flow cytometry. Staining of MVs for parental cell markers were summarised in Table 2.9 & Table 2.10. Note that we initially limited our *in vivo* MV subtype staining strategy to two antibody fluorophore-conjugates (PE and APC). In the case of neutrophil and monocyte ($Ly6C^{high}$ subset) MVs we used anti-CD11b and anti-Ly6G or -Ly6C, respectively. However, this was found to be sub-optimal for clear separation of the subtypes by dot plot analysis and in subsequent *in vivo* experiments we switched to the three antibodies combined (PE, PE-Cy and APC). The reasoning for using two antibody/fluorochromes and its limitations for MV subtype analysis in mouse blood are described in the Results section in this chapter. In addition to subtype-specific markers (PE and APC), we also included annexin V (FITC) in staining mixes for detection of phosphatidylserine (PS) as a potential 'generic' MV marker[324,332–334].

4.5 Results

4.5.1 Kidney ischaemia reperfusion injury (IRI): a model of sterile peripheral organ injury

Model development and evaluation: Tissue distribution of neutrophils and monocytes

Published kidney IRI model protocols differ considerably depending on the purpose of studies, primarily with respect to the use of unilateral or bilateral ischaemia, duration of ischaemia (20-60min) and reperfusion period (1-96h)[305,495–497,511,524–526]. To avoid the release of excessive apoptotic/necrotic factors from the kidney as a result of extended ischaemic period, or uraemia as a result of loss of renal function, we carried out a moderate unilateral renal ischaemia protocol of 30min to maintain renal function in the contralateral kidney. Additionally, we aimed to optimise the IRI model for the assessment of early MV release as a primary response to the local injury, thus we assessed reperfusion within acute timepoints up to 4h in preliminary studies (data not shown) and found significant production of MVs within 1h reperfusion.

To evaluate induction of local and remote inflammatory effects by the IRI protocol, we analysed the distribution of inflammatory Ly6C^{high} monocytes and neutrophils within the kidneys, lungs and in the circulation. After 1h reperfusion, significant increases in the number of neutrophils (Figure 4.1) and Ly6C^{high} subset monocytes (Figure 4.2) were observed in the ischaemic left kidney compared to sham-operated and untreated controls, suggesting an early margination or recruitment response at 1h post-reperfusion. In the kidney IRI mice, increased numbers of neutrophils were observed in the blood, lungs and contralateral uninjured right kidney, indicating occurrence of neutrophilia during IRI, in line with previously reported findings[510]. In sham-operated mice, neutrophil numbers increased, but to a lesser extent, only reaching statistical significance in the lungs. Ly6C^{high} monocytes showed a different picture, with no significant changes in blood, lungs or right kidney with some small statistically non-significant decrease. These findings indicate that the unilateral renal IRI model produced an early localised vascular inflammation in the ischaemic tissues and that in the case of neutrophils, this was accompanied by systemic increases, although sham surgery appeared to contribute to this effect with increased neutrophil margination in the lungs.

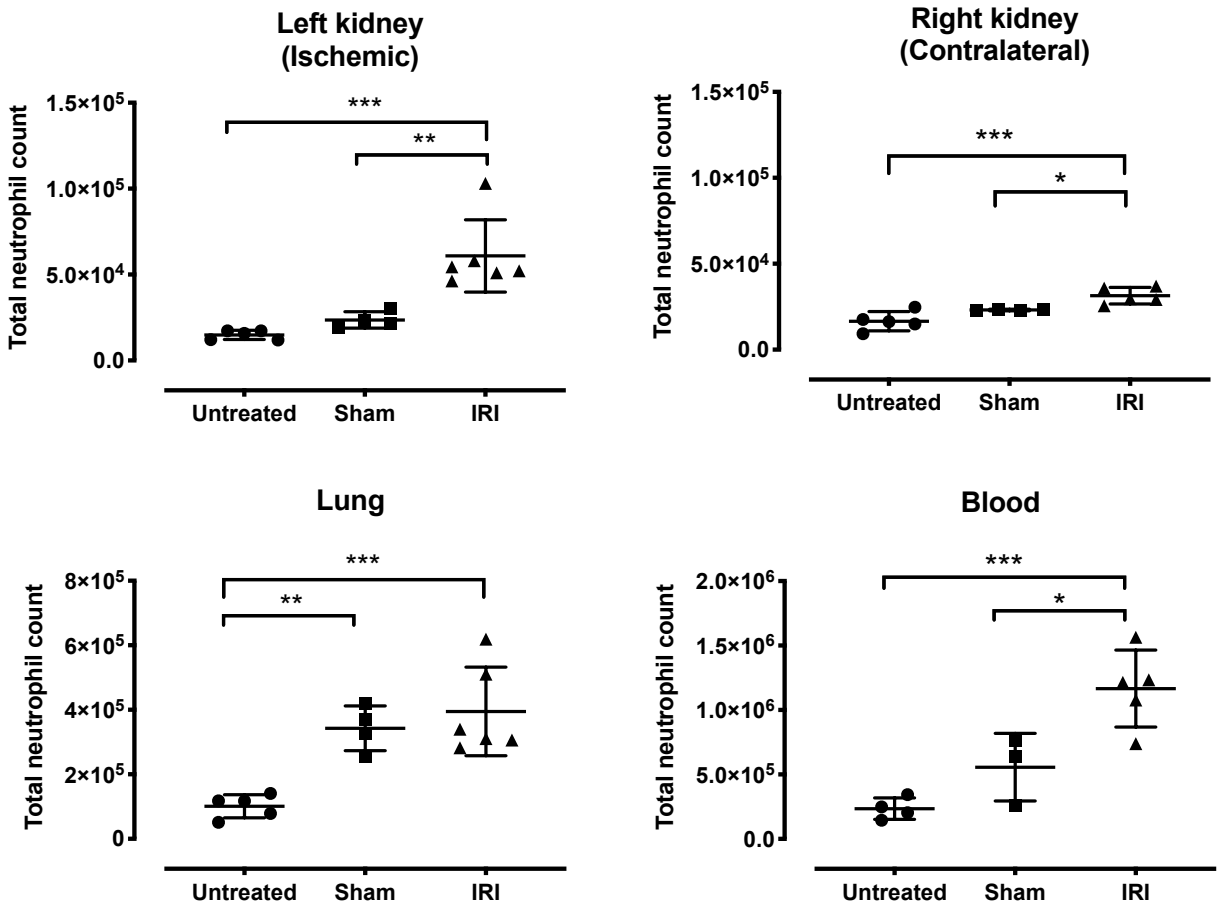

Figure 4.1 Tissue distribution of neutrophils during kidney IRI in mice.

*The kidneys, lungs and blood were harvested from mice after left kidney ischaemia (30min) and reperfusion (1h), and from control untreated and sham-operated mice. Kidney IRI resulted in significantly increased numbers of neutrophils in both kidneys and blood compared to sham-operated mice, while significant increases were seen in all tissues compared to untreated control mice. Sham operation elicited increase in neutrophil numbers in the lung compared to untreated. (Mean ± SD, n=4-6, *p<0.05, **p<0.01, ***p<0.001, one-way ANOVA with Bonferroni's multiple comparisons test.)*

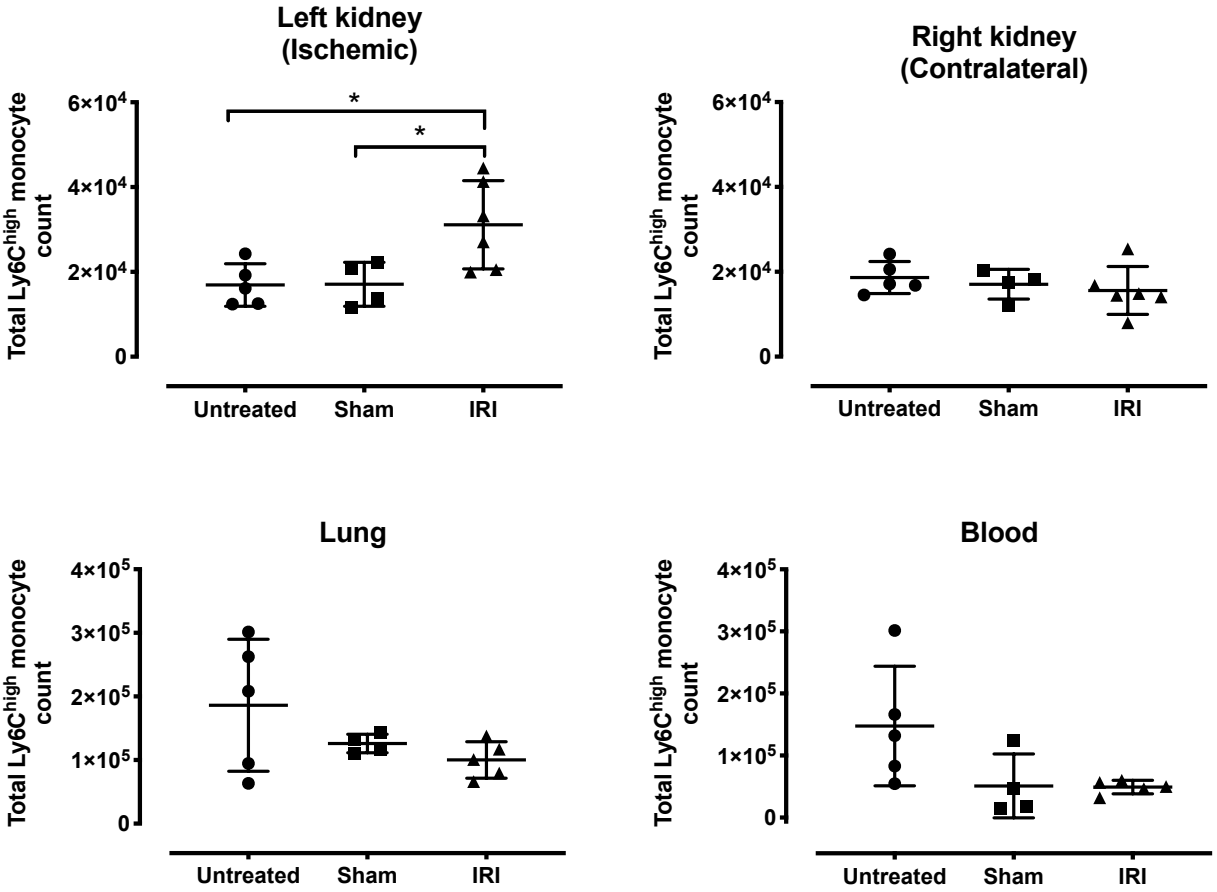

Figure 4.2 Tissue distribution of Ly6C^{high} monocytes during kidney IRI in mice.

*The kidneys, lungs and blood were harvested from mice after left kidney ischaemia (30min) and reperfusion (1h), and from control untreated and sham-operated mice. Kidney IRI resulted in significantly increased numbers of Ly6C^{high} monocytes in the ischaemic (left) kidney compared to sham, while no significant increase was seen in all other tissues and blood. (Mean ± SD, n=4-6, *p<0.05, one-way ANOVA with Bonferroni's multiple comparisons test.)*

Analysis of MV subpopulations in mouse plasma by flow cytometry

In the previous chapter we analysed MVs produced from a single cell line and found the identification of MVs possible using a single plasma membrane cell marker. Here, we aimed to identify circulating MV subtypes derived from various vascular cell types including endothelial cells, platelets, neutrophils, macrophages and monocytes. We identified each MV subtype based on antibody staining of 2-3 surface markers conjugated with bright fluorophores using flow cytometry, either PE and APC/AlexaFluor 647 and others including PE-Cy7 that minimised spectral overlap.

During preliminary kidney IRI experiments, we evaluated different antibodies and staining strategies. Of several markers tested for the identification of endothelial-MVs including CD144, CD146 and CD105, we found that CD31 produced a more consistent measurement. As CD31 is also likely to be expressed on platelets, endothelial MVs were identified by the expression of CD31, and the lack of CD41 expression, a platelet-specific marker[527]. CD11b was used to identify myeloid-derived MVs and these were then double stained with Ly6G or Ly6C to identify their neutrophil or monocyte origin. In the kidney IRI model the final antibody panel for MVs was: platelet-derived (CD41+), endothelial-derived (CD31+, CD41+), neutrophil-derived (CD11b+, Ly6G+), monocyte-derived (CD11b+, Ly6C+) (Figure 4.3). Macrophage-derived MVs was also assessed on the basis of their F4/80 expression (higher than monocytes) and CD45, but we did not detect any MVs using these markers.

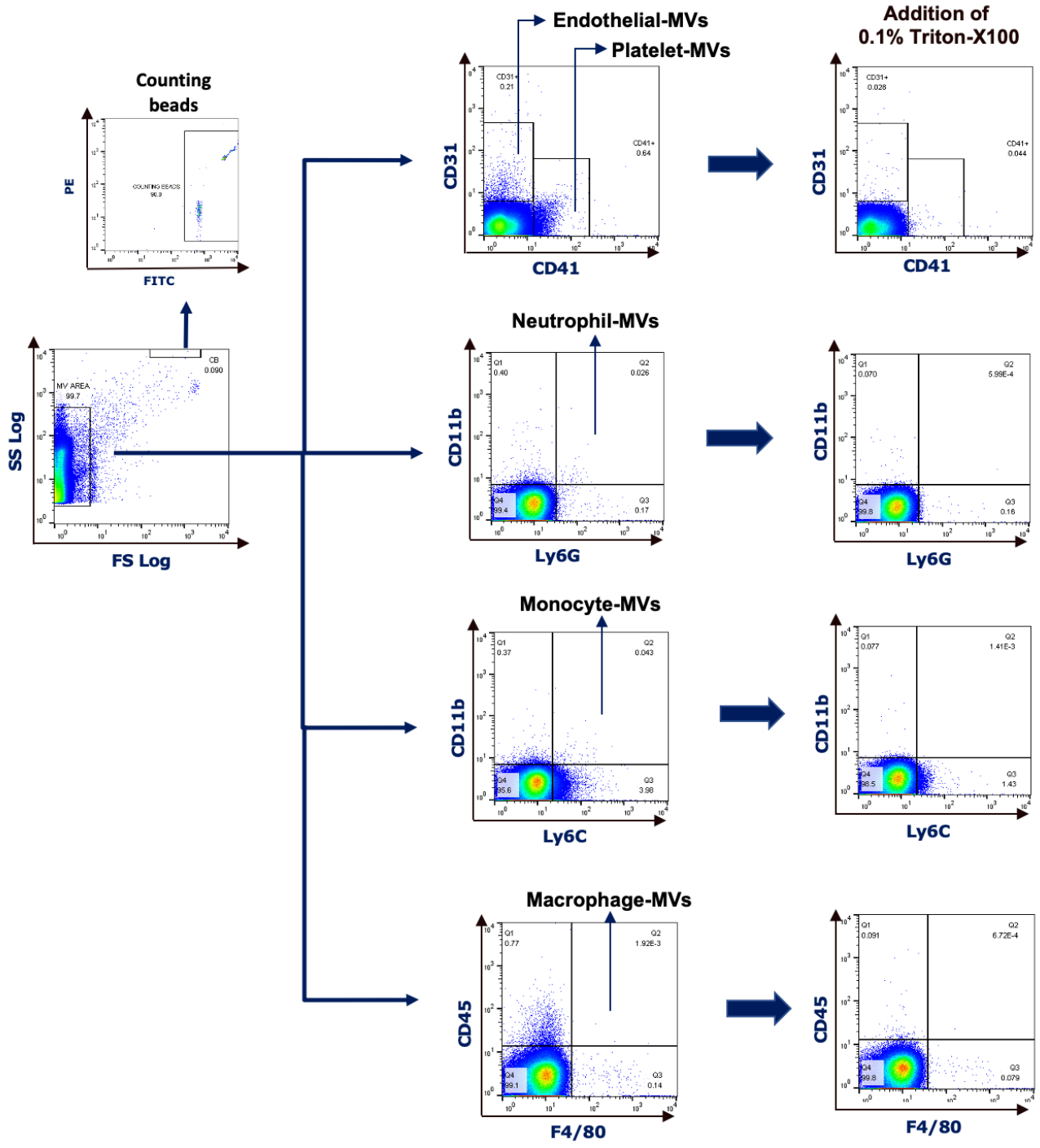

Figure 4.3 Flow cytometry gating of MVs in mouse plasma during kidney IRI.

Circulating MVs from unilateral kidney IRI (30min ischaemia, 1h reperfusion) mouse plasma were characterised by flow cytometry. Surface markers used for MV identification were: platelet-MVs (CD41+), endothelial-MVs (CD31+, CD41-), neutrophil-MVs (CD11b+, Ly6G+), monocyte-MVs (CD11b+, Ly6C+) and macrophage-MVs (CD45+, F4/80+). (Representative figure, n=1)

Production of MVs during kidney ischaemia reperfusion injury (IRI)

Using these gating strategies, we found a significantly elevated level of all MV subtypes investigated (platelet, endothelial, neutrophil- and monocytes-derived) at 1h reperfusion after 30min unilateral renal ischaemia in mice, as compared to sham-operated and control untreated mice (Figure 4.4). Interestingly, significantly increased levels of CD11b+Ly6C+ monocyte-MVs were detected in sham operated mice compared to untreated control, suggesting specific activation of monocytes from sterile abdominal surgery alone. However, the largest increase specific to IRI was that of platelet-MVs and endothelial-MVs, suggestive of primary haemostasis and injury to vessel walls.

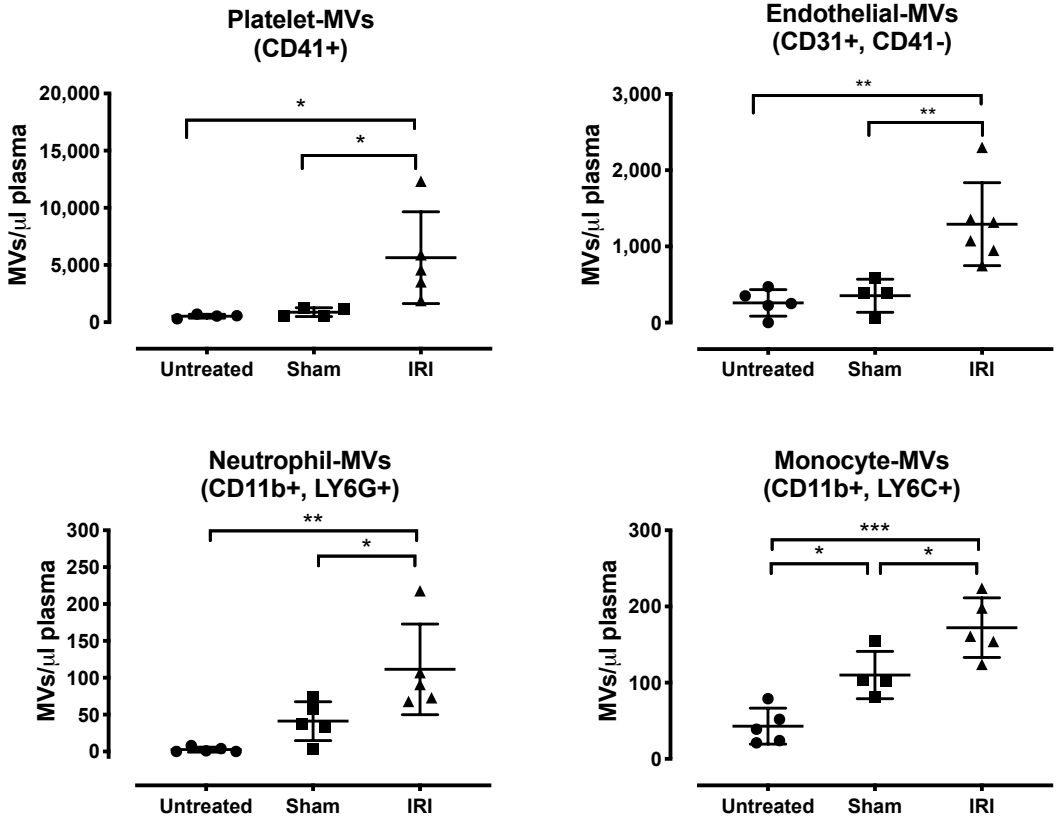

Figure 4.4 Circulating MV subtypes during kidney IRI in mice.

*Circulating MV subtypes were quantified in plasma of mice by flow cytometry after left kidney ischaemia (30min) and reperfusion (1h) and from sham-operated and control untreated mice. Significant elevation of circulating MVs from platelets (CD41+), endothelial cells (CD31+, CD41-), neutrophils (CD11b+, Ly6G+) and monocyte-MVs (CD11b+, Ly6C+) were detected in the plasma of kidney IRI mice, as compared to both sham operated and control untreated mice. Sham operation elicited significant increase in monocyte-MVs compared to untreated controls. (Mean ± SD, n=4-6, *p<0.05, **p<0.01, ***p<0.001, one-way ANOVA with* Bonferroni's *multiple comparisons test).*

4.5.2 Kidney IRI with subclinical endotoxaemia: a model of SIRS and peripheral organ injury

Model development and evaluation: Tissue distribution of neutrophil and monocyte

AKI occurs frequently in sepsis patients and may be a major trigger for indirect ALI. To investigate the potent interaction of a preceding systemic inflammation and AKI on MV production, we used a subclinical non-injurious LPS-pretreatment (20ng, i.v., 2h) in combination with kidney IRI procedure (30min ischaemia and 1h reperfusion) to enable evaluation of any interaction between preceding endotoxaemia and the superimposed AKI.

As before, we assessed the trafficking of neutrophils and Ly6C^{high} monocytes to obtain a picture of the local and systemic inflammatory responses. LPS pretreatment produced a striking several-fold increase in neutrophil recruitment to the ischaemic kidney during IRI (Figure 4.5). Although the number of experiments performed were low (n=2-4), there was evidence of neutrophilia and increases in neutrophils in the contralateral kidney and the lungs with LPS pretreatment, regardless of the surgery performed (untreated, sham-operated or IRI). A different pattern was observed with Ly6C^{high} monocytes, with LPS-pretreatment induced increases in both kidneys and the lungs, regardless of the surgery performed (untreated, sham-operated or IRI) (Figure 4.6). In contrast to neutrophils in LPS-pretreated mice, there appeared to be no enhanced recruitment of monocytes to the injured kidney or increase in circulating monocytes by LPS pretreatment. These results indicate distinctive trafficking behaviour of neutrophils and monocytes during local organ injury when superimposed with a relatively mild systemic inflammation, both of which could have an impact on their activation states and MV release.

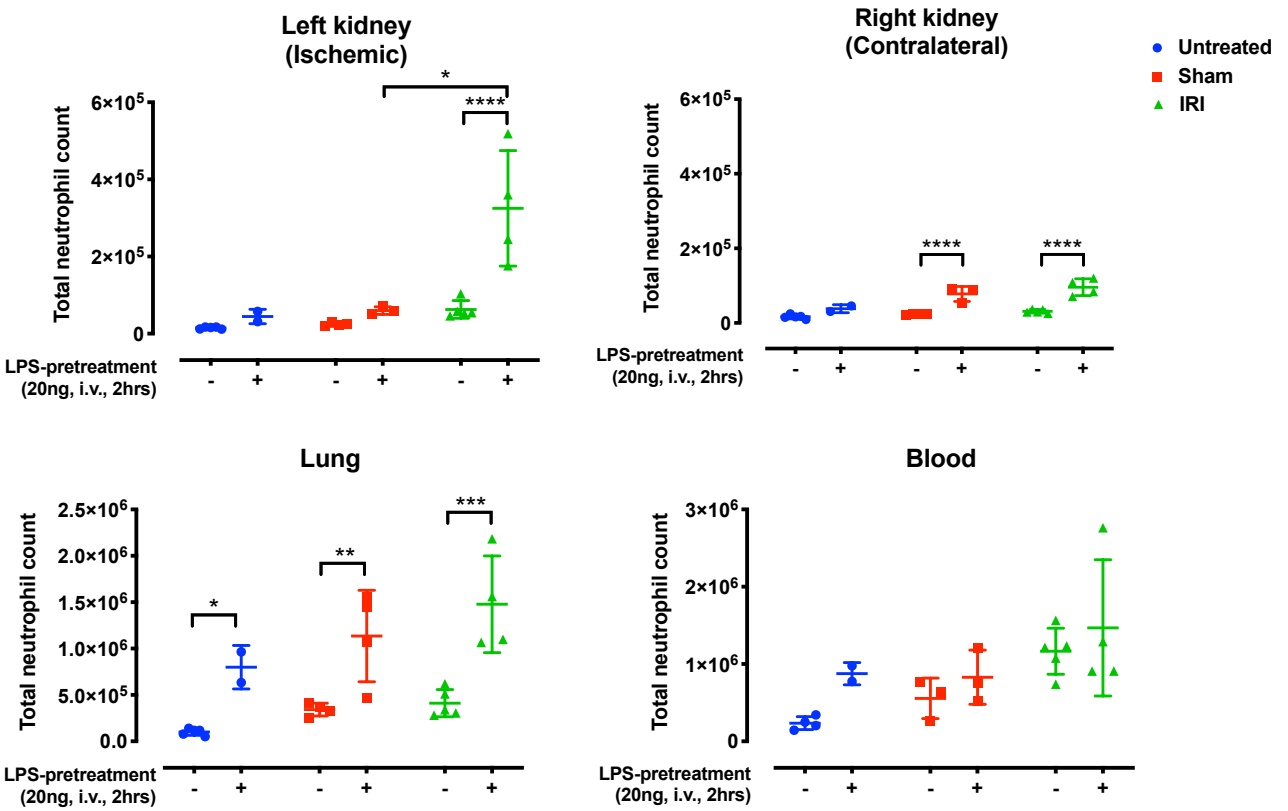

Figure 4.5 Tissue distribution of neutrophils during kidney IRI in untreated and LPS-pretreated mice.

*Both kidneys, the lungs and blood were harvested from mice after left kidney ischaemia (30min) and reperfusion (1h) and from control untreated and sham-operated mice, with or without prior LPS-pretreatment (20ng, i.v., 2h). LPS-pretreatment resulted in significant increased numbers of neutrophils in the ischaemic (left) kidney compared to non-LPS-treated IRI mice and sham-operated LPS-pretreated mice. Significant increases were also seen in the contralateral right kidney and the lung with LPS-priming, regardless of surgery performed (untreated, sham-operated or IRI). (Mean ± SD, n=2-4, *p<0.05, **p<0.01, ***p<0.001, ****p<0.0001, two-way ANOVA with Bonferroni's multiple comparisons test).*

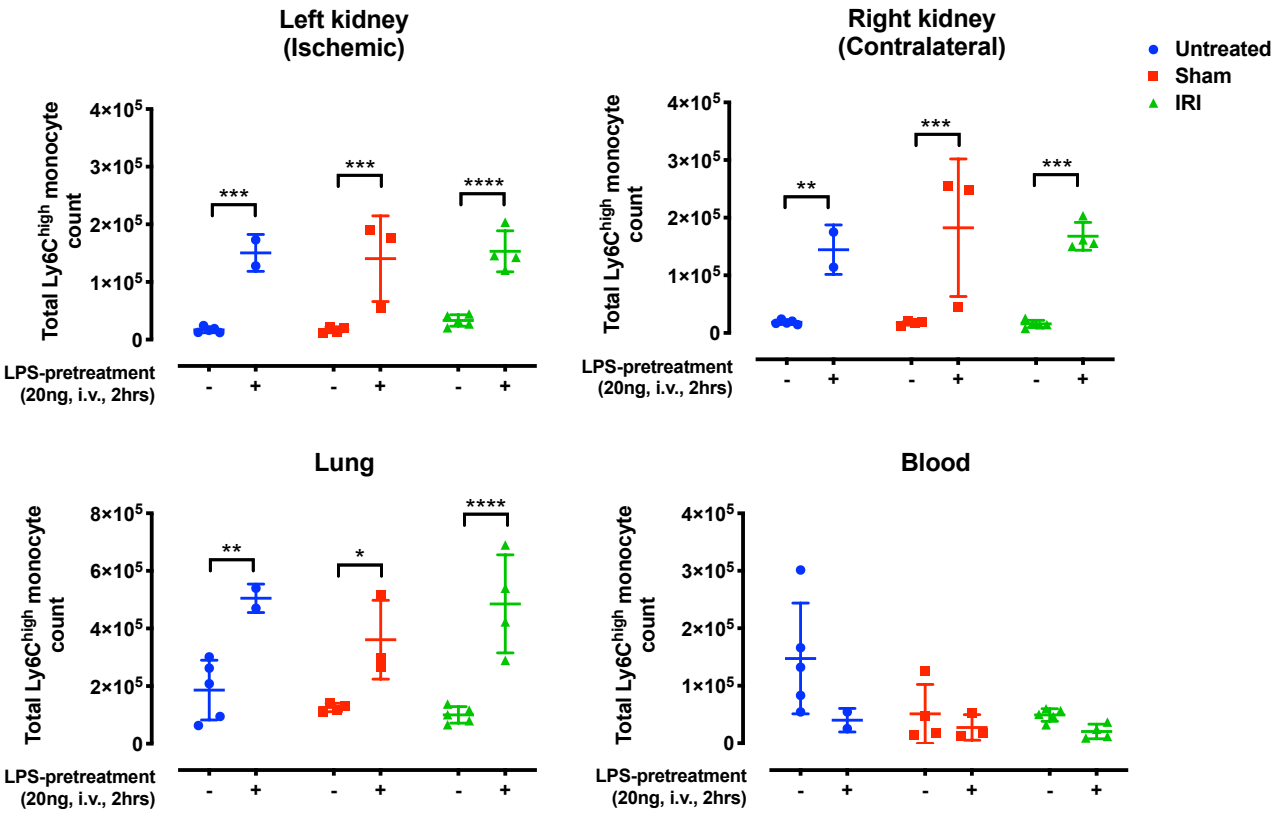

Figure 4.6 Tissue distribution of Ly6C^{high} monocytes during kidney IRI in untreated and LPS-pretreated mice.

*Both kidneys, the lungs and blood were harvested from mice after left kidney ischaemia (30min) and reperfusion (1h) and from control untreated and sham-operated mice, with or without prior LPS-pretreatment (20ng, i.v., 2h). LPS-pretreatment resulted in significantly increased numbers of Ly6C^{high} monocytes in all tissues, but not the blood, regardless of surgery performed (untreated, sham-operated or IRI). No difference was detected between sham operation and IRI with LPS-pretreatment. (Mean ± SD, n=2-4, *p<0.05, **p<0.01, ***p<0.001, ****p<0.0001, two-way ANOVA with Bonferroni's multiple comparisons test).*

Analysis of MV subpopulations by flow cytometry

In these experiments with low-dose LPS-pretreatment before kidney IRI, we observed substantial increases in circulating monocyte- and neutrophil-MVs, which revealed some limitations of the flow cytometry staining and gating strategy for myeloid MV subtypes (Figure 4.7). Using anti-CD11b and anti-Ly6C antibodies, two CD11b+, Ly6C+ MV subpopulations were apparent with higher MV numbers: a CD11b+, Ly6C+ population previously designated as $Ly6C^{high}$ monocyte-derived and a population with lower Ly6C expression 'CD11b+, Ly6C-low'. Subsequent analysis using Ly6C and Ly6G staining together (see Figure 4.9), indicated that CD11b+, Ly6C-low MVs were neutrophil-derived (Ly6G+), whereas CD11b+, Ly6C+ were $Ly6C^{high}$ monocyte-derived (Ly6G-). The data for monocyte MVs were therefore based on gated CD11b+, Ly6C+ MVs, but all other MVs were identified as before (endothelial and platelet-MVs). Again, we did not find an F4/80+ population and these data are not included in the analysis.

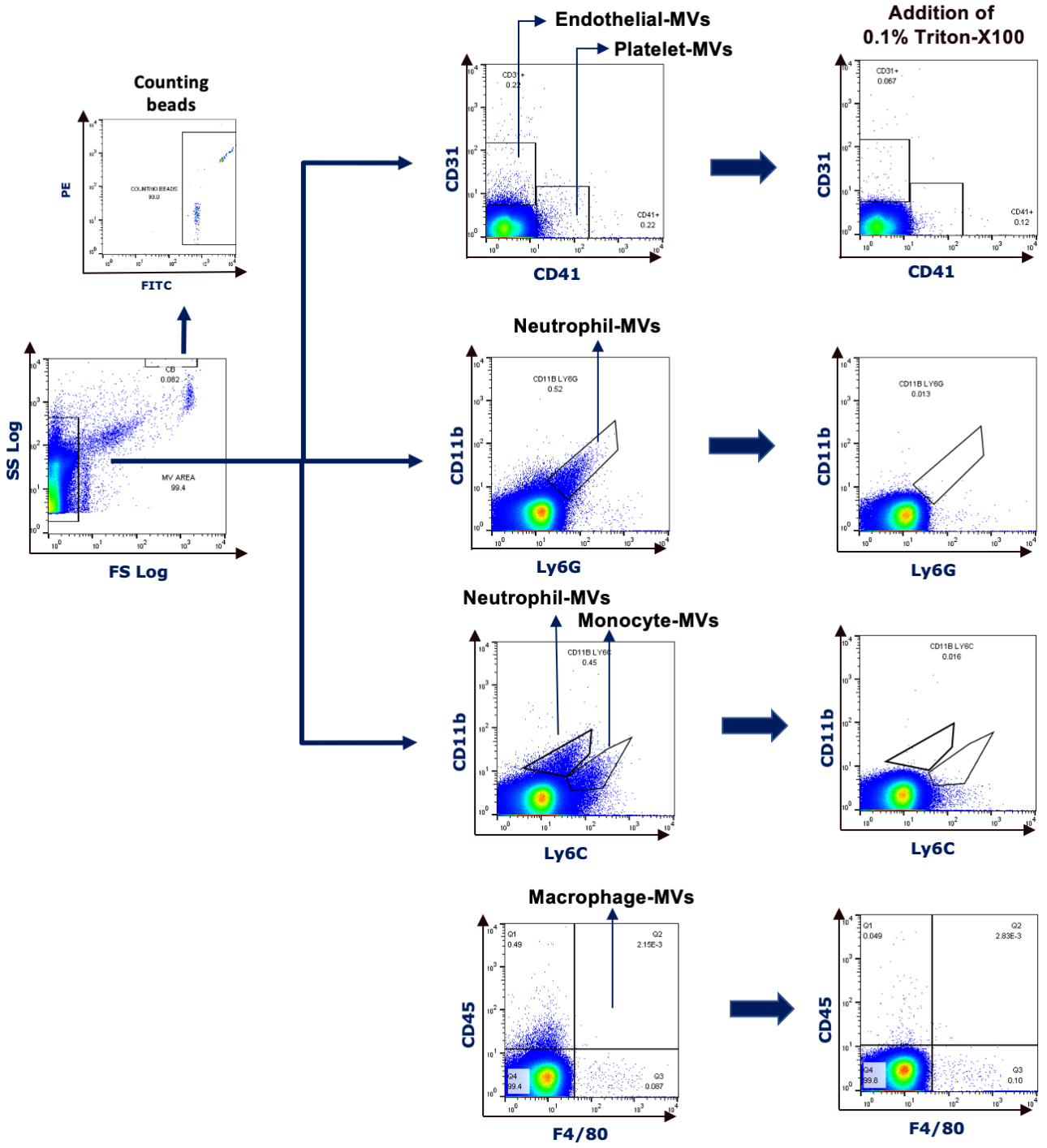

Figure 4.7 Flow cytometry gating of MVs in mouse plasma during kidney IRI with LPS-pretreatment.

Circulating MVs from LPS (20ng, i.v., 2h)-pretreated, unilateral kidney IRI (30min ischaemia, 1h reperfusion) mouse plasma were characterised by flow cytometry. Surface markers used for MVs identification were: platelet-MVs (CD41+), endothelial-MVs (CD31+, CD41-), neutrophil-MVs (CD11b+, Ly6G+), monocyte-MVs (CD11b+, Ly6C+) and macrophage-MVs (CD45+, F4/80+). (Representative figure, n=1)

Production of MVs during kidney IRI with subclinical endotoxaemia

As suggested by the flow cytometry dot plots, we found that low-dose LPS pretreatment produced very large increases in circulating myeloid MV subtypes (neutrophil- and monocyte-MVs) relative to kidney IRI but there was no obvious increase between LPS-pretreated sham, and LPS-pretreated IRI mice (Figure 4.8). In sharp contrast, LPS-pretreatment elicited a significant decrease in circulating platelet- and endothelial-MVs during kidney IRI, as compared to non-LPS-pretreated IRI mice.

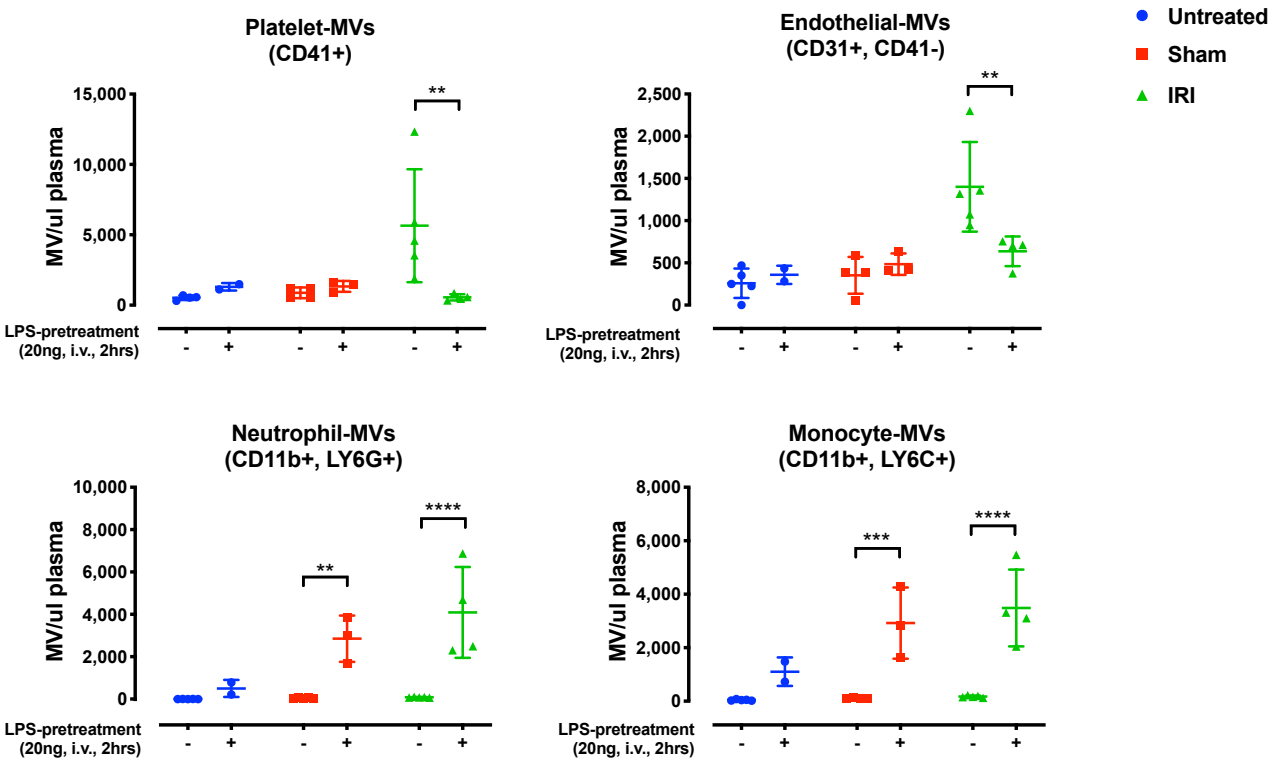

Figure 4.8 Circulating MV subtypes during kidney IRI in untreated and LPS-pretreated mice. *Circulating MV subtypes were quantified plasma of mice by flow cytometry after left kidney ischaemia (30min) and reperfusion (1h) and from control untreated and sham-operated mice, with or without prior LPS-pretreatment (20ng, i.v., 2h). LPS-pretreatment resulted in significant reduction in platelet- and endothelial-MVs compared to non-LPS-pretreated mice during kidney IRI. Increased levels of monocyte- and neutrophil-MVs were observed in LPS-pretreated mice, regardless of surgery performed (sham-operated or IRI). (Mean ± SD, n=2-4, **p<0.01, ***p<0.001, ****p<0.0001, two-way ANOVA with Bonferroni's multiple comparisons test.)*

4.5.3 Intravenous LPS: a model of systemic inflammation

Our aim was to investigate MV production kinetics during acute endotoxaemia but to avoid the severity of the clinical response and minimise secondary physiological effects that could affect MV production and recovery. Based on previous studies of LPS dose response in the group[187,291], a single bolus, moderate 2μg/mouse dose of LPS was used, which produced minor or no visible clinical symptoms (e.g. lethargy, huddling or piloerection). As this model has been thoroughly elaborated by our group previously[187], no further model development was conducted.

Analysis of MV subpopulations by flow cytometry.

Due to the limitations identified from the use of 2 antibody fluorophore-conjugates staining described above, we expanded the staining panels to 3 antibody fluorophore-conjugates to differentiate neutrophil- and monocyte-MVs with higher precision. In addition to platelet-, endothelial-, neutrophil-, monocyte- and macrophage-MVs, we also investigated erythrocyte-MVs in this model, as they have been shown to induce indirect ALI *in vivo*[391,442]. Additional MV detection panels such as CD3 and CD19 were also tested for the detection of lymphocyte-derived MVs, as well as F4/80 and CD45 for macrophage-derived MVs. However, levels of lymphocyte- and macrophage-MVs were undetectable within the acute timepoints (up to 4h) investigated (data not shown). Using these gating strategies, plasma MVs from either untreated or LPS-treated mice were analysed. MVs identified include neutrophil-MVs (CD11b+, Ly6C+, Ly6G+), monocyte-MVs (CD11b+, Ly6C+, Ly6G-), platelet-MVs (CD41+), endothelial-MVs (CD31+, CD41-) and erythrocyte-MVs (TER-119+) (Figure 4.9). As we were mainly interested in MVs released by vascular cell types[432], no further markers were examined.

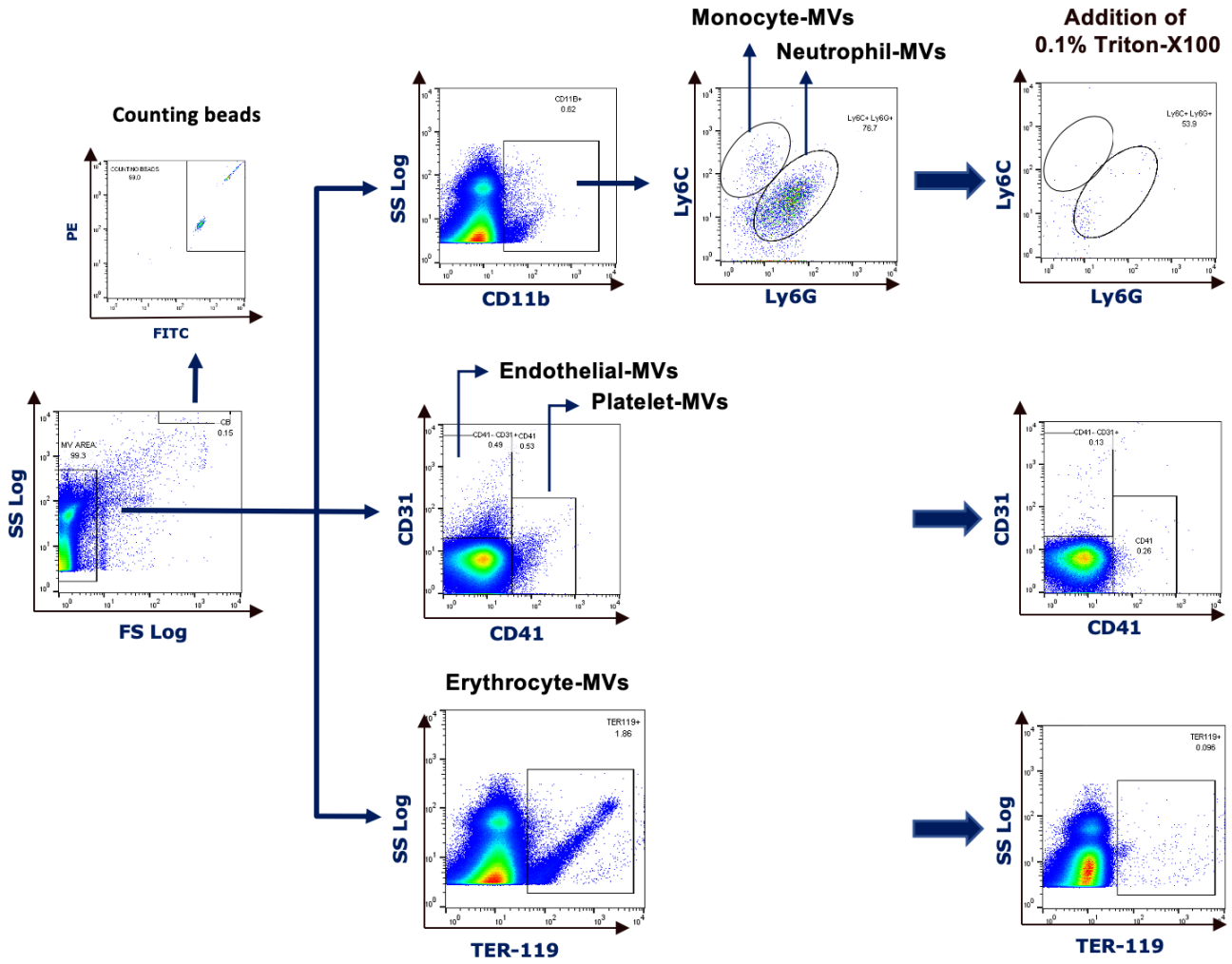

Figure 4.9 Flow cytometry gating of MVs in mouse plasma.

Circulating MVs from LPS (2µg, i.v., 1h)-treated mouse plasma were characterised by flow cytometry. MVs identified include neutrophil-MVs (CD11b+, Ly6C+, Ly6G+), monocyte-MVs (CD11b+, Ly6C+, Ly6G-), platelet-MVs (CD41+), endothelial-MVs (CD31+, CD41-) and erythrocyte-MVs (TER-119+). (Representative figure, n=1)

Kinetics of circulating MVs during endotoxaemia.

A marked elevation of circulating neutrophil-derived MVs (~100-fold) was observed at 1h post-LPS (Figure 4.10), which decreased over time but remained higher than baseline up to the 4h timepoint. These findings demonstrate that neutrophil-derived MVs (CD11b+Ly6C+Ly6G+) are the most acutely increased circulating MV subtype following systemic LPS challenge, consistent with observations in patients during early-stage infectious and sterile SIRS in the bloodstream[420,427]. The same pattern was observed with monocyte-derived MVs (CD11b+Ly6C+Ly6G-) with acute and sustained elevation, albeit at much lower baseline and induced levels (~20-fold). In contrast, level of MVs derived from platelets, endothelial cells and erythrocytes were relatively high at baseline but did not change over the investigated timepoints with LPS challenge.

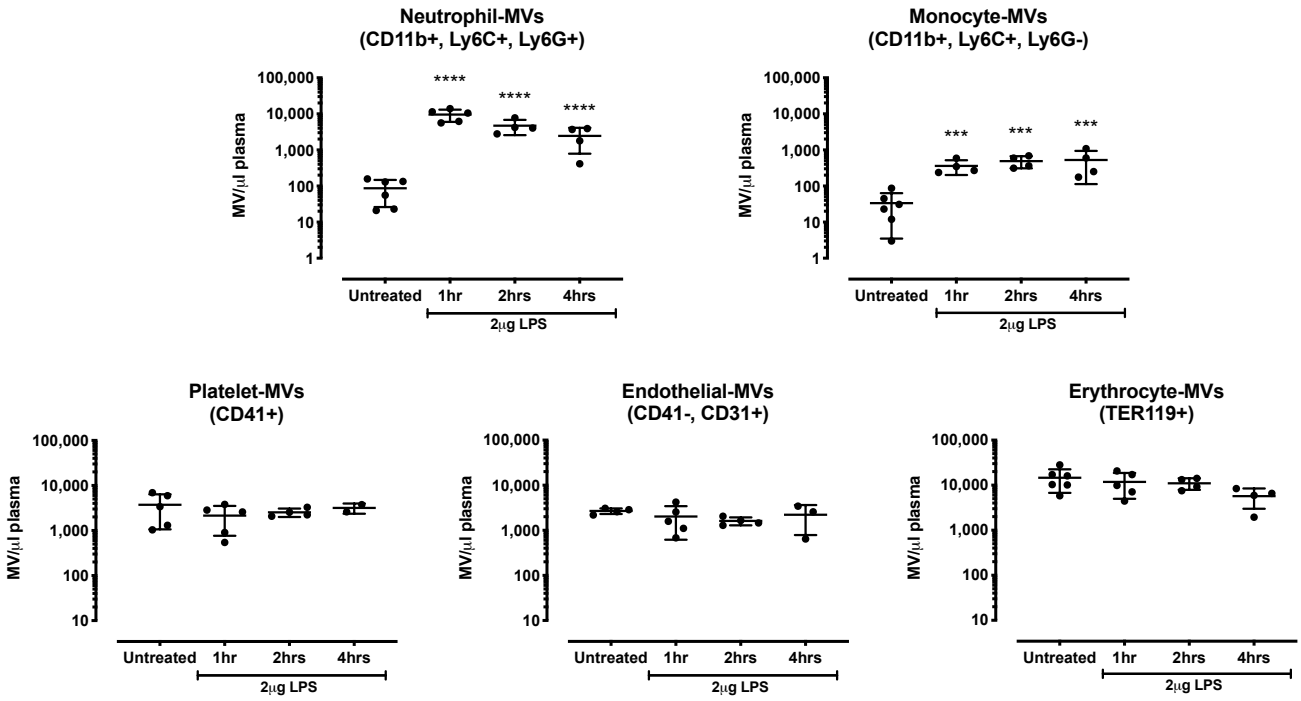

Figure 4.10 Kinetics of *in vivo* MVs production following i.v. LPS challenge.

*Circulating MV subtypes were quantified plasma of mice by flow cytometry following i.v. 2μg LPS injection up to 4h. Significant elevation of circulating neutrophil-derived MVs (~100-fold) and monocyte-derived MVs (~20-fold) was observed at 1h timepoint, as compared to untreated control mice. No significant increase in the level of MVs released by other vascular cell types (platelet-, endothelial-, erythrocyte-derived) was detected. (Mean ± SD, n=3-6, ***p<0.001, ****p<0.0001, one-way ANOVA with Bonferroni's multiple comparisons test)*

4.5.4 PS expression on circulating MV subtypes (all models)

In addition to MV subtype-specific markers, all PPP were co-stained with annexin V for evaluation of PS expression on MVs in all three of the models investigated. Although PS translocation is often considered an essential step in the MV release process and surface PS expression on MVs has been evaluated in sepsis patients[432], its detection by annexin V varied considerably here, in an all or none fashion, both between the different MV subtypes and between the injury models (summarised in Figure 4.11). Distinctive patterns in the annexin V staining included the relatively higher proportion of annexin V+ platelet- and endothelial-MVs in the kidney IR model that appeared to be lost with LPS-pretreatment, and the lack of annexin V staining in neutrophil- and monocyte-MVs in the endotoxaemia models. These preliminary findings using controlled physiological models of organ injury and endotoxaemia suggest that PS expression may be an important tool to dissect out circulating MV dynamics in relation to different systemic insults.

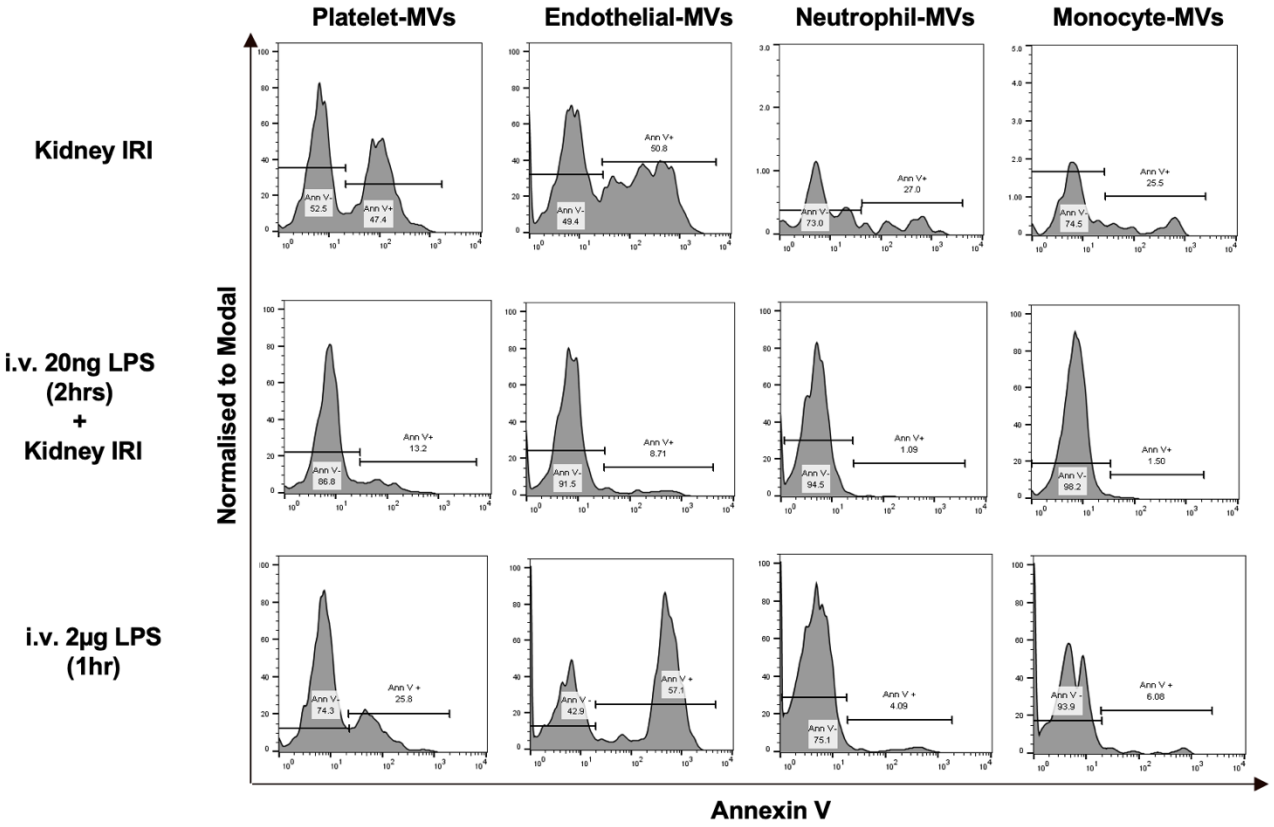

Figure 4.11 Representative histograms of PS expression on MV subtypes during kidney IRI, kidney IRI with subclinical endotoxaemia and clinical endotoxaemia models.

Plasma MVs obtained from mice underwent 30min unilateral renal ischaemia with 1h reperfusion (kidney IRI), i.v. 20ng LPS (2h) prior to kidney IRI, or i.v. 2µg LPS (1h) treatments, were analysed based on their cellular origin subtypes (platelet-, endothelial-, neutrophil- and monocytes-derived). Each MV subtypes was then quantified based on their annexin V binding (x-axis), as an indicator of PS expression. Percentage of annexin V- and annexin V+ subpopulations in each MV subtypes were indicated by horizontal bars drawn across each histogram peaks. (Representative figure, n=1 from each treatment group)

4.6 Discussion

4.6.1 Summary

This chapter investigated the early production of MVs during a sterile peripheral organ injury and systemic inflammation, and combination of both, using models of kidney IRI and intravenous LPS. Kidney IRI elicited substantial increases in the level of platelet- and endothelial-MVs, and smaller but significant increases in monocyte- and neutrophil-MVs were also observed. In contrast, the LPS model of endotoxaemia induced an exclusive increase in neutrophil- and monocyte-MVs. Interestingly, low-dose LPS treatment prior to kidney IRI reduced the number of platelet- and endothelial-derived MVs to baseline levels, suggesting a substantial shift in their production or clearance rates, requiring further investigation. Post hoc analysis showed that PS expressions of each MV subtype varied considerably between subtypes and between each inflammatory model investigated. Collectively, we found that the MV production profile differed significantly between sterile peripheral organ injury and systemic inflammation, where different subtypes of circulating MVs could have differing roles in the propagation of extrapulmonary inflammation and in the modulation of indirect ALI.

4.6.2 Kidney IRI cell biology

It is often clinically unclear if sepsis/SIRS occur as a cause or consequence of AKI, as 40% of AKI patients were found to develop sepsis after AKI diagnosis and 28% had sepsis before development of AKI[528]. Therefore, the development of indirect ALI can result from the effect of superimposed mediators released from both AKI and sepsis, adding complexity to the disease pathogenesis. We employed moderate local (unilateral kidney ischaemia) and systemic (endotoxaemia) treatments and measurements within acute timepoints to focus on MV production in response to the initial insult rather than any secondary systemic responses. In the case of AKI-induced indirect ALI, the published models usually employ an ischaemic period of >30min and ligation of both kidneys to induce high mortality and morbidity, limiting the ability to discern the direct relationship between the kidney-lung crosstalk versus the secondary systemic responses to renal failure[529]. Therefore, we used a unilateral ischaemia of moderate duration (30min) with the function of the contralateral kidney retained to avoid renal dysfunction toxicity. As evidence of leukocytes margination was reported within 2h post-

ischaemia[510] and evidence of lung inflammation reported within 4h post-ischaemia[495], we carried out preliminary studies comparing circulating MVs levels during acute reperfusion timepoints at 1h. This protocol was of sufficient severity to elicit the early recruitment of neutrophils and monocytes to injured kidney, as well as evidence of systemic neutrophil increases. Moreover, following kidney IR there were consistent increases in circulating levels of platelet-, endothelial-, neutrophil- and monocyte-MVs. It may be speculated that in this early post-ischaemic period, circulating MVs are derived from in the injured kidney as part the local response to IRI. Moreover, at least some of the systemically released MVs are likely to interact with or be taken up by cells within the pulmonary vasculature. It is of note therefore that neutrophil numbers increased in the lungs, but this appeared to be in response to the abdominal surgery rather than the kidney IRI.

4.6.3 MV production during AKI and IRI in other organs.

Our findings that circulating platelet- and endothelial-derived MVs were the predominant subtypes following kidney IRI are in line with clinical findings in patients with chronic kidney disease[530,531] and chronic renal failure[503,504]. However, our study appears to be the first evaluation of acutely released MVs during the development of kidney injury. Acute production of MVs has been described in other models of single organ IRI, particularly liver (endothelial-, platelet- and neutrophil-MVs)[505] and heart (platelet-MVs)[532], suggesting shared mechanisms of induction. Although the exact mechanism of MV production during IRI is unclear, various DAMPs, cytokines and the complement system have been implicated in the inflammatory mechanism of IRI, including ATP, ROS, C5a and TNF-α[533–536], all of which are potent inducers of MVs production.

AKI and indirect ALI are often associated with a background of systemic inflammation due to various causes (e.g. sepsis, major surgery, trauma), which interact with kidney ischaemia as part of the injury process. In these cases, MVs entering the pulmonary circulation are likely to be a product of both local and systemic inflammation. We hypothesised that the increased level of endothelial- and platelet-MVs we observed here were reflective of endothelial dysfunction and a pro-thrombosis state as a result of vascular injury from IR. Although circulating neutrophil- and monocyte-MVs were lower than that of endothelial- and platelet-MVs, their levels were consistently increased during IRI. Our

results showing the tissue distribution of neutrophils and Ly6C^{high} monocytes suggest the potential of MV production by these marginated cells at the site of injury as an acute response, however these findings may require real-time multiphoton imaging for further verification.

4.6.4 Two-hit model of AKI

We performed a low-dose LPS systemic challenge, aiming to 'prime' the inflammatory responses to kidney IRI and to better simulate the AKI conditions during sepsis. The LPS-pretreatment produced a more pronounced neutrophil recruitment to the injured kidney, presumably due to increased availability of neutrophils mobilised from the bone marrow reservoir[187]. Furthermore, LPS produced increased numbers of circulating neutrophil- and monocyte-derived MVs, albeit through enhancing the response to sham surgery rather than a specific potentiation of IRI-induced MV production. However, a very different phenomenon was produced with levels of circulating platelet-MVs and endothelial cell MVs. Unlike the myeloid-MVs, levels of endothelial- and platelet-MVs did not increase, but rather decreased with LPS-pretreatment in IRI mice, returning close to baseline levels. We can consider two likely explanations for this intriguing phenomenon. First, pre-exposure of animals to LPS has been shown to induce tolerance to renal IRI[537–539] and IRI in other organs[540–542], a phenomenon called endotoxin tolerance, potentially via immunosuppressive responses in circulating monocytes[543–545]. We consider this explanation less likely due to the relatively low-dose of LPS used and the apparent selectivity of the suppressive effect being applied only to platelet- and endothelial-MVs. Second, we speculate the reduced levels of these MVs reflect a combination of their lack of increased production by LPS (as compared to myeloid-MVs) and their enhanced clearance during systemic inflammation. Circulating platelet-MVs have previously been shown to have very short half-lives[400], so the dynamics of their clearance is certainly an important determinant of their apparent levels in the circulation. Although further investigation on the total production of MVs during kidney IRI via depletion of intravascular macrophages could shed light on the understanding of the response dynamics, depletion of monocytes/macrophages has been shown to protect animals against renal IRI[546,547], precluding this investigative approach.

4.6.5 MV production during endotoxaemia.

In contrast to propagation of inflammation from a single organ injury model, we investigated MV production in LPS-induced endotoxaemia as a response to generalised inflammation initiated throughout the vasculature. As a single insult, moderate dose of LPS produced large and sustained increases in neutrophil-MVs and to a lesser degree, monocyte-MVs. The dichotomy with non-myeloid-MVs was evident again, with no detectable increases in circulating platelet-, endothelial- or erythrocyte-derived MVs. These differences in MV subtype profiles presumably reflect the responsiveness of their parent cells to LPS or secondary *in vivo* generated MV-inducing agonists (e.g. cytokines). Our data on the early increases in myeloid-MVs resemble those in acute sepsis[420], burns patients[427] and healthy volunteers injected with LPS[438,548], although significant increases in non-myeloid-MVs were also observed. In animal models of polymicrobial sepsis (CLP), increased levels of various MV subtypes including monocytes-, neutrophils-, endothelial- and platelet-derived MVs, were consistently observed, but at a much later timepoints (>24h)[440,517–519]. In LPS models of endotoxaemia, MV subtypes (their cell type origin) were not often characterised, and instead, MVs analyses were focussed mainly on tissue factor expression and their associated procoagulant activity[520–522]. Here in this study, we carried out a thorough characterisation of MV subtypes during acute phase of endotoxaemia. Based on the rapid release and abundance of myeloid-derived MVs in plasma during endotoxaemia, we hypothesise that myeloid-MVs may play a significant role in eliciting pulmonary vascular inflammation during systemic inflammation.

4.6.6 Phosphatidylserine (PS) expression on MVs.

We assessed MV subtype expression of surface PS expression using Annexin V, a calcium-dependent phospholipid-binding protein that has a high affinity for the anionic phospholipid PS. Although the release of annexin V+ MV has been described in several models of IRI *in vivo*[335,357,452,505], our data showed that a mixture of annexin V+ and annexin V- MVs were present in circulating blood. Assuming annexin V binding we measured was a direct representation of PS expression levels, then the findings are consistent with presence of distinct PS+ and PS- subpopulations of MVs described previously in various *in vitro* and *in vivo* models[343–346]. Although PS expression may not have value as a generic marker of MVs, it remains an important indicator of MV functionality in relation their roles

in potentiating coagulation reactions[335–338], which is critical to specific disease processes such as IRI. PS expression is also a primary determinant of MV uptake by mononuclear phagocytes as described in Chapter 3. On this basis, we speculate that differences in MV PS expression may affect their residence time within the circulation and this may vary between the subtypes and the different *in vivo* model insults. For instance, high proportion of annexin V+ platelet- and endothelial-MVs following kidney IRI was lost with LPS-pretreatment, coinciding with their reduction in circulating levels. Interestingly, the scavenging of PS-expressing MVs using diannexin was shown to protect against liver IRI[357,549], suggesting important pathological role of PS-expressing MVs in IRI. Although PS expression may provide additional insights in the disease evolution and may serve as a useful biomarker (e.g. higher level of PS-expressing MVs in patients may indicate IRI occurrence in septic patients), PS expression-based MV characterisation studies may require more cautious interpretation[432,434,550–552], as MV subtypes that express lower level of PS may be missed.

4.7 Conclusion

As the first step to understand the role of MVs in the pathogenesis of indirect ALI, in this chapter we investigated mechanisms of extrapulmonary inflammation as clinically relevant drivers of the disease: (1) organ injury related to local vascular inflammation (kidney IRI) and (2) direct induction of systemic inflammation (LPS-induced endotoxaemia). Compared to *in vitro*-generated MVs, *in vivo* produced MVs represent a more physiologically relevant source, suitable for evaluating *in vivo* remote organ injury effects, such as indirect ALI. Previous studies have demonstrated effects of *in vitro*-generated MVs from erythrocytes and human endothelial cells in rodent models of indirect ALI[391,442–444], but the relevance of this approach to indirect ALI arising from endogenously-generated MVs is questionable. Thus, despite providing invaluable insights, *in vitro* MVs generated from single population of cells with cell-specific stimuli may not be representative of endogenously produced MVs *in vivo*. However, there are major challenges that limit the use of *in vivo*-derived MVs, primary amongst these are the mixture of MV subtypes, the limited numbers of MVs available due to rapid RES clearance and the complexity/reproducibility of *in vivo* challenge models. To some extent, we were successful in addressing the latter point in the design of organ and systemic inflammation models here.

Chapter 5

Pilot studies on activity of circulating microvesicles in an IPL model of indirect ALI

Parts of the content of this chapter has been presented as a conference abstract:

Investigation into the Roles of Circulating Microvesicles Within the Pulmonary Vasculature Using Ex Vivo Isolated Perfused Lung. *Y. Y. Tan, K. P. O'Dea, A. Pac Soo, M. Takata. American Journal of Respiratory and Critical Care Medicine 2019; 199: A7317.*

Chapter 5 Pilot studies on activity of circulating microvesicles in an IPL model of indirect ALI

5.1 Abstract

Background

Microvesicles (MVs) have been implicated as biomarkers and mediators of sepsis pathophysiology, but their specific roles in the pathogenesis of indirect acute lung injury (ALI) remain undefined. We recently demonstrated that endotoxaemia markedly enhanced uptake of circulating MVs by lung-marginated monocytes, suggesting that systemic inflammation may substantively enhance the effects of MVs in the lungs. Previous studies on the potential roles of MVs in indirect ALI have been limited to injections of *in vitro*-generated MVs into mice, which do not define the direct effects of MV within the pulmonary vasculature, nor reveal the properties of endogenously released circulating MVs. Here, we use a novel approach to address the role of MVs in indirect ALI, directly assessing the biological activities of MVs within the lungs using *ex vivo* isolated perfused lung (IPL) challenged with *in vivo*-generated MVs derived from endotoxaemic 'donor' mice.

Methods

C57BL/6 mice were injected with a moderate dose of LPS (2μg, i.v., 1h) and plasma MVs were isolated by differential centrifugation. The IPL was prepared from a separate mouse, untreated or pretreated with low-dose LPS (20ng, i.v., 2h). MVs recovered from one donor mouse were directly infused into the IPL perfusate buffer and recirculated for 4h. Lung oedema was determined by wet-to-dry weight ratio and BALF protein levels, and cell activation by flow cytometric analysis of lung single cell suspensions, and soluble mediators in perfusates by ELISA.

Results

MVs from LPS-treated mice, but not untreated mice, induced upregulation of ICAM-1 and VCAM-1 on endothelial cells, and CD86 on Ly6C^{high} monocytes and interstitial macrophages (CD11b+, F4/80+, Ly6C-low, MHCII+) in IPLs of LPS-pretreated mice, but not IPLs of non-LPS-pretreated mice. However, MVs from both control and LPS-treated mice did not induce significant increases in lung permeability or perfusate cytokines measurements, both of which reach relatively high baseline levels in LPS-pretreated IPLs during the 4h perfusion period without MV treatment.

Conclusion

We successfully developed a mouse model of *in vivo* MV-to-*ex vivo* IPL challenge to simulate indirect ALI. These preliminary findings showed, for the first time, that *in vivo*-generated MVs are capable of directly modulating pulmonary vascular inflammation in the absence of any systemic factors. Despite the evidence of MV-induced activation of endothelial cells and lung-marginated monocytes, we consider that further definition of the *in vivo* MV preparation and modification of the IPL protocol are necessary to investigate the contribution of endogenously released, circulating MVs to indirect ALI.

5.2 Background

5.2.1 MVs in sepsis-induced ALI

Despite several *in vivo* and clinical studies demonstrating an increased level of circulating MVs in animal models of sepsis and sepsis patients as discussed in Chapter 4, the inflammatory functions of these MVs and their contribution to organ-specific inflammation/injuries has not been defined. The clinical evidence appears to be contradictory in the relationship between circulating MVs and clinical severity in SIRS patients. We recently observed direct correlations between circulating neutrophil-MVs (CD66b+/CD11b+) and clinical severity in severe burns injury patients admitted to the ICU[427]. Others have also reported that neutrophil-MVs are associated with mortality in critically-ill patients admitted to ICU[377], and increased level of endothelial-derived, ACE-positive MVs serve as an predictor of ARDS development in septic patients[431]. In contrast, some studies found an inverse correlation between MV levels with disease outcome. In ARDS patients, higher level of circulating leukocyte-MVs (CD45+) were found to associate with better survivor outcome[435]. In sepsis patients, higher levels of circulating MV (Annexin V+) levels correlated with lesser chance of developing ARDS[433], and higher levels of endothelial- (CD31+/CD42-) and platelet-derived (CD31+/CD42+) MVs were found to predict more favourable outcome in mortality and organ dysfunction[436].

When functional activities of sepsis-associated MVs were studied, MVs (mainly platelet-derived) from septic patients were shown to induce apoptosis on vascular endothelial cells *in vitro*[439], whereas MVs (mainly leukocyte-derived) obtained from septic rats that underwent CLP were found to induce systemic vasodilation *in vivo*[440]. In contrast, protective effects of total MVs (mainly platelet- and endothelial-derived) from septic shock patients has also been reported in the maintenance of vascular reactivity *in vivo*[429]. In the context of indirect ALI, systemic administration of *in vitro*-generated MVs from erythrocytes[391,442] and human endothelial cells[443,444] have been shown to produce some features of indirect ALI in mice *in vivo*. However, it is unclear if these responses measured *in vivo* developed from direct effects of MVs within the pulmonary vasculature or secondary to MV-induced systemic responses. Moreover, as cells may release qualitatively distinctive MV phenotypes depending on the inducing stimulus, functional studies using *in vitro* generated MVs may not be representative of MVs generated under *in vivo* conditions where parent cells encounter multiple agonists and vascular-bed

specific environments, thereby affecting their MV generation and phenotype. There is, therefore, a need to perform more defined and systematic modelling of circulating MV production *in vivo* and their direct effects within the pulmonary vasculature contributing to indirect ALI.

5.2.2 Pulmonary vascular inflammation during indirect ALI

To produce acute lung injury symptoms in animal models arise from extrapulmonary causes, "two-hit" models were commonly used to reproduce comorbidities and risk factors present in patients[553]. For example, combination of intraperitoneal endotoxin injection or fecal peritonitis with "second-hit" intratracheal acid aspiration, intestinal ischaemia-reperfusion or haemorrhage were used to induce full-blown pulmonary oedema[554–557]. However, whilst these injurious models are useful for the endpoint injury measurements, they are less helpful in the understanding of specific mediator release and their direct role in disease pathophysiology and propagation mechanism. Instead, a reductionist approach in disease modelling such as the IPL allows a more systematic approach in the understanding of the direct effects of MVs in elicitng pulmonary vascular inflammation and injury.

We previously utilised the mouse IPL system to investigate uptake of *in vitro* produced MVs by lung vascular cells (Chapter 3). The exclusion of systemic factors, including uptake within other vascular beds, enabled us to quantify changes in uptake by different pulmonary cell populations during subclinical endotoxaemia. As a next step in elucidating the pulmonary-specific biological roles of circulating MVs, we decided to investigate the feasibility of a direct adoptive transfer of circulating MVs from a donor mouse into a recipient IPL. With characterisation of circulating MV subtype production profiles in the kidney IRI and intravenous LPS models described in the previous chapter, we considered the suitability and benefits of each model. Based on the higher levels of circulating MVs produced and various technical considerations, the moderate dose LPS-induced endotoxaemia model was chosen over the IRI model for this investigation. Although not investigated further in this study, the role of MVs released during the 'sterile' isolated kidney injury in propagation of inflammation to the lungs would be an important system for future investigation.

5.3 Aims

Based on the previously described phenomena of increased MV uptake in the lungs and increased levels of circulating myeloid-MVs during endotoxaemia, we hypothesised that transfer of MVs from moderate-dose LPS-treated mice to the IPL of low-dose LPS-pretreated mice would lead to pulmonary vascular inflammation and lung oedema. To test this, we aimed to:

1) Develop and optimise a prolonged isolated perfused lung (IPL) system for transfer and evaluation of *in vivo*-derived MV function.
2) Compare the inflammatory/injurious activities of MVs from untreated and LPS-treated donor mice in the IPL from untreated and LPS-pretreated mice.

5.4 Methods

5.4.1 MV production from untreated or *in vivo* endotoxaemic mice

C57BL/6 mice were untreated or injected i.v. with 2μg LPS for 1h. Mice were anaesthetised and 1ml of blood was exsanguinated with 20IU heparin via the IVC. Blood was centrifuged at 1,000 x *g* for 10min at 4°C to remove cells and the plasma supernatant centrifuged at 1,000 x *g* for a further 5min at 4°C to obtain platelet-poor plasma (PPP). PPP was centrifuged at 20,000 x g for 30min to pellet MVs. MVs were washed and resuspended in pre-warmed IPL perfusate buffer for infusion into the IPL circuit. Total preparation of MVs obtained from one donor (untreated or LPS-treated) was adoptively transferred to one IPL recipient (1:1 donor-to-recipient treatment ratio).

5.4.2 *Ex vivo* isolated perfused lung (IPL)

IPLs were prepared from untreated or low-dose LPS (20ng, i.v., 2h)-pretreated C57BL/6 mice. In brief, IPL was perfused with RPMI-1640 supplemented with 4% (v/v) BSA-RPMI at a rate of 25 ml/kg/min and ventilated with 5%CO_2 at 5cmH_2O PEEP, 6-7ml/kg tidal volume and sustained inflation performed at 25cmH_2O at every 15min interval. Total preparation of MVs from one donor mouse (untreated or LPS-treated) were infused into the non-recirculating perfusion circuit of IPL for 4h (Figure 5.1). Basic randomisation was performed by alternating MV treatments (from untreated and LPS-treated mice) in the IPL to avoid system drift effects and to identify anomalies. At the end of 4h experimentation, IPL perfusate was collected for analysis of soluble cytokines by ELISA after removal of residual cells and MVs by centrifugation at 300 x g for 10min followed by 20,000 x g for 30min. The right lower lobe of the lungs was tied off and oedema was determined by wet-to-dry weight ratio measurement and the remainder of the lungs was lavaged with 0.65ml of saline to collect bronchoalveolar lavage fluid (BALF). The left lung was used to prepare single cell suspension for flow cytometric analysis.

5.4.3 Single cell suspension for flow cytometry analysis

Single cell suspensions of the lungs were prepared by simultaneous disaggregation and fixation to preserve cell integrity and minimise changes in phenotype during processing. In brief, lungs were mechanically disaggregated in 2ml fixative for 1min, passed through a 40μm nylon filter and washed with cold FACS Wash Buffer (FWB). Cells were pelleted by centrifugation at 400 x g for 10min at 4°C,

resuspended in 1-step Fix/Lyse Solution (1X) for 1min to remove red blood cells, and washed twice with FWB prior to antibody staining. Antibodies used were summarised in Table 2.7. Lung endothelial cells were identified as CD45-, CD41-, ICAM-2+ and CD31+ population (Figure 2.9), Ly6C^{high} monocytes as CD11b+, F4/80+, Ly6C-high population, Ly6C^{low} monocytes as CD11b+, F4/80+, Ly6C-low, MHCII- population, interstitial macrophages as CD11b+, F4/80+, Ly6C-low, MHCII+ population, neutrophils as CD11b+, F4/80-, Ly6C-med, Ly6G+ population (Figure 2.10).

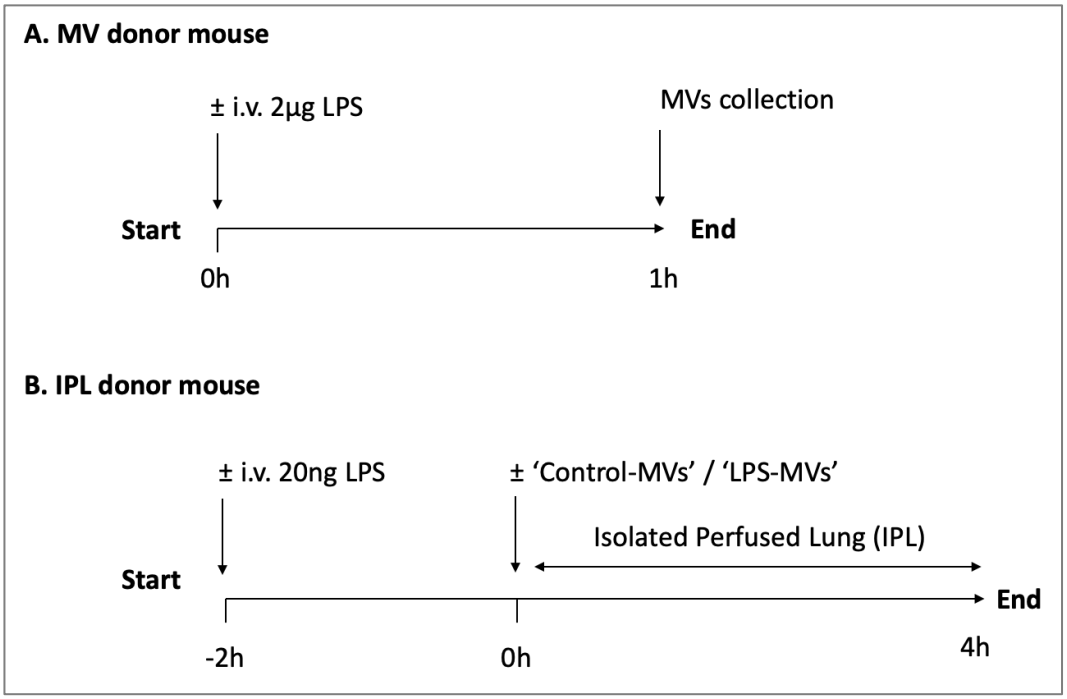

Figure 5.1 *In vivo* MV-to-*ex vivo* IPL(4h) adoptive transfer methodology.

C57BL/6 mice were untreated or injected with LPS (2μg, i.v., 1h) and plasma MVs were isolated by differential centrifugation. The IPL was prepared from a separate mouse, untreated or pretreated with low-dose LPS (20ng, i.v., 2h). MVs recovered from one donor mouse were directly infused into the IPL perfusate buffer and recirculated for 4h.

5.5 Results

5.5.1 Optimisation and evaluation of the IPL system

Respiratory and vascular stability of 4h IPL

To allow sufficient time to be able to detect a range of MV effects in the IPL model, including transcriptional upregulation of endothelial cell adhesion molecule (CAM) expression, we decided to extend the recirculating perfusion protocol to 4h, beyond that of the 2-3h perfusion periods previously used in the group[294,295]. The IPL system is prone to instability and therefore several optimisation steps and precautions were taken to ensure reproducibility including stringent cleaning routines for the tubing and connectors, perfusion buffer sterility, pH and osmolality, as detailed in Chapter 2 methods. To verify the stability of IPL preparation, the physiology of IPL preparations was monitored by measurements of airway respiratory and pulmonary vascular mechanics. The collection of data and calculation of these lung physiological parameters were described in detail in Chapter 2 (**Equation 2**, **Equation 3**, **Equation 4**). These parameters are commonly used to assess and characterise the pulmonary responses in the IPL to various pharmacological agents and biological variables[558–561].

As previously discussed, subclinical endotoxaemia induces enhanced pulmonary vascular uptake of circulating MVs via functionally primed lung-marginated marginated Ly6C^{high} monocytes. Therefore, we performed optimisation of the IPL using preparations from control untreated and low-dose LPS (20ng, i.v., 2h)-pretreated mice, to enable reproducible assessment of the MV effects in both conditions. Respiratory resistance (Rrs) and elastance (Ers) did not change significantly over 4h in untreated or LPS-pretreated IPLs (Rrs (min-max): control 0.55-0.65 vs. LPS 0.52-0.71 cmH_2O sec/ml; Ers (min-max): control 0.47-0.51 vs. LPS 0.47-0.54 cmH_2O kg/ml), with no significant difference in percentage change over 4h, suggesting stability of the lungs throughout (Figure 5.2). LPS-pretreated IPLs appeared to have a slightly higher pulmonary vascular resistance (PVR) compared to control IPLs (PVR (min-max): control 5.0-6.3 vs. LPS 5.8-7.5 mmHg min/ml), with an overall percentage increase in control and LPS-pretreated IPLs of 19.72±17.35% and 31.33±23.86%, respectively, over the course of 4h (Figure 5.3). However, none of these differences reached statistical significance between control and LPS-pretreated IPLs. As a positive control, thrombin was infused into the perfusate at the start of IPL, which was shown to induce 59% (n=1) increase in PVR, whereas injurious

ventilation (high-stretch and atelectasis) were shown previously by our group to induce 50-100% increase in Ers and Rrs[295]. In summary, the IPL physiological parameters remained stable with no clear deterioration by the 4h timepoint in both control and LPS-pretreated models. Moreover, as the low-dose LPS-pretreatment of mice did not appear to produce any lung respiratory or vascular dysfunction, direct comparisons of MV treatment effects between these IPL models was possible.

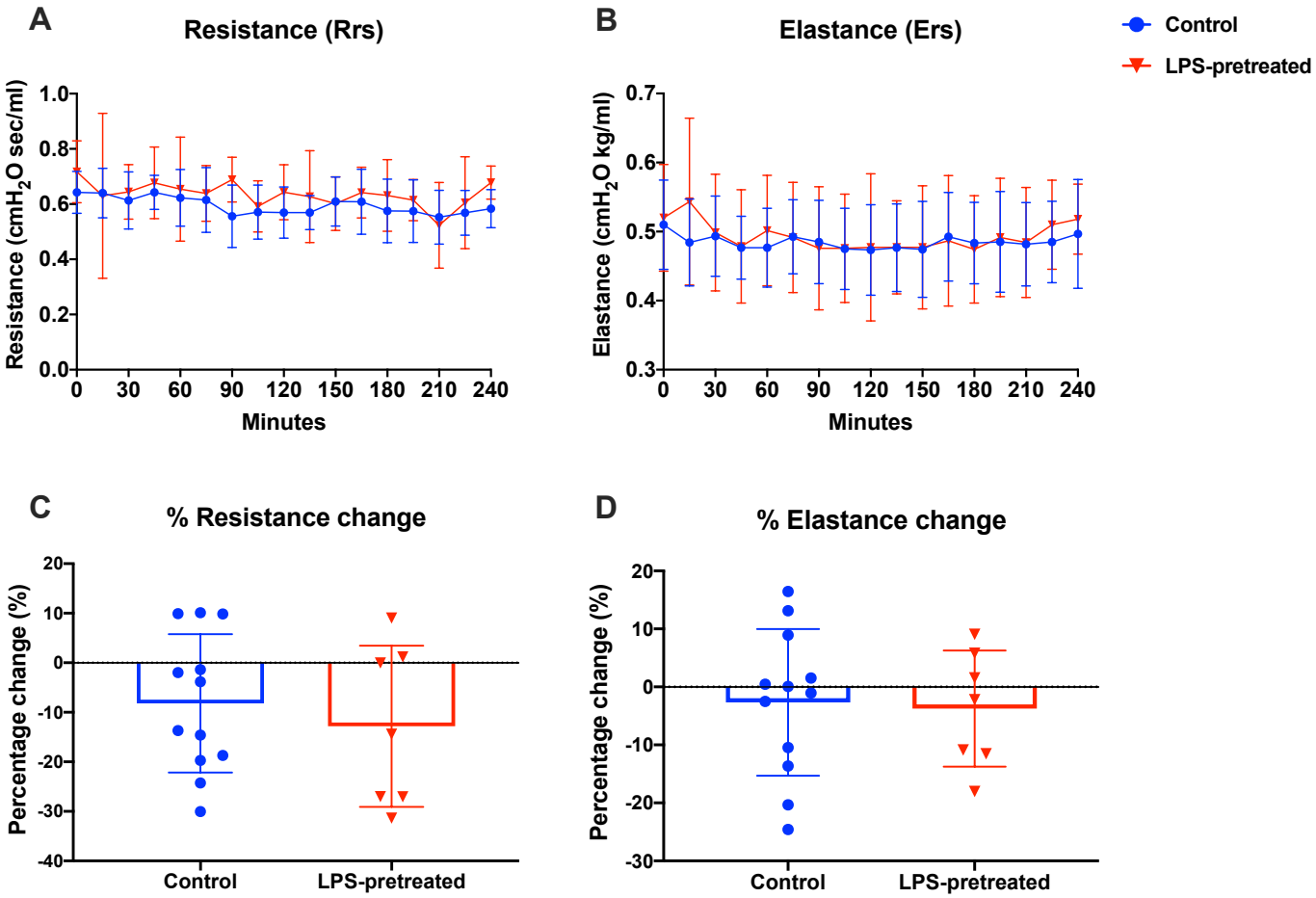

Figure 5.2 Lung respiratory mechanics over 4h IPL.

(A) Respiratory resistance (Rrs) and (B) elastance (Ers) were calculated every 15min during inspiratory pauses over 4h of IPLs obtained from both untreated and LPS (20ng, i.v., 2h)-pretreated mice. (C, D) Percentage change in Rrs and Ers was calculated by differences between data points at 0h and 4h, divided by data points at 0h. No statistical significance was found in the change of Rrs and Ers over 4h in LPS-pretreated or control IPLs, suggesting respiratory stability of the lungs throughout. (Mean ± SD, n=6-11, two-tailed unpaired t-test.)

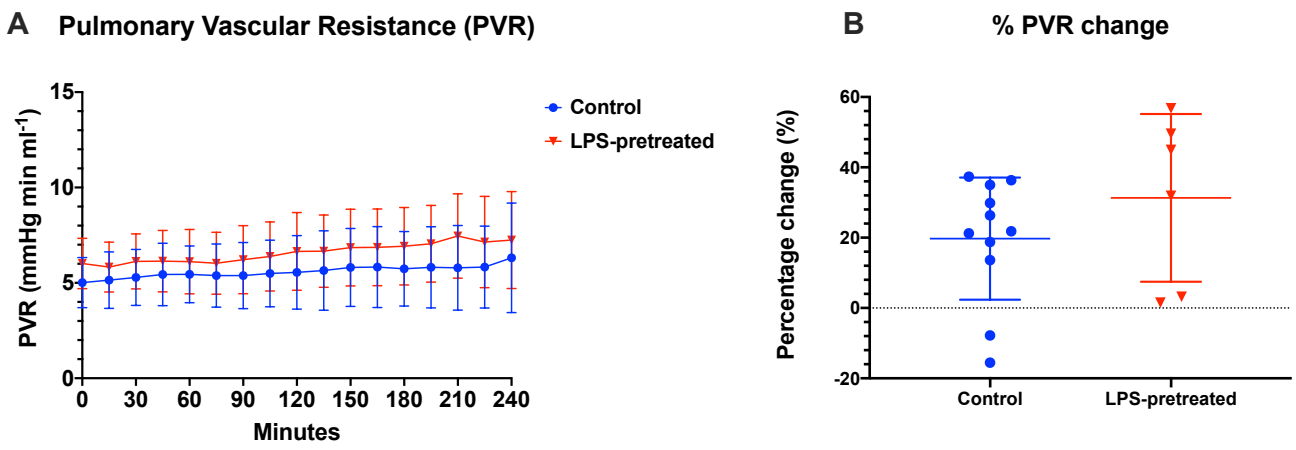

Figure 5.3 Lung vascular mechanics over 4h IPL.

(A) Pulmonary vascular resistance (PVR) was calculated every 15min during inspiratory pauses over 4h of IPLs obtained from both untreated and LPS (20ng, i.v., 2h)-pretreated mice. (B) Percentage change in PVR was calculated by differences between data points at 0h and 4h, divided by data points at 0h. No statistical significance was found in the percentage change of PVR over 4h in LPS-pretreated or control IPLs, suggesting vascular stability of the lungs throughout. (Mean ± SD, n=6-11, two-tailed unpaired t-test.)

Leukocytes retention in IPLs after 4h perfusion

Previous research in the group demonstrated that approximately half of intravascular Ly6C^{high} and Ly6C^{low} monocytes remained marginated within the pulmonary vasculature following IPL set up after initial flush-out perfusion[294562]. To verify the presence of lung-marginated leukocytes after 4h of lung perfusion, leukocytes were quantified by flow cytometry in single cell suspensions from either control or LPS-pretreated IPLs. Numbers of Ly6C^{high} and Ly6C^{low} monocytes in control IPLs were comparable to those previously found[294], and in the case of Ly6C^{high} monocytes and neutrophils, much higher numbers were found in LPS-pretreated IPLs compared to control IPLs, due to additional margination during endotoxaemia[187] (Figure 5.4). Although not possible to directly assess their viability with the methods used, the retention of these cells within in the pulmonary microcirculation suggests an active role throughout the perfusion protocol.

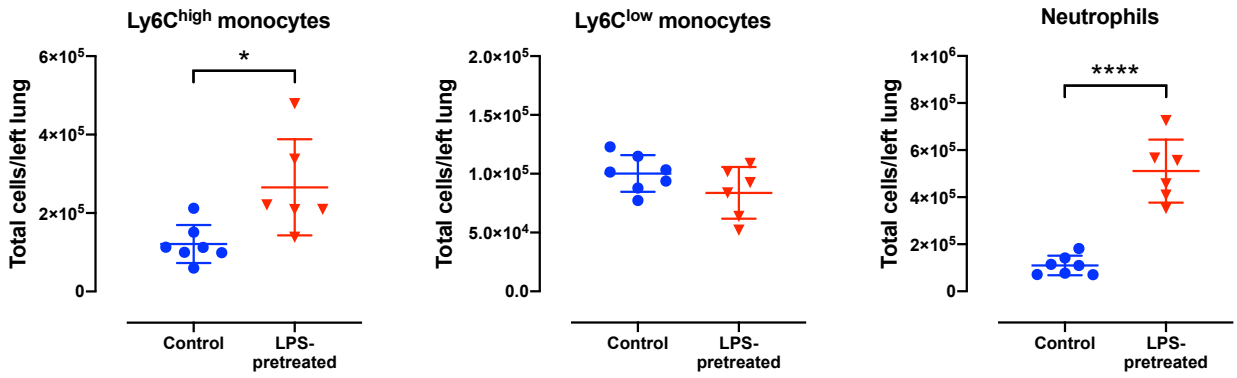

Figure 5.4 Lung-marginated leukocytes are retained in the lungs after 4h perfusion.
*Lungs of untreated or LPS (20ng, i.v., 2h)-pretreated mice were isolated and perfused briefly at 0.1ml/min to remove non-adherent blood cells until the lungs turned translucently white. The lungs were then perfused in a closed, recirculating circuit at 25ml/kg/min for 4h. Left lungs were homogenised for flow cytometry quantification of leukocytes. LPS-pretreated IPLs contained significantly higher numbers of lung-marginated Ly6C^{high} monocyte and neutrophils compared to control IPLs. (Mean ± SD, n=6-7, *p<0.05, ****p<0.0001, two-tailed unpaired t-test.)*

5.5.2 Activation of pulmonary vascular cells in MV-treated IPLs.

Activation of endothelial cells in LPS-pretreated IPLs by MVs from endotoxaemic mice

MVs obtained from untreated controls or endotoxaemic mice (2μg, i.v., 1h LPS-treated) were adoptively transferred to IPLs prepared from either untreated or low-dose LPS (20ng, i.v., 2h)-pretreated mice in 1:1 donor-to-recipient treatment ratio. Neither of the MV treatments significantly altered the lung respiratory and vascular mechanics (data not shown), indicating there were no gross effects on lung physiological dysfunction with these treatments. For quantification of pulmonary vascular cell responses by flow cytometry, single cell suspensions were prepared by simultaneous disaggregation and fixation to preserve cell integrity and minimise changes in phenotype during processing[450]. Lung endothelial cells were identified by the co-expression of ICAM-2 and CD31 (Figure 2.9)[563] and their activation determined by upregulated expression of their cell adhesion molecules ICAM-1, VCAM-1 and E-selectin. Infusion of MVs from LPS-treated mice ("LPS-MVs") induced significant upregulation of endothelial ICAM-1 and VCAM-1 expression in LPS-pretreated IPLs, but not in control IPLs (Figure 5.5). Importantly, MVs from untreated mice donors ("control-MVs") had no effect on endothelial cell CAM expression in LPS-pretreated IPLs. E-selectin expression, which is normally very low at baseline[291], was not increased in any of the treatments (data not shown).

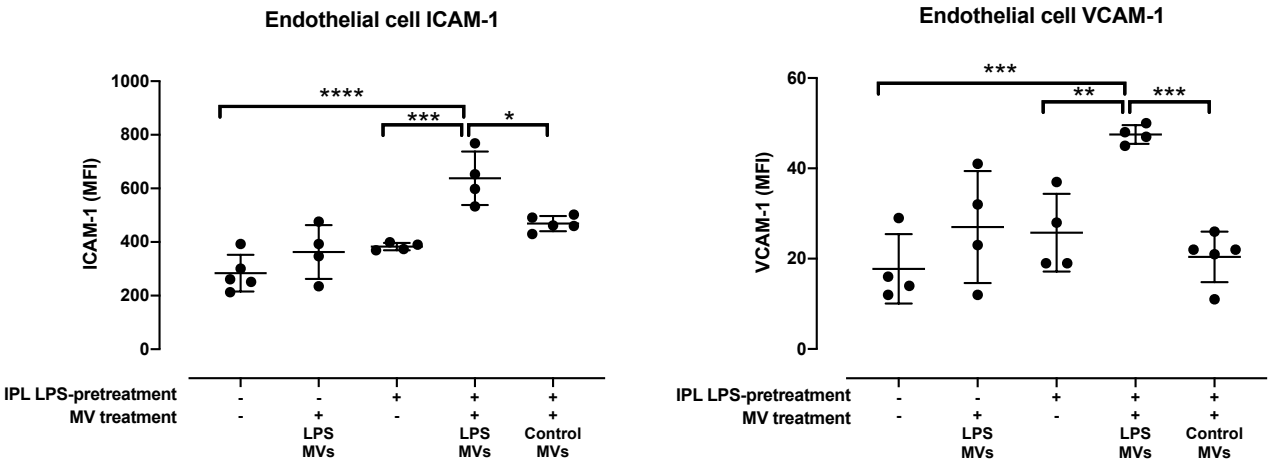

Figure 5.5 Upregulation of cell adhesion molecules on lung endothelial cells by endotoxaemic MVs in LPS-pretreated IPL.

*MVs isolated from either untreated ("control-MVs") or LPS (2μg, i.v., 1h)-treated ("LPS-MVs") mouse plasma were infused into the closed, recirculating circuit of IPLs prepared from either untreated or LPS (20ng, i.v., 2h)-pretreated mice for 4h. Expression of ICAM-1 and VCAM-1 on lung endothelial cells were assessed by flow cytometric analysis of lung single cell suspensions. "LPS-MVs" induced significant upregulation in ICAM-1 and VCAM-1 expressions on lung endothelial cells in LPS-pretreated IPLs but not in control IPLs. "Control-MVs" had no effects in LPS-pretreated IPLs. (Mean ± SD, n=4-5, *p<0.05, **p<0.01, ***p<0.001, ****p<0.0001, one-way ANOVA with Bonferroni's multiple comparisons test.)*

Activation of monocytes/macrophages in LPS-pretreated IPLs by MVs from endotoxaemic mice

We analysed MV-induced upregulation of CD86 expression as an activation marker on Ly6C^{high} monocytes (CD11b+, F4/80+, Ly6C^{high}), Ly6C^{low} monocytes (CD11b+, F4/80+, Ly6C^{low}, MHCII-) and interstitial macrophages (CD11b+, F4/80+, Ly6C^{low}, MHCII+) (Figure 2.10)[294,562]. MVs from LPS challenged mice "LPS-MVs" induced upregulation of CD86 on Ly6C^{high} monocytes and interstitial macrophages in the LPS-pretreated IPL, but not in the control IPL (Figure 5.6). As with endothelial responses, MVs from untreated mice donors ("control-MVs") did not induce monocyte/macrophage CD86 upregulation in the LPS-pretreated IPLs. No significant changes were detected in the expression of CD86 on Ly6C^{low} monocytes under all treatment conditions. Neutrophil activation, assessed by surface expression of CD11b, was apparent with LPS-pretreatment without MVs, and addition of MVs did not produce any further response (Figure 5.7). These findings, together with previous studies by the group[1,187,291], suggest an important role for lung-marginated Ly6C^{high} monocytes and circulating endogenous MVs in the potentiation of pulmonary vascular endothelial cell activation during endotoxaemia.

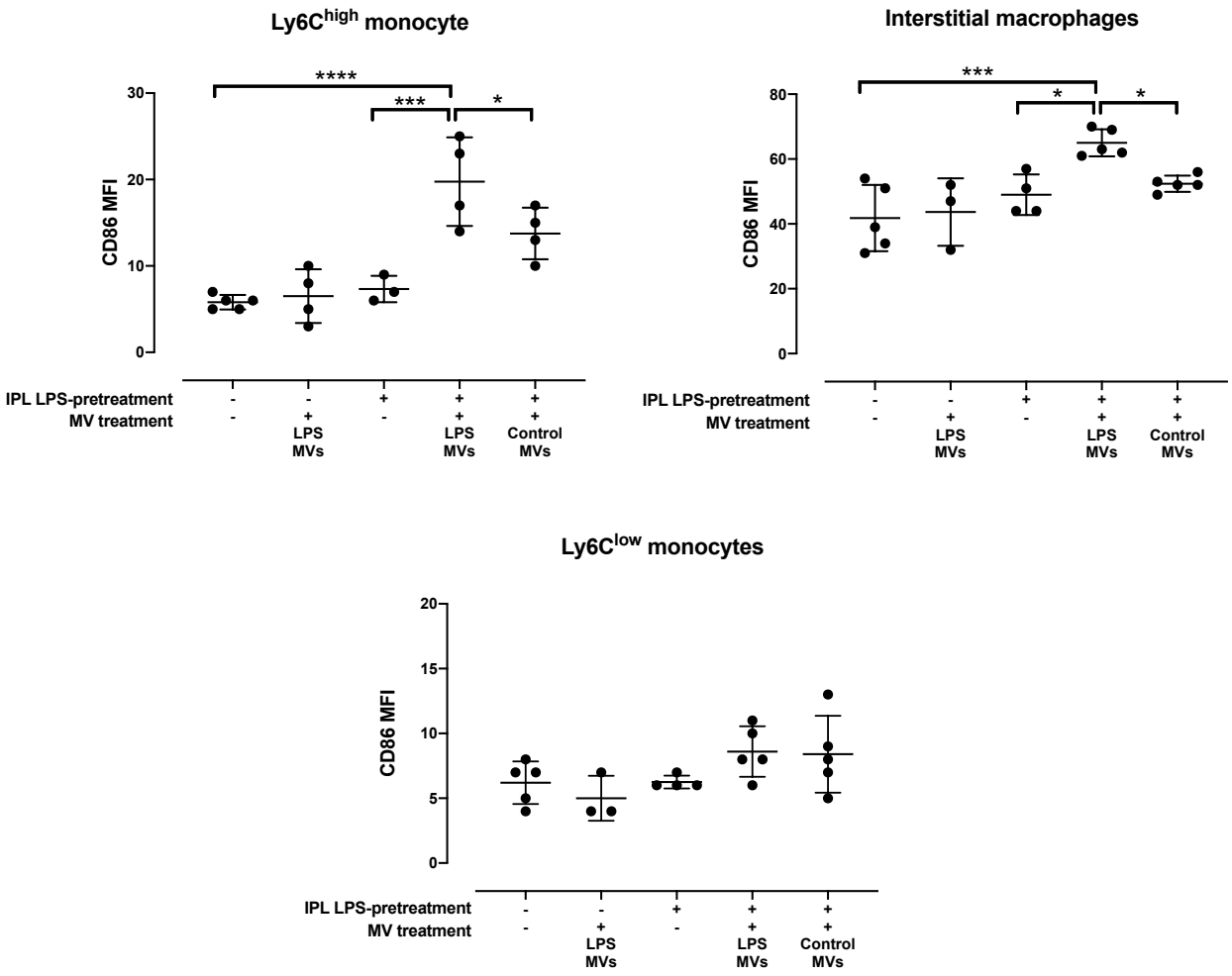

Figure 5.6 Upregulation of CD86 on lung-marginated Ly6C^{high} monocytes and interstitial macrophages by endotoxaemic MVs in LPS-pretreated IPL.

*MVs isolated from either untreated ("control-MVs") or LPS (2μg, i.v., 1h)-treated ("LPS-MVs") mouse plasma were infused into the closed, recirculating circuit of IPLs prepared from either untreated or LPS (20ng, i.v., 2h)-pretreated mice for 4h. Expressions of CD86 on lung monocytes and macrophages were assessed by flow cytometric analysis of lung single cell suspensions. "LPS-MVs" induced significant upregulation in CD86 expressions on Ly6C^{high} monocytes and interstitial macrophages in LPS-pretreated IPLs, but not in control IPLs. "Control-MVs" had no effects in LPS-pretreated IPLs. CD86 expression on Ly6C^{low} monocytes remained unchanged across all treatment groups. (Mean ± SD, n=3-5, *p<0.05, ***p<0.001, ****p<0.0001, one-way ANOVA with Bonferroni's multiple comparisons test)*

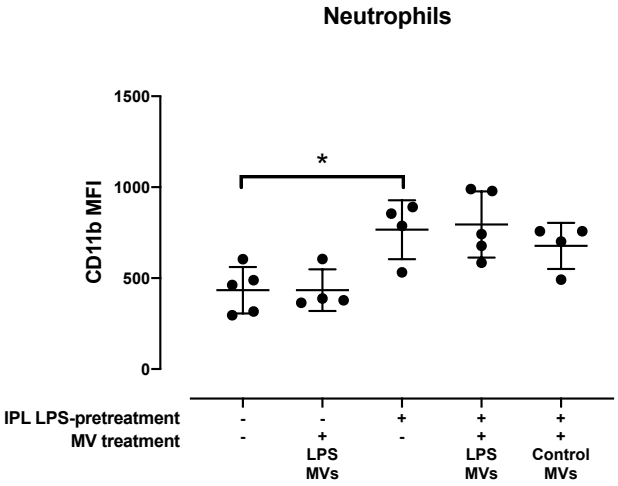

Figure 5.7 Upregulation of CD11b on lung-marginated neutrophils in LPS-pretreated IPL.
*MVs isolated from either untreated ("control-MVs") or LPS (2µg, i.v., 1h)-treated ("LPS-MVs") mouse plasma were infused into the closed, recirculating circuit of IPLs prepared from either untreated or LPS (20ng, i.v., 2h)-pretreated mice for 4h. Expression of CD11b on lung neutrophils was assessed by flow cytometric analysis of lung single cell suspensions. LPS-pretreatment induced increased expression of CD11b on neutrophils, but no further response was elicited by MV treatment in IPLs. (Mean ± SD, n=4-5, *p<0.05, one-way ANOVA with Bonferroni's multiple comparisons test.)*

5.5.3 Measurement of lung oedema in MV-treated IPLs.

In the same experiments, lung oedema was assessed by lung wet-to-dry weight ratio and total bronchoalveolar lavage fluid (BALF) protein at the end of the 4h IPL protocol (Figure 5.8). It was found that LPS-pretreatment alone increased lung permeability during the 4h protocol, evidenced by both the wet-to-dry weight ratio and BALF protein measurements. However, treatment with "LPS-MVs" did not elicit any further increase in oedema but instead, attenuated it significantly. This finding was unexpected considering the clear response pattern of pulmonary vascular cell activations in response to "LPS-MVs" in LPS-pretreated IPL described above. Furthermore, "control-MVs" produced a similar suppression of oedema formation in the LPS-pretreated IPL, further suggesting that the effect was distinct from the pro-inflammatory response to "LPS-MVs". It should be noted at this stage that it is normal for a gradual accumulation of lung water in the IPL system (wet-to-dry weight ratio of ±5.5 in untreated control IPL vs. ±4.3 in untreated non-perfused lungs) and that perfusion much beyond 4h duration would result in non-specific oedema[294,564].

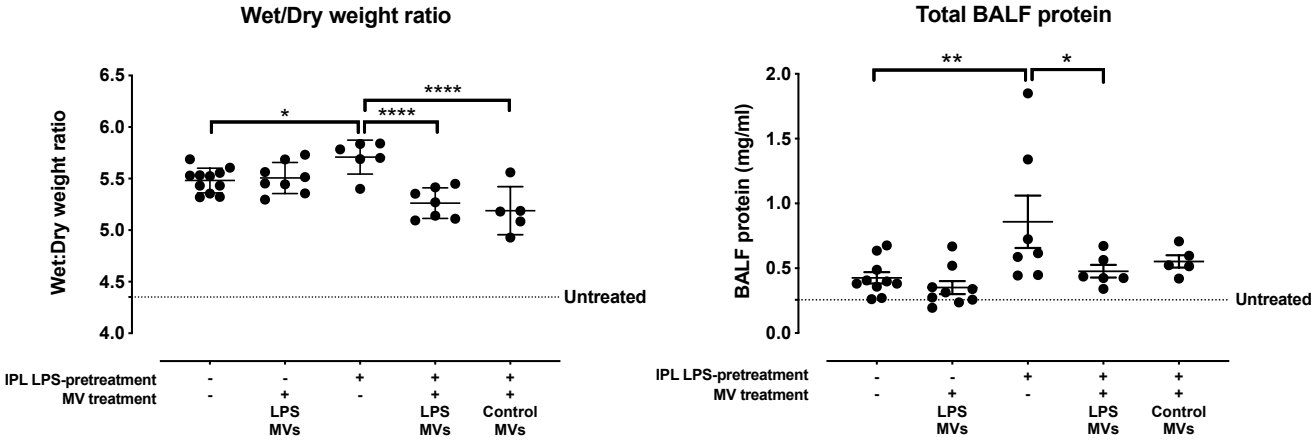

Figure 5.8 Assessment of lung injury change in IPL via change in lung permeability.

*MVs isolated from either untreated ("control-MVs") or LPS (2μg, i.v., 1h)-treated ("LPS-MVs") mouse plasma were infused into the closed, recirculating circuit of IPLs prepared from either untreated or LPS (20ng, i.v., 2h)-pretreated mice for 4h. Lung injury was assessed by lung wet-to-dry weight ratio and total BALF protein as indicators of lung permeability change. LPS-pretreatment of IPLs induced significant increase in lung permeability, which were attenuated by both "LPS-MVs" and "Control-MVs". (Mean ± SD, n=5-10, *p<0.05, **p<0.01, ****p<0.0001, one-way ANOVA with Bonferroni's multiple comparisons)*

5.5.4 Measurement of soluble markers of inflammation and injury in MV-treated IPLs.

Release of soluble inflammation and injury markers (KC, IL-6, VEGF and RAGE) into perfusates was measured at the end of the 4h IPL protocol (Figure 5.9). Interestingly, treatment with “LPS MVs” in the control IPL, but not in LPS-pretreated IPL, produced a relatively small but signifiant increase in the levels of perfusate RAGE, despite the lack of oedema formation in this treatment group. However, there were no other significant differences in the cytokines levels across all treatment groups. Therefore, despite the clear effects of “LPS-MVs” on cell activation and LPS-pretreatment on enhanced oedema, neither of these translated to equivalent changes in the soluble markers. It should be noted at this stage that the levels of all markers were elevated at the end of 4h in the untreated control IPL compared to the baseline levels observed previously[294], indicating constitutive release and accumulation of metabolites, or some degree of inflammation during the continuous recirculating perfusion protocol. Therefore, IPL perfusion much beyond 4h duration may result in non-specific release of inflammatory mediators.

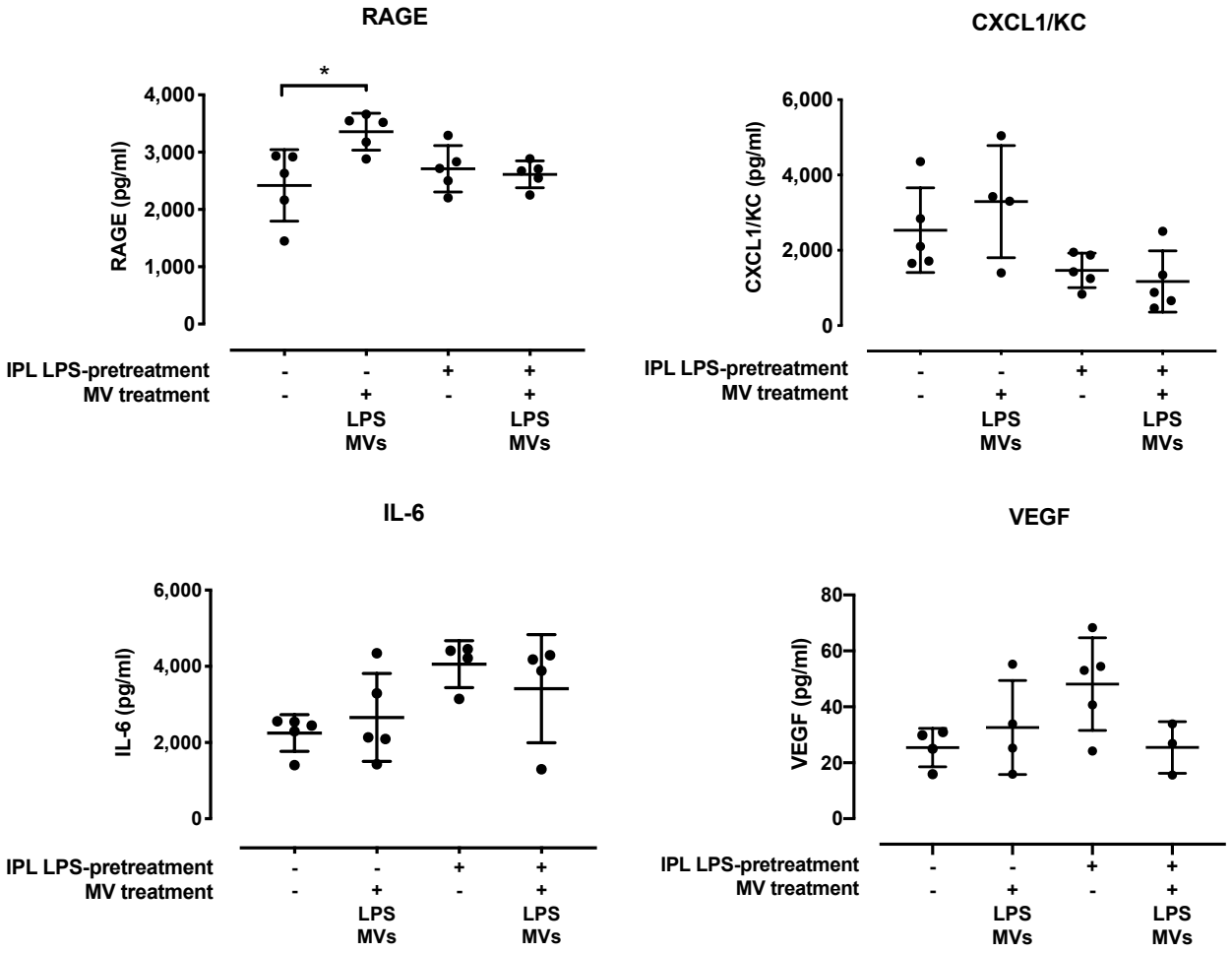

Figure 5.9 Cytokines released into IPL perfusate.

*MVs isolated from either untreated ("control-MVs") or LPS (2µg, i.v., 1h)-treated ("LPS-MVs") mouse plasma were infused into the closed, recirculating circuit of IPLs prepared from either untreated or LPS (20ng, i.v., 2h)-pretreated mice for 4h. IPL perfusates were differentially centrifuged to remove cells and any remnant MVs. Soluble cytokines released into the IPL perfusate was assessed by ELISA. "LPS-MVs" induced significant increase in RAGE in LPS-pretreated IPLs. (Mean ± SD, n=3-5, *p<0.05, one-way ANOVA with Bonferroni's multiple comparisons)*

5.6 Discussion

5.6.1 Summary

This chapter explored a unique combination of *in vivo*-generated MVs-to-*ex vivo* IPL adoptive transfer strategy to delineate the pulmonary-specific effects of circulating MVs produced during inflammation on pulmonary vascular injury/inflammation. Based on the kinetics of circulating MV subtypes during endotoxaemia (Chapter 4), the early 1h timepoint after LPS injection was selected for harvest of total MVs and used for MV challenge in the IPL. When infused into LPS-pretreated IPLs *ex vivo*, these MVs elicited an activation response in lung endothelial cells, Ly6C^{high} monocytes and interstitial macrophages. However, we also observed 'protective' roles for MVs in attenuating the development of oedema during IPL and no clear effect on the relatively high levels of soluble mediators in perfusate. Collectively, these preliminary results demonstrate some clear functionality of circulating MVs during endotoxaemia, but further refinement of the approaches may be necessary for demonstrating clearer signals to permit further dissection of MV biology.

5.6.2 Optimisation of IPL for prolonged assays.

Despite its distinct advantages for the study of pulmonary vascular inflammation in isolation from systemic variables, IPL has most frequently been used for the investigation of direct ALI aetiologies, including pneumonia associated alveolar injury[311], ventilator-induced lung injury[295,312], lung ischaemia-reperfusion injury[294,313]. In the context of pulmonary vascular injury, IPL serves as a useful model for the measurement of airway and vascular reactivity in response to various biological or pharmacological mediators[314,315,317,558,565]. However, not many studies utilise IPL to investigate responses to insults within the pulmonary vasculature, potentially owing to the difficulty in maintaining IPL for sufficient periods to measure transcriptional responses. In order to detect the effect of MVs in these pilot experiments, we decided to run the IPL for 4h with recirculation of the perfusate to allow for transcriptional changes and for any injury to endothelial cells to develop that may be secondary to mediator release from other inflammatory cells interacting with MVs (e.g. marginated monocytes). It has been shown that the upregulation of adhesion molecules such as ICAM-1 and VCAM-1 can be detected in IPL maintained between 3-4h, perfused with either allogeneic blood or cell culture media-based perfusate buffer[564,566,567]. However, IPL perfused with recirculating circuit can be unstable,

where inflammation and oedema can occur or be amplified overtime due to accumulation of metabolites. Although the exchange of IPL perfusate every hour with fresh perfusate medium may have an added advantage for the maintenance of IPL stability as shown by our group previously in a direct ALI model[295], we considered this approach unsuitable for an indirect ALI investigation due to potential loss of the infused MVs in the perfusate during exchange. Therefore, we took extensive precautions to minimise non-specific responses in the prolonged IPL protocol. Buffer composition was optimised for reproducibility, using a serum-free and sterile cell culture-grade albumin buffer with the osmolality value specifically adjusted for mice. On top of physiological buffer optimisation, several other steps were taken to improve the IPL stability, such as application of positive end expiratory pressure (PEEP) throughout preparation procedure, recruitment of lungs with sustained inflation every 15min intervals and the use of relatively slow perfusion flow rate. Stringent cleaning routines for the tubing and connectors, and their replacement, were also implemented, with care taken to randomise test groups to control for any drift in the system mechanism between new tube replacements. Over time, with incremental improvements and precision in the setup and maintenance of procedure, a reliable 4h IPL protocol was achieved with minimal development of oedema.

5.6.3 LPS-priming in the potentiation of lung injury in IPL.

In our previous study (Chapter 3 and publication[1]), we demonstrated that low-dose LPS endotoxaemia produced a dramatic increase in MV uptake by lung-marginated monocytes. We therefore implemented this condition in the IPL model with comparison to control IPL from untreated mice. An LPS 'priming' effect, was clearly demonstrated by the "LPS-MV" challenge in eliciting cell activation responses in LPS-pretreated IPLs, but not in control IPLs, and the lack of responses in "control-MV"-treated LPS-pretreated IPLs. However, LPS-pretreatment alone increased activation of neutrophils and produced oedema, neither of which were augmented by MV challenge, but instead appeared to reverse the oedema formation. These effects of LPS pretreatment on neutrophils and oedema presumably represent ehancement of lung inflammation prior to or during IPL, and as such may be distinct from the priming effect on monocytes and endothelial activation. It has been shown that infusion of LPS into IPL perfusate could potentiate the lung response to other mediators[565,568], such as PAF and methacholine, but on its own, LPS does not usually elicit any change in lung wet-to-dry

weight ratio, especially in absence of blood components in IPL perfusate[230]. Here, airway respiratory and vascular reactivity mechanics were measured to ensure low-dose LPS-pretreatment of IPL mouse donor would not elicit significant inflammation and injury, which could potentially mask any inflammatory changes in response to MV treatment. It was previously found that IPLs obtained from LPS-treated rats exhibit significant increase in pulmonary perfusion pressure[317], whereas IPLs of guinea pigs challenged with LPS infused in the perfusate buffer did not exhibit any significant change in both pulmonary artery pressure and pulmonary capillary pressure[240]. As such, to achieve a 'primed state' of the lungs for investigation of pulmonary vascular cell responses during systemic inflammation, *in vivo* low-dose LPS treatment of mice prior to isolation of the lungs may be more physiologically relevant (new populations of monocytes and neutrophils had time to mobilised from bone marrow and marginate to the lungs[187]), compared to infusion of LPS into perfusate buffer of IPL obtained from untreated mice. Furthermore, the lack of significant difference between control and LPS-pretreated IPL in lung airway and vascular mechanics, as well as the preservation of lung-marginated monocytes after 4h perfusion in IPL, supported the use of low-dose LPS-pretreatment IPL model for following investigations with MVs.

5.6.4 MV-mediated endothelial activation and indirect ALI

To our knowledge, the ability of MVs to elicit activation in various lung vascular cell types in LPS-pretreated IPL is the first evidence for direct pulmonary specific effects of circulating MVs in the lungs. A role for MVs in indirect ALI has been suggested previously by systemic administration of *in vitro* generated MVs. Although some of the studies that used MVs generated from stored red blood cells may be relevant to transfusion-induced ALI[391,442,569], studies using *in vitro* human umbilical vein endothelial cells (HUVEC) to generate endothelial-derived MVs may not be representative of the *in vivo* endogenously produced MVs during systemic inflammation[443,444]. Although endothelial-derived MVs is currently being investigated as biomarker for diagnosis and prognosis in early sepsis in clinical trial (NCT01998139), we observed in this study (Chapter 4) that during LPS challenge, only levels of neutrophil- and monocyte-derived MVs were acutely increased, whereas levels of endothelial-, erythrocyte- and platelet-derived MVs did not change significantly throughout. Although leukocyte-derived MVs were previously shown to activate monocytes[377] and endothelial cells *in vitro*[570,571], yet

again, MVs investigated in these studies were generated *in vitro* with cell-specific stimulus in isolation. As each cell type may release quantitatively and qualitatively distinctive MV phenotypes depending on the stimulus they encounter, functional studies using *in vitro*-generated MVs, without clear rationale for a particular chosen MV subtype or stimulus used, may limit our understanding of the true biological properties of endogenous, disease-relevant MV.

On the recipient side, although MV treatment on endothelial cells *in vitro* may provide a clearer molecular effect, the complex biological interaction of vascular cells such as lung-marginated monocytes with the endothelium may not be reciprocated *in vitro*. As discussed above, the 'primed state' of the lungs may require *in vivo* LPS challenge to mobilise and marginate the cells to pulmonary vasculature, and may not be achieved by *in vitro* LPS treatment of cell culture. Furthermore, endothelial permeability studied using *in vitro* cultured endothelial cells were found to exhibit phenotypic differences from that of ex vivo IPL[230], where some agents found to increase endothelial permeability *in vitro* has no effects in IPL. In contrast, *in vivo* models that employ direct injection of MVs into intact animals for functional studies may not provide extra information, as the site or mode of MV action could not be defined due to complex influences from other remote systemic organs. In the case of the lungs, it is unclear whether MVs act directly within the pulmonary vasculature, indirectly in remote vascular beds (e.g. the splanchnic circulation) or systemically within circulating blood (e.g. via complement or coagulation pathway activation). Based on these considerations, we have taken our unique approach of adoptively transferring total circulating MVs from an endotoxaemic donor mouse, to an IPL from another recipient mouse to evaluate the direct contribution of MVs to pulmonary responses.

5.6.5 MV-mediated lung oedema and inflammation

The reduction of lung oedema by both "control-MVs" and "LPS-MVs", despite their activation of pulmonary cells by the latter, was both unexpected and difficult to interpret. It is possible that the induction mechanisms of each response differ, and that in the IPL preparation, MVs trigger endothelial activation but not permeability increase. The unavoidable but very gradual increases in tissue water (i.e. wet-to-dry weight ratio increases) during IPL are mostly likely due the effects of blood-free

perfusion of capillaries and loss of lymphatic drainage[563]. The reduction of permeability by MV treatment suggests the involvement of permeability-reversing signalling pathways, such as sphingosine-1-phosphate (S1P), which was found to be expressed in high levels in MVs derived from bone marrow mesenchymal stem cells (MSCs)[572], and has been an area of promising therapeutic research targeting oedema as a central mechanism of organ injury in sepsis/SIRS[563] and primary graft dysfunction in lung transplantation[573]. Although the presence of MCS-derived MVs in our total MV preparation from LPS-treated mice is undefined, it possible that MVs buffer the system against the vascular leak in some way, but as the MV effect appears to be specific to the LPS-pretreated IPL, it seems more likely to be related to an inflammatory process rather than the IPL procedure per se. Anti-inflammatory effects of neutrophil-[380,574–576] and platelet-derived[577–579] MVs have also been described, however these were mainly demonstrated through inhibition of cytokines release, which we did not observe here in this study. Other than MVs, there might be other particulates known to co-isolate with MVs preparations through centrifugation present in our MVs preparation, such as high-density lipoproteins (HDLs)[580], which were also found to also exert protective effects on endothelial function and integrity[581], possibly through S1P-associated molecular mechanism[582,583]. To address these uncertainties, a more defined MV preparation is required, ideally isolated from individual MV subtypes based on surface expressed markers to eliminate co-isolated particulates and other unknown MV subtypes.

We measured a limited panel of soluble markers of inflammatory and injury in this study but found no obvious differences between treatment groups apart from a modest but significant increase in RAGE in control IPL infused with “LPS-MVs”. Although only four markers were studied (KC, IL-6, VEGF and RAGE), these are commonly measured in IPL as markers of inflammation[294,310–312,584]. However, baseline levels of KC, IL-6 and RAGE were relatively high in the control IPL, at comparable levels to those detected previously by our group in lung ischaemia-reperfusion IPL model[294]. Therefore, the development of such intrinsic IPL system noise by 4h perfusion may have masked detection of any MV-induced signal. Despite the unexpected and ambiguous effects in lung oedema and cytokines release, the clear MV-induced endothelial transcriptionally regulated responses suggests an alternative signalling process or the involvement of other pro-inflammatory cytokines, such as TNF-

α, which are induced by MVs at early timepoints and could stimulate downstream endothelial CAM upregulation.

5.6.6 Limitations of experimental design & further improvement.

As it was not possible to quantify MVs with a generic marker, thus the dose of MVs for each IPL were based on using the total MV population obtained from one donor mouse, either untreated or LPS-treated. Instead of a matched MV quantity comparison, by this approach we evaluated the effect of exposing the pulmonary vascular to the normal circulating MV pool versus the LPS challenge-modified pool, which appeared to differ in composition only with respect to the increase in myeloid-MV subtypes (neutrophil- and monocyte-MVs). Despite physiologically stable, 4h of recirculating IPL runtime causes accumulation of metabolites and unavoidable oedema. When used for measurement of intricate changes in immune response such as perfusate cytokines and minor increase in lung water, these effects are masked by the high background noise intrinsic to the IPL system. Thus, as measurements of lung oedema and the production of cytokines in IPL maintained for 4h were inconclusive in this study potentially due to prolonged IPL runtime, improvement in the signal-to-noise ratio is a necessary next step, including a more ‘defined’ MV preparation and shorter IPL runtime. These limitations are further discussed and improved in the next chapter.

5.7 Conclusion

To evaluate the role of systemically released MVs in indirect ALI, here we investigated the feasibility of a direct adoptive transfer of circulating *in vivo* MVs from a donor mouse into a recipient *ex vivo* IPL. We demonstrated in the previous chapter an exclusive acute increase in MVs derived from neutrophils and monocytes during endotoxaemia in mice. Here, we further demonstrated that when these total MVs derived from endotoxaemic mice were transferred to LPS-pretreated IPL, they induced a direct activation of lung-marginated monocytes and endothelial cells *ex vivo*. The lack of responses in the "control-MVs"-treated LPS-pretreated IPL, and in the "LPS-MVs"-treated control IPL, demonstrated the essential role of both endotoxaemia-induced MVs and a "primed-state" of the lung for cellular activation in the pulmonary vasculature. Together, these findings shown for the first time that *in vivo*-generated endotoxaemic MVs are capable of directly modulating pulmonary vascular injury within the lung.

Chapter 6

Circulating myeloid-derived microvesicles mediate indirect ALI during systemic inflammation

Parts of the content of this chapter have been presented as a conference abstract:

Circulating Neutrophil-derived Microvesicles During Endotoxaemia Induce Pulmonary Vascular Injury. *Y. Y. Tan, K. P. O'Dea, M. Takata. American Journal of Respiratory and Critical Care Medicine 2020; 201: A2670.*

Chapter 6 Circulating myeloid-derived microvesicles mediate indirect ALI during systemic inflammation

6.1 Abstract

Background

Circulating neutrophil-derived microvesicles (MVs) increase dramatically during acute systemic inflammation of infectious and non-infectious aetiologies and were found to correlate with disease severity and mortality. However, their functional role in the propagation of organ injury is largely unknown. Here, using an *ex vivo* isolated perfused lung (IPL) model, we investigated the biological effects of circulating MVs from endotoxaemic mice on pulmonary vascular responses in IPL, in particular focusing on differential effects of individual MV subtypes, i.e. myeloid- vs. platelet-derived MVs.

Methods

C57BL/6 mice were pretreated with clodronate liposomes (i.v., 48h) to deplete intravascular macrophages, followed by LPS (2μg, i.v., 1h) to induce endotoxaemia. At 1h post-LPS, platelet poor plasmas were analysed by flow cytometry, and MVs isolated by differential centrifugation, with or without individual MV subtypes further separated using immunoaffinity magnetic bead separation. The recipient IPL was prepared from a separate mouse pretreated with low-dose LPS (20ng, i.v., 2h), with or without clodronate liposome pretreatment (i.v., 24h prior) to deplete lung monocytes. Isolated MVs were infused into the recirculating IPL for 2h. Lung inflammation/injury was assessed by lung wet-to-dry weight ratio and IPL perfusate cytokines by ELISA.

Results

When intravascular macrophages were depleted, myeloid- and platelet-derived MVs were the most predominant MV subtypes produced during endotoxaemia. Infusion of total endotoxaemic mouse MVs (including all subtypes) into LPS-pretreated IPLs resulted in significant pulmonary oedema, which was abolished in the monocyte-depleted IPLs. Infusion of myeloid-MVs (CD11b+ selected) produced a comparable level of oedema to the total MVs, while platelet-MVs (CD41+ selected) produced a statistically significant, but much lower level of oedema. Infusion of myeloid-MVs, but not platelet-MVs, increased the release of pro-inflammatory cytokines and soluble markers of endothelial injury in IPL perfusates.

Conclusion

We demonstrated for the first time, that circulating MVs generated *in vivo* during systemic inflammation induce pulmonary vascular injury and the myeloid-derived MV subtype was the primary contributor to this lung monocyte-dependent response. Therefore, myeloid-derived MVs can serve as vehicles for long-range pro-inflammatory signalling by their parent cells to induce indirect acute lung injury.

6.2 Background

6.2.1 MV production-clearance dynamics

It has been previously demonstrated that the systemically administered MVs are rapidly removed from the circulation within 10min, where only 10% of injected dose remain in the blood by 30min post-injection, and that this occurs mainly via the reticuloendothelial system (RES) in the liver and spleen under non-inflammatory conditions[397,398,400]. Therefore, the level of endogenously produced circulating MVs measured at any one timepoint reflects only the balance between rate of production and clearance[342,585]. Our recent study on *in vivo* MV uptake indicated that the MV clearance dynamics may be further altered by the development of enhanced uptake capacity by monocytes during low-grade systemic inflammation[1], in part due to their expansion in blood from the bone marrow reservoir[1]. These findings based on the clearance of injected MVs or observations of MV dynamics following a defined insult suggest that there is a substantial underestimation of the total production of MVs in response to inflammatory insults, especially if they are generated systemically during endotoxaemia or other SIRS conditions. Therefore, to evaluate the total production of all endogenously released MVs and their biological activities in the models such as the IPL, the factor of MV clearance should be minimised or eliminated.

6.2.2 MV subtypes in sepsis/SIRS

In a comprehensive analysis of vascular MV subtypes in septic patients, an increase was demonstrated in MVs number across all subtypes investigated including platelet-, endothelial-, erythrocyte-, leukocyte-, neutrophil-, monocyte-, T cell- and B cell-derived [432]. However, other studies that measured a less comprehensive panels have also demonstrated increases in circulating level of platelets-[421–424], leukocytes-[380,425–428] and endothelial-derived MVs[429–431], which were most commonly detected in sepsis patients. Although MV levels generally increase in septic patients, they were found to inversely correlate with disease severity, mortality and development of ARDS[433–437]. Due to disease heterogeneity in sepsis and varying degree of organs dysfunction in patients, MV clearance and production dynamics will likely vary considerably over time in each individual, and the time of sampling may be critical in determining their relationship to the disease progression. We previously investigated MV levels in severe burns patients within 24h of admission to ICU and found that neutrophil-MVs were

most consistently elevated across different patients and related to clinical severity[427]. In parallel, large increases in neutrophil-MVs were observed in patients with meningococcal sepsis within the first 10h of admission[420], whereas in another study neutrophil-MVs sampled upon ICU admission were found to predict mortality[377]. Based on acute abundance increase in neutrophil-MVs in patients and here in this study following LPS injection, it seems likely that these MVs have some role in organ injury, yet *in vivo* data on the functional activities of different MV subtypes is only available for endothelial-[443,444], erythrocyte-[391,442] and monocyte-MVs[586,587]. As discussed in the previous chapter, using a relatively crude preparation of plasma derived MVs may produce diverse effects in the IPL endpoints that limit any meaningful interpretation. Thus, when studying the functional activity of *in vivo* MVs containing a mixture of subtypes, it may be essential examine subtype individually using appropriate immunoaffinity isolation methods.

6.2.3 Lung-marginated monocytes and neutrophils in ALI

The margination and activation of neutrophils and monocytes within the pulmonary circulation, in direct contact with capillary walls, is a core process in indirect ALI pathogenesis. Numbers of each population increase several-fold during even relatively low-grade systemic inflammation, and, in a primed state, they respond vigorously *in situ* to subsequent intravascular insults[187,291]. Depletion of intravascular monocytes in the lung were found to sufficiently attenuate pulmonary vascular inflammation and oedema *in vivo* and *ex vivo*[294–299]. Based on the potentially crucial roles of lung marginated monocytes in ALI and the increase in MV uptake capacity during endotoxaemia[1], we hypothesised that they would play a significant role in MV-mediated effects in the IPL.

6.3 Aims

In Chapters 4 & 5, we demonstrated the selective increase in numbers of neutrophil- and monocyte-derived MVs during endotoxaemia and found preliminary evidence suggesting a pro-inflammatory role for these MVs in pulmonary vascular inflammation in *ex vivo* IPL. However, we recognised there were limitations in our approach that required modification to define circulating MV functions in the IPL. We considered it likely that the MVs harvested were not truly representative of the total MV output during endotoxaemia due the previous studies showing that a majority of MVs are cleared rapidly by the RES. Additionally, 4h of recirculating IPL produced significant background in the measurement of lung oedema and perfusate cytokines, reducing the detection sensitivity of the functional outcome measurements. To further consolidate our findings, we aimed to optimise the *in vivo* MV-to-*ex vivo* IPL transfer model to address the roles of selected MV subtypes and the contribution of lung-marginated monocytes to indirect ALI.

The specific aims were to:

1) Investigate the total production of MVs *in vivo* during endotoxaemia by inhibition of RES clearance.
2) Investigate the role of lung-marginated monocytes in MV-induced pulmonary vascular inflammation/injury.
3) Isolate and purify individual *in vivo* MV subtypes from endotoxaemic mice.
4) Investigate the contribution of specific MV subtypes in pulmonary vascular inflammation/injury.

6.4 Methods

6.4.1 MV production from untreated or *in vivo* endotoxaemic mice

C57BL/6 mice received i.v. injection 200μl of clodronate liposomes 48h prior to the LPS injection (2μg, i.v.) for 1h. Clodronate liposome treatment for 48h enables the depletion of intravascular macrophages, which reduces MVs clearance and enables recovery of MVs more representative of the total intravascular output during endotoxaemia, but allow repopulation of monocytes in the circulation to normal levels. MVs were isolated from blood by differential centrifugation (2.8.3 & 2.8.4), and the washed MV pellet was either resuspended in pre-warmed IPL perfusate buffer for infusion into the IPL circuit, or in 0.2μm filtered PBS for magnetic-beads isolation.

6.4.2 Immunoaffinity magnetic beads isolation of MV subtypes

MVs isolated from PPP were resuspended in PBS and incubated with bead-conjugated antibodies at pre-titrated concentration of 1μl bead-conjugated antibody/biotin-conjugated antibody to 10^6 'target MVs', for 30min on ice. For the positive selection or depletion of myeloid-derived MVs, directly conjugated anti-CD11b magnetic beads (Miltenyi Biotec) were used, whereas for platelet-derived MVs, primary anti-CD41 biotin (Miltenyi Biotec) and anti-biotin magnetic beads (Miltenyi Biotec) were incubated together with MVs for 30min on ice. For depletion of other MV populations, MVs were incubated with a mixed cocktail of pre-titrated biotinylated antibodies (1 in 100 final dilution of each antibody) (anti-TER119 for RBC-, anti-CD31 for endothelial-, anti-CD41 for platelet-, and anti-CD11b for myeloid-derived MVs) (Biolegend) for 15min, followed by anti-biotin magnetic beads, for 30min on ice. MV subpopulations were fractionated through magnetised columns, and the positively selected, bead-bound MV fractions were recovered from the magnetic column and the negatively selected, bead-free MV fractions were recovered from the flow through. The desired MV fractions were analysed by flow cytometry, centrifuged at 20,000g for 30min and resuspended in pre-warmed IPL perfusate buffer for infusion into the IPL circuit. Percentage recovery and percentage depletion of MVs after immunoaffinity magnetic beads isolation were calculated using **Equation 5** & **Equation 6** as below:

Percentage recovery: $\frac{\text{No.of MV subtype in desired fraction}^*}{\text{No.of MV subtype before fractionation}} \times 100\%$

Equation 5 Calculation of MV subtype percentage recovery after immunoaffinity magnetic beads isolation.

Percentage depletion: $\left(1 - \frac{\text{No.of MV subtype in desired fraction}^*}{\text{No.of MV subtype before fractionation}}\right) \times 100\%$

Equation 6 Calculation of MV subtype percentage depletion after immunoaffinity magnetic beads isolation.

*For negative selection and depletion of myeloid MVs, the 'desired fraction' is unbound flow through.

*For positive selection of myeloid MVs, the 'desired fraction' is column elute.

6.4.3 *Ex vivo* isolated perfused lungs (IPL)

C57BL/6 mice were pretreated with low-dose LPS (i.v. 20ng, 2h) with or without i.v. clodronate liposome pretreatment (i.v., 24h prior) for intravascular lung monocytes depletion. IPL was performed as described before (5.4.2), with exception of a shorter runtime of 2h, after infusion of MVs into the non-recirculating perfusion circuit (Figure 6.1). For "total MV" treatment, MVs from one donor mouse (treated with i.v. 48hrs clodronate liposomes, i.v. 2μg LPS for 1h) was infused into the IPL (1:1 donor-to-recipient adoptive transfer). For "magnetic beads-isolated MV" treatment, standardised concentration of $9x10^7$ CD11b-selected myeloid-MVs or CD41-selected platelet-MVs were infused into the recirculating IPL perfusion circuit. At the end of 2h experimentation, IPL perfusate was collected for analysis of soluble cytokines by ELISA after removal of residual cells and MVs by centrifugation at 300 x g for 10min followed by 20,000 x g for 30min. The right lower lobe of lung was tied off and oedema was determined by wet-to-dry weight ratio measurement.

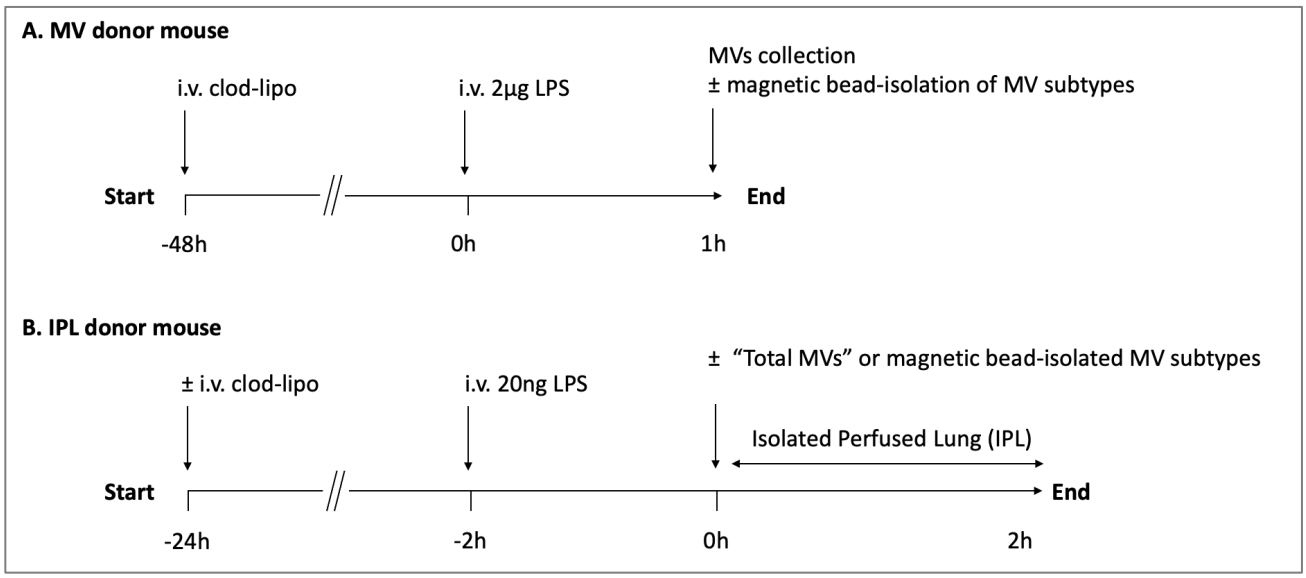

Figure 6.1 Total *in vivo* MV-to-*ex vivo* IPL (2h) adoptive transfer methodology.

C57BL/6 mice were pretreated with clodronate liposomes (i.v. clod-lipo, 48h) to deplete intravascular macrophages, followed by LPS (2µg, i.v., 1h) to induce endotoxaemia. MVs were isolated by differential centrifugation, with or without individual MV subtypes further separated using immunoaffinity magnetic beads. The recipient IPL was prepared from a separate mouse pretreated with low-dose LPS (i.v., 20ng, 2h), with or without clodronate liposome pretreatment (i.v., 24h before) to deplete lung monocytes. Isolated MVs were infused into the recirculating IPL for 2h.

6.5 Results

6.5.1 Investigation of total circulating MV levels during endotoxaemia.

Elevation of all circulating MV subtype levels by depletion of intravascular macrophages.

To evaluate levels of circulating MVs during endotoxaemia under depressed RES clearance conditions, we injected clodronate liposomes for 48h to deplete intravascular macrophages, as previously described[1,187,297]. Similar MV gating strategies were used, as demonstrated in previous chapter: neutrophil-MVs CD11b+, Ly6C+, Ly6G+; monocyte-MVs CD11b+, Ly6C+, Ly6G-; platelet-MVs CD41+; endothelial-MVs CD31+, CD41-; and erythrocyte-MVs TER-119+ (Figure 6.2). At 48h post-clodronate liposome (when $Ly6C^{high}$ monocytes are replenished from the bone marrow) and 1h post-LPS injection, numbers of all circulating MV subtypes were ≥10-fold higher in clodronate liposome-treated than control mice (1h LPS-treated only) (Figure 6.3). Platelet- and neutrophil-MVs were the two most abundant circulating MV subtype populations under systemic RES-depleted conditions, followed by monocyte-, erythrocyte- and endothelial-derived MVs. These findings suggest the rapid clearance of MVs from blood and that the circulating MV populations under normal production-clearance equilibrium are not necessarily representative of the total intravascular MV output during acute inflammation.

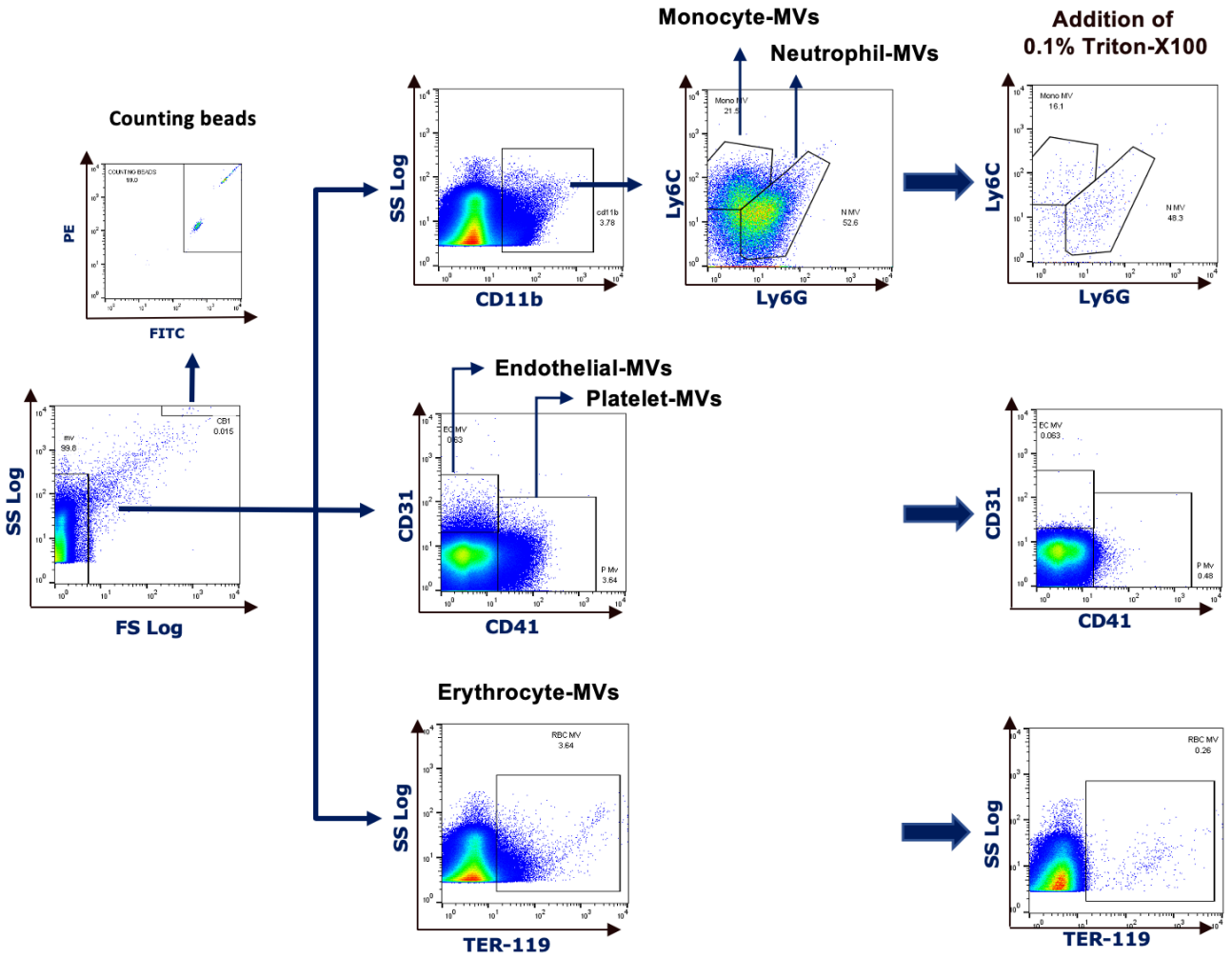

Figure 6.2 Flow cytometry gating of MVs in intravascular macrophage-depleted mouse plasma. *Representative flow cytometry plots of MVs obtained from plasma of mice treated with clodronate liposomes (i.v., 48h), followed by LPS (2µg, i.v., 1h). MVs identified include neutrophil-MVs (CD11b+, Ly6C+, Ly6G+), monocyte-MVs (CD11b+, Ly6C+, Ly6G-), platelet-MVs (CD41+), endothelial-MVs (CD31+, CD41-) and erythrocyte-MVs (TER-119+). (Representative figure, n=1)*

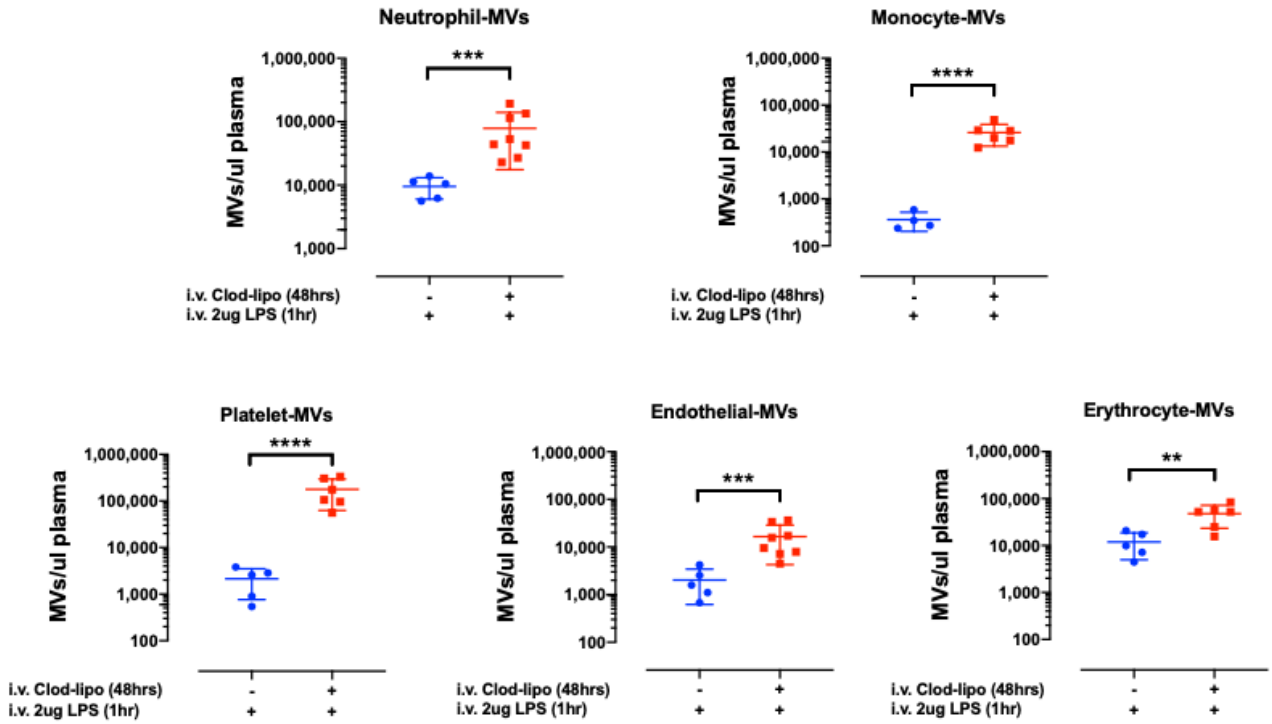

Figure 6.3 Evaluation of all circulating MV levels during endotoxaemia via systemic depletion of intravascular macrophages.

*MV concentrations were compared between mice treated with LPS (2µg, i.v., 1h), with or without clodronate liposome pretreatment (i.v., 48h before LPS treatment). MV concentration in PPP was determined by flow cytometry. Platelet- and neutrophil-MVs were the two most abundant circulating MV subtype populations under RES-depleted (clodronate liposome-pretreated) conditions, followed by monocyte-, erythrocyte- and endothelial-derived MVs. (Mean ± SD, n=4-6, **p<0.01, ***p<0.001, ****p<0.0001, unpaired t-test)*

Characterisation of PS expression on circulating MV subtypes in response to depletion of intravascular macrophages.

As in the previous study (Chapter 4) we measured PS expression using FITC-conjugated annexin V in all samples as a generic marker of MVs. As shown in representative histogram overlays (Figure 6.4) there appeared to be some changes in PS levels associated with the suppression of MV clearance by the RES. This was most noticeable with an overall increase in the fraction of PS+ myeloid-derived MVs (histograms shifted to the right), and a reduction in average PS expressions across all MV subtypes other than monocyte MVs (inset MFI values), suggesting there may be some phenotypic differences between MVs that are cleared by the RES and those that remain in the circulation.

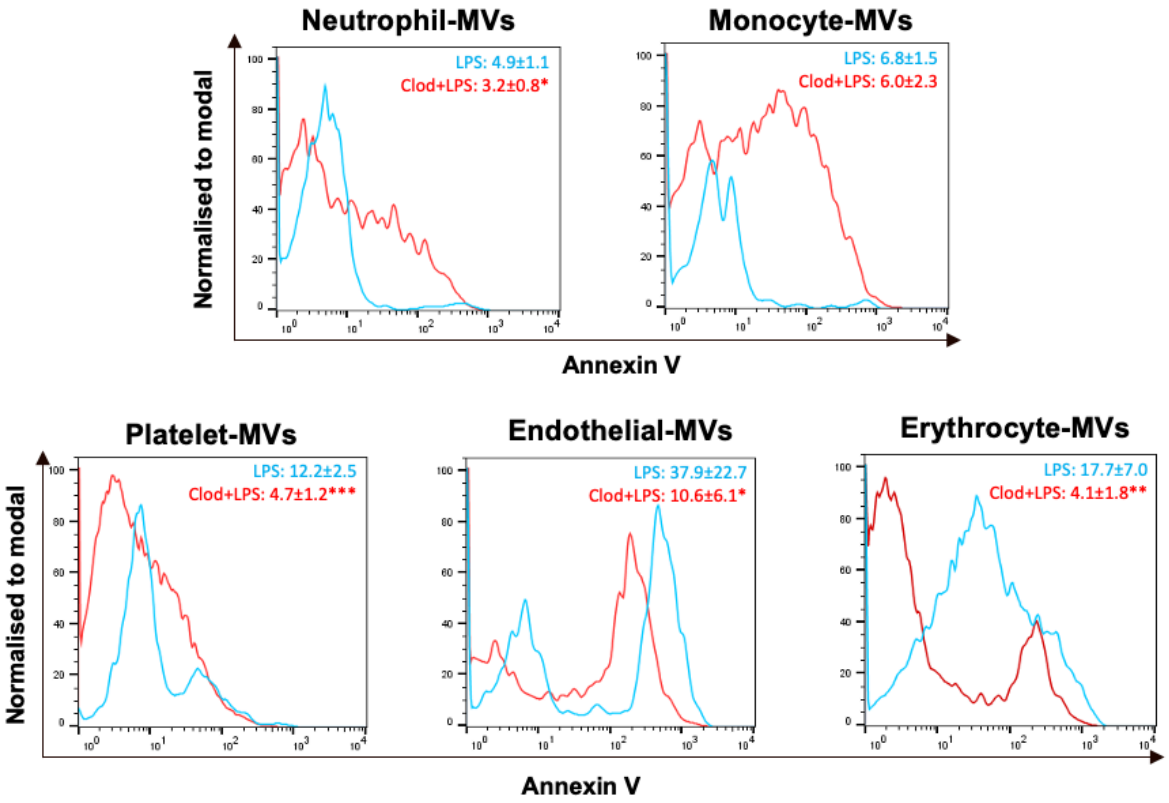

Figure 6.4 PS expression on all circulating MV subtypes during endotoxaemia in normal and intravascular macrophage-depleted mice.

*Annexin V staining of MV subtypes, indicating their PS expression, was determined by flow cytometry. MVs obtained from endotoxaemic mice treated with LPS (2μg, i.v., 1h), shown in blue, was compared to MVs obtained from mice pretreated with clodronate liposomes (i.v., 48h) before LPS treatment, shown in red. (Mean fluorescence intensity (MFI) of PS expressions presented in mean ± SD in top right corner insets, n=5, *p<0.05, **p<0.01, ***p<0.001, unpaired t-tests.)*

6.5.2 Circulating MVs from endotoxaemic mice induce indirect ALI via intravascular monocytes.

To investigate the direct contribution of circulating MVs to ALI during systemic inflammation, we used i.v. clodronate liposome pretreatment to minimise MV clearance by the RES, followed by LPS treatment to induce endotoxaemia as an *in vivo* MV source, and thereby model the exposure of the pulmonary vasculature to a more representative population of MVs. These 'total' circulating MVs from one donor mouse were infused into the closed, recirculating perfusion circuit of a recipient IPL pretreated with low-dose LPS as described previously in Chapter 5, with the exception that IPL was shortened from 4h to 2h enable the measurement of lung oedema and perfusate cytokines with reduced background noise. The role of lung-marginated monocytes was also assessed in the IPL with prior i.v. clodronate liposome treatment for 24h, which depletes only $Ly6C^{high}$ and $Ly6C^{low}$ monocytes, leaving neutrophils and interstitial macrophages untouched, as described previously in our group[187,294] (Figure 6.5)

MVs induced a very consistent increase in IPL wet-to-dry weight ratio after 2h recirculating perfusion, but there was no change in BALF protein concentration, indicative of an interstitial oedema (Figure 6.6). The MV-induced oedema was completely reversed in IPLs from monocyte-depleted mice, suggesting the critical role of lung-marginated monocytes. Levels of a lung injury marker, RAGE, in the IPL perfusate, also increased significantly compared to the control IPL, which was again significantly attenuated by monocyte depletion in the IPL, further suggesting a vascular compartment driven response. However, no significant changes were found in the levels of a panel of other cytokines and chemokines by MV treatment, including KC, TNF-α, MIP-1α, MIP-2, MCP-1, RANTES, GM-CSF, IL-6, IL-1β, IL-10, as well as endothelial cell injury markers Endothelin-1 (ET-1), Angiotensin converting enzyme (ACE), Angiopoietin-2 (Angpt-2) and vascular endothelial growth factor (VEGF) (Table 6.1). Interestingly, increased level of MIP-1α, MCP-1, IL-10 and Angpt-2 was detected in monocyte-depleted IPL, as compared to non-monocyte-depleted IPL, suggesting effects of monocyte depletion on circulating cytokines level in IPL perfusate.

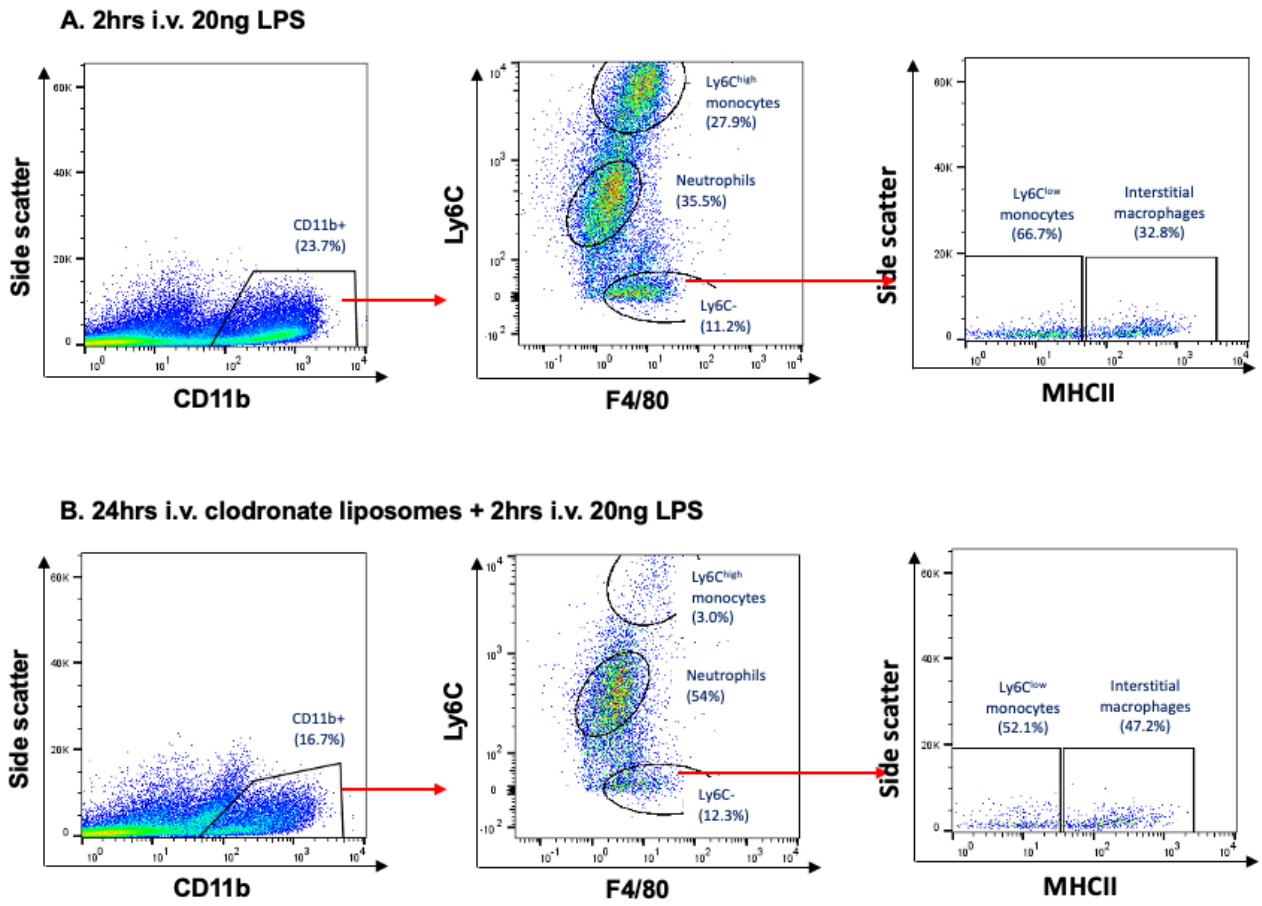

Figure 6.5 Depletion of intravascular monocytes in IPL.

Representative flow cytometry plots demonstrating in vivo depletion of monocytes prior to isolation of lungs for IPL by clodronate liposome pretreatment (i.v., 24h), followed by low-dose LPS (20ng, i.v., 2h)-pretreatment in mice. Only Ly6C^{high} and Ly6C^{low} monocytes were significantly depleted, due to their intravascular localisation, whereas neutrophils and interstitial macrophages remained untouched by i.v. clodronate liposome treatment, as described previously[187,294]*. (Representative figure, n=1)*

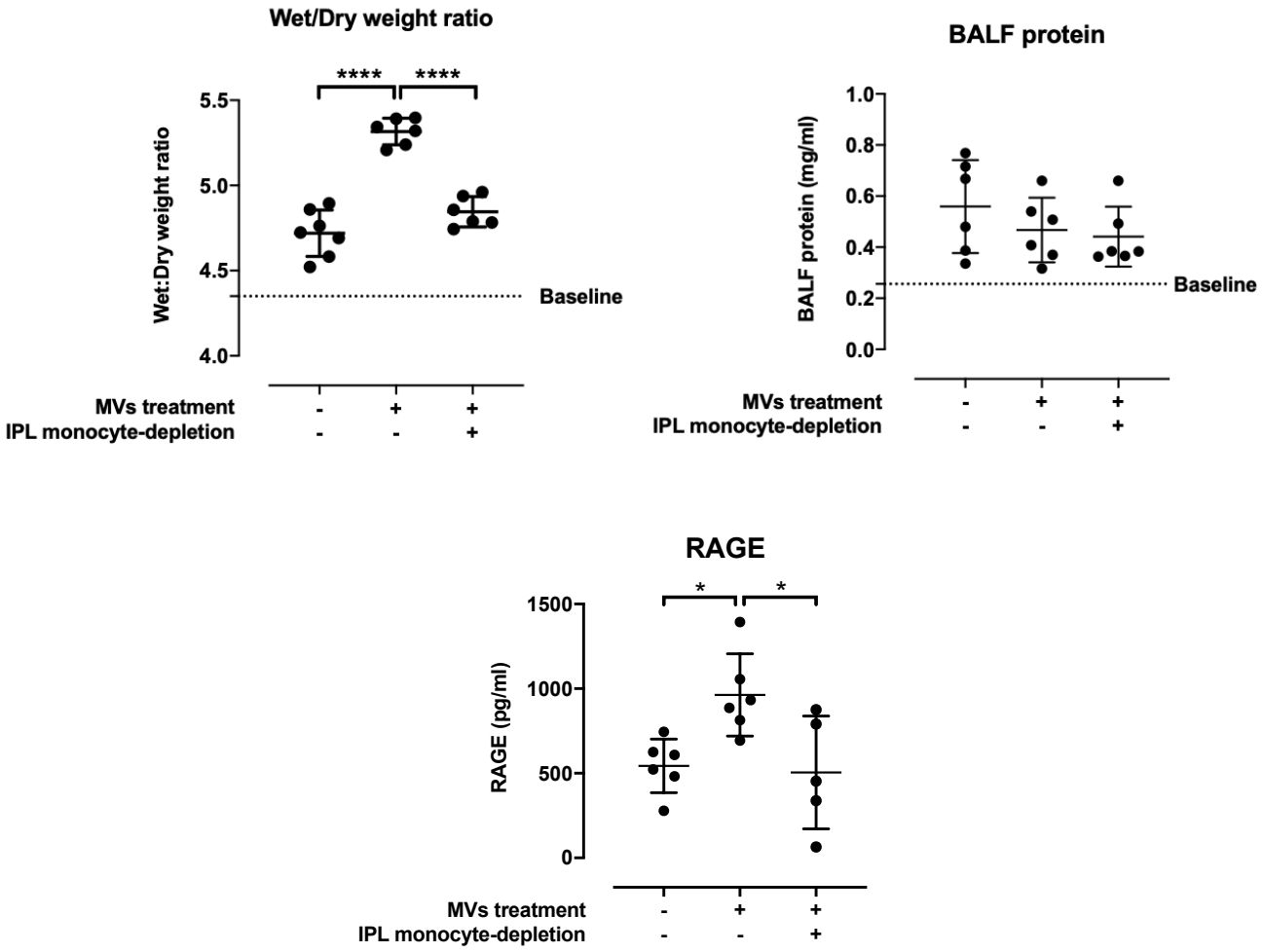

Figure 6.6 Circulating MVs from clodronate liposome-pretreated endotoxaemic mice induce a monocyte-dependent lung injury in LPS-pretreated IPL.

*Total MVs were obtained from macrophage-depleted (48h i.v. clodronate liposome-pretreated), LPS (i.v. 2μg, 1h)-treated mice and infused into a close, recirculating circuit of low-dose LPS (i.v., 20ng, 2h)-pretreated IPL for 2h. Endotoxaemic mouse plasma MVs induced an increase in lung wet-to-dry weight ratio, and an increased production of lung injury marker, RAGE into the perfusate, measured by ELISA. These effects were abolished in IPLs obtained from clodronate liposome (i.v., 24h prior to low-dose LPS pretreatment)-treated mice, which were depleted of lung intravascular monocytes. No change in BALF protein was detected across all treatment groups. Dotted lines represent baseline measurement of non-perfused lung from untreated mouse. (Mean ± SD, n=5-7, *p<0.05, ****p<0.0001, one-way ANOVA with Bonferroni's multiple comparisons test).*

Analyte	Concentration (pg/ml)		
MV treatment	-	+	+
IPL monocyte depletion	-	-	+
KC	475±195	395±443	736±507
TNF-α	39±37	364±414	455±339
MIP-1α	80±58	299±385	848±416$^{\#}$
MIP-2	422±610	434±710	1275±1060
MCP-1	165±43	115±52	426±146$^{\#}$
RANTES	616±295	703±552	440±284
GM-CSF	3±2	3±5	6±4
IL-6	731±480	1217±653	1138±756
ET-1	0.13±0.08	0.14±0.18	0.25±0.07
ACE	41431±7404	37040±6007	38400±6245
Angpt-2	4252±469	4407±235	5912±891$^{\#\#\#}$
VEGF	14±4	14±4	14±2
IL-1β	3±4	4±4	2±3
IL-10	63±25	58±30	123±42$^{\#\#}$

Table 6.1 Cytokines, chemokines and endothelial injury markers released into IPL perfusate. *Total MVs were obtained from macrophage-depleted (48h i.v. clodronate liposome-pretreated), LPS (i.v. 2μg, 1h)-treated mice and infused into a close, recirculating circuit of low-dose LPS (i.v., 20ng, 2h)-pretreated IPL for 2h. Perfusates were collected and centrifuged at 20,000 x g for 30min to remove cells and remnant MVs. A panel of soluble mediators were measured by ELISA. No significant difference in the level of all soluble mediators was detected by MV treatment. Monocyte depletion in IPL increased levels of MIP-1α, MCP-1, IL-10 and Angpt-2, compared to non-monocyte-depleted, MV-treated IPLs. (Mean ± SD, n=6-7, $^{\#}p<0.05$ vs. MV treated, non-monocyte depleted IPL, one-way ANOVA with Bonferroni's multiple comparisons test)*

6.5.3 Isolation and purification of circulating MV subtypes from endotoxaemic mice.

As myeloid-MVs and platelet-MVs were the most abundant MV subtypes released during early endotoxaemia, we aimed to purify them from the plasma of endotoxaemic mice for the investigation of their individual functional activity. The 'right-side-out' biogenesis of MVs causes them to carry distinctive surface markers originating directly from the plasma membrane of their parental cells. This characteristic enables the isolation and purification of different MV subtypes based on classical surface markers that define their parent cells.

Negative selection of myeloid-MVs

We initially investigated MV subtype immunoaffinity-based isolation by an indirect "negative selection", rather than direct "positive selection" approach, as we considered 'untouched' MVs without surface-bound immunoaffinity microbeads was preferable for functional studies. For isolation of myeloid-MVs by negative selection, we used a combination of biotin-conjugated antibodies followed by anti-biotin magnetic microbeads to remove other major MV populations: anti-TER119 for erythrocyte-MVs, anti-CD31 for endothelial-MVs, and anti-CD41 for platelet-MVs (Figure 6.7). After application to the magnetised columns, flow-through of unbound material was found to contain mainly the neutrophil-derived MVs (CD11b+, Ly6C+, Ly6G+) with a percentage recovery of 75±12% (n=3) from the original plasma. Percentage depletion of other identified MVs (platelet-, endothelial- and erythrocytes-derived) was >85%**.** However, we considered that the purity of the neutrophil MV-enriched fraction was insufficient for use in the IPL as we could not rule out the presence of other unidentified MV subtypes. Furthermore, without adequate generic markers available[358] to monitor MV purity, the negative selection approach may not produce conclusive finding in the IPL.

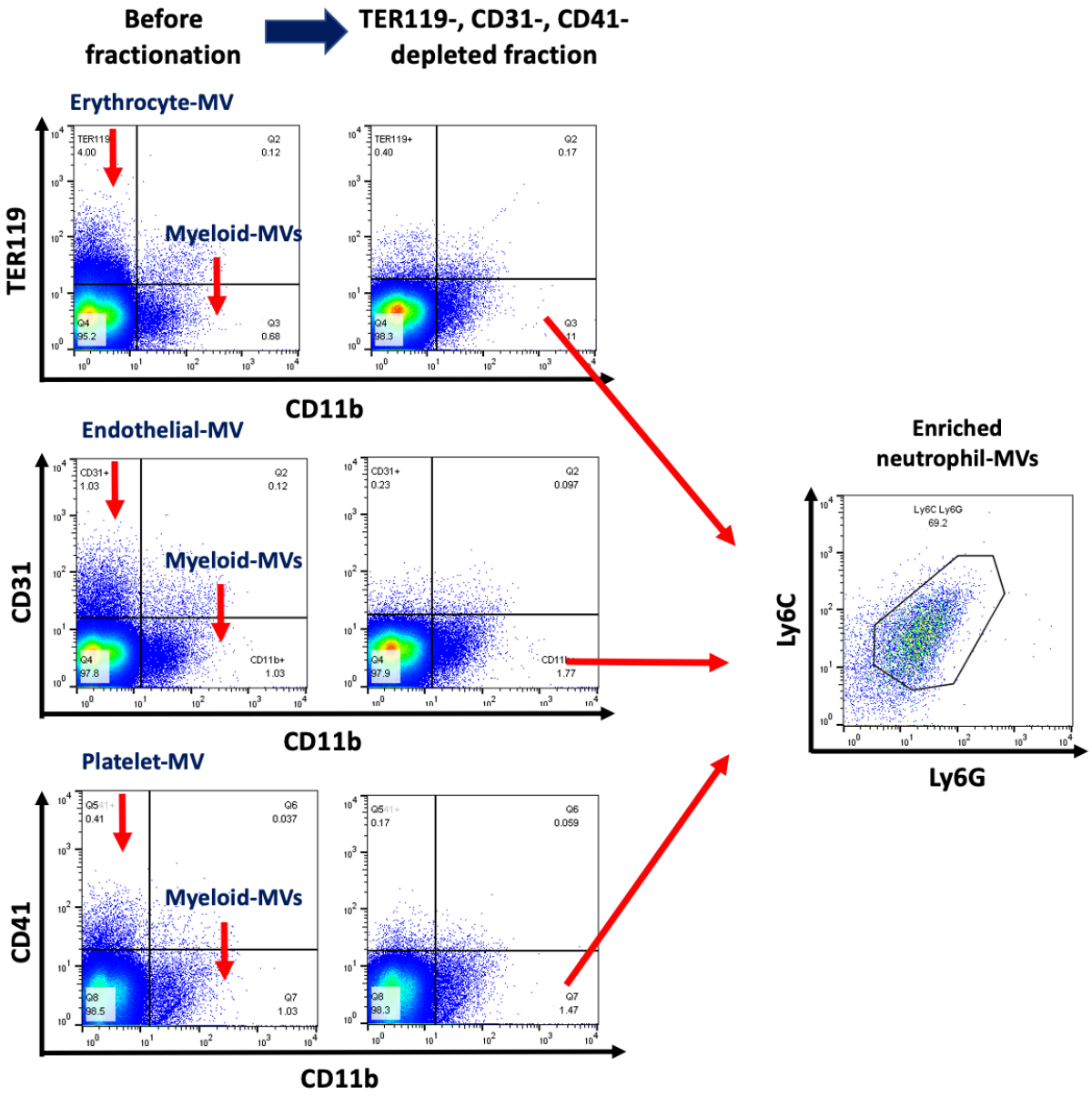

Figure 6.7 Negative selection of myeloid-MVs by immunoaffinity magnetic beads.

MVs obtained from endotoxaemic mice were labelled with anti-TER119 for erythrocyte-, anti-CD31 for endothelial-, and anti-CD41 for platelet-derived MVs, followed by anti-biotin magnetic beads. MVs were then passed through a magnetised column to fractionate the bead-bound MVs from unbound MVs in flow-through. 'Before fractionation' flow cytometry plots shown the presence of various MV subpopulations before magnetic separation, whereas the 'TER119-, CD31-, CD41-depleted fraction' in unbound flow through showed the depletion of erythrocyte-, endothelial- and platelet-MVs and the enrichment of the neutrophil-derived MVs (CD11b+, Ly6C+ and Ly6G+) after fractionation. (Representative figure, n=1)

Positive selection of myeloid-MVs

For positive selection of MV subtypes from clodronate liposome-pretreated, endotoxaemic mouse plasma, we decided to use anti-CD11b-conjugated beads to enrich for myeloid-MVs and anti-CD41 for platelet-MVs. Phenotype analysis of the selected MV subtypes was based on alternative markers from the beads conjugates: for the CD11b-selected fraction, expression of Ly6C and Ly6G were used; for the CD41-selected fraction, expression of CD61 and CD31 were used (Figure 6.8). In CD11b positive selection of MVs, percentage recovery of myeloid MVs was 94.5±8.6%, whereas percentage depletion of platelet MVs in the CD11b-selected fraction was 96.8±2.1% (n=6). In CD41 positive selection of MVs, percentage recovery of platelet MVs was 74.8±19.9%, whereas percentage depletion of myeloid MVs in the CD41-selected fraction was 96.6±2.2% (n=5). Overall, this method was successfully developed for isolation of the respective MV subtypes, suitable for the subsequent functional studies in *ex vivo* IPL.

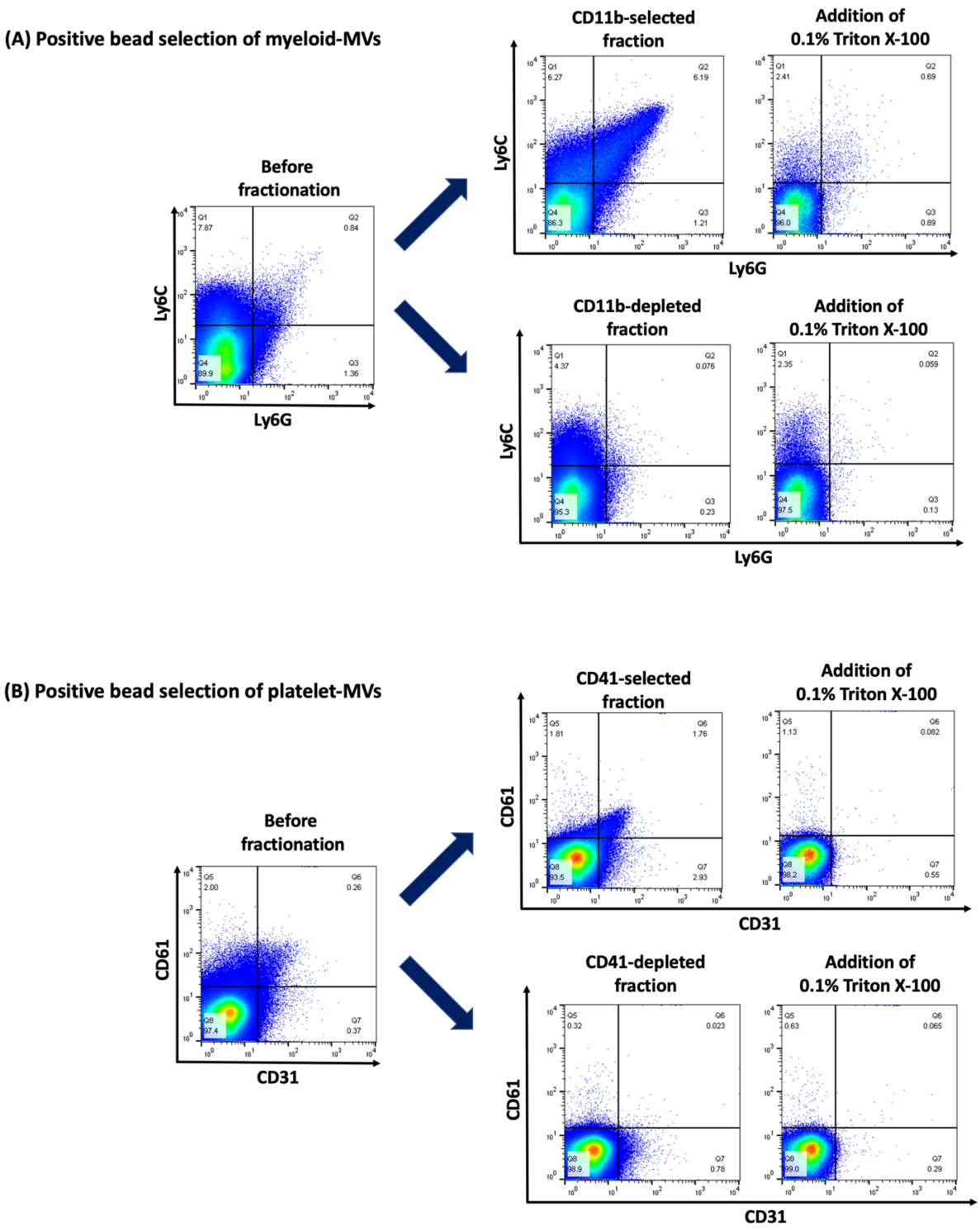

Figure 6.8 Positive selection of myeloid- and platelet-MVs by immunoaffinity magnetic beads. *MVs obtained from macrophage-depleted, endotoxaemic mice were incubated with either (A) anti-CD11b microbeads, or (B) anti-CD41 biotin antibody, followed by anti-biotin microbeads. MVs were then passed through a magnetised column to fractionate the bead-bound MVs from unbound MVs in the flow-through. The CD11b-selected fraction and CD41-selected fraction were identified by their expression of Ly6C, Ly6G for myeloid-MVs, and CD61, CD31 for platelet-MVs, respectively. The detergent sensitivity of these bead-isolated MVs by 0.1% (v/v) Triton x-100 treatment and their absence in the flow-through, further verified their MV identities. (Representative figure, n=1)*

6.5.4 Myeloid-MVs but not platelet-MVs from endotoxaemic mice induce indirect ALI.

We assessed the biological activities of "positively selected" myeloid-MVs and platelet-MV subtypes in the IPL model. Equal numbers of each MV subtypes ($9x10^7$), obtained from two clodronate liposome-pretreated, endotoxaemic donor mice were infused into the recirculating IPL perfusion circuit for 2h. Myeloid-MVs caused significant oedema in the LPS-pretreated IPL (Figure 6.9), at a similar level to that elicited by total unfractionated MVs (Figure 6.6). Platelet-MVs on the other hand, produced a much smaller, but statistically significant increase compared to control IPL. As with total MVs, there was no change in BALF protein content, indicating interstitial oedema. A panel of soluble mediators and markers of inflammation/injury released into the IPL perfusate after the 2h recirculating perfusion were also determined. Myeloid-MVs induced significant increases in levels of pro-inflammatory cytokines (KC, TNF-α, MIP-1α, MIP-2, MCP-1, RANTES, GM-CSF and IL-6), as well as soluble markers of endothelial injury (Endothelin-1 (ET-1), Angiotensin converting enzyme (ACE), Angiopoietin-2 (Angpt-2) and vascular endothelial growth factor (VEGF)) in IPL perfusates (Table 6.2). Contrasting with myeloid-MVs, platelet-MVs had virtually no effect on the level of soluble mediators, except a significant increase Angiopoietin-2, which level was similar to those of induced by myeloid-MVs. Other pro- and anti-inflammatory markers such as IL-1β, IL-10 and TGB-β (data not shown) were assessed but no change between treatment groups was detected. These findings demonstrate that myeloid-MVs are capable of inducing potent pro-inflammatory responses directly within the pulmonary vasculature.

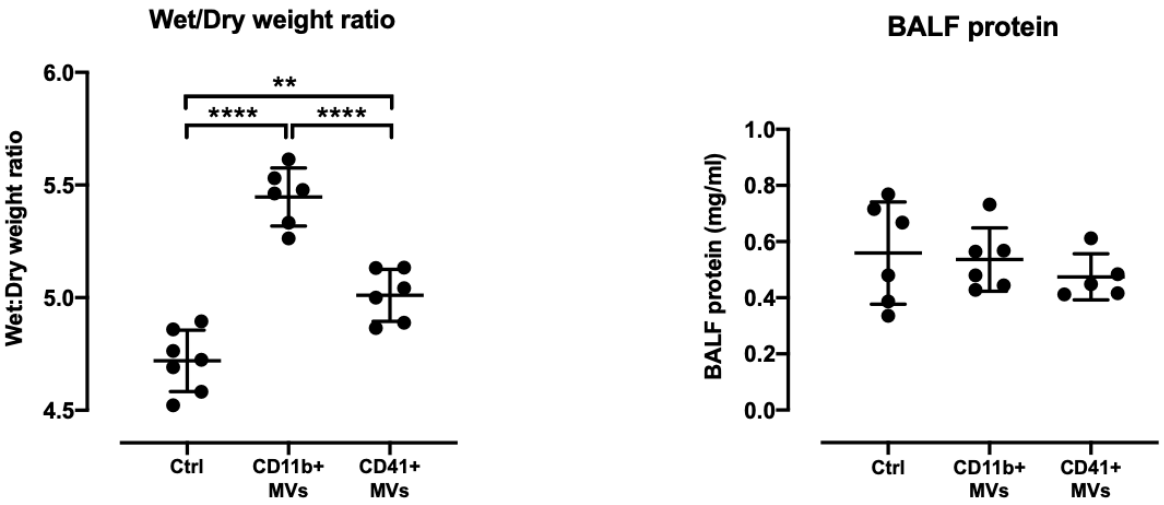

Figure 6.9 Myeloid-MVs induce significant oedema in LPS-pretreated IPL.

*Myeloid- or platelet-MVs ($9x10^7$ for both) obtained from macrophage-depleted, endotoxaemic mice isolated by immunoaffinity magnetic beads, were infused into low-dose LPS-pretreated IPLs and recirculated for 2h. Infusion of myeloid-MVs (positively selected by CD11b) elicited a significant oedema, while platelet-MVs (positively selected by CD41) produced a smaller but significant oedema, with wet-to-dry weight ratios similar to the level of the control IPL. No change in BALF protein was detected across all treatment groups. (Mean ± SD, n=6-7, **p<0.01, ****p>0.0001, one-way ANOVA with Bonferroni's multiple comparisons test)*

Analyte	Concentration (pg/ml)		
	Untreated	CD11b+ MVs	CD41+ MVs
RAGE	543±159	3265±1947**	515±255
KC	475±195	1505±535***	281±142
TNF-α	39±37	1856±1081***	165±273
MIP-1α	80±58	1044±187****	102±68
MIP-2	422±610	1852±980**	72±13
MCP-1	165±43	271±33**	162±65
RANTES	616±295	1449±200**	974±382
GM-CSF	3±2	19±10***	6±5
IL-6	731±480	2309±261***	1308±737
ET-1	0.13±0.08	0.33±0.14*	0.21±0.13
ACE	41431±7404	59006±13613*	34278±4227
Angpt-2	4252±469	6241±1240**	6074±593**
VEGF	14±4	18±2$^{\#}$	12±3
IL-1β	3±4	6±3	6±5
IL-10	63±25	56±18	68±17

Table 6.2 Myeloid-MVs induced significant release of pro-inflammatory mediators in LPS-pretreated IPL perfusate.

*Myeloid- or platelet-MVs (9x10^{7} for both) obtained from macrophage-depleted, endotoxaemic mice isolated by immunoaffinity magnetic beads, were infused into low-dose LPS-pretreated IPLs and recirculated for 2h. Perfusates were collected and centrifuged at 20,000 x g for 30min to remove MVs. A panel of soluble mediators were measured by ELISA. Infusion of myeloid-MVs induced significant release of all tested mediators, whereas platelet-MVs only induced release of angiopoietin-2 level to a similar level as that of myeloid-MVs. No difference in the level of IL-1β, IL-10 and TGB-β (undetectable, not shown) was found across all treatment groups. (Mean ± SD, n=6-7, *p<0.05, **p<0.001, ***p<0.0005, ****p<0.0001 vs. untreated control, $^{\#}$p<0.05 vs. platelet-MVs, one-way ANOVA with Bonferroni's multiple comparisons test)*

6.5.5 Preliminary investigation on the feasibility of depleting myeloid-MVs for IPL studies.

To assess the relative contribution of myeloid-MVs to the total MV-induced pulmonary inflammation/injury, we performed some pilot experiments on the effect of immunoaffinity depletion of myeloid-MVs. This was done using the same method as for positive selection of CD11b+ (Figure 6.8) but using the unbound flow through containing the CD11b-depleted fraction instead. MV subtypes analysed by flow cytometry shows that the CD11b-depleted fraction contained platelet-, endothelial- and erythrocyte-derived MVs, but not neutrophil- and monocyte-MVs (Figure 6.10). Percentage depletion of myeloid MVs in the CD11b-depleted fraction was 95.6±2.6% (n=5). However, a distinct Ly6C+, Ly6G- population was present the CD11b-depleted fraction, likely to be the CD11b-Ly6C+ population observed in plasma previously (Figure 4.7), but the cellular origin of which is unknown at this stage. In comparison to total MVs, when CD11b-depleted MV fraction was infused into IPL, the wet-to-dry weight ratio remained significantly higher than the no MV control IPL, but with more variable results than the increases induced by total MVs (Figure 6.11). With the limited repeats performed (n=3), further evaluation of this approach is necessary, and we did not rule out the possibility that other active MV subtypes may be present in the CD11b-depleted preparation.

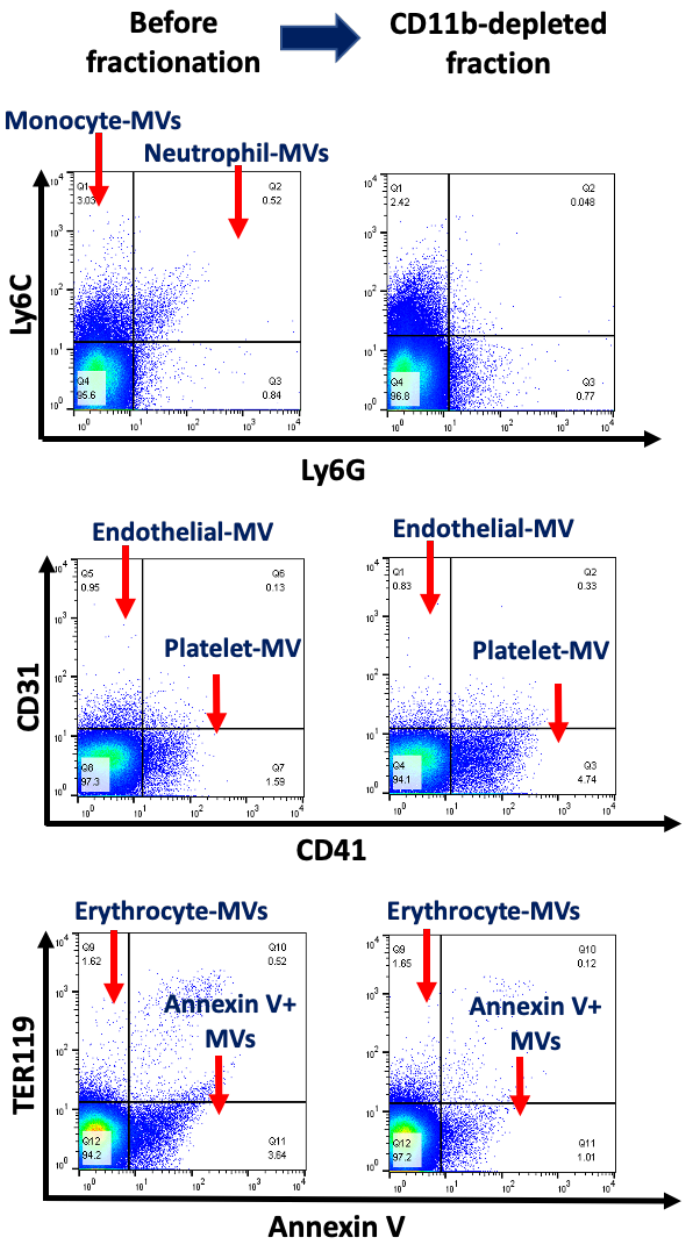

Figure 6.10 Depletion of myeloid-MVs by immunoaffinity magnetic beads.

MVs obtained from macrophage-depleted, endotoxaemic mice were incubated with anti-CD11b microbeads and passed through a magnetised column to fractionate the bead-bound MVs from unbound MVs in flow through. MV subtypes were identified before and after fractionation. Neutrophil- or monocyte-MVs were depleted from the CD11b-depleted fraction, but not platelet-, endothelial- and erythrocyte-MVs. (Representative figure, n=1)

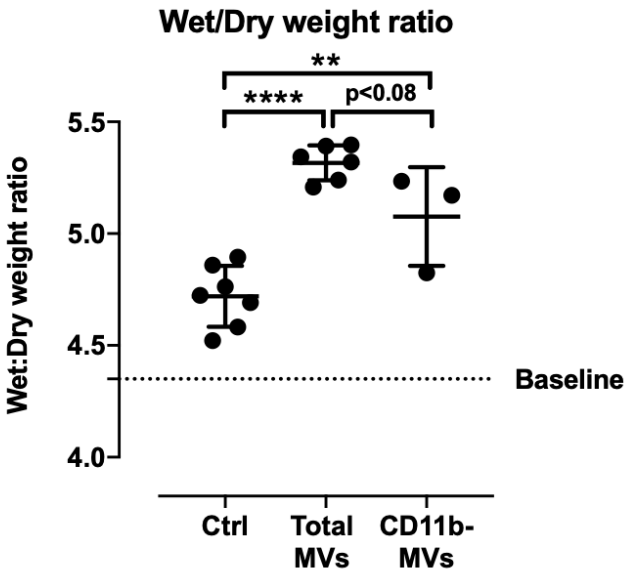

Figure 6.11 Preliminary evaluation of CD11b-depleted MVs in IPL.

*MVs were obtained from macrophage-depleted (48h i.v. clodronate liposome-pretreated), LPS (i.v. 2μg, 1h)-treated mice and infused into a close, recirculating circuit of low-dose LPS (i.v., 20ng, 2h)-pretreated IPL for 2h. Infusion of the total endotoxaemic mouse plasma MVs (total MVs) induced a significant increase in lung wet-to-dry weight ratio and this effect was partially mitigated (p<0.08) when MVs were depleted of myeloid-MVs ("CD11b- MVs"). Dotted lines represent baseline measurement of non-perfused lung from untreated mouse. (Mean ± SD, n=3-7, **p<0.01, ****p<0.0001, one-way ANOVA with Bonferroni's multiple comparisons test)*

6.6 Discussion

6.6.1 Summary

This chapter utilised the *in vivo*-to-*ex vivo* adoptive transfer method with a shortened IPL protocol and immunoaffinity isolation-based methods to delineate the direct effects of myeloid- and platelet-MVs subtypes produced on pulmonary vascular injury/inflammation. We also developed a method for recovery of a more representative population of *in vivo* endogenously produced MVs using clodronate liposome treatment to suppress rapid MV clearance by the RES. With these approaches, we observed that total MVs induced interstitial oedema that was reversed by lung intravascular monocyte depletion. When MV subtypes isolated by positive selection were infused into LPS-primed IPLs, myeloid-MVs, but not platelet-MVs, elicited significant interstitial oedema and an early potent release of pro-inflammatory cytokines in IPL perfusates. Collectively, these results highlight the injurious properties of *in vivo*-generated, myeloid-derived MVs during inflammation and the role of lung-marginated $Ly6C^{high}$ monocytes in the potentiation of indirect ALI during systemic inflammation. Together with results on MV production and pulmonary vascular cells activation described in Chapter 4 and 5, major findings of this study are summarised in Figure 6.12.

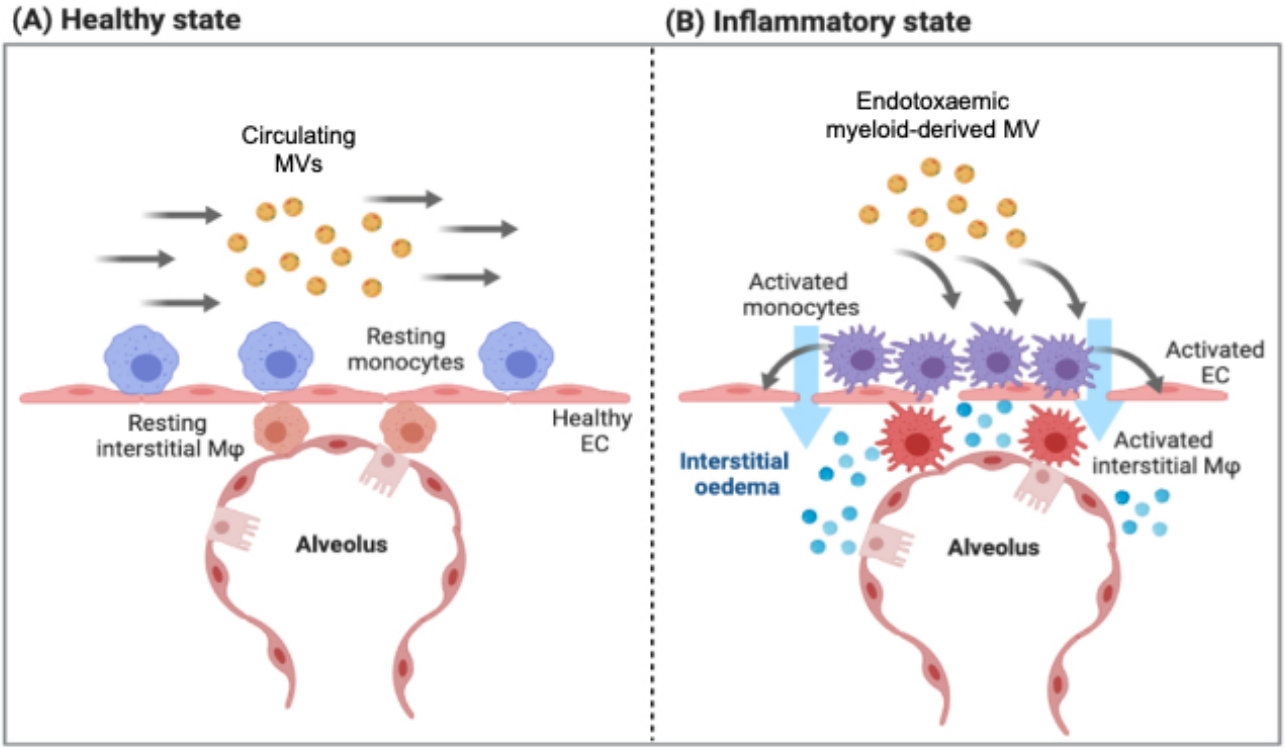

Figure 6.12 Summary of the inflammatory mechanisms involved in MVs-induced indirect ALI. *During healthy state (left), MV uptake in the pulmonary vasculature is negligible. During systemic inflammatory state (right), endotoxaemic-derived myeloid-derived MVs interact with lung-marginated monocytes and causes activation of Ly6C^{high} monocytes, pulmonary endothelial cells and interstitial macrophages, alongside with the release of pro-inflammatory mediators and interstitial oedema. (Made with BioRender)*

6.6.2 Intravascular macrophage depletion for the assessment of total MVs production.

Resident intravascular macrophages in various organs were shown to play a major role in the clearance and elimination of circulating MVs[397,400]. In this chapter, we depleted the intravascular macrophages, using i.v. injection of clodronate liposomes to investigate the total production of MVs during inflammation. As the depletion of intravascular macrophages would also deplete circulating and marginated monocytes, which plays an important part in vascular inflammation, clodronate liposomes were injected for 48h. This allowed ample time for the repopulation of Ly6C^{high} subset monocytes in the circulation to normal levels[172,187,297,588] and ensured the production of monocyte-MVs as a major constituent of the myeloid CD11b+ MV population. However, the repopulation of monocytes would also restore the clearance of MVs to a certain degree, as monocytes internalise MVs and liver endothelial cells also contribute to uptake[1,397]. Therefore, it is important to note that the

total production of MVs investigated here would still have been underestimated to a certain degree via this approach.

Despite providing valuable insights, when circulating levels of MVs were measured in clinical studies, the endogenous MV clearance in the body was often not taken into account. For example, when the circulating level of MVs were compared between healthy volunteers and septic patients, it is possible that the higher levels in the latter reflect reduced clearance and not increased production alone. This may be particularly pronounced for constitutively released MVs such as platelet-MVs that are present in the bloodstream of sepsis patients at high baseline level, but were often found to have no correlation with mortality[589,590]. By contrast, changes in the levels of inducible MVs that are very low at baseline, such as acutely released myeloid-MV, specifically neutrophil-MVs, are more likely to reflect increased production and were shown to correlate with disease severity and mortality[377,427].

In addition to some substantial increases in circulating MVs following clodronate liposome treatment, the varying proportions of surface PS expressed by MV subtypes, appeared to be affected by the level of endogenous clearance *in vivo* by intravascular macrophages. When intravascular macrophages were depleted, the fraction of PS+ myeloid-derived MVs increased, but the average PS expressions across all other MV subtypes decreased. These findings were unexpected as we hypothesised that the rapidly cleared PS+ MV under normal conditions would remain in the circulation with clodronate liposome treatment, based on PS as a key ligand in MV uptake by monocytes[475] and macrophages[416]. Nonetheless, it is important to note that identification of MVs in various clinical studies based on the expression of PS, could lead to an overemphasis on certain MV subtype with higher proportion of PS-expressing subpopulation, or MV phenotype with higher PS expression. Overall, the understanding of the MV uptake-clearance dynamics during disease progression may shed more light into the underlying mechanism behind the consistently reported inverse correlation between circulating MV levels in septic/ARDS patients with disease severity or mortality[433–437].

6.6.3 Role of lung monocytes in indirect ALI.

Lung-marginated monocytes have previously been implicated in the development of ALI[187,291,294,295,297,450], and the depletion of intravascular monocytes in the lung were found to sufficiently attenuate pulmonary vascular inflammation and oedema *in vivo* and *ex vivo*[294–299]. To delineate the role of lung-marginated monocytes in MV-induced lung injury, intravascular monocytes were depleted prior to IPL in this study. Our group has previously demonstrated that i.v. injection of clodronate liposomes for 24h effectively depleted vascular Ly6C^{high} and Ly6C^{low} monocytes, leaving numbers of the interstitial macrophages, alveolar macrophages and vascular neutrophils unaffected[294]. As shown in Chapter 3 and in our recently published paper[1], MVs are preferentially internalised by lung-marginated Ly6C^{high} monocytes, suggesting they would play some role in the development of inflammation/injury. By depletion of lung-marginated vascular monocytes, we found that monocytes do indeed contribute to MV-induced lung oedema, but cytokine levels in perfusates appeared to be unaffected. The latter observation suggests MV-induced oedema and inflammation are separate pathways and that monocytes may not be the primary producers of pulmonary cytokines. However, it should be borne in mind that the MV-induced cytokine levels were variable, lacking statistical significance in most cases. Moreover, monocyte depletion resulted in increased levels of MIP-1α, MCP-1, IL-10 and Angpt-2. Regarding the mechanism of monocyte-mediated oedema, in the absence of perfusate cytokine differences, other mediators such as eicosanoids and/or juxtracrine signalling seem likely candidates.

6.6.4 Fractionation of MVs by immunoaffinity magnetic beads and their functional activities.

The ‘right-side-out’ biogenesis of MVs facilitated their subtype fractionation based on their respective expression of parental cell markers. To our knowledge, only one study evaluated functional activity of different endogenous MV subtypes, where non-platelet derived MVs obtained from patient plasma were found to induce endothelial dysfunction *in vitro*[591]. In that study, *in vitro* endothelial cells were incubated with either anti-CD61 bead-selected platelet-MVs, anti-CD61 bead-depleted non-platelet MVs or anti-CD61 beads alone. Here, we performed direct comparison between bead-bound MVs (myeloid-MVs vs. platelet-MVs) and carried out a separate analysis comparing between bead-free MVs (total MVs vs. CD11b-depleted MVs). Certainly, it would be ideal to study the functional activity

of MVs in the IPL with bead-free myeloid-MVs, as we inferred that the presence of beads on MVs may interfere with their interaction with target cells. However, MACS microbeads (Miltenyi biotech) used here are 50nm in size and MVs are typically sized between 0.1-1μm. MVs are thus about 2-20 times larger than the beads. Although positive immunoaffinity selection is not ideal, it does ensure that any activity observed can be attributed primarily to the bead-bound MV subtype contrasting with the relatively undefined content of negatively selected MVs. In the latter case, additional purification steps such as size-exclusion chromatography would help to eliminate lipoproteins[592,593], though this would not exclude unknown MV subtypes such as the Ly6C+ single positive MV population identified in our CD11b-depleted preparation. As infusion of bead-bound platelet-MVs produced significantly less oedema and virtually no cytokine response, they conveniently served as control for beads and the isolation procedure itself, negating the need for bead-alone controls and consistent with 3Rs guidelines. Although the work on MV subtype depletion was incomplete, it may be a useful complimentary approach to positive selection, by removing other potentially active MV subtypes in addition to myeloid MVs.

6.6.5 Pulmonary injury and inflammation in indirect ALI.

The use of a shorter 2h IPL protocol and total MVs from clodronate liposome-treated endotoxaemic mice appeared to enable an enhancement of signal-to-noise ratio in the detection of lung oedema and release of soluble mediators. In the LPS-pretreated IPL without MV treatment, the wet-to-dry weight ratio reduced from 5.71±0.16 (Figure 5.8) to 4.72±0.14 (Figure 6.6) at the end of the 4h and 2h protocols, respectively. While for soluble mediators, RAGE, IL-6 and KC were between 4-6 times lower with the shorter 2h protocol. In addition to reduction of background ‘noise’, the doses of total MV infused into IPL were increased from approximately $1x10^7$ (one donor LPS-treated mouse) to $9x10^7$ (two donor clodronate liposome and LPS-treated mouse), significantly enhancing the ‘signal’ for clearer outcome measurement.

We evaluated the direct contribution of endogenously released MVs in ALI using the IPL model in two stages: initially determining whether circulating MVs are pro-injurious per se under the conditions employed, and then exploring in more detail the response to different MV subtypes fractions. The

formation of lung oedema and release of soluble mediators in *ex vivo* IPL has been widely reported in models of direct ALI[294,295,310,311,594,595] but not indirect ALI. It is recognised that there is fundamental difference between the pathophysiology of direct and indirect ALI, where epithelial injury is more severe in direct ALI and endothelial injury is more severe in indirect ALI[29,32,227,596]. Consistent with these compartment-specific origins of ALI, we demonstrated that total MV induced an interstitial oedema based on the wet-to-dry weight increase with no change in BAL protein levels (ruling out an alveolar transudate or exudate). We found that myeloid-MVs, but not platelet-MVs, produced an identical pattern of compartmentalised interstitial oedema and release of RAGE into IPL perfusate, which has been used as a gold standard plasma biomarker of ALI, released mainly by lung epithelial and endothelial cells[597–599], as well as other vascular cell types[600,601]. When total MVs were obtained from one donor mouse and infused into IPL, we used a dose of about $9x10^7$ 'total' MVs from all the subtypes identified by flow cytometry, of which ~50% were myeloid-MVs. Therefore, we decided to standardise the positively-selected MV subtype number to $9x10^7$ for each MV subtype-challenged IPL, to match to the total number of circulating MVs experienced by the lungs during systemic inflammation. This results in a final concentration of 36,000MVs/μl in the recirculating IPL (2.5ml perfusate), which was much lower than the concentration of myeloid MVs found in macrophage-depleted, LPS-treated mouse plasma (about 100,000MVs/μl of neutrophil- and monocyte-MVs). This higher relative dose of myeloid-MVs in the CD11b-selected MVs relative to total MV challenges, could explain the higher levels of RAGE and other cytokines released. Furthermore, the more consistent cytokine responses in the CD11b-selected MVs relative to total MV challenges may be attributed to the standardisation of MV number in replacement of the one-to-one donor-recipient adoptive transfer method, suggesting a dose-dependent relationship between active MV number and cytokine release.

Interestingly, we found that platelet-MVs elicited a modest but significant increase in lung oedema and the release of angiopoietin-2 but not any other soluble mediators measured. As the percentage depletion of myeloid-MVs in the CD41-selected fraction was 96.6±2.2%, it is therefore unlikely that these significant responses were mediated by residual myeloid-MVs (<4%). Despite its role in the regulation of vascular permeability[602–604], angiopoietin-2 alone has been shown to be insufficient in inducing vascular leakage without collaboration of other angiogenic factors such as VEGF and

angiopoietin-1[605–608]. We have shown here that myeloid-MVs, induced a statistically significant increase in VEGF compared to platelet-MVs, which together with angiopoietin-2, could triggered a more significant increase in endothelial permeability, as compared to platelet-MVs. Moreover, VEGF released by Ly6C^{high} monocytes has been shown to contribute to increased vascular permeability in ventilator-induced lung injury[300], further suggesting the role of lung-marginated Ly6C^{high} monocytes in MV-induced indirect ALI. Angiopoietin-2 were also found to contribute to the development of indirect ALI via neutrophil-endothelial interaction *in vitro* and *in vivo*[609], further suggesting the role of neutrophil-derived MVs in the phenomenon observed in this study. Circulating level of platelet-MVs have frequently been shown to elevate in patients with sepsis/SIRS and some studies have shown that platelet-MVs are pro-inflammatory and possess aggregating and pro-adhesion properties[420,423,424,610]. Therefore, the lack of platelet-MVs activity in modulating significant inflammation in the IPL presents an interesting finding in the area of MVs research. However, the direct relationship between lung permeability change and cytokines release was not explored in the scope of this study, which presents an interesting area for further investigation.

6.7 Conclusion

In conclusion, we have shown here that with a relatively brief exposure to physiologically relevant quantities of circulating MVs, there is a substantive pulmonary vascular response of acute inflammation and increased permeability, hallmarks of the early stages of indirect ALI. The attribution of this activity to myeloid-MVs is in line with the critical roles of this lineage of cells in ALI, and as such, certain effects ascribed to their parent cell effector molecules may instead be derived from MVs. Hence, these findings suggest an alternative paradigm of indirect ALI in sepsis and SIRS, where MVs may dominate over the secreted pro-inflammatory mediators as endocrine mediators of their parent cell effector functions. As such, reducing MV-induced pulmonary vascular responses could be an effective vascular-bed specific clinical approach in the attenuating ALI and its propagation of systemic inflammation.

Chapter 7

Conclusion and future directions

Chapter 7 Conclusion & future directions

7.1 Summary of work

Since the recognition of MVs as functional entities in immunology research, the role of circulating MVs as biomarker of sepsis has been widely investigated in clinical studies. However, their functional role in the pathogenesis of sepsis-induced pulmonary vascular inflammation, especially in indirect ALI, has not been determined. Despite the established mechanism of monocyte margination and sequestration in the lungs during systemic inflammation, their interaction with circulating mediators and its subsequent functional responses has rarely been reported. In this project, we firstly investigated the dynamics and mechanism of MV uptake using an *in vitro* macrophage cell line generated MVs, with which we ascertained the role of lung-marginated Ly6C^{high} monocytes in the homing of MVs to the lung microvasculature during inflammation[1]. Secondly, we extended these findings to characterise the *in vivo* endogenous production of MVs during inflammation, comparing MV subtypes produced in animal models of systemic infection (LPS-induced endotoxaemia) and local sterile inflammation (unilateral kidney IRI). We adoptively transferred MVs from endotoxaemic mice to normal and LPS-primed IPL systems to examine their inflammatory properties in the lungs. After observing a range of biological effects with total MVs, we focussed on the isolation and transfer of MV subtypes and demonstrated that myeloid-derived MVs alone can produce significant lung oedema and acute release of inflammatory mediators within the pulmonary vasculature. This chapter will discuss some of the major findings of this study, and their implications and future opportunities.

7.1.1 Monocytes mediate homing of circulating MVs to the lungs during inflammation via a phosphatidylserine (PS)-mediated receptor mechanism

In Chapter 3, using an *in vitro* macrophage cell line (J774A.1) to generate MVs via the ATP-P2X$_7$ receptor signalling pathway, we demonstrated that during subclinical endotoxaemia, the expanded population of Ly6C^{high} monocytes marginated to the lungs also exhibited increased MV uptake, while uptake by liver Kupffer cells was reduced. Utilising the preparation of an *ex vivo* model of IPL to eliminate systemic variables, we demonstrated that systemic inflammation enhanced the uptake capacity of MVs by lung-marginated Ly6C^{high} monocytes “per se”, independently of any change in systemic clearance processes. To further investigate the mechanism involved, we developed a novel

technique to obtain lung-marginated monocytes for *in vitro* experimentation. Using this model, we demonstrated that the mechanism of MV uptake by these lung-marginated monocytes are mediated through an active, endocytic process that involved the recognition of PS on MVs via integrin and scavenger receptors[1]. These findings on monocyte-mediated homing of circulating MVs to the lungs during low-grade systemic inflammation, via PS and other potential recognition mechanisms, should be considered when the biodistribution of exogenously administered MVs are studied, especially in the field of EV-based therapeutics, either with MSC-derived MVs or synthetically engineered exosomes, where tissue targeting poses a significant hindrance in technological advancement.

Despite wider application of these findings using a convenient *in vitro* method for MV generation, our long-term aim remained focussed on the role of endogenously released circulating MVs during sepsis/SIRS in indirect ALI. Therefore, we proceeded to extend these findings to investigate the *in vivo* endogenously produced MVs during systemic inflammation. Despite the common use of various individual stimuli to generate MVs *in vitro* such as ATP, fMLP, PMA, calcium ionophore, TNF and LPS[364], switching to *in vivo*-produced MVs as the next step enabled us to study the true biological properties of MVs released during disease state and to extrapolate their clinical relevance. Interestingly, in Chapters 4 and 6 we discovered that not all *in vivo*-generated MVs express PS. This finding not only negates the use of annexin V as a general marker of MVs, but also raises the possibility that MVs, even if generated from the same cell source, may be taken up differentially by target cells *in vivo* based on their differing surface PS expression. Thus, PS expression may vary according to the manner of MV release and their parental cell source, which may also have differing consequences for the responses they elicit in target cells. There is a body of evidence implicating PS in anti-inflammatory responses by macrophages during apoptotic cell clearance[611,612] and uptake of PS-positive MVs, particularly that of neutrophil-derived[613–615]. It is therefore of note that MVs released from necroptotic cells are also PS-positive[349,350], despite the assumption that in direct contrast to apoptosis, necroptosis is an overall a pro-inflammatory pathway of cell death. Therefore, further studies should consider such functional and biological heterogeneity of MVs, with respect to their interaction with target cells, the mechanism involved in their uptake and their subsequent impact on cell function.

7.1.2 MV subtype profiles differ significantly in animal models of sepsis and sterile organ injury

In Chapter 4, we aimed to characterise the production of MVs in two clinically relevant animal models of inflammation, representative of sepsis (i.v. LPS-induced endotoxaemia) and sterile remote organ injury (kidney IRI). We demonstrated that MV subtype production and profiles differ significantly under differing states of inflammation. In the endotoxaemia model, the predominant MV subtypes were of neutrophil- and monocyte-origin, whereas in kidney IRI, platelet- and endothelial-derived MVs were predominated. As the MV subtype profile of the endotoxaemia model coincided with our recent clinical finding in burn injury patients where neutrophil- and monocyte-MVs were increased acutely[427], and it was technically more feasible to run this model in adoptive transfer experiments, we decided to investigate MVs produced during endotoxaemia and not kidney IRI in the indirect ALI IPL model. In Chapter 5, we established the *in vivo* MV-to-*ex vivo* IPL system, showing that MVs from one donor mouse could produce inflammation (endothelial and monocyte activation) in IPLs from LPS-treated mice. Nevertheless, our findings on MV production in the model of kidney IRI remains an interesting area of investigation to determine whether these MVs can contribute to organ-to-organ propagation of inflammation and how distinct profiles of MV subtypes produce differing effects within the pulmonary vasculature.

Although we were able to recover sufficient amount of MVs from the circulating blood of LPS-treated mice for *ex vivo* functional studies, the natural *in vivo* production-clearance equilibrium of MVs limits MV recovery to only a small and potentially phenotypically unrepresentative portion of the total *in vivo* output. The more potent or biologically active MV subtypes may have a much shorter half-life in the blood and exerting their biological activities rapidly, in contrast to those MVs remaining in the circulation and therefore more likely to be sampled and analysed. This notion should be taken into consideration when MVs are investigated in clinical setting, and attempts made in the mouse system to compare the MVs from normal and macrophage-depleted mice. In order to recover the total *in vivo* produced circulating MVs for functional studies, we depleted intravascular macrophages, known to be the major clearance system of circulating MVs, in Chapter 6. Although challenging to address

these questions in patients due to ethical consideration, it would be informative to assess functional activities of MVs obtained in the early prodromal or pre-ICU period during the acute production phase and follow up at a later stage where production may have slowed and clearance could play a greater role in determining circulating MV profile. Moreover, as LPS infusion in human volunteers showed increases in circulating MV levels within hours[438], human endotoxaemia model may be an useful alternative to study MV production during early timepoint under controlled condition as a comparator to patient samples.

7.1.3 Myeloid-derived MVs elicit a monocyte-dependent lung injury during inflammation

When MVs from macrophage-depleted mouse donors were adoptively transferred to IPLs, they consistently produced a rapid (≤2h) and significant interstitial oedema, a standard injury parameter in the development of indirect ALI. This process was also found to be dependent on the presence of lung intravascular monocytes, where their depletion prior to the IPL procedure prevented oedema formation. Our group has previously shown the role of lung-marginated monocytes both in the context of direct[294,295,297] and indirect ALI[187,291]. However, this study demonstrated for the first time, the interaction of lung-marginated monocytes with an endogenous meditator of inflammation released during endotoxaemia, i.e. MVs, contribute to the development of indirect ALI.

MVs from the same or different cell sources have been shown to carry a spectrum of biological activities, sometimes opposing (e.g. pro- and anti-inflammatory), under *in vitro* conditions. Such opposing effects expressed within the pulmonary circulation may potentially obscure measurement of MV subtype activities in the IPL. Using an *in vivo* endogenous MV production model approach which contains a mixture of multiple MV subtypes, this heterogeneity may be even more pronounced in the IPL than *in vitro* due the further release of MV in response to secondary stimuli, such as cytokines released by the IPL. When MV subtypes were isolated from endotoxaemic plasma based on their surface parental cell marker, we found a sharp contrast between the activities of myeloid-derived and platelet-derived MVs. The pro-inflammatory and pro-injurious responses measured in IPL was mainly attributed to the MVs of myeloid-origin (isolated by anti-CD11b-beads), rather than platelet-origin (isolated by anti-CD41-beads). It was apparent that total MVs and myeloid-MVs produced similar

levels of oedema, but inflammatory mediator release was lower and more variable with total MVs. Although we attribute this difference in part to the higher challenge dose of myeloid-MVs present in the immunoaffinity magnetic beads preparation and the standardisation of the MV number used, other factors could be important following total MV infusion, such as competition in binding to target cells between non-active MV and active MV subtypes. Future investigations could include a more in-depth analysis of the different MV subtypes and any co-isolates in the MV preparation to guide the improvement on MV isolation procedures required.

7.1.4 The role of neutrophil-derived MVs

These findings together point to the pulmonary microvasculature as a unique site for expression of inflammatory MV subtype activity, strongly suggesting a key role for myeloid MVs in indirect ALI pathogenesis, most likely neutrophil-derived MVs in particular, based on their abundance in plasma during endotoxaemia and our recent findings in burns patients[427]. Neutrophilia is a common consequence of systemic infection or inflammation where neutrophil number increases in the circulating blood as an early host defense response. These neutrophils could release MVs in the circulation and in different vascular beds, including the lung capillaries where they would come into close proximity with lung-marginated monocytes. Recently, two types of MVs released from neutrophils have been described: neutrophil-derived trails (NDTRs) and neutrophil-derived MVs (NDMVs)[616]. It has been suggested that NDTRs generated by migrating neutrophils are pro-inflammatory, whereas NDMVs generated from neutrophils which arrived at the inflammatory foci are anti-inflammatory.

As described above, we were not able to discern whether the MVs recovered from the circulating blood were released from circulating, marginated, or migrating neutrophils in this study. It is therefore interesting to speculate that neutrophil-MVs could perform a key role in intercellular communication between lung-marginated neutrophils and monocytes and as such, would represent a potential means of local communication and coordination of effector functions. Thus, this study could further benefit from the use of intravital microscopy to label neutrophils and their real time release of MVs, as recently explored using mouse cremaster muscle[575,617]. Especially in the setting of IPL, it would be interesting

to observe if MVs are released endogenously from pulmonary vascular cells, and as such could be monitored as emerging markers of indirect ALI. Furthermore, intravital microscopy of IPL may provide additional information on whether MVs released by lung-marginated neutrophils occurring in proximity to the lung-marginated monocytes, interact differently than those released by circulating neutrophils which travelled long distance to the lungs.

7.2 Future work

Although this study provided important insights into the role of lung-marginated monocytes and myeloid-derived MVs in pulmonary vascular inflammation in indirect ALI, our findings also give rise to further important questions that merit future investigations.

7.2.1 MV interaction with target cell and consequences

Although we demonstrated that lung-marginated Ly6C^{high} monocytes internalise *in vitro* generated MVs via their surface-exposed PS, further experiments are needed to determine pulmonary target cell interactions of *in vivo*-derived myeloid MVs with their more heterogeneous PS expression. There are several possible mechanisms in which MVs could elicit endothelial inflammation and injury via lung-marginated monocytes: 1) direct MV uptake by monocyte, through which monocytes are activated and release pro-inflammatory and pro-injurious factors, 2) monocytes capture MVs on their surface and present them to endothelial cells for internalisation, and 3) monocytes are activated by MV binding and release activating factors to stimulate the release of MV content from these MVs onto endothelial cell surface. In the first instance, neutrophil MVs have been found to directly induce monocyte activation[377], including the release of cytokine such as TNF-α, IL-6, MIP-1α, suggesting the crucial role of monocytes in mediating inflammatory responses. However, depletion of lung monocyte in IPL did not seem to mitigate these responses in this study, though it was not further characterised with immunoaffinity magnetic bead-isolated myeloid-MVs. In the second instance, neutrophil-MVs may directly mediate endothelial responses, as they have been shown to directly induce CAM upregulation on endothelial cells *in vitro*[570,571]. However, although direct activation of endothelium by MVs is possible through their internalisation[618], this may have to operate via monocyte capture and presentation to the endothelial cells under physiological flow conditions, as we found a significantly lower MV uptake by endothelial cells than monocytes *in vivo* and *ex vivo*[1]. In the third instance, MVs may activate monocytes and elicit chemokine and lipid mediator release, which in turn activate the release of MV content onto endothelial cell surface through MV lysis or active production. For example, neutrophil MVs were found to release reactive oxygen species (ROS) and leukotriene B_4 (LTB_4) into extra-vesicular space, upon direct stimulation by fMLF (chemoattractant) and arachidonic acid[380], likely to be produced by monocytes/macrophage. In another study, neutrophil MVs were found

to induce permeability increase in endothelial and epithelial cells via MV-associated myeloperoxidase (MPO)[381,619].

7.2.2 Molecular cargo mediators in myeloid MVs

We did not investigate the cargoes of the myeloid-MVs in this study, but based on previous literature, there are several potential molecular mechanisms capable of causing inflammation and regulating endothelial permeability. It has been demonstrated that various miRNAs, proteins and cytokines can be carried by MVs depending on the stimuli and/or cell source[370,380,620]. Several enzymatic and cytotoxic mediators have been implicated as pro-inflammatory and pro-injurious neutrophil-derived MV-associated effectors, such as MPO, ROS, leukotriene, elastase, proteinase 3 and matrix metalloproteinase-9[378–381]. Other than neutrophil enzymes, neutrophil-derived MVs were also found to contribute to vascular inflammation in atherosclerosis via delivery of miRNA (miR-155)[621]. Interestingly, miR-155 were also found to be carried by dendritic cells-derived exosomes and were found to enhance endotoxin-induced inflammation in mice[622]. Together, these studies suggest that EV-associated miRNA such as miR-155 may have a role in myeloid-MV effects in the pulmonary vasculature. Additionally, our group has previously demonstrated the effect of MVs containing TNF-α released by alveolar macrophages in the alveolar space, as a crucial mediator of direct ALI[375,376], suggesting a role of MV-associated cytokines in the pathogenesis of ALI. Overall, as MVs can carry a wide range of mediators, further analysis of their content using proteome, lipidome (eicosanoid/oxylipins) and RNAome (miRNA) analysis focussing on relevant MV subtype (i.e. myeloid- or neutrophil-derived) isolated by positive magnetic bead selection, with comparisons to the less active MV subtype (i.e. platelet-derived), may shed more light in the molecular cargo responsible in the pathogenesis of sepsis-induced indirect ALI.

7.2.3 Is purity an issue? Are exosomes involved?

Reports on circulating exosomes in sepsis/SIRS patients are limited, but elevated levels of plasma exosomes were recently found to correlate with severity of organ failure and mortality in septic patients[623]. However, as the study used ExoQuick to obtain exosomes, a method which co-precipitates smaller MVs (<200nm), the identity of the exosome preparation is uncertain. In a sepsis

CLP mouse model, miRNAs were also found to be released in the blood via EVs (exosomes and MVs) and mediate inflammatory responses *in vivo* and *in vitro*[519]. It is therefore unclear to date if functional activity of exosomes and MVs are as distinctive from each other as how they have been defined. Recently, the ISEV has suggested the use of "small EVs" to encompass both exosomes and MVs, as it is now recognised that there is a lack of specific marker to distinguish exosomes from MVs[328,329]. Undeniably, our 'total MVs' preparation from differential centrifugation may contain exosomes and other co-isolates such as HDL. However, the positively selected MVs by anti-CD11b immunoaffinity magnetic beads should facilitate the removal of exosomes and lipoproteins, which are unlikely to express CD11b on the surface. As the CD11b positive selection method isolated a broad MV subtype of myeloid origin, further investigation using more specific antibody-conjugated magnetics beads may provide more information on the MV subtype-specific activities. For example, anti-Ly6G can be used to specifically isolate neutrophil-MVs, anti-CD115 for monocyte/macrophage-MVs, or anti-Ly6B.2 (7/4 antigen) for neutrophil- and Ly6C^{high} monocyte-MVs to assess any combined or synergistic activity between these MV subtypes.

7.2.4 Translational and therapeutic opportunities

In an effort to explore the translational potential of these findings, I have collaborated with another PhD student in our group to examine the functional activities of MVs in an *in vitro* monocyte-endothelial co-culture system. Interestingly, although these human MVs were obtained by *ex vivo* treatment of human whole blood with LPS, similar results were obtained, demonstrating the pro-inflammatory properties of neutrophil-derived (isolated by CD66b-beads), but not platelet-derived MVs (isolated by CD61-beads) via a monocyte-dependent mechanism.

It would therefore be an ideal next step to investigate MVs obtained from patients with sepsis/SIRS in this *in vitro* co-culture system to further ascertain their immunomodulatory properties, ideally with samples obtained at an early timepoint as discussed above. However, the methods of blood collection from patients, especially in the field of EVs research remain inconsistent, significantly affecting the quality of research and hinders translational discoveries. For instance, Lacroix et al. has shown that pre-analytical parameters such as delay before first centrifugation, agitation of tubes during

transportation and centrifugation protocol, significantly impact on the measurement of circulating EVs[624]. Specifically, freeze-thaw cycle was found to increase MV number significantly, especially that of platelet-derived due to platelet activation and fragmentation. Moreover, freeze-thawing was shown to degrade structural and biological activity of EVs by decreasing their size, degrading RNA and causes leakage of EV-associated proteins[625,626]. Therefore, functional activity of MVs should ideally be studied with fresh plasma samples obtained from patients if possible, as we did in this mouse study.

The immunoaffinity magnetic beads method developed in this study can be used not only to demonstrate MV subtype-specific functional activity, it is also a useful tool to purify MV subtypes from patient samples for subsequent omics analysis to examine their lipids, RNA or protein content/cargo as described above. Overall, if the mechanism of MV-cell interaction can be established using these human endotoxaemia or patient MVs *in vitro* and the mouse models to identify therapeutic targets, it may be possible to extend these findings to the human *ex vivo* lung perfusion system, which is now increasingly used as a preclinical testing platform for ALI therapeutics[627], to bridge the gap between animal models and patient clinical trials.

7.3 Concluding remarks

In brief, this study has proven our initial hypothesis that MVs (especially that of myeloid-derived) and their interaction with lung-marginated monocytes play a crucial role in the propagation of systemic inflammation to the lung, which drives the progression of pulmonary vascular inflammation in the development of indirect ALI. While further work is required to elucidate the specific molecular mechanism involved, we demonstrated here a proof-of-concept finding for biomarker application in patients with sepsis/SIRS. Furthermore, the interaction between marginated monocytes and circulating MVs serve as a reference point for potential development of therapeutic strategies in sepsis-induced indirect ALI.

Chapter 8

References

Chapter 8 References

1. O'Dea, K. P. *et al.* Monocytes mediate homing of circulating microvesicles to the pulmonary vasculature during low-grade systemic inflammation. *J. Extracell. Vesicles* **9**, 1706708 (2020).
2. Ashbaugh, D. David Ashbaugh reminisces. *The Lancet Respiratory Medicine* vol. 5 474 (2017).
3. Cutts, S. *et al.* History of acute respiratory distress syndrome. *Lancet. Respir. Med.* **4**, 547–548 (2016).
4. Raghavendran, K. & Napolitano, L. M. Definition of ALI/ARDS. *Critical Care Clinics* vol. 27 429–437 (2011).
5. Bernard, G. R. *et al.* The American-European Consensus Conference on ARDS: Definitions, mechanisms, relevant outcomes, and clinical trial coordination. in *American Journal of Respiratory and Critical Care Medicine* vol. 149 818–824 (American Thoracic Society, 1994).
6. Ranieri, V. M. *et al.* Acute respiratory distress syndrome: The Berlin definition. *JAMA - J. Am. Med. Assoc.* (2012) doi:10.1001/jama.2012.5669.
7. Rubenfeld, G. D. *et al.* Incidence and outcomes of acute lung injury. *N. Engl. J. Med.* **353**, 1685–1693 (2005).
8. Brun-Buisson, C. *et al.* Epidemiology and outcome of acute lung injury in European intensive care units Results from the ALIVE study. *Intensive Care Med.* **30**, 51–61 (2004).
9. Bersten, A. D., Edibam, C., Hunt, T. & Moran, J. Incidence and mortality of acute lung injury and the acute respiratory distress syndrome in three Australian States. *Am. J. Respir. Crit. Care Med.* **165**, 443–448 (2002).
10. Luhr, O. R. *et al.* Incidence and mortality after acute respiratory failure and acute respiratory distress syndrome in Sweden, Denmark, and Iceland. *Am. J. Respir. Crit. Care Med.* **159**, 1849–1861 (1999).
11. Phua, J. *et al.* Has mortality from acute respiratory distress syndrome decreased over time?: A systematic review. *American Journal of Respiratory and Critical Care Medicine* vol. 179 220–227 (2009).
12. Rubenfeld, G. D. & Herridge, M. S. Epidemiology and outcomes of acute lung injury. *Chest* **131**, 554–562 (2007).
13. Quartin, A. A. *et al.* Acute lung injury outside of the ICU incidence in respiratory isolation on a general ward. *Chest* **135**, 261–268 (2009).
14. Johnson, E. R. & Matthay, M. A. Acute lung injury: Epidemiology, pathogenesis, and treatment. *Journal of Aerosol Medicine and Pulmonary Drug Delivery* vol. 23 243–252 (2010).
15. Bellingan, G. J. The pulmonary physician in critical care·6: The pathogenesis of ALI/ARDS. *Thorax* vol. 57 540–546 (2002).
16. Matthay, M. A. & Zimmerman, G. A. Acute lung injury and the acute respiratory distress syndrome: Four decades of inquiry into pathogenesis and rational management. *American Journal of Respiratory Cell and Molecular Biology* (2005) doi:10.1165/rcmb.F305.
17. Ware, L. B. & Matthay, M. A. The acute respiratory distress syndrome. *N. Engl. J. Med.* **342**, 1334–1349 (2000).
18. Bhargava, M. & Wendt, C. H. Biomarkers in acute lung injury. *Translational Research* vol. 159 205–217 (2012).
19. Fremont, R. D. *et al.* Acute Lung Injury in Patients With Traumatic Injuries: Utility of a Panel of Biomarkers for Diagnosis and Pathogenesis. *J. Trauma Inj. Infect. Crit. Care* **68**, 1121–1127 (2010).
20. McClintock, D., Zhuo, H., Wickersham, N., Matthay, M. A. & Ware, L. B. Biomarkers of inflammation, coagulation and fibrinolysis predict mortality in acute lung injury. *Crit. Care* **12**, R41 (2008).

21. Wang, Y. *et al.* The preventive effect of antiplatelet therapy in acute respiratory distress syndrome: A meta-analysis. *Crit. Care* **22**, (2018).

22. Bajwa, E. K., Malhotra, C. K., Thompson, B. T., Christiani, D. C. & Gong, M. N. Statin therapy as prevention against development of acute respiratory distress syndrome: An observational study. *Crit. Care Med.* **40**, 1470–1477 (2012).

23. Nieman, G. F. *et al.* Prevention and treatment of acute lung injury with time-controlled adaptive ventilation: physiologically informed modification of airway pressure release ventilation. *Annals of Intensive Care* vol. 10 3 (2020).

24. Raghavendran, K. *et al.* Pharmacotherapy of Acute Lung Injury and Acute Respiratory Distress Syndrome. *Curr. Med. Chem.* **15**, 1911 (2008).

25. Sweeney, R., Griffiths, M. & Mcauley, D. Treatment of acute lung injury: Current and emerging pharmacological therapies. *Semin. Respir. Crit. Care Med.* **34**, 487–498 (2013).

26. Calfee, C. S. & Matthay, M. A. Nonventilatory treatments for acute lung injury and ARDS. *Chest* **131**, 913–920 (2007).

27. Sadikot, R. T., Kolanjiyil, A. V, Kleinstreuer, C. & Rubinstein, I. Nanomedicine for Treatment of Acute Lung Injury and Acute Respiratory Distress Syndrome. *Biomed. Hub* **2**, 1–12 (2017).

28. Guillamat-Prats, R. *et al.* Cell therapy for the treatment of acute lung injury: Alveolar type II cells or mesenchymal stem cells? in *European Respiratory Journal* vol. 48 PA945 (European Respiratory Society (ERS), 2016).

29. Shaver, C. M. & Bastarache, J. A. Clinical and biological heterogeneity in acute respiratory distress syndrome: Direct versus indirect lung injury. *Clinics in Chest Medicine* (2014) doi:10.1016/j.ccm.2014.08.004.

30. Doi, K., Ishizu, T., Fujita, T. & Noiri, E. Lung injury following acute kidney injury: Kidney-lung crosstalk. *Clinical and Experimental Nephrology* vol. 15 464–470 (2011).

31. Pelosi, P. *et al.* Pulmonary and extrapulmonary acute respiratory distress syndrome are different. *European Respiratory Journal, Supplement* vol. 22 48s-56s (2003).

32. Gattinoni, L. *et al.* Acute respiratory distress syndrome caused by pulmonary and extrapulmonary disease: Different syndromes? *Am. J. Respir. Crit. Care Med.* **158**, 3–11 (1998).

33. Rocco, P. R. M. & Zin, W. A. Pulmonary and extrapulmonary acute respiratory distress syndrome: Are they different? *Current Opinion in Critical Care* vol. 11 10–17 (2005).

34. Rocco, P. R. M. & Pelosi, P. Pulmonary and extrapulmonary acute respiratory distress syndrome: Myth or reality? *Current Opinion in Critical Care* vol. 14 50–55 (2008).

35. Morisawa, K. *et al.* Difference in pulmonary permeability between indirect and direct acute respiratory distress syndrome assessed by the transpulmonary thermodilution technique: a prospective, observational, multi-institutional study. *J. Intensive Care* **2**, 24 (2014).

36. Sehgal, I. S., Dhooria, S., Behera, D. & Agarwal, R. Acute respiratory distress syndrome: Pulmonary and extrapulmonary not so similar. *Indian J. Crit. Care Med.* **20**, 194–197 (2016).

37. Suntharalingam, G., Regan, K., Keogh, B. F., Morgan, C. J. & Evans, T. W. Influence of direct and indirect etiology on acute outcome and 6-month functional recovery in acute respiratory distress syndrome. *Crit. Care Med.* (2001) doi:10.1097/00003246-200103000-00016.

38. Luo, L. *et al.* Clinical Predictors of Hospital Mortality Differ Between Direct and Indirect ARDS. *Chest* **151**, 755–763 (2017).

39. Anan, K., Kawamura, K., Suga, M. & Ichikado, K. Clinical differences between pulmonary and extrapulmonary acute respiratory distress syndrome: A retrospective cohort study of prospectively collected data in Japan. *J. Thorac. Dis.* **10**, 5796–5803 (2018).

40. Thille, A. W., Richard, J. C. M., Maggiore, S. M., Ranieri, V. M. & Brochard, L. Alveolar recruitment in pulmonary and extrapulmonary acute respiratory distress syndrome:

Comparison using pressure-volume curve or static compliance. *Anesthesiology* **106**, 212–217 (2007).

41. Agarwal, R., Srinivas, R., Nath, A. & Jindal, S. K. Is the mortality higher in the pulmonary vs the extrapulmonary ARDS? A metaanalysis. *Chest* (2008) doi:10.1378/chest.07-2182.

42. Callister, M. E. J. & Evans, T. W. Pulmonary versus extrapulmonary acute respiratory distress syndrome: Different diseases or just a useful concept? *Current Opinion in Critical Care* vol. 8 21–25 (2002).

43. Ackermann, M. *et al.* Pulmonary vascular endothelialitis, thrombosis, and angiogenesis in Covid-19. *N. Engl. J. Med.* **383**, 120–128 (2020).

44. Patel, B. V *et al.* Pulmonary Angiopathy in Severe COVID-19: Physiologic, Imaging and Hematologic Observations. *Am. J. Respir. Crit. Care Med.* **202**, 690–699 (2020).

45. Calabrese, F. *et al.* Pulmonary pathology and COVID-19: lessons from autopsy. The experience of European Pulmonary Pathologists. *Virchows Archiv* (2020) doi:10.1007/s00428-020-02886-6.

46. Tian, S. *et al.* Pathological study of the 2019 novel coronavirus disease (COVID-19) through postmortem core biopsies. *Mod. Pathol.* **33**, 1007–1014 (2020).

47. Magro, C. *et al.* Complement associated microvascular injury and thrombosis in the pathogenesis of severe COVID-19 infection: A report of five cases. *Transl. Res.* **220**, 1–13 (2020).

48. Sinha, P. & Calfee, C. S. Phenotypes in acute respiratory distress syndrome: Moving towards precision medicine. *Current Opinion in Critical Care* vol. 25 12–20 (2019).

49. Wilson, J. G. & Calfee, C. S. ARDS Subphenotypes: Understanding a Heterogeneous Syndrome. *Critical Care* vol. 24 102 (2020).

50. Calfee, C. S. *et al.* Subphenotypes in acute respiratory distress syndrome: Latent class analysis of data from two randomised controlled trials. *Lancet Respir. Med.* **2**, 611–620 (2014).

51. Bellani, G. *et al.* Epidemiology, patterns of care, and mortality for patients with acute respiratory distress syndrome in intensive care units in 50 countries. *JAMA - J. Am. Med. Assoc.* **315**, 788–800 (2016).

52. Vincent, J. L. *et al.* International study of the prevalence and outcomes of infection in intensive care units. *JAMA - J. Am. Med. Assoc.* **302**, 2323–2329 (2009).

53. Stapleton, R. D. *et al.* Causes and timing of death in patients with ARDS. *Chest* **128**, 525–532 (2005).

54. Englert, J. A., Bobba, C. & Baron, R. M. Integrating molecular pathogenesis and clinical translation in sepsis-induced acute respiratory distress syndrome. *JCI Insight* vol. 4 (2019).

55. Bone, R. C. *et al.* Definitions for sepsis and organ failure and guidelines for the use of innovative therapies in sepsis. in *Chest* vol. 101 1644–1655 (1992).

56. Fujishima, S. Organ dysfunction as a new standard for defining sepsis. *Inflammation and Regeneration* vol. 36 24 (2016).

57. Singer, M. *et al.* The Third International Consensus Definitions for Sepsis and Septic Shock (Sepsis-3). *Jama* **315**, 801–10 (2016).

58. Vincent, J. L., Opal, S. M., Marshall, J. C. & Tracey, K. J. Sepsis definitions: Time for change. *The Lancet* vol. 381 774–775 (2013).

59. Pool, R., Gomez, H. & Kellum, J. A. Mechanisms of Organ Dysfunction in Sepsis. *Critical Care Clinics* vol. 34 63–80 (2018).

60. Spapen, H. D., Jacobs, R. & Honoré, P. M. Sepsis-induced multi-organ dysfunction syndrome—a mechanistic approach. *J. Emerg. Crit. Care Med.* **1**, 27–27 (2017).

61. Rudd, K. E. *et al.* Global, regional, and national sepsis incidence and mortality, 1990–2017:

analysis for the Global Burden of Disease Study. *Lancet* (2020) doi:10.1016/S0140-6736(19)32989-7.

62. MacFie, J. *et al.* Gut origin of sepsis: A prospective study investigating associations between bacterial translocation, gastric microflora, and septic morbidity. *Gut* **45**, 223–228 (1999).

63. Fukushima, R., Alexander, J. W., Gianotti, L., Pyles, T. & Ogle, C. K. Bacterial translocation-related mortality may be associated with neutrophil-mediated organ damage. *Shock* (1995).

64. Matzinger, P. The danger model: A renewed sense of self. *Science* vol. 296 301–305 (2002).

65. Chen, G. Y. & Nuñez, G. Sterile inflammation: sensing and reacting to damage. *Nat. Rev. Immunol.* **10**, 826–37 (2010).

66. Bone, R. C. Sir Isaac Newton, sepsis, SIRS, and CARS. *Critical Care Medicine* (1996) doi:10.1097/00003246-199607000-00010.

67. Hotchkiss, R. S., Coopersmith, C. M., McDunn, J. E. & Ferguson, T. A. The sepsis seesaw: Tilting toward immunosuppression. *Nature Medicine* (2009) doi:10.1038/nm0509-496.

68. Remick, D. G. Pathophysiology of sepsis. *Am. J. Pathol.* (2007) doi:10.2353/ajpath.2007.060872.

69. Osuchowski, M. F., Welch, K., Siddiqui, J. & Remick, D. G. Circulating Cytokine/Inhibitor Profiles Reshape the Understanding of the SIRS/CARS Continuum in Sepsis and Predict Mortality. *J. Immunol.* **177**, 1967–1974 (2006).

70. Cavaillon, J. M., Adrie, C., Fitting, C. & Adib-Conquy, M. Reprogramming of circulatory cells in sepsis and SIRS. *Journal of Endotoxin Research* (2005) doi:10.1179/096805105X58733.

71. Cavaillon, J. M., Adib-Conquy, M., Cloëz-Tayarani, I. & Fitting, C. Immunodepression in sepsis and SIRS assessed by ex vivo cytokine production is not a generalized phenomenon: A review. *Journal of Endotoxin Research* (2001) doi:10.1179/096805101101532576.

72. Lopes De Miranda, M., Balarini, M., Caixeta, D. & Bouskela, E. Microcirculatory dysfunction in sepsis: Pathophysiology, clinical monitoring, and potential therapies. *American Journal of Physiology - Heart and Circulatory Physiology* vol. 311 H24–H35 (2016).

73. Bateman, R. M., Sharpe, M. D., Jagger, J. E. & Ellis, C. G. Sepsis impairs microvascular autoregulation and delays capillary response within hypoxic capillaries. *Crit. Care* **19**, (2015).

74. Ince, C. The microcirculation is the motor of sepsis. *Critical Care* vol. 9 (2005).

75. Faix, J. D. Biomarkers of sepsis. *Critical Reviews in Clinical Laboratory Sciences* vol. 50 23–36 (2013).

76. Landelle, C. *et al.* Low monocyte human leukocyte antigen-DR is independently associated with nosocomial infections after septic shock. *Intensive Care Med.* **36**, 1859–1866 (2010).

77. Monneret, G. *et al.* Persisting low monocyte human leukocyte antigen-DR expression predicts mortality in septic shock. *Intensive Care Med.* **32**, 1175–1183 (2006).

78. Shozushima, T. *et al.* Usefulness of presepsin (sCD14-ST) measurements as a marker for the diagnosis and severity of sepsis that satisfied diagnostic criteria of systemic inflammatory response syndrome. *J. Infect. Chemother.* **17**, 764–769 (2011).

79. Bopp, C. *et al.* sRAGE is Elevated in Septic Patients and Associated With Patients Outcome. *J. Surg. Res.* **147**, 79–83 (2008).

80. Genel, F. *et al.* Evaluation of adhesion molecules CD64, CD11b and CD62L in neutrophils and monocytes of peripheral blood for early diagnosis of neonatal infection. *World J. Pediatr.* **8**, 72–75 (2012).

81. Bouchon, A., Facchetti, F., Weigand, M. A. & Colonna, M. TREM-1 amplifies inflammation and is a crucial mediator of septic shock. *Nature* **410**, 1103–1107 (2001).

82. Simon, L., Gauvin, F., Amre, D. K., Saint-Louis, P. & Lacroix, J. Serum procalcitonin and C-reactive protein levels as markers of bacterial infection: A systematic review and meta-analysis.

Clinical Infectious Diseases vol. 39 206–217 (2004).

83. Marshall, J. C. Why have clinical trials in sepsis failed? *Trends in Molecular Medicine* vol. 20 195–203 (2014).

84. Fisher, C. J. *et al.* Treatment of septic shock with the tumor necrosis factor receptor:Fc fusion protein. The Soluble TNF Receptor Sepsis Study Group. *N. Engl. J. Med.* **334**, 1697–1702 (1996).

85. Opal, S. M. *et al.* Confirmatory interleukin-1 receptor antagonist trial in severe sepsis: A phase III, randomized, double-blind, placebo-controlled, multicenter trial. *Critical Care Medicine* vol. 25 1115–1124 (1997).

86. Opal, S. M. *et al.* Effect of eritoran, an antagonist of MD2-TLR4, on mortality in patients with severe sepsis: The ACCESS randomized trial. *JAMA - J. Am. Med. Assoc.* **309**, 1154–1162 (2013).

87. Levin, M. *et al.* Recombinant bactericidal/permeability-increasing protein (rBPI21) as adjunctive treatment for children with severe meningococcal sepsis: A randomised trial. *Lancet* **356**, 961–967 (2000).

88. Angus, D. C. The search for effective therapy for sepsis: Back to the drawing board? *JAMA - Journal of the American Medical Association* vol. 306 2614–2615 (2011).

89. Davies, R., O'Dea, K. & Gordon, A. Immune therapy in sepsis: Are we ready to try again? *Journal of the Intensive Care Society* vol. 19 326–344 (2018).

90. Deutschman, C. S. & Tracey, K. J. Sepsis: Current dogma and new perspectives. *Immunity* **40**, 463–475 (2014).

91. Murphy, K. *Immunobiology, 8th Edition*. *Garland Science* (2012).

92. Amarante-Mendes, G. P. *et al.* Pattern recognition receptors and the host cell death molecular machinery. *Frontiers in Immunology* vol. 9 2379 (2018).

93. Takeuchi, O. & Akira, S. Pattern Recognition Receptors and Inflammation. *Cell* vol. 140 805–820 (2010).

94. Wiersinga, W. J., Leopold, S. J., Cranendonk, D. R. & van der Poll, T. Host innate immune responses to sepsis. *Virulence* vol. 5 36–44 (2014).

95. Andersson, U. & Tracey, K. J. HMGB1 is a therapeutic target for sterile inflammation and infection. *Annu. Rev. Immunol.* **29**, 139–162 (2011).

96. Ahmed, A. I., Soliman, R. A. & Samir, S. Cell Free DNA and Procalcitonin as Early Markers of Complications in ICU Patients with Multiple Trauma and Major Surgery. *Clin. Lab.* **62**, 2395–2404 (2016).

97. Cohen, M. J. *et al.* Early release of high mobility group box nuclear protein 1 after severe trauma in humans: role of injury severity and tissue hypoperfusion. *Crit. Care* **13**, (2009).

98. Alhamdi, Y. *et al.* Circulating histones are major mediators of cardiac injury in patients with sepsis. *Crit. Care Med.* **43**, 2094–2103 (2015).

99. Horst, K. *et al.* Impact of haemorrhagic shock intensity on the dynamic of alarmins release in porcine poly-trauma animal model. *Eur. J. Trauma Emerg. Surg.* **42**, 67–75 (2016).

100. Kawai, C. *et al.* Circulating extracellular histones are clinically relevant mediators of multiple organ injury. *Am. J. Pathol.* **186**, 829–843 (2016).

101. Singleton, K. D. & Wischmeyer, P. E. Effects of HSP70.1/3 gene knockout on acute respiratory distress syndrome and the inflammatory response following sepsis. *Am. J. Physiol. - Lung Cell. Mol. Physiol.* **290**, (2006).

102. Sursal, T. *et al.* Plasma bacterial and mitochondrial DNA distinguish bacterial sepsis from sterile systemic inflammatory response syndrome and quantify inflammatory tissue injury in nonhuman primates. *Shock* **39**, 55–62 (2013).

103. Gentile, L. F. & Moldawer, L. L. DAMPs, PAMPs, and the origins of SIRS in bacterial sepsis. *Shock* vol. 39 113–114 (2013).

104. Kawasaki, T. & Kawai, T. Toll-like receptor signaling pathways. *Frontiers in Immunology* vol. 5 461 (2014).

105. Pålsson-McDermott, E. M. & O'Neill, L. A. J. Signal transduction by the lipopolysaccharide receptor, Toll-like receptor-4. *Immunology* vol. 113 153–162 (2004).

106. Cuenda, A. & Rousseau, S. p38 MAP-Kinases pathway regulation, function and role in human diseases. *Biochimica et Biophysica Acta - Molecular Cell Research* vol. 1773 1358–1375 (2007).

107. Hoffmann, A., Levchenko, A., Scott, M. L. & Baltimore, D. The IκB-NF-κB signaling module: Temporal control and selective gene activation. *Science (80-.).* **298**, 1241–1245 (2002).

108. Beyaert, R. *et al.* The p38/RK mitogen-activated protein kinase pathway regulates interleukin-6 synthesis in response to tumour necrosis factor. *EMBO J.* **15**, 1914–1923 (1996).

109. Lee, J. C. *et al.* A protein kinase involved in the regulation of inflammatory cytokine biosynthesis. *Nature* **372**, 739–746 (1994).

110. Kalogeris, T., Baines, C. P., Krenz, M. & Korthuis, R. J. Cell Biology of Ischemia/Reperfusion Injury. in *International Review of Cell and Molecular Biology* vol. 298 229–317 (Elsevier Inc., 2012).

111. Kalogeris, T., Baines, C. P., Krenz, M. & Korthuis, R. J. Ischemia/Reperfusion. *Compr. Physiol.* **7**, 113–170 (2017).

112. Wu, M. Y. *et al.* Current Mechanistic Concepts in Ischemia and Reperfusion Injury. *Cellular Physiology and Biochemistry* vol. 46 1650–1667 (2018).

113. Galley, H. F. Oxidative stress and mitochondrial dysfunction in sepsis. *British Journal of Anaesthesia* vol. 107 57–64 (2011).

114. Bar-Or, D. *et al.* Sepsis, oxidative stress, and hypoxia: Are there clues to better treatment? *Redox Rep.* **20**, 193–197 (2015).

115. Pedoto, A. *et al.* Acidosis stimulates nitric oxide production and lung damage in rats. *Am. J. Respir. Crit. Care Med.* **159**, 397–402 (1999).

116. Phan, S. H., Gannon, D. E., Varani, J., Ryan, U. S. & Ward, P. A. Xanthine oxidase activity in rat pulmonary artery endothelial cells and its alteration by activated neutrophils. *Am. J. Pathol.* **134**, 1201–1211 (1989).

117. Phan, Q. T. *et al.* Neutrophils use superoxide to control bacterial infection at a distance. *PLoS Pathog.* **14**, e1007157 (2018).

118. Esterházy, D., King, M. S., Yakovlev, G. & Hirst, J. Production of reactive oxygen species by complex I (NADH:ubiquinone oxidoreductase) from Escherichia coli and comparison to the enzyme from mitochondria. *Biochemistry* **47**, 3964–3971 (2008).

119. Hernandez, L. A., Grisham, M. B. & Granger, D. N. A role for iron in oxidant-mediated ischemic injury to intestinal microvasculature. *Am. J. Physiol. - Gastrointest. Liver Physiol.* **253**, G49-53 (1987).

120. Veith, A. & Moorthy, B. Role of cytochrome P450s In the generation and metabolism of reactive oxygen species. *Current Opinion in Toxicology* vol. 7 44–51 (2018).

121. Calfee, C. S., Gallagher, D., Abbott, J., Thompson, B. T. & Matthay, M. A. Plasma angiopoietin-2 in clinical acute lung injury: Prognostic and pathogenetic significance. *Crit. Care Med.* **40**, 1731–1737 (2012).

122. Gloire, G., Legrand-Poels, S. & Piette, J. NF-κB activation by reactive oxygen species: Fifteen years later. *Biochem. Pharmacol.* **72**, 1493–1505 (2006).

123. Riedemann, N. C., Guo, R. F. & Ward, P. A. Novel strategies for the treatment of sepsis. *Nature Medicine* vol. 9 517–524 (2003).

124. Zanotti, S., Kumar, A. & Kumar, A. Cytokine modulation in sepsis and septic shock. *Expert Opinion on Investigational Drugs* vol. 11 1061–1075 (2002).

125. Mera, S. *et al.* Multiplex cytokine profiling in patients with sepsis. *APMIS* **119**, 155–163 (2011).

126. Gogos, C. A., Drosou, E., Bassaris, H. P. & Skoutelis, A. Pro- versus anti-inflammatory cytokine profile in patients with severe sepsis: A marker for prognosis and future therapeutic options. *J. Infect. Dis.* **181**, 176–180 (2000).

127. Chaudhry, H. *et al.* Role of cytokines as a double-edged sword in sepsis. *In Vivo* vol. 27 669–684 (2013).

128. Zhang, J. M. & An, J. Cytokines, inflammation, and pain. *International Anesthesiology Clinics* vol. 45 27–37 (2007).

129. Turner, M. D., Nedjai, B., Hurst, T. & Pennington, D. J. Cytokines and chemokines: At the crossroads of cell signalling and inflammatory disease. *Biochimica et Biophysica Acta - Molecular Cell Research* vol. 1843 2563–2582 (2014).

130. BOGDAN, C. & NATHAN, C. Modulation of Macrophage Function by Transforming Growth Factor β, Interleukin-4, and Interleukin-10. *Ann. N. Y. Acad. Sci.* **685**, 713–739 (1993).

131. Turner, M. *et al.* Induction of the interleukin 1 receptor antagonist protein by transforming growth factor-β. *Eur. J. Immunol.* **21**, 1635–1639 (1991).

132. Hamilton, J. A. Colony-stimulating factors in inflammation and autoimmunity. *Nature Reviews Immunology* vol. 8 533–544 (2008).

133. Sokol, C. L. & Luster, A. D. The chemokine system in innate immunity. *Cold Spring Harb. Perspect. Biol.* **7**, 1–20 (2015).

134. Griffith, J. W., Sokol, C. L. & Luster, A. D. Chemokines and chemokine receptors: Positioning cells for host defense and immunity. *Annual Review of Immunology* vol. 32 659–702 (2014).

135. Imai, T. *et al.* Identification and molecular characterization of fractalkine receptor CX3CR1, which mediates both leukocyte migration and adhesion. *Cell* **91**, 521–530 (1997).

136. Cavaillon, J. M., Munoz, C., Fitting, C., Misset, B. & Carlet, J. Circulating cytokines: The tip of the iceberg? *Circ. Shock* (1992).

137. Schädler, D. *et al.* A multicenter randomized controlled study of an extracorporeal cytokine hemoadsorption device in septic patients. *Crit. Care* **17**, P62 (2013).

138. Schädler, D. *et al.* The effect of a novel extracorporeal cytokine hemoadsorption device on IL-6 elimination in septic patients: A randomized controlled trial. *PLoS One* **12**, (2017).

139. Funk, C. D. Prostaglandins and leukotrienes: Advances in eicosanoid biology. *Science* vol. 294 1871–1875 (2001).

140. Nakahata, N. Thromboxane A2: Physiology/pathophysiology, cellular signal transduction and pharmacology. *Pharmacology and Therapeutics* vol. 118 18–35 (2008).

141. Czarnetzki, B. Increased monocyte chemotaxis towards leukotriene B4 and platelet activating factor in patients with inflammatory dermatoses. *Clin. Exp. Immunol.* **54**, 486–92 (1983).

142. Gabrijelcic, J. *et al.* Neutrophil airway influx by platelet-activating factor in asthma: Role of adhesion molecules and LTB4 expression. *Eur. Respir. J.* **22**, 290–297 (2003).

143. Durán, W. N., Milazzo, V. J., Sabido, F. & Hobson, R. W. Platelet-activating factor modulates leukocyte adhesion to endothelium in ischemia-reperfusion. *Microvasc. Res.* **51**, 108–115 (1996).

144. Dalli, J. *et al.* Human Sepsis Eicosanoid and Proresolving Lipid Mediator Temporal Profiles: Correlations with Survival and Clinical Outcomes. *Crit. Care Med.* **45**, 58–68 (2017).

145. Bernard, G. R. *et al.* The effects of ibuprofen on the physiology and survival of patients with sepsis. *N. Engl. J. Med.* **336**, 912–918 (1997).

146. Haupt, M. T., Jastremski, M. S., Clemmer, T. P., Metz, C. A. & Goris, G. B. Effect of ibuprofen

in patients with severe sepsis: A randomized, double-blind, multicenter study. *Crit. Care Med.* **19**, 1339–1347 (1991).

147. Memiş, D., Karamanlioglu, B., Turan, A., Koyuncu, O. & Pamukçu, Z. Effects of lornoxicam on the physiology of severe sepsis. *Crit. Care* **8**, (2004).

148. Suputtamongkol, Y. *et al.* A double-blind placebo-controlled study of an infusion of lexipafant (platelet-activating factor receptor antagonist) in patients with severe sepsis. *Antimicrob. Agents Chemother.* **44**, 693–696 (2000).

149. Loscalzo, J. & Jin. Vascular nitric oxide: formation and function. *J. Blood Med.* **1**, 147 (2010).

150. Kilbourn, R. G., Szabó, C. & Traber, D. L. Beneficial versus detrimental effects of nitric oxide synthase inhibitors in circulatory shock: Lessons learned from experimental and clinical studies. *Shock* (1997) doi:10.1097/00024382-199704000-00001.

151. Kuebler, W. M., Yang, Y., Samapati, R. & Uhlig, S. Vascular barrier regulation by PAF, ceramide, caveolae, and no-an intricate signaling network with discrepant effects in the pulmonary and systemic vasculature. *Cellular Physiology and Biochemistry* (2010) doi:10.1159/000315103.

152. López, A. *et al.* Multiple-center, randomized, placebo-controlled, double-blind study of the nitric oxide synthase inhibitor 546C88: Effect on survival in patients with septic shock. *Crit. Care Med.* **32**, 21–30 (2004).

153. Yan, C. & Gao, H. New insights for C5a and C5a receptors in sepsis. *Frontiers in Immunology* vol. 3 (2012).

154. Gressner, O. A., Koch, A., Sanson, E., Trautwein, C. & Tacke, F. High C5a levels are associated with increased mortality in sepsis patients - No enhancing effect by actin-free Gc-globulin. *Clin. Biochem.* **41**, 974–980 (2008).

155. Karasu, E., Nilsson, B., Köhl, J., Lambris, J. D. & Huber-Lang, M. Targeting complement pathways in polytrauma- And sepsis-induced multiple-organ dysfunction. *Frontiers in Immunology* vol. 10 543 (2019).

156. Hu, X., Chakravarty, S. D. & Ivashkiv, L. B. Regulation of interferon and Toll-like receptor signaling during macrophage activation by opposing feedforward and feedback inhibition mechanisms. *Immunological Reviews* vol. 226 41–56 (2008).

157. Chertov, O. *et al.* Identification of human neutrophil-derived cathepsin G and azurocidin/CAP37 as chemoattractants for mononuclear cells and neutrophils. *J. Exp. Med.* **186**, 739–747 (1997).

158. Soehnlein, O. *et al.* Neutrophil secretion products pave the way for inflammatory monocytes. *Blood* **112**, 1461–1471 (2008).

159. Prame Kumar, K., Nicholls, A. J. & Wong, C. H. Y. Partners in crime: neutrophils and monocytes/macrophages in inflammation and disease. *Cell and Tissue Research* vol. 371 551–565 (2018).

160. Takano, T. *et al.* Neutrophil survival factors (TNF-alpha, GM-CSF, and G-CSF) produced by macrophages in cats infected with feline infectious peritonitis virus contribute to the pathogenesis of granulomatous lesions. *Arch. Virol.* **154**, 775–781 (2009).

161. Henderson, R. B., Hobbs, J. A. R., Mathies, M. & Hogg, N. Rapid recruitment of inflammatory monocytes is independent of neutrophil migration. *Blood* **102**, 328–335 (2003).

162. Gibbings, S. L. *et al.* Three unique interstitial macrophages in the murine lung at steady state. *Am. J. Respir. Cell Mol. Biol.* (2017) doi:10.1165/rcmb.2016-0361OC.

163. Chiu, S. & Bharat, A. Role of monocytes and macrophages in regulating immune response following lung transplantation. *Current Opinion in Organ Transplantation* vol. 21 239–245 (2016).

164. Geissmann, F., Jung, S. & Littman, D. R. Blood monocytes consist of two principal subsets with distinct migratory properties. *Immunity* **19**, 71–82 (2003).

165. Palframan, R. T. *et al.* Inflammatory chemokine transport and presentation in HEV: A remote control mechanism for monocyte recruitment to lymph nodes in inflamed tissues. *J. Exp. Med.* **194**, 1361–1373 (2001).

166. Auffray, C. *et al.* Monitoring of blood vessels and tissues by a population of monocytes with patrolling behavior. *Science (80-.).* **317**, 666–670 (2007).

167. Ingersoll, M. A. M. *et al.* Comparison of gene expression profiles between human and mouse monocyte subsets. *Blood* **115**, 10–20 (2010).

168. Ziegler-Heitbrock, L. Blood monocytes and their subsets: Established features and open questions. *Frontiers in Immunology* vol. 6 423 (2015).

169. Sprangers, S., Vries, T. J. D. & Everts, V. Monocyte Heterogeneity: Consequences for Monocyte-Derived Immune Cells. *Journal of Immunology Research* (2016) doi:10.1155/2016/1475435.

170. Ziegler-Heitbrock, L. & Hofer, T. P. J. Toward a refined definition of monocyte subsets. *Frontiers in Immunology* (2013) doi:10.3389/fimmu.2013.00023.

171. Patel, A. A. *et al.* The fate and lifespan of human monocyte subsets in steady state and systemic inflammation. *J. Exp. Med.* **214**, 1913–1923 (2017).

172. Sunderkötter, C. *et al.* Subpopulations of Mouse Blood Monocytes Differ in Maturation Stage and Inflammatory Response. *J. Immunol.* **172**, 4410–4417 (2004).

173. Rodero, M. P. *et al.* Immune surveillance of the lung by migrating tissue monocytes. *Elife* **4**, 1–23 (2015).

174. Chong, S. Z. *et al.* CXCR4 identifies transitional bone marrow premonocytes that replenish the mature monocyte pool for peripheral responses. *J. Exp. Med.* **213**, 2293–2314 (2016).

175. Hou, P. C. *et al.* Endothelial Permeability and Hemostasis in Septic Shock: Results From the ProCESS Trial. *Chest* **152**, 22–31 (2017).

176. Borregaard, N. Neutrophils, from Marrow to Microbes. *Immunity* vol. 33 657–670 (2010).

177. Rosales, C. Neutrophil: A cell with many roles in inflammation or several cell types? *Frontiers in Physiology* vol. 9 (2018).

178. Nicolás-Ávila, J. Á., Adrover, J. M. & Hidalgo, A. Neutrophils in Homeostasis, Immunity, and Cancer. *Immunity* vol. 46 15–28 (2017).

179. Ella, K., Mócsai, A. & Káldi, K. Circadian regulation of neutrophils: Control by a cell-autonomous clock or systemic factors? *European Journal of Clinical Investigation* vol. 48 e12965 (2018).

180. Häger, M., Cowland, J. B. & Borregaard, N. Neutrophil granules in health and disease. *Journal of Internal Medicine* vol. 268 25–34 (2010).

181. Selders, G. S., Fetz, A. E., Radic, M. Z. & Bowlin, G. L. An overview of the role of neutrophils in innate immunity, inflammation and host-biomaterial integration. *Regen. Biomater.* **4**, 55–68 (2017).

182. Lahoz-Beneytez, J. *et al.* Human neutrophil kinetics: Modeling of stable isotope labeling data supports short blood neutrophil half-lives. *Blood* **127**, 3431–3438 (2016).

183. Adrover, J. M., Nicolás-Ávila, J. A. & Hidalgo, A. Aging: A Temporal Dimension for Neutrophils. *Trends in Immunology* vol. 37 334–345 (2016).

184. Zhang, D. *et al.* Neutrophil ageing is regulated by the microbiome. *Nature* **525**, 528–532 (2015).

185. McCracken, J. M. & Allen, L. A. H. Regulation of human neutrophil apoptosis and lifespan in health and disease. *J. Cell Death* **7**, 15–23 (2014).

186. Swain, S. D., Rohn, T. T. & Quinn, M. T. Neutrophil priming in host defense: Role of oxidants as priming agents. *Antioxidants and Redox Signaling* vol. 4 69–83 (2002).

187. O'Dea, K. P. *et al.* Mobilization and margination of bone marrow Gr-1high monocytes during subclinical endotoxemia predisposes the lungs toward acute injury. *J. Immunol.* **182**, 1155–66

(2009).

188. Zhang, X. & Morrison, D. C. Lipopolysaccharide-induced selective priming effects on tumor necrosis factor α and nitric oxide production in mouse peritoneal macrophages. *J. Exp. Med.* **177**, 511–516 (1993).

189. Henricson, B. E., Manthey, C. L., Perera, P. Y., Hamilton, T. A. & Vogel, S. N. Dissociation of lipopolysaccharide (LPS)-inducible gene expression in murine macrophages pretreated with smooth LPS versus monophosphoryl lipid A. *Infect. Immun.* **61**, 2325–2333 (1993).

190. Ozmen, L. *et al.* Interleukin 12, interferon γ, and tumor necrosis factor α are the key cytokines of the generalized shwartzman reaction. *J. Exp. Med.* **180**, 907–915 (1994).

191. Volk, H. D. *et al.* Monocyte deactivation - Rationale for a new therapeutic strategy in sepsis. *Intensive Care Medicine, Supplement* vol. 22 (1996).

192. Biswas, S. K. & Lopez-Collazo, E. Endotoxin tolerance: new mechanisms, molecules and clinical significance. *Trends in Immunology* vol. 30 475–487 (2009).

193. Murry, C. E., Jennings, R. B. & Reimer, K. A. Preconditioning with ischemia: A delay of lethal cell injury in ischemic myocardium. *Circulation* (1986) doi:10.1161/01.CIR.74.5.1124.

194. Rosenzweig, H. L. *et al.* Endotoxin preconditioning prevents cellular inflammatory response during ischemic neuroprotection in mice. in *Stroke* vol. 35 2576–2581 (Lippincott Williams & Wilkins, 2004).

195. Hoogerwerf, J. J. *et al.* Priming of alveolar macrophages upon instillation of lipopolysaccharide in the human lung. *Am. J. Respir. Cell Mol. Biol.* **42**, 349–356 (2010).

196. Kraatz, J., Clair, L., Rodriguez, J. L. & West, M. A. Macrophage TNF secretion in endotoxin tolerance: Role of SAPK, p38, and MAPK. *J. Surg. Res.* **83**, 158–164 (1999).

197. Schaeffer, V. *et al.* The priming effect of C5a on monocytes is predominantly mediated by the p38 MAPK pathway. *Shock* **27**, 623–630 (2007).

198. Adib-Conquy, M. *et al.* NF-κB expression in mononuclear cells of patients with sepsis resembles that observed in lipopolysaccharide tolerance. *Am. J. Respir. Crit. Care Med.* **162**, 1877–1883 (2000).

199. Munoz, C. *et al.* Dysregulation of in vitro cytokine production by monocytes during sepsis. *J. Clin. Invest.* **88**, 1747–1754 (1991).

200. Van Deuren, M. *et al.* Differential expression of proinflammatory cytokines and their inhibitors during the course of meningococcal infections. *J. Infect. Dis.* **169**, 157–161 (1994).

201. Tracey, K. J. The inflammatory reflex. *Nature* (2002) doi:10.1038/nature01321.

202. Jaffe, E. A. Cell biology of endothelial cells. *Hum. Pathol.* **18**, 234–239 (1987).

203. Aird, W. C. Phenotypic heterogeneity of the endothelium: I. Structure, function, and mechanisms. *Circulation Research* vol. 100 158–173 (2007).

204. Zimmerman, G. A., McIntyre, T. M. & Prescott, S. M. Thrombin stimulates the adherence of neutrophils to human endothelial cells in vitro. *J. Clin. Invest.* **76**, 2235–2246 (1985).

205. Zimmerman, G. A., Prescott, S. M. & McIntyre, T. M. Endothelial cell interactions with granulocytes: tethering and signaling molecules. *Immunology Today* vol. 13 93–100 (1992).

206. Springer, T. A. Traffic signals for lymphocyte recirculation and leukocyte emigration: The multistep paradigm. *Cell* vol. 76 301–314 (1994).

207. Butcher, E. C. Leukocyte-endothelial cell recognition: Three (or more) steps to specificity and diversity. *Cell* vol. 67 1033–1036 (1991).

208. Herter, J. & Zarbock, A. Integrin Regulation during Leukocyte Recruitment. *J. Immunol.* **190**, 4451–4457 (2013).

209. Zwartz, G. *et al.* Relationship between Molecular and Cellular Dissociation Rates for VLA-4/VCAM-1 Interaction in the Absence of Shear Stress. *Biophys. J.* **86**, 1243–1252 (2004).

210. Altieri, D. C. Occupancy of CD11b/CD18 (Mac-1) divalent ion binding site(s) induces leukocyte adhesion. *J. Immunol.* (1991).

211. Gerritsen, M. E. Functional heterogeneity of vascular endothelial cells. *Biochem. Pharmacol.* **36**, 2701–2711 (1987).

212. Vassiliou, A. G. *et al.* Elevated biomarkers of endothelial dysfunction/activation at ICU admission are associated with sepsis development. *Cytokine* **69**, 240–247 (2014).

213. Mikacenic, C. *et al.* Biomarkers of endothelial activation are associated with poor outcome in critical illness. *PLoS One* (2015) doi:10.1371/journal.pone.0141251.

214. Skibsted, S. *et al.* Biomarkers of endothelial cell activation in early sepsis. *Shock* **39**, 427–432 (2013).

215. Laudes, I. J. *et al.* Disturbed Homeostasis of Lung Intercellular Adhesion Molecule-1 and Vascular Cell Adhesion Molecule-1 during Sepsis. *Am. J. Pathol.* **164**, 1435–1445 (2004).

216. Wu, R., Xu, Y., Song, X. & Meng, X. Gene expression of adhesion molecules in pulmonary and hepatic microvascular endothelial cells during sepsis. *Chinese J. Traumatol. - English Ed.* (2002).

217. Amalakuhan, B. *et al.* Endothelial adhesion molecules and multiple organ failure in patients with severe sepsis. *Cytokine* **88**, 267–273 (2016).

218. Stevens, T. *et al.* Lung vascular cell heterogeneity: Endothelium, smooth muscle, and fibroblasts. in *Proceedings of the American Thoracic Society* vol. 5 783–791 (American Thoracic Society, 2008).

219. Kibria, G., Heath, D., Smith, P. & Biggar, R. Pulmonary endothelial pavement patterns. *Thorax* **35**, 186–191 (1980).

220. Paolinelli, R., Corada, M., Orsenigo, F. & Dejana, E. The molecular basis of the blood brain barrier differentiation and maintenance. Is it still a mystery? *Pharmacological Research* vol. 63 165–171 (2011).

221. Del Vecchio, P. J. *et al.* Culture and characterization of pulmonary microvascular endothelial cells. *Vitr. Cell. Dev. Biol. - Anim.* **28 A**, 711–715 (1992).

222. Parker, J. C. & Yoshikawa, S. Vascular segmental permeabilities at high peak inflation pressure in isolated rat lungs. *American Journal of Physiology - Lung Cellular and Molecular Physiology* vol. 283 L1203–L1209 (2002).

223. Lamm, W. J. E., Luchtel, D. & Albert, R. K. Sites of leakage in three models of acute lung injury. *J. Appl. Physiol.* **64**, 1079–1083 (1988).

224. Qiao, R. L. & Bhattacharya, J. Segmental barrier properties of the pulmonary microvascular bed. *J. Appl. Physiol.* **71**, 2152–2159 (1991).

225. Bhattacharya, J. Hydraulic conductivity of lung venules determined by split-drop technique. *J. Appl. Physiol.* **64**, 2562–2567 (1988).

226. Lin, W., Jacobs, E., Schapira, R. M., Presberg, K. & Effros, R. M. Stop-flow studies of distribution of filtration in rat lungs. *J. Appl. Physiol.* **84**, 47–52 (1998).

227. Millar, F. R., Summers, C., Griffiths, M. J., Toshner, M. R. & Proudfoot, A. G. The pulmonary endothelium in acute respiratory distress syndrome: Insights and therapeutic opportunities. *Thorax* (2016) doi:10.1136/thoraxjnl-2015-207461.

228. Sukriti, S., Tauseef, M., Yazbeck, P. & Mehta, D. Mechanisms regulating endothelial permeability. *Pulmonary Circulation* vol. 4 535–551 (2014).

229. Minshall, R. D. & Malik, A. B. Transport Across the Endothelium: Regulation of Endothelial Permeability. in *The Vascular Endothelium I* 107–144 (Springer Berlin Heidelberg, 2006). doi:10.1007/3-540-32967-6_4.

230. Uhlig, S. *et al.* Differential regulation of lung endothelial permeability in vitro and in situ. *Cell. Physiol. Biochem.* **34**, 1–19 (2014).

231. Mong, P. Y., Petrulio, C., Kaufman, H. L. & Wang, Q. Activation of Rho Kinase by TNF-α Is Required for JNK Activation in Human Pulmonary Microvascular Endothelial Cells. *J. Immunol.* **180**, 550–558 (2008).

232. Joshi, A. D. *et al.* Heat shock protein 90 inhibitors prevent lps-induced endothelial barrier dysfunction by disrupting Rhoa signaling. *Am. J. Respir. Cell Mol. Biol.* **50**, 170–179 (2014).

233. Vandenbroucke, E., Mehta, D., Minshall, R. & Malik, A. B. Regulation of endothelial junctional permeability. in *Annals of the New York Academy of Sciences* vol. 1123 134–145 (Blackwell Publishing Inc., 2008).

234. Nwariaku, F. E. *et al.* Rho inhibition decreases TNF-induced endothelial MAPK activation and monolayer permeability. *J. Appl. Physiol.* **95**, 1889–1895 (2003).

235. Goldblum, S. E., Hennig, B., Jay, M., Yoneda, K. & McClain, C. J. Tumor necrosis factor α-induced pulmonary vascular endothelial injury. *Infect. Immun.* **57**, 1218–1226 (1989).

236. Hocking, D. C., Phillips, P. G., Ferro, T. J. & Johnson, A. Mechanisms of pulmonary edema induced by tumor necrosis factor-α. *Circ. Res.* **67**, 68–77 (1990).

237. Uhlig, S. *et al.* Functional and fine structural changes in isolated rat lungs challenged with endotoxin ex vivo and in vitro. *Am. J. Pathol.* **146**, 1235–47 (1995).

238. Schulman, C. I., Wright, J. K., Nwariaku, F., Sarosi, G. & Turnage, R. H. The effect of tumor necrosis factor-α on microvascular permeability in an isolated, perfused lung. *Shock* **18**, 75–81 (2002).

239. Winn, R., Nickelson, S. & Rice, C. L. Fluid filtration coefficient of isolated goat lungs was unchanged by endotoxin. *J. Appl. Physiol.* **64**, 2463–2467 (1988).

240. Horgan, M. J., Palace, G. P., Everitt, J. E. & Malik, A. B. TNF-α release in endotoxemia contributes to neutrophil-dependent pulmonary edema. *Am. J. Physiol. - Hear. Circ. Physiol.* **264**, (1993).

241. Chian, C. F. *et al.* Apocynin attenuates lipopolysaccharide-induced lung injury in an isolated and perfused rat lung model. *Shock* **38**, 196–202 (2012).

242. Lo, S. K., Everitt, J., Gu, J. & Malik, A. B. Tumor necrosis factor mediates experimental pulmonary edema by ICAM-1 and CD18-dependent mechanisms. *J. Clin. Invest.* **89**, 981–988 (1992).

243. Dodam, J. R., Olson, N. C. & Friedman, M. Differential effects of tumor necrosis factor-α and platelet-activating factor on bovine pulmonary artery endothelial cells in vitro. *Exp. Lung Res.* **20**, 131–141 (1994).

244. Göggel, R. & Uhlig, S. The inositol trisphosphate pathway mediates platelet-activating-factor-induced pulmonary oedema. *Eur. Respir. J.* **25**, 849–857 (2005).

245. Adamson, R. H. *et al.* Rho and rho kinase modulation of barrier properties: Cultured endothelial cells and intact microvessels of rats and mice. *J. Physiol.* **539**, 295–308 (2002).

246. Adamson, R. H., Zeng, M., Adamson, G. N., Lenz, J. F. & Curry, F. E. PAF- and bradykinin-induced hyperpermeability of rat venules is independent of actin-myosin contraction. *Am. J. Physiol. - Hear. Circ. Physiol.* **285**, (2003).

247. Orfanos, S. E., Mavrommati, I., Korovesi, I. & Roussos, C. Pulmonary endothelium in acute lung injury: From basic science to the critically ill. *Intensive Care Medicine* (2004) doi:10.1007/s00134-004-2370-x.

248. Aaronson, P. I., Robertson, T. P. & Ward, J. P. T. Endothelium-derived mediators and hypoxic pulmonary vasoconstriction. *Respir. Physiol. Neurobiol.* **132**, 107–120 (2002).

249. Machuca, T. N. *et al.* The role of the endothelin-1 pathway as a biomarker for donor lung assessment in clinical ex vivo lung perfusion. *J. Hear. Lung Transplant.* (2015) doi:10.1016/j.healun.2015.01.003.

250. Rubens, C. *et al.* Big endothelin-1 and endothelin-1 plasma levels are correlated with the

severity of primary pulmonary hypertension. *Chest* (2001) doi:10.1378/chest.120.5.1562.

251. Eppihimer, M. J., Wolitzky, B., Anderson, D. C., Labow, M. A. & Granger, D. N. Heterogeneity of Expression of E- and P-Selectins In Vivo. *Circ. Res.* **79**, 560–569 (1996).

252. Panes, J. *et al.* Regional differences in constitutive and induced ICAM-1 expression in vivo. *Am. J. Physiol. - Hear. Circ. Physiol.* **269**, (1995).

253. Mura, M., Dos Santos, C. C., Stewart, D. & Liu, M. Vascular endothelial growth factor and related molecules in acute lung injury. *Journal of Applied Physiology* vol. 97 1605–1617 (2004).

254. Kaner, R. J. *et al.* Lung overexpression of the vascular endothelial growth factor gene induces pulmonary edema. *Am. J. Respir. Cell Mol. Biol.* **22**, 657–664 (2000).

255. Krenn, K., Klepetko, W., Taghavi, S., Paulus, P. & Aharinejad, S. Vascular endothelial growth factor increases pulmonary vascular permeability in cystic fibrosis patients undergoing lung transplantation. *Eur. J. Cardio-thoracic Surg.* (2007) doi:10.1016/j.ejcts.2007.04.006.

256. Mordant, P. *et al.* Mesenchymal stem cell treatment is associated with decreased perfusate concentration of interleukin-8 during ex vivo perfusion of donor lungs after 18-hour preservation. *J. Hear. Lung Transplant.* (2016) doi:10.1016/j.healun.2016.04.017.

257. Serraf, A. *et al.* Pulmonary vascular endothelial growth factor and nitric oxide interaction during total cardiopulmonary bypass in neonatal pigs. *J. Thorac. Cardiovasc. Surg.* (2003) doi:10.1067/mtc.2003.402.

258. Thickett, D. R., Armstrong, L., Christie, S. J. & Millar, A. B. Vascular endothelial growth factor may contribute to increased vascular permeability in acute respiratory distress syndrome. *Am. J. Respir. Crit. Care Med.* **164**, 1601–1605 (2001).

259. Schlosser, K. *et al.* High circulating angiopoietin-2 levels exacerbate pulmonary inflammation but not vascular leak or mortality in endotoxin-induced lung injury in mice. *Thorax* (2018) doi:10.1136/thoraxjnl-2017-210413.

260. Agrawal, A. *et al.* Plasma angiopoietin-2 predicts the onset of acute lung injury in critically ill patients. *Am. J. Respir. Crit. Care Med.* **187**, 736–742 (2013).

261. Clark, P. R., Manes, T. D., Pober, J. S. & Kluger, M. S. Increased ICAM-1 expression causes endothelial cell leakiness, cytoskeletal reorganization and junctional alterations. *J. Invest. Dermatol.* **127**, 762–774 (2007).

262. Mulligan, M. S. *et al.* Neutrophil-dependent acute lung injury: Requirement for P-selectin (GMP-140). *J. Clin. Invest.* **90**, 1600–1607 (1992).

263. Mauer, A. M., Athens, J. W., Ashenbrucker, H., Cartwright, G. E. & Wintrobe, M. M. LEUKOKINETIC STUDIES. II. A METHOD FOR LABELING GRANULOCYTES IN VITRO WITH RADIOACTIVE DIISOPROPYLFLUOROPHOSPHATE (DFP32)*. *J. Clin. Invest.* (1960) doi:10.1172/jci104167.

264. ATHENS, J. W. *et al.* Leukokinetic studies. III. The distribution of granulocytes in the blood of normal subjects. *J. Clin. Invest.* **40**, 159–164 (1961).

265. ATHENS, J. W. *et al.* Leukokinetic studies. IV. The total blood, circulating and marginal granulocyte pools and the granulocyte turnover rate in normal subjects. *J. Clin. Invest.* **40**, 989–995 (1961).

266. Doerschuk, C. M. Mechanisms of leukocyte sequestration in inflamed lungs. *Microcirculation* **8**, 71–88 (2001).

267. Gebb, S. A. *et al.* Sites of leukocyte sequestration in the pulmonary microcirculation. *J. Appl. Physiol.* (1995) doi:10.1152/jappl.1995.79.2.493.

268. Kuebler, W. M., Kuhnle, G. E. H., Groh, J. & Goetz, A. E. Leukocyte kinetics in pulmonary microcirculation: Intravital fluorescence microscopic study. *J. Appl. Physiol.* **76**, 65–71 (1994).

269. Kuebler, W. M., Kuhnle, G. E. H., Groh, J. & Goetz, A. E. Contribution of selectins to leucocyte sequestration in pulmonary microvessels by intravital microscopy in rabbits. *J. Physiol.* **501**,

375–386 (1997).

270. Kubo, H. *et al.* L- and P-selectin and CD11/CD18 in intracapillary neutrophil sequestration in rabbit lungs. *Am. J. Respir. Crit. Care Med.* **159**, 267–274 (1999).

271. Doerschuk, C. M., Tasaka, S. & Wang, Q. CD11/CD18-Dependent and -independent neutrophil emigration in the lungs: How do neutrophils know which route to take? *American Journal of Respiratory Cell and Molecular Biology* vol. 23 133–136 (2000).

272. Ohgami, M., Doerschuk, C. M., Gie, R. P., English, D. & Hogg, J. C. Monocyte kinetics in rabbits. *J. Appl. Physiol.* **70**, 152–157 (1991).

273. Downey, G. P. *et al.* Retention of leukocytes in capillaries: Role of cell size and deformability. *J. Appl. Physiol.* (1990) doi:10.1152/jappl.1990.69.5.1767.

274. Doherty, D. E., Downey, G. P., Schwab, B., Elson, E. & Worthen, G. S. Lipolysaccharide-induced monocyte retention in the lung. Role of monocyte stiffness, actin assembly, and CD18-dependent adherence. *J. Immunol.* **153**, (1994).

275. Ohgami, M., Doerschuk, C. M., Gie, R. P., English, D. & Hogg, J. C. Late effects of endotoxin on the accumulation and function of monocytes in rabbit lungs. *Am. Rev. Respir. Dis.* (1992) doi:10.1164/ajrccm/146.1.190.

276. O'Dea, K. P., Wilson, M. R. & Takata, M. Marginated GR1-High Monocytes Play a Significant Role in Development of Acute Lung Injury With Systemic Septic Stimuli in Mice. in *Proc Am Thorac Soc.* vol. 3 Poster Presentation, ATS annual meeting, San Diego (2006).

277. Granton, E., Kim, J. H., Podstawka, J. & Yipp, B. G. The Lung Microvasculature Is a Functional Immune Niche. *Trends in Immunology* vol. 39 890–899 (2018).

278. Yipp, B. G. *et al.* The lung is a host defense niche for immediate neutrophil-mediated vascular protection. *Sci. Immunol.* **2**, (2017).

279. Grommes, J. & Soehnlein, O. Contribution of neutrophils to acute lung injury. *Mol. Med.* **17**, 293–307 (2011).

280. Ward, P. A. Role of complement, chemokines, and regulatory cytokines in acute lung injury. in *Annals of the New York Academy of Sciences* (1996). doi:10.1111/j.1749-6632.1996.tb32572.x.

281. Guo, R. F. & Ward, P. A. Mediators and regulation of neutrophil accumulation in inflammatory responses in lung: Insights from the IgG immune complex model. *Free Radic. Biol. Med.* (2002) doi:10.1016/S0891-5849(02)00823-7.

282. Guthrie, L. A., McPhail, L. C., Henson, P. M. & Johnston, R. B. Priming of neutrophils for enhanced release of oxygen metabolites by bacterial lipopolysaccharide: Evidence for increased activity of the superoxide-producing enzyme. *J. Exp. Med.* (1984) doi:10.1084/jem.160.6.1656.

283. Ayala, A. *et al.* Shock-induced neutrophil mediated priming for acute lung injury in mice: Divergent effects of TLR-4 and TLR-4/FasL deficiency. *Am. J. Pathol.* (2002) doi:10.1016/S0002-9440(10)64504-X.

284. Singh, N. R. P. *et al.* Acute lung injury results from failure of neutrophil de-priming: A new hypothesis. *European Journal of Clinical Investigation* (2012) doi:10.1111/j.1365-2362.2012.02720.x.

285. Matute-Bello, G., Frevert, C. W. & Martin, T. R. Animal models of acute lung injury. *American Journal of Physiology - Lung Cellular and Molecular Physiology* vol. 295 L379-99 (2008).

286. Maunder, R. J., Hackman, R. C., Riff, E., Albert, R. K. & Springmeyer, S. C. Occurrence of the adult respiratory distress syndrome in neutropenic patients. *Am. Rev. Respir. Dis.* **133**, 313–316 (1986).

287. Ognibene, F. P. *et al.* Adult Respiratory Distress Syndrome in Patients with Severe Neutropenia. *N. Engl. J. Med.* **315**, 547–551 (1986).

288. Laufe, M. D., Simon, R. H., Flint, A. & Keller, J. B. Adult respiratory distress syndrome in neutropenic patients. *Am. J. Med.* **80**, 1022–1026 (1986).

289. Warner, A. E. & Brain, J. D. The cell biology and pathogenic role of pulmonary intravascular macrophages. *American Journal of Physiology - Lung Cellular and Molecular Physiology* vol. 258 (1990).

290. Staub, N. C. Pulmonary intravascular macrophages. *Annual Review of Physiology* vol. 56 47–67 (1994).

291. O'Dea, K. P. *et al.* Lung-marginated monocytes modulate pulmonary microvascular injury during early endotoxemia. *Am. J. Respir. Crit. Care Med.* **172**, 1119–1127 (2005).

292. Charavaryamath, C., Janardhan, K. S., Caldwell, S. & Singh, B. Pulmonary intravascular monocytes/macrophages in a rat model of sepsis. *Anat. Rec. - Part A Discov. Mol. Cell. Evol. Biol.* **288**, 1259–1271 (2006).

293. Warner, A. E. Pulmonary intravascular macrophages: Role in acute lung injury. *Clin. Chest Med.* **17**, 125–135 (1996).

294. Tatham, K. C. *et al.* Intravascular donor monocytes play a central role in lung transplant ischaemia-reperfusion injury. *Thorax* thoraxjnl-2016-208977 (2018) doi:10.1136/thoraxjnl-2016-208977.

295. Wakabayashi, K. *et al.* Volutrauma, but not Atelectrauma, Induces Systemic Cytokine Production by Lung-Marginated Monocytes*. *Crit. Care Med.* **42**, e49–e57 (2014).

296. Dhaliwal, K. *et al.* Monocytes control second-phase neutrophil emigration in established lipopolysaccharide-induced murine lung injury. *Am. J. Respir. Crit. Care Med.* **186**, 514–524 (2012).

297. Wilson, M. R. *et al.* Role of lung-marginated monocytes in an in vivo mouse model of ventilator-induced lung injury. *Am. J. Respir. Crit. Care Med.* **179**, 914–922 (2009).

298. Jiang, Z., Zhou, Q., Gu, C., Li, D. & Zhu, L. Depletion of circulating monocytes suppresses IL-17 and HMGB1 expression in mice with LPS-induced acute lung injury. **312**, (2017).

299. Zheng, Z. *et al.* Donor pulmonary intravascular nonclassical monocytes recruit recipient neutrophils and mediate primary lung allograft dysfunction. *Sci. Transl. Med.* **9**, (2017).

300. Shi, C. S. *et al.* VEGF production by Ly6C+high monocytes contributes to ventilator-induced lung injury. *PLoS One* (2016) doi:10.1371/journal.pone.0165317.

301. Huang, T. H. *et al.* Cyclooxygenase-2 activity regulates recruitment of VEGF-secreting Ly6Chigh monocytes in ventilator-induced lung injury. *Int. J. Mol. Sci.* (2019) doi:10.3390/ijms20071771.

302. Matute-Bello, G. *et al.* An official American Thoracic Society workshop report: features and measurements of experimental acute lung injury in animals. *Am. J. Respir. Cell Mol. Biol.* **44**, 725–738 (2011).

303. Aeffner, F., Bolon, B. & Davis, I. C. Mouse Models of Acute Respiratory Distress Syndrome: A Review of Analytical Approaches, Pathologic Features, and Common Measurements. *Toxicol. Pathol.* (2015) doi:10.1177/0192623315598399.

304. Menezes, S. L. S. *et al.* Pulmonary and extrapulmonary acute lung injury: Inflammatory and ultrastructural analyses. *J. Appl. Physiol.* **98**, 1777–1783 (2005).

305. Bhargava, R. *et al.* Intratracheal IL-6 Protects against Lung Inflammation in Direct, but Not Indirect, Causes of Acute Lung Injury in Mice. *PLoS One* **8**, (2013).

306. Hoegl, S. *et al.* Capturing the multifactorial nature of ARDS – "Two-hit" approach to model murine acute lung injury. *Physiol. Rep.* **6**, (2018).

307. Hepokoski, M. *et al.* Ventilator-induced lung injury increases expression of endothelial inflammatory mediators in the kidney. *Am. J. Physiol. - Ren. Physiol.* **312**, F654–F660 (2017).

308. Broccard, A. F., Vannay, C., Feihl, F. & Schaller, M. D. Impact of low pulmonary vascular

pressure on ventilator-induced lung injury. *Crit. Care Med.* **30**, 2183–2190 (2002).

309. Ermert, L., Duncker, H. R., Rosseau, S., Schutte, H. & Seeger, W. Morphometric analysis of pulmonary intracapillary leukocyte pools in ex vivo-perfused rabbit lungs. *Am. J. Physiol. - Lung Cell. Mol. Physiol.* **267**, (1994).

310. Von Bethmann, A. N. *et al.* Hyperventilation induces release of cytokines from perfused mouse lung. *Am. J. Respir. Crit. Care Med.* **157**, 263–272 (1998).

311. Markovic, N. *et al.* Mediators released from LPS-challenged lungs induce inflammatory responses in liver vascular endothelial cells and neutrophilic leukocytes. *Am. J. Physiol. - Gastrointest. Liver Physiol.* (2009) doi:10.1152/ajpgi.00278.2009.

312. Held, H.-D., Boettcher, S., Hamann, L. & Uhlig, S. Ventilation-induced chemokine and cytokine release is associated with activation of nuclear factor-kappaB and is blocked by steroids. *Am J Respir Crit Care Med Internet* **163**, 711–716 (2001).

313. Zhang, Q., Matsuzaki, I., Chatterjee, S. & Fisher, A. B. Activation of endothelial NADPH oxidase during normoxic lung ischemia is KATP channel dependent. *Am. J. Physiol. - Lung Cell. Mol. Physiol.* **289**, L954–L961 (2005).

314. Yang, Y. *et al.* Platelet-activating factor reduces endothelial nitric oxide production: Role of acid sphingomyelinase. *Eur. Respir. J.* **36**, 417–427 (2010).

315. Waypa, G. B., Vincent, P. A., Morton, C. A. & Minnear, F. L. Thrombin increases fluid flux in isolated rat lungs by a hemodynamic and not a permeability mechanism. *J Appl Physiol* **80**, 1197–1204 (1996).

316. Horgan, M. J., Fenton, J. W. & Malik, A. B. α-Thrombin-induced pulmonary vasoconstriction. *J. Appl. Physiol.* **63**, 1993–2000 (1987).

317. GRIFFITHS, M. J. D. J. D., CURZEN, N. P. P., MITCHELL, J. A. A. & Evans, T. W. W. In vivo treatment with endotoxin increases rat pulmonary vascular contractility despite NOS induction. *Am. J. Respir. Crit. Care Med.* **156**, 654–658 (1997).

318. Niehaus, G. D. & Mehendale, S. R. Quantifying rat pulmonary intravascular mononuclear phagocytes. *Anat. Rec.* **252**, 626–636 (1998).

319. Richter, N., Raddatz, G., Steinhoff, G., Schäfers, H. J. & Schlitt, H. J. Transimission of donor lymphocytes in clinical lung transplantation. *Transpl. Int.* (1994) doi:10.1007/BF00346035.

320. Paantjens, A. W. M. *et al.* Chimerism of dendritic cell subsets in peripheral blood after lung transplantation. *J. Hear. Lung Transplant.* (2011) doi:10.1016/j.healun.2011.01.706.

321. Trams, E. G., Lauter, C. J., Norman Salem, J. & Heine, U. Exfoliation of membrane ecto-enzymes in the form of micro-vesicles. *BBA - Biomembr.* **645**, 63–70 (1981).

322. Raposo, G. & Stoorvogel, W. Extracellular vesicles: Exosomes, microvesicles, and friends. *J. Cell Biol.* **200**, 373–383 (2013).

323. Witwer, K. W. *et al.* Standardization of sample collection, isolation and analysis methods in extracellular vesicle research. *J. Extracell. vesicles* **2**, 1–25 (2013).

324. Cocucci, E. & Meldolesi, J. Ectosomes and exosomes: Shedding the confusion between extracellular vesicles. *Trends in Cell Biology* vol. 25 364–372 (2015).

325. Emanueli, C., Shearn, A. I. U., Angelini, G. D. & Sahoo, S. Exosomes and exosomal miRNAs in cardiovascular protection and repair. *Vascular Pharmacology* vol. 71 24–30 (2015).

326. Oksvold, M. P. *et al.* Expression of B-Cell surface antigens in subpopulations of exosomes released from B-cell lymphoma cells. *Clin. Ther.* **36**, 847-862.e1 (2014).

327. Sahoo, S. *et al.* Exosomes from human CD34+ stem cells mediate their proangiogenic paracrine activity. *Circ. Res.* **109**, 724–728 (2011).

328. Yáñez-Mó, M. *et al.* Biological properties of extracellular vesicles and their physiological functions. *J. Extracell. vesicles* **4**, 27066 (2015).

329. Théry, C. *et al.* Minimal information for studies of extracellular vesicles 2018 (MISEV2018): a position statement of the International Society for Extracellular Vesicles and update of the MISEV2014 guidelines. *J. Extracell. Vesicles* **7**, (2018).

330. Daleke, D. L. Regulation of transbilayer plasma membrane phospholipid asymmetry. *Journal of Lipid Research* (2003) doi:10.1194/jlr.R200019-JLR200.

331. Bevers, E. M., Comfurius, P., Dekkers, D. W. C. & Zwaal, R. F. A. Lipid translocation across the plasma membrane of mammalian cells. *Biochimica et Biophysica Acta - Molecular and Cell Biology of Lipids* (1999) doi:10.1016/S1388-1981(99)00110-9.

332. McVey, M., Tabuchi, A. & Kuebler, W. M. Microparticles and acute lung injury. *Am J Physiol Lung Cell Mol Physiol* **303**, L364-81 (2012).

333. Bevers, E. M. & Williamson, P. L. Getting to the Outer Leaflet: Physiology of Phosphatidylserine Exposure at the Plasma Membrane. *Physiol. Rev.* **96**, 605–645 (2016).

334. Morel, O., Jesel, L., Freyssinet, J. M. & Toti, F. Cellular mechanisms underlying the formation of circulating microparticles. *Arterioscler. Thromb. Vasc. Biol.* **31**, 15–26 (2011).

335. Jeanneteau, J. *et al.* Microparticle release in remote ischemic conditioning mechanism. *Am. J. Physiol. - Hear. Circ. Physiol.* **303**, H871–H877 (2012).

336. Ma, F., Liu, H., Shen, Y., Zhang, Y. & Pan, S. Platelet-derived microvesicles are involved in cardio-protective effects of remote preconditioning. *Int. J. Clin. Exp. Pathol.* **8**, 10832–10839 (2015).

337. Fink, K. *et al.* Circulating annexin V positive microparticles in patients after successful cardiopulmonary resuscitation. *Crit. Care* **15**, R251 (2011).

338. Thiagarajan, P. & Tait, J. F. Collagen-induced exposure of anionic phospholipid in platelets and platelet-derived microparticles. *J. Biol. Chem.* **266**, 24302–24307 (1991).

339. Nomura, S. & Shimizu, M. Clinical significance of procoagulant microparticles. *Journal of Intensive Care* vol. 3 (2015).

340. Tans, G. *et al.* Comparison of anticoagulant and procoagulant activities of stimulated platelets and platelet-derived microparticles. *Blood* **77**, 2641–2648 (1991).

341. VanWijk, M. J., VanBavel, E., Sturk, A. & Nieuwland, R. Microparticles in cardiovascular diseases. *Cardiovascular Research* vol. 59 277–287 (2003).

342. Ayers, L. *et al.* Dynamic microvesicle release and clearance within the cardiovascular system: triggers and mechanisms. *Clin. Sci.* **129**, 915–931 (2015).

343. Perez-Pujol, S., Marker, P. H. & Key, N. S. Platelet microparticles are heterogeneous and highly dependent on the activation mechanism: Studies using a new digital flow cytometer. *Cytom. Part A* **71A**, 38–45 (2007).

344. Latham, S. L. *et al.* Immuno-analysis of microparticles: Probing at the limits of detection. *Sci. Rep.* **5**, 1–13 (2015).

345. Connor, D. E., Exner, T., Ma, D. D. F. & Joseph, J. E. The majority of circulating platelet-derived microparticles fail to bind annexin V, lack phospholipid-dependent procoagulant activity and demonstrate greater expression of glycoprotein Ib. *Thromb. Haemost.* **103**, 1044–1052 (2010).

346. Arraud, N. *et al.* Extracellular vesicles from blood plasma: Determination of their morphology, size, phenotype and concentration. *J. Thromb. Haemost.* **12**, 614–627 (2014).

347. Heijnen, H. F., Schiel, A. E., Fijnheer, R., Geuze, H. J. & Sixma, J. J. Activated platelets release two types of membrane vesicles: microvesicles by surface shedding and exosomes derived from exocytosis of multivesicular bodies and alpha-granules. *Blood* **94**, 3791–9 (1999).

348. Laulagnier, K. *et al.* Mast cell- and dendritic cell-derived display a specific lipid composition and an unusual membrane organization. *Biochem. J.* **380**, 161–171 (2004).

349. Shlomovitz, I., Speir, M. & Gerlic, M. Flipping the dogma - Phosphatidylserine in non-apoptotic cell death. *Cell Communication and Signaling* vol. 17 1–12 (2019).

350. Shlomovitz, I. *et al.* Proteomic analysis of necroptotic extracellular vesicles. *bioRxiv* 2020.04.11.037192 (2020) doi:10.1101/2020.04.11.037192.

351. Zargarian, S. *et al.* Phosphatidylserine externalization, “necroptotic bodies” release, and phagocytosis during necroptosis. *PLoS Biol.* **15**, e2002711 (2017).

352. Zakharova, L., Svetlova, M. & Fomina, A. F. T cell exosomes induce cholesterol accumulation in human monocytes via phosphatidylserine receptor. *J. Cell. Physiol.* **212**, 174–181 (2007).

353. Dey-Hazra, E. *et al.* Detection of circulating microparticles by flow cytometry: Influence of centrifugation, filtration of buffer, and freezing. *Vasc. Health Risk Manag.* **6**, 1125–1133 (2010).

354. Boulanger, C. M., Amabile, N. & Tedgui, A. Circulating microparticles: A potential prognostic marker for atherosclerotic vascular disease. *Hypertension* **48**, 180–186 (2006).

355. Garcia, S. *et al.* Phenotypic assessment of endothelial microparticles in patients with heart failure and after heart transplantation: Switch from cell activation to apoptosis. *J. Hear. Lung Transplant.* (2005) doi:10.1016/j.healun.2005.07.006.

356. Shet, A. S. *et al.* Sickle blood contains tissue factor-positive microparticles derived from endothelial cells and monocytes. *Blood* **102**, 2678–2683 (2003).

357. Teoh, N. C. *et al.* Microparticles mediate hepatic ischemia-reperfusion injury and are the targets of Diannexin (ASP8597). *PLoS One* **9**, 1–13 (2014).

358. De Rond, L. *et al.* Comparison of generic fluorescent markers for detection of extracellular vesicles by flow cytometry. *Clin. Chem.* **64**, 680–689 (2018).

359. ENJETI, A. K., LINCZ, L. & Seldon, M. Bio-maleimide as a generic stain for detection and quantitation of microparticles. *Int. J. Lab. Hematol.* **30**, 196–199 (2008).

360. Takov, K., Yellon, D. M. & Davidson, S. M. Confounding factors in vesicle uptake studies using fluorescent lipophilic membrane dyes. *J. Extracell. Vesicles* **6**, (2017).

361. Furi, I., Momen-Heravi, F. & Szabo, G. Extracellular vesicle isolation: Present and future. *Annals of Translational Medicine* vol. 5 263 (2017).

362. van der Vlist, E. J., Nolte-’t Hoen, E. N. M. M., Stoorvogel, W., Arkesteijn, G. J. A. a & Wauben, M. H. M. M. Fluorescent labeling of nano-sized vesicles released by cells and subsequent quantitative and qualitative analysis by high-resolution flow cytometry. *Nat. Protoc.* **7**, 1311–26 (2012).

363. Cointe, S. *et al.* Standardization of microparticle enumeration across different flow cytometry platforms: results of a multicenter collaborative workshop. *J. Thromb. Haemost.* **15**, 187–193 (2017).

364. Said, A. S., Rogers, S. C. & Doctor, A. Physiologic impact of circulating RBC microparticles upon blood-vascular interactions. *Frontiers in Physiology* vol. 8 1120 (2018).

365. Burger, D. *et al.* Microparticles: biomarkers and beyond. *Clin. Sci.* **124**, 423–441 (2013).

366. González-Cano, P. *et al.* Mycobacterium tuberculosis H37Rv induces ectosome release in human polymorphonuclear neutrophils. *Tuberculosis* **90**, 125–134 (2010).

367. Simoncini, S. *et al.* Trail/Apo2L mediates the release of procoagulant endothelial microparticles induced by thrombin in vitro: a potential mechanism linking inflammation and coagulation. *Circ. Res.* **104**, 943–951 (2009).

368. Terrisse, A. D. *et al.* Internalization of microparticles by endothelial cells promotes platelet/endothelial cell interaction under flow. *J. Thromb. Haemost.* **8**, 2810–2819 (2010).

369. Burger, D. *et al.* Endothelial microparticle formation by angiotensin II is mediated via ang II receptor type I/NADPH Oxidase/rho kinase pathways targeted to lipid rafts. *Arterioscler. Thromb. Vasc. Biol.* **31**, 1898–1907 (2011).

370. Fitzgerald, W. *et al.* A System of Cytokines Encapsulated in ExtraCellular Vesicles. *Sci. Rep.* **8**, (2018).

371. Raeven, P., Zipperle, J. & Drechsler, S. *Extracellular vesicles as markers and mediators in sepsis*. *Theranostics* vol. 8 3348–3365 (2018).

372. Del Conde, I. *et al.* Tissue-factor-bearing microvesicles arise from lipid rafts and fuse with activated platelets to initiate coagulation. *Blood* **106**, 1604–1611 (2005).

373. Wang, J. G. *et al.* Monocytic microparticles activate endothelial cells in an IL-1β-dependent manner. *Blood* **118**, 2366–2374 (2011).

374. Milbank, E. *et al.* Microparticles from apoptotic RAW 264.7 macrophage cells carry tumour necrosis factor-α functionally active on cardiomyocytes from adult mice. *J. Extracell. Vesicles* (2015) doi:10.3402/jev.v4.28621.

375. Soni, S. *et al.* ATP redirects cytokine trafficking and promotes novel membrane TNF signaling *via* microvesicles. *FASEB J.* **33**, 6442–6455 (2019).

376. Soni, S. *et al.* Alveolar macrophage-derived microvesicles mediate acute lung injury. *Thorax* **71**, 1020–1029 (2016).

377. Danesh, A. *et al.* Granulocyte-derived extracellular vesicles activate monocytes and are associated with mortality in intensive care unit patients. *Front. Immunol.* **9**, (2018).

378. Gasser, O. *et al.* Characterisation and properties of ectosomes released by human polymorphonuclear neutrophils. *Exp. Cell Res.* **285**, 243–257 (2003).

379. Hess, C. *et al.* Ectosomes released by human neutrophils are specialized functional units. *J. Immunol.* **163**, 4564–4573 (1999).

380. Dalli, J. *et al.* Heterogeneity in neutrophil microparticles reveals distinct proteome and functional properties. *Mol. Cell. Proteomics* **12**, 2205–19 (2013).

381. Slater, T. W. *et al.* Neutrophil Microparticles Deliver Active Myeloperoxidase to Injured Mucosa To Inhibit Epithelial Wound Healing. *J. Immunol.* **198**, 2886–2897 (2017).

382. Wang, Y. *et al.* Platelet-derived microparticles regulates thrombin generation via phophatidylserine in abdominal sepsis. *J. Cell. Physiol.* **233**, 1051–1060 (2018).

383. Wang, Y., Luo, L., Mörgelin, M. & Thorlacius, H. Rac1 regulates sepsis-induced formation of platelet-derived microparticles and thrombin generation. *Biochem. Biophys. Res. Commun.* **487**, 887–891 (2017).

384. Pasquet, J. M., Toti, F., Nurden, A. T. & Dachary-Prigent, J. Procoagulant activity and active calpain in platelet-derived microparticles. *Thromb. Res.* (1996) doi:10.1016/0049-3848(96)00101-6.

385. Morel, N. *et al.* Generation of procoagulant microparticles in cerebrospinal fluid and peripheral blood after traumatic brain injury. *J Trauma* **64**, 698–704 (2008).

386. Morel, O., Morel, N., Freyssinet, J.-M. & Toti, F. Platelet microparticles and vascular cells interactions: a checkpoint between the haemostatic and thrombotic responses. *Platelets* **19**, 9–23 (2008).

387. Bernal-Mizrachi, L. *et al.* High levels of circulating endothelial microparticles in patients with acute coronary syndromes. *Am. Heart J.* **145**, 962–970 (2003).

388. Jimenez, J. J. *et al.* Endothelial microparticles released in thrombotic thrombocytopenic purpura express von Willebrand factor and markers of endothelial activation. *Br. J. Haematol.* **123**, 896–902 (2003).

389. Taraboletti, G. *et al.* Shedding of the matrix metalloproteinases MMP-2, MMP-9, and MT1-MMP as membrane vesicle-associated components by endothelial cells. *Am. J. Pathol.* **160**, 673–80 (2002).

390. Pérez-Casal, M., Downey, C., Fukudome, K., Marx, G. & Toh, C. H. Activated protein C induces the release of microparticle-associated endothelial protein C receptor. *Blood* **105**, 1515–1522 (2005).

391. Zecher, D., Cumpelik, A. & Schifferli, J. A. Erythrocyte-derived microvesicles amplify systemic

inflammation by thrombin-dependent activation of complement. *Arterioscler. Thromb. Vasc. Biol.* **34**, 313–320 (2014).

392. Hashemi Tayer, A. *et al.* Procoagulant Activity of Red Blood Cell-Derived Microvesicles during Red Cell Storage. *Transfus. Med. Hemotherapy* **46**, 224–230 (2019).

393. Russell, A. E. *et al.* Biological membranes in EV biogenesis, stability, uptake, and cargo transfer: an ISEV position paper arising from the ISEV membranes and EVs workshop. in *Journal of Extracellular Vesicles* vol. 8 1684862 (Taylor and Francis Ltd., 2019).

394. Mulcahy, L. A., Pink, R. C. & Carter, D. R. F. Routes and mechanisms of extracellular vesicle uptake. *J. Extracell. Vesicles* **3**, 1–14 (2014).

395. Parolini, I. *et al.* Microenvironmental pH is a key factor for exosome traffic in tumor cells. *J. Biol. Chem.* **284**, 34211–34222 (2009).

396. Margolis, L. & Sadovsky, Y. The biology of extracellular vesicles: The known unknowns. *PLoS Biol.* **17**, e3000363 (2019).

397. Willekens, F. L. A. A. *et al.* Liver Kupffer cells rapidly remove red blood cell-derived vesicles from the circulation by scavenger receptors. *Blood* **105**, 2141–2145 (2005).

398. Dasgupta, S. K., Le, A., Chavakis, T., Rumbaut, R. E. & Thiagarajan, P. Developmental endothelial locus-1 (del-1) mediates clearance of platelet microparticles by the endothelium. *Circulation* **125**, 1664–1672 (2012).

399. Al Faraj, A. *et al.* Endothelial Cell–derived Microparticles Loaded with Iron Oxide Nanoparticles: Feasibility of MR Imaging Monitoring in Mice. *Radiology* **263**, 169–178 (2012).

400. Rand, M. L., Wang, H., Bang, K. W. A., Packham, M. A. & Freedman, J. Rapid clearance of procoagulant platelet-derived microparticles from the circulation of rabbits [3]. *Journal of Thrombosis and Haemostasis* vol. 4 1621–1623 (2006).

401. Yi, Y. W. *et al.* Advances in analysis of biodistribution of exosomes by molecular imaging. *International Journal of Molecular Sciences* vol. 21 (2020).

402. Gangadaran, P., Hong, C. M. & Ahn, B. C. An update on in vivo imaging of extracellular vesicles as drug delivery vehicles. *Frontiers in Pharmacology* (2018) doi:10.3389/fphar.2018.00169.

403. Smyth, T. *et al.* Biodistribution and delivery efficiency of unmodified tumor-derived exosomes. *J. Control. Release* **199**, 145–155 (2015).

404. Ohno, S. *et al.* Systemically Injected Exosomes Targeted to EGFR Deliver Antitumor MicroRNA to Breast Cancer Cells. *Mol. Ther.* **21**, 185–191 (2012).

405. Tian, Y. *et al.* A doxorubicin delivery platform using engineered natural membrane vesicle exosomes for targeted tumor therapy. *Biomaterials* **35**, 2383–2390 (2014).

406. Grange, C. *et al.* Biodistribution of mesenchymal stem cell-derived extracellular vesicles in a model of acute kidney injury monitored by optical imaging. *Int. J. Mol. Med.* **33**, 1055–1063 (2014).

407. Herrera, M. B. B. *et al.* Exogenous mesenchymal stem cells localize to the kidney by means of CD44 following acute tubular injury. *Kidney Int.* **72**, 430–441 (2007).

408. Camussi, G., Deregibus, M. C. C. & Cantaluppi, V. Role of stem-cell-derived microvesicles in the paracrine action of stem cells. *Biochem. Soc. Trans.* **41**, 283–287 (2013).

409. Gatti, S. *et al.* Microvesicles derived from human adult mesenchymal stem cells protect against ischaemia-reperfusion-induced acute and chronic kidney injury. *Nephrol. Dial. Transplant.* **26**, 1474–1483 (2011).

410. Bruno, S. *et al.* Microvesicles derived from mesenchymal stem cells enhance survival in a lethal model of acute kidney injury. *PLoS One* **7**, e33115 (2012).

411. Balachandran, B. & Yuana, Y. Extracellular vesicles-based drug delivery system for cancer treatment. *Cogent Med.* **6**, (2019).

412. Schneberger, D., Aharonson-Raz, K. & Singh, B. Pulmonary intravascular macrophages and lung health: What are we missing? *AJP Lung Cell. Mol. Physiol.* **302**, L498–L503 (2012).

413. Ravichandran, K. S. & Lorenz, U. Engulfment of apoptotic cells: signals for a good meal. *Nat. Rev. Immunol.* **7**, 964–974 (2007).

414. Flannagan, R. S., Canton, J., Furuya, W., Glogauer, M. & Grinstein, S. The phosphatidylserine receptor TIM4 utilizes integrins as coreceptors to effect phagocytosis. *Mol. Biol. Cell* **25**, 1511–1522 (2014).

415. Buzás, E. I., Tóth, E., Sódar, B. W. & Szabó-Taylor, K. Molecular interactions at the surface of extracellular vesicles. *Seminars in Immunopathology* vol. 40 453–464 (2018).

416. Dasgupta, S. K. *et al.* Lactadherin and clearance of platelet-derived microvesicles. *Blood* **113**, 1332–1339 (2009).

417. Wu, Y., Tibrewal, N. & Birge, R. B. Phosphatidylserine recognition by phagocytes: a view to a kill. *Trends Cell Biol.* **16**, 189–197 (2006).

418. Véron, P. *et al.* Accumulation of MFG-E8/lactadherin on exosomes from immature dendritic cells. *Blood Cells, Mol. Dis.* **35**, 81–88 (2005).

419. Fitzner, D. *et al.* Selective transfer of exosomes from oligodendrocytes to microglia by macropinocytosis. *J. Cell Sci.* **124**, 447–458 (2011).

420. Nieuwland, R. *et al.* Cellular origin and procoagulant properties of microparticles in meningococcal sepsis. *Blood* **95**, 930–935 (2000).

421. Joop, K. *et al.* Microparticles from patients with multiple organ dysfunction syndrome and sepsis support coagulation through multiple mechanisms. *Thromb. Haemost.* **85**, 810–820 (2001).

422. Larsson, A., Lundahl, T., Eriksson, M., Lundkvist, K. & Lindahl, T. Endotoxin induced platelet microvesicle formation measured by flow cytometry. *Platelets* **7**, 153–158 (1996).

423. Lundahl, T. H. *et al.* Activated platelets and impaired platelet function in intensive care patients analyzed by flow cytometry. in *Blood Coagulation and Fibrinolysis* vol. 7 218–220 (Lippincott Williams and Wilkins, 1996).

424. Ogura, H. *et al.* Activated platelets enhance microparticle formation and platelet-leukocyte interaction in severe trauma and sepsis. *J. Trauma* **50**, 801–9 (2001).

425. Matsumoto, H. *et al.* CLINICAL SIGNIFICANCE of TISSUE FACTOR and CD13 DOUBLEPOSITIVE MICROPARTICLES in SIRS PATIENTS with TRAUMA and SEVERE SEPSIS. *Shock* **47**, 409–415 (2017).

426. Huisse, M. G. *et al.* Leukocyte activation: The link between inflammation and coagulation during heatstroke. A study of patients during the 2003 heat wave in Paris. *Crit. Care Med.* **36**, 2288–2295 (2008).

427. O'Dea, K. P. *et al.* Circulating microvesicles are elevated acutely following major burns injury and associated with clinical severity. *PLoS One* **11**, 1–17 (2016).

428. Fujimi, S. *et al.* Increased production of leukocyte microparticles with enhanced expression of adhesion molecules from activated polymorphonuclear leukocytes in severely injured patients. *J Trauma* **54**, 114–120 (2003).

429. Mostefai, H. A. *et al.* Circulating microparticles from patients with septic shock exert protective role in vascular function. *Am. J. Respir. Crit. Care Med.* **178**, 1148–1155 (2008).

430. Lehner, G. F. *et al.* Characterization of microvesicles in septic shock using high-sensitivity flow cytometry. *Shock* **46**, 373–381 (2016).

431. Takei, Y. *et al.* Increase in circulating ACE-positive endothelial microparticles during acute lung injury. *Eur. Respir. J.* **54**, 1801188 (2019).

432. Zhang, Y. *et al.* Circulating Microparticles, Blood Cells, and Endothelium Induce Procoagulant Activity in Sepsis Through Phosphatidylserine Exposure. *Shock* **45**, 299–307 (2016).

433. Shaver, C. M. *et al.* Circulating microparticle levels are reduced in patients with ARDS. *Crit. Care* **21**, 120 (2017).

434. Trepesch, C. *et al.* High intravascular tissue factor-but not extracellular microvesicles-in septic patients is associated with a high SAPS II score. *J. Intensive Care* (2016) doi:10.1186/s40560-016-0160-5.

435. Guervilly, C. *et al.* High levels of circulating leukocyte microparticles are associated with better outcome in acute respiratory distress syndrome. *Crit. Care* **15**, R31 (2011).

436. Soriano, A. O. *et al.* Levels of endothelial and platelet microparticles and their interactions with leukocytes negatively correlate with organ dysfunction and predict mortality in severe sepsis. *Crit Care Med* **33**, 2540–2546 (2005).

437. Curry, N., Raja, A., Beavis, J., Stanworth, S. & Harrison, P. Levels of procoagulant microvesicles are elevated after traumatic injury and platelet microvesicles are negatively correlated with mortality. *J. Extracell. Vesicles* **3**, (2014).

438. Aras, O. *et al.* Induction of microparticle- and cell-associated intravascular tissue factor in human endotoxemia. *Blood* **103**, 4545–4553 (2004).

439. Azevedo, L. C. P. *et al.* Platelet-derived exosomes from septic shock patients induce myocardial dysfunction. *Crit. Care* **11**, R120 (2007).

440. Mortaza, S. *et al.* Detrimental hemodynamic and inflammatory effects of microparticles originating from septic rats. *Crit. Care Med.* **37**, 2045–50 (2009).

441. Li, H., Meng, X., Liang, X., Gao, Y. & Cai, S. Administration of microparticles from blood of the lipopolysaccharide-treated rats serves to induce pathologic changes of acute respiratory distress syndrome. *Exp. Biol. Med.* (2015) doi:10.1177/1535370215591830.

442. Belizaire, R. M. *et al.* Microparticles from stored red blood cells activate neutrophils and cause lung injury after hemorrhage and resuscitation. *J. Am. Coll. Surg.* **214**, 648–655 (2012).

443. Buesing, K. L. *et al.* Endothelial microparticles induce inflammation in acute lung injury. *J. Surg. Res.* **166**, 32–39 (2011).

444. Densmore, J. C. *et al.* Endothelium-derived microparticles induce endothelial dysfunction and acute lung injury. *Shock* **26**, 464–471 (2006).

445. Bloch, K. D., Takata, M., Ph, D., Steudel, W. & Zapol, W. M. Congenital NOS2 Deficiency Protects Mice from LPS- induced Hyporesponsiveness to Inhaled Nitric Oxide. 1744–1753 (1999).

446. Yoo, H. Y. *et al.* Optimization of isolated perfused/ventilated mouse lung to study hypoxic pulmonary vasoconstriction. *Pulm. Circ.* **3**, 396–405 (2013).

447. Waymouth, C. Osmolality of mammalian blood and of media for culture of mammalian cells. *In Vitro* **6**, 109–127 (1970).

448. Bailey, L. E. & Ong, S. D. Krebs-Henseleit solution as a physiological buffer in perfused and superfused preparations. *J. Pharmacol. Methods* **1**, 171–175 (1978).

449. Thomas, L. M. & Salter, R. D. Activation of macrophages by P2X7-induced microvesicles from myeloid cells is mediated by phospholipids and is partially dependent on TLR4. *J. Immunol.* **185**, 3740–9 (2010).

450. O'Dea, K. P., Dokpesi, J. O., Tatham, K. C., Wilson, M. R. & Takata, M. Regulation of monocyte subset proinflammatory responses within the lung microvasculature by the p38 MAPK/MK2 pathway. *AJP Lung Cell. Mol. Physiol.* **301**, L812-21 (2011).

451. Wiklander, O. P. B. B. *et al.* Extracellular vesicle in vivo biodistribution is determined by cell source, route of administration and targeting. *J. Extracell. Vesicles* **4**, 1–13 (2015).

452. Augustine, D. *et al.* Dynamic release and clearance of circulating microparticles during cardiac stress. *Circ. Res.* **114**, 109–113 (2014).

453. Lai, C. P. *et al.* Dynamic biodistribution of extracellular vesicles in vivo using a multimodal

imaging reporter. *ACS Nano* **8**, 483–494 (2014).

454. Takahashi, Y. *et al.* Visualization and in vivo tracking of the exosomes of murine melanoma B16-BL6 cells in mice after intravenous injection. *J. Biotechnol.* **165**, 77–84 (2013).

455. Jang, S. C. *et al.* In vivo kinetic biodistribution of nano-sized outer membrane vesicles derived from bacteria. *Small* **11**, 456–461 (2015).

456. Bruno, S. *et al.* Mesenchymal Stem Cell-Derived Microvesicles Protect Against Acute Tubular Injury. *J Am Soc Nephrol* **20**, 1053–1067 (2009).

457. Warner, A. E., Molina, R. M., Bellows, C. E. & Brain, J. D. Endotoxemia enhances pulmonary mononuclear cell uptake of circulating particles and pathogens in a species without pulmonary intravascular macrophages. in *Chest* vol. 105 50S-51S (American College of Chest Physicians, 1994).

458. Crescitelli, R. *et al.* Distinct RNA profiles in subpopulations of extracellular vesicles: Apoptotic bodies, microvesicles and exosomes. *J. Extracell. Vesicles* (2013) doi:10.3402/jev.v2i0.20677.

459. Faille, D. *et al.* Endocytosis and intracellular processing of platelet microparticles by brain endothelial cells. *J. Cell. Mol. Med.* **16**, 1731–1738 (2012).

460. Czernek, L., Chworos, A. & Duechler, M. The Uptake of Extracellular Vesicles is Affected by the Differentiation Status of Myeloid Cells. *Scand. J. Immunol.* **82**, 506–514 (2015).

461. Feng, D. *et al.* Cellular internalization of exosomes occurs through phagocytosis. *Traffic* **11**, 675–687 (2010).

462. Morelli, A. E. *et al.* Endocytosis, intracellular sorting, and processing of exosomes by dendritic cells. *Blood* **104**, 3257–3266 (2004).

463. Montecalvo, A. *et al.* Mechanism of transfer of functional microRNAs between mouse dendritic cells via exosomes. *Blood* **119**, 756–766 (2012).

464. Ishii, M. *et al.* Energy-dependent endocytosis is involved in the absorption of indomethacin nanoparticles in the small intestine. *Int. J. Mol. Sci.* **20**, (2019).

465. Obregon, C., Rothen-Rutishauser, B., Gerber, P., Gehr, P. & Nicod, L. P. Active Uptake of Dendritic Cell-Derived Exovesicles by Epithelial Cells Induces the Release of Inflammatory Mediators through a TNF-α-Mediated Pathway. *Am. J. Pathol.* **175**, 696–705 (2009).

466. Patiño, T., Soriano, J., Barrios, L., Ibáñez, E. & Nogués, C. Surface modification of microparticles causes differential uptake responses in normal and tumoral human breast epithelial cells. *Sci. Rep.* **5**, 11371 (2015).

467. Falati, S. *et al.* Accumulation of tissue factor into developing thrombi in vivo is dependent upon microparticle P-selectin glycoprotein ligand 1 and platelet P-selectin. *J. Exp. Med.* **197**, 1585–1598 (2003).

468. Qu, Y. & Dubyak, G. R. P2X7 receptors regulate multiple types of membrane trafficking responses and non-classical secretion pathways. *Purinergic Signal.* **5**, 163–173 (2009).

469. MacKenzie, A. *et al.* Rapid secretion of interleukin-1β by microvesicle shedding. *Immunity* **15**, 825–835 (2001).

470. Qiu, Q., Xiong, W., Yang, C., Gagnon, C. & Hardy, P. Lymphocyte-derived microparticles induce bronchial epithelial cells' pro-inflammatory cytokine production and apoptosis. *Mol. Immunol.* **55**, 220–230 (2013).

471. Bastos-Amador, P. *et al.* Capture of cell-derived microvesicles (exosomes and apoptotic bodies) by human plasmacytoid dendritic cells. *J. Leukoc. Biol.* **91**, 751–758 (2012).

472. Wang, F. *et al.* The biomolecular corona is retained during nanoparticle uptake and protects the cells from the damage induced by cationic nanoparticles until degraded in the lysosomes. *Nanomedicine Nanotechnology, Biol. Med.* **9**, 1159–1168 (2013).

473. Yan, Y. *et al.* Differential roles of the protein corona in the cellular uptake of nanoporous polymer particles by monocyte and macrophage cell lines. *ACS Nano* **7**, 10960–10970 (2013).

474. Arrighetti, N. *et al.* Exosome-like Nanovectors for Drug Delivery in Cancer. *Curr. Med. Chem.* **26**, 6132–6148 (2018).

475. Köppler, B., Cohen, C., Schlöndorff, D. & Mack, M. Differential mechanisms of microparticle transfer to B cells and monocytes: Anti-inflammatory properties of microparticles. *Eur. J. Immunol.* **36**, 648–660 (2006).

476. B??ttcher, A. *et al.* Involvement of phosphatidylserine, ??v??3, CD14, CD36, and complement C1q in the phagocytosis of primary necrotic lymphocytes by macrophages. *Arthritis Rheum.* **54**, 927–938 (2006).

477. Oshima, K., Aoki, N., Kato, T., Kitajima, K. & Matsuda, T. Secretion of a peripheral membrane protein, MFG-E8, as a complex with membrane vesicles: A possible role in membrane secretion. *Eur. J. Biochem.* **269**, 1209–1218 (2002).

478. Hanayama, R. *et al.* Identification of a factor that links apoptotic cells to phagocytes. *Nature* **417**, 182–187 (2002).

479. Rautou, P. E. & MacKman, N. Del-etion of microvesicles from the circulation. *Circulation* **125**, 1601–1604 (2012).

480. Hanayama, R., Tanaka, M., Miwa, K. & Nagata, S. Expression of Developmental Endothelial Locus-1 in a Subset of Macrophages for Engulfment of Apoptotic Cells. *J. Immunol.* **172**, 3876–3882 (2004).

481. Ghosh, A. *et al.* Platelet CD36 mediates interactions with endothelial cell-derived microparticles and contributes to thrombosis in mice. *J. Clin. Invest.* **118**, 1934–1943 (2008).

482. Getts, D. R. *et al.* Therapeutic Inflammatory Monocyte Modulation Using Immune-Modifying Microparticles. *Sci. Transl. Med.* **6**, 219ra7-219ra7 (2014).

483. Danesh, A. *et al.* Exosomes from RBC units bind to monocytes and induce pro-inflammatory cytokines, boosting T cell responses in vitro. *Blood* **123**, 687–696 (2013).

484. Ismail, N. *et al.* Macrophage microvesicles induce macrophage differentiation and miR-223 transfer. *Blood* **121**, 984–995 (2013).

485. Bardelli, C. *et al.* Autocrine activation of human monocyte/macrophages by monocyte-derived microparticles and modulation by PPAR?? ligands. *Br. J. Pharmacol.* **165**, 716–728 (2012).

486. Chertow, G. M., Christiansen, C. L., Cleary, P. D., Munro, C. & Lazarus, J. M. Prognostic Stratification in Critically Ill Patients With Acute Renal Failure Requiring Dialysis. *Arch. Intern. Med.* **155**, 1505–1511 (1995).

487. Doi, K. & Rabb, H. Impact of acute kidney injury on distant organ function: Recent findings and potential therapeutic targets. *Kidney International* vol. 89 555–564 (2016).

488. Sureka, B., Bansal, K. & Arora, A. Pulmonary edema − cardiogenic or noncardiogenic? *J. Fam. Med. Prim. Care* **4**, 290 (2015).

489. Grams, M. E. & Rabb, H. The distant organ effects of acute kidney injury. *Kidney Int.* **81**, 942–948 (2012).

490. Faubel, S. & Edelstein, C. L. Mechanisms and mediators of lung injury after acute kidney injury. *Nat. Rev. Nephrol.* **12**, 48–60 (2016).

491. Zhao, H. *et al.* Necroptosis and parthanatos are involved in remote lung injury after receiving ischemic renal allografts in rats. *Kidney Int.* **87**, 738–748 (2015).

492. Daemen, M. A. R. C., De Vries, B., Van't Veer, C., Wolfs, T. G. A. M. & Buurman, W. A. Apoptosis and chemokine induction after renal ischemia-reperfusion. *Transplantation* **71**, 1007–1011 (2001).

493. White, L. E., Santora, R. J., Cui, Y., Moore, F. A. & Hassoun, H. T. TNFR1-dependent pulmonary apoptosis during ischemic acute kidney injury. *Am. J. Physiol. - Lung Cell. Mol. Physiol.* **303**, L449 (2012).

494. Feltes, C. M., Hassoun, H. T., Lie, M. L., Cheadle, C. & Rabb, H. Pulmonary endothelial cell

activation during experimental acute kidney injury. *Shock* **36**, 170–6 (2011).

495. Deng, J., Hu, X., Yuen, P. S. T. T. & Star, R. A. Alpha-melanocyte-stimulating hormone inhibits lung injury after renal ischemia/reperfusion. *Am. J. Respir. Crit. Care Med.* **169**, 749–756 (2004).

496. Hassoun, H. T. *et al.* Ischemic acute kidney injury induces a distant organ functional and genomic response distinguishable from bilateral nephrectomy. *Am J Physiol Ren. Physiol* **293**, F30-40 (2007).

497. Hassoun, H. T. *et al.* Kidney ischemia-reperfusion injury induces caspase-dependent pulmonary apoptosis. *Am. J. Physiol. - Ren. Physiol.* **297**, F125 (2009).

498. Karimi, Z. *et al.* Renal ischemia/reperfusion against nephrectomy for induction of acute lung injury in rats. *Ren. Fail.* **38**, 1503–1515 (2016).

499. Colletti, L. M. *et al.* Chemokine expression during hepatic ischemia/reperfusion-induced lung injury in the rat: The role of epithelial neutrophil activating protein. *J. Clin. Invest.* **95**, 134–141 (1995).

500. Caty, M. G., Guice, K. S., Oldham, K. T., Remick, D. G. & Kunkel, S. I. Evidence for tumor necrosis factor-induced pulmonary microvascular injury after intestinal ischemia-reperfusion injury. *Ann. Surg.* **212**, 694–700 (1990).

501. Dwivedi, A. J. *et al.* Adrenomedullin and Adrenomedullin Binding Protein-1 Prevent Acute Lung Injury after Gut Ischemia-Reperfusion. *J. Am. Coll. Surg.* **205**, 284–293 (2007).

502. Seekamp, A. *et al.* Role of β2 integrins and ICAM-1 in lung injury following ischemia-reperfusion of rat hind limbs. *Am. J. Pathol.* (1993).

503. Faure, V. *et al.* Elevation of circulating endothelial microparticles in patients with chronic renal failure. *J. Thromb. Haemost.* **4**, 566–573 (2006).

504. Amabile, N. *et al.* Circulating endothelial microparticles are associated with vascular dysfunction in patients with end-stage renal failure. *J. Am. Soc. Nephrol.* **16**, 3381–3388 (2005).

505. Freeman, C. M. *et al.* Characterization of microparticles after hepatic ischemia-reperfusion injury. *PLoS One* **9**, (2014).

506. Choi, H. Y. *et al.* Microparticles from kidney-derived mesenchymal stem cells act as carriers of proangiogenic signals and contribute to recovery from acute kidney injury. *PLoS One* **9**, (2014).

507. Bitzer, M., Ben-Dov, I. Z. & Thum, T. Microparticles and microRNAs of endothelial progenitor cells ameliorate acute kidney injury. *Kidney International* vol. 82 375–377 (2012).

508. Ranghino, A. *et al.* The effects of glomerular and tubular renal progenitors and derived extracellular vesicles on recovery from acute kidney injury. *Stem Cell Res. Ther.* **8**, 1–15 (2017).

509. Dominguez, J. M., Dominguez, J. H., Xie, D. & Kelly, K. J. Human extracellular microvesicles from renal tubules reverse kidney ischemia-reperfusion injury in rats. *PLoS One* **13**, e0202550 (2019).

510. Awad, A. S. *et al.* Compartmentalization of neutrophils in the kidney and lung following acute ischemic kidney injury. *Kidney Int.* **75**, 689–98 (2009).

511. Hoke, T. S. *et al.* Acute Renal Failure after Bilateral Nephrectomy Is Associated with Cytokine-Mediated Pulmonary Injury. *J. Am. Soc. Nephrol.* **18**, 155–164 (2007).

512. Klein, C. L. *et al.* Interleukin-6 mediates lung injury following ischemic acute kidney injury or bilateral nephrectomy. *Kidney Int.* **74**, 901–909 (2008).

513. White, L. E., Cui, Y., Shelak, C. M. F. F., Lie, M. L. & Hassoun, H. T. Lung endothelial cell apoptosis during ischemic acute kidney injury. *Shock* **38**, 320–327 (2012).

514. Remick, D. G. & Ward, P. A. Evaluation of endotoxin models for the study of sepsis. *Shock* vol. 24 7–11 (2005).

515. Moldawer, L., Manohar, P., Bolgos, G., Rodriguez, J. & Wollenberg, G. Blockade of tumor necrosis factor reduces lipopolysaccharide lethality, but not the lethality of cecal ligation and puncture. *Shock* **4**, 89–95 (1995).

516. Johnson, B. L., Iii, Kuethe, J. W. & Caldwell, C. C. Neutrophil derived microvesicles: emerging role of a key mediator to the immune response. *Endocr. Metab. Immune Disord. Drug Targets* **14**, 210–7 (2014).

517. Zafrani, L. *et al.* Calpastatin controls polymicrobial sepsis by limiting procoagulant microparticle release. *Am. J. Respir. Crit. Care Med.* **185**, 744–755 (2012).

518. Herrmann, I. K. *et al.* Differentiating sepsis from non-infectious systemic inflammation based on microvesicle-bacteria aggregation. *Nanoscale* **7**, 13511–20 (2015).

519. Xu, J. *et al.* Circulating Plasma Extracellular Vesicles from Septic Mice Induce Inflammation via MicroRNA- and TLR7-Dependent Mechanisms. *J. Immunol.* **201**, 3392–3400 (2018).

520. Wang, J. G., Manly, D., Kirchhofer, D., Pawlinski, R. & Mackman, N. Levels of microparticle tissue factor activity correlate with coagulation activation in endotoxemic mice. *J. Thromb. Haemost.* **7**, 1092–1098 (2009).

521. Zubairova, L. D., Zubairov, D. M., Andrushko, I. A., Svintenok, G. Y. & Mustafin, I. G. Cell microvesicles during experimental endotoxemia. *Bull. Exp. Biol. Med.* **142**, 573–576 (2006).

522. Eriksson, M., Nelson, D., Nordgren, A. & Larsson, A. Increased platelet microvesicle formation is associated with mortality in a porcine model of endotoxemia. *Acta Anaesthesiol. Scand.* **42**, 551–557 (1998).

523. Lorincz, A. M. *et al.* Functionally and morphologically distinct populations of extracellular vesicles produced by human neutrophilic granulocytes. *J. Leukoc. Biol.* **98**, 583–589 (2015).

524. Rabb, H. *et al.* Acute renal failure leads to dysregulation of lung salt and water channels. *Kidney Int.* **63**, 600–606 (2003).

525. Kramer, A. A. *et al.* Renal ischemia/reperfusion leads to macrophage-mediated increase in pulmonary vascular permeability. *Kidney Int.* **55**, 2362–2367 (1999).

526. Doi, K. *et al.* The high-mobility group protein B1-Toll-like receptor 4 pathway contributes to the acute lung injury induced by bilateral nephrectomy. *Kidney Int.* **86**, 316–326 (2014).

527. Periard, D. *et al.* Are circulating endothelial-derived and platelet-derived microparticles a pathogenic factor in the cisplatin-induced stroke? *Stroke* **38**, 1636–1638 (2007).

528. Mehta, R. L. *et al.* Sepsis as a cause and consequence of acute kidney injury: Program to Improve Care in Acute Renal Disease. *Intensive Care Med.* **37**, 241–248 (2011).

529. Basu, R. K., Donaworth, E., Wheeler, D. S., Devarajan, P. & Wong, H. R. Antecedent acute kidney injury worsens subsequent endotoxin-induced lung inflammation in a two-hit mouse model. *Am. J. Physiol. Renal Physiol.* **301**, F597-604 (2011).

530. Mörtberg, J. *et al.* Increased concentrations of platelet- and endothelial-derived microparticles in patients with myocardial infarction and reduced renal function- a descriptive study. *BMC Nephrol.* **20**, 1–9 (2019).

531. Chen, Y. L. *et al.* Levels of circulating microparticles in patients with chronic cardiorenal disease. *J. Atheroscler. Thromb.* **22**, 247–256 (2015).

532. Hartopo, A. B., Puspitawati, I., Gharini, P. P. R. & Setianto, B. Y. Platelet microparticle number is associated with the extent of myocardial damage in acute myocardial infarction. *Arch. Med. Sci.* **12**, 529–537 (2016).

533. Kvietys, P. R. & Granger, D. N. Role of reactive oxygen and nitrogen species in the vascular responses to inflammation. *Free Radical Biology and Medicine* vol. 52 556–592 (2012).

534. Kristiansen, S. B. *et al.* Role of pannexin and adenosine triphosphate (ATP) following myocardial ischemia/reperfusion. *Scand. Cardiovasc. J.* **52**, 340–343 (2018).

535. Donnahoo, K. K. *et al.* Early kidney TNF-α expression mediates neutrophil infiltration and injury

after renal ischemia-reperfusion. *Am. J. Physiol. - Regul. Integr. Comp. Physiol.* **277**, (1999).

536. de Vries, B. *et al.* Complement Factor C5a Mediates Renal Ischemia-Reperfusion Injury Independent from Neutrophils. *J. Immunol.* **170**, 3883–3889 (2003).

537. Dai, Y. *et al.* MiR-146a is essential for lipopolysaccharide (LPS)-induced cross-tolerance against kidney ischemia/reperfusion injury in mice. *Sci. Rep.* **6**, (2016).

538. Heemann, U. *et al.* Lipopolysaccharide pretreatment protects from renal ischemia/reperfusion injury: Possible connection to an interleukin-6-dependent pathway. *Am. J. Pathol.* **156**, 287–293 (2000).

539. Godet, C. *et al.* Endotoxin tolerance enhances interleukin-10 renal expression and decreases ischemia-reperfusion renal injury in rats. *Shock* **25**, 384–388 (2006).

540. Colletti, L. M., Remick, D. G. & Campbell, D. A. LPS Pretreatment Protects from Hepatic Ischemia/Reperfusion. *J. Surg. Res.* **57**, 337–343 (1994).

541. Eising, G. P., Mao, L., Schmid-Schonbein, G. W., Engler, R. L. & Ross, J. Effects of induced tolerance to bacterial lipopolysaccharide on myocardial infarct size in rats. *Cardiovasc. Res.* **31**, 73–81 (1996).

542. Ackermann, M. *et al.* Cytokine synthesis in the liver of endotoxin-tolerant and normal rats during hemorrhagic shock. *J. Endotoxin Res.* **7**, 105–112 (2001).

543. del Fresno, C. *et al.* Inflammatory responses associated with acute coronary syndrome up-regulate IRAK-M and induce endotoxin tolerance in circulating monocytes. *J. Endotoxin Res.* **13**, 39–52 (2007).

544. del Fresno, C. *et al.* Monocytes from cystic fibrosis patients are locked in an LPS tolerance state: Down-regulation of TREM-1 as putative underlying mechanism. *PLoS One* **3**, e2667 (2008).

545. del Fresno, C. *et al.* Potent Phagocytic Activity with Impaired Antigen Presentation Identifying Lipopolysaccharide-Tolerant Human Monocytes: Demonstration in Isolated Monocytes from Cystic Fibrosis Patients. *J. Immunol.* (2009) doi:10.4049/jimmunol.0803350.

546. Ferenbach, D. A. *et al.* Macrophage/monocyte depletion by clodronate, but not diphtheria toxin, improves renal ischemia/reperfusion injury in mice. *Kidney Int.* **82**, 928–933 (2012).

547. Jo, S. K., Sung, S. A., Cho, W. Y., Go, K. J. & Kim, H. K. Macrophages contribute to the initiation of ischaemic acute renal failure in rats. *Nephrol. Dial. Transplant.* (2006) doi:10.1093/ndt/gfk047.

548. Paues Göranson, S. *et al.* Circulating H3Cit is elevated in a human model of endotoxemia and can be detected bound to microvesicles. *Sci. Rep.* (2018) doi:10.1038/s41598-018-31013-4.

549. Teoh, N. C. *et al.* Diannexin, a Novel Annexin V Homodimer, Provides Prolonged Protection Against Hepatic Ischemia-Reperfusion Injury in Mice. *Gastroenterology* **133**, 632–646 (2007).

550. Hellum, M. *et al.* Microparticle-associated tissue factor activity correlates with plasma levels of bacterial lipopolysaccharides in meningococcal septic shock. *Thromb. Res.* (2014) doi:10.1016/j.thromres.2013.12.031.

551. Delabranche, X. *et al.* Early Detection of Disseminated Intravascular Coagulation during Septic Shock: A Multicenter Prospective Study. *Crit. Care Med.* (2016) doi:10.1097/CCM.0000000000001836.

552. Lehner, G. F. *et al.* Hemofiltration induces generation of leukocyte-derived CD31+/CD41− microvesicles in sepsis. *Ann. Intensive Care* (2017) doi:10.1186/s13613-017-0312-3.

553. Matthay, M. A. *et al.* Future research directions in acute lung injury: Summary of a National Heart, Lung, and Blood Institute Working Group. in *American Journal of Respiratory and Critical Care Medicine* vol. 167 1027–1035 (2003).

554. Murphy, T. J. *et al.* Linking the 'two-hit' response following injury to enhanced TLR4 reactivity. *J Leukoc Biol* **77**, 16–23 (2005).

555. Nemzek, J. a *et al.* Immunopathology of a two-hit murine model of acid aspiration lung injury. *Am. J. Physiol. Lung Cell. Mol. Physiol.* **278**, L512–L520 (2000).

556. Steinberg, J., Halter, J., Schiller, H., Gatto, L. & Nieman, G. The development of acute respiratory distress syndrome after gut ischemia/reperfusion injury followed by fecal peritonitis in pigs: A clinically relevant model. *Shock* **23**, 129–137 (2005).

557. Lyden, S. P. *et al.* Transient inhibition of CD18-dependent leukocyte functions after hemorrhage and polymicrobial sepsis. *Surgery* **123**, 679–691 (1998).

558. Held, H. D., Martin, C. & Uhlig, S. Characterization of airway and vascular responses in murine lungs. *Br. J. Pharmacol.* **126**, 1191–1199 (1999).

559. Al-Robaiy, S., Hiebl, B., Simm, A., Silber, R.-E. & Bartling, B. Physiological parameters of the isolated perfused mouse lung and their dependency on age. *J. Cell. Biotechnol.* **1**, 3–14 (2015).

560. Tuchscherer, H. A., Webster, E. B. & Chesler, N. C. Pulmonary vascular resistance and impedance in isolated mouse lungs: Effects of pulmonary emboli. *Ann. Biomed. Eng.* **34**, 660–668 (2006).

561. Spöhr, F. *et al.* 4-Aminopyridine restores impaired hypoxic pulmonary vasoconstriction in endotoxemic mice. *Anesthesiology* **107**, 597–604 (2007).

562. Patel, B. V *et al.* In vivo compartmental analysis of leukocytes in mouse lungs. *Am. J. Physiol. Lung Cell. Mol. Physiol.* **309**, L639-52 (2015).

563. Zhu, Y. G. *et al.* Human mesenchymal stem cell microvesicles for treatment of Escherichia coli endotoxin-induced acute lung injury in mice. *Stem Cells* **32**, 116–125 (2014).

564. Vogel, S. M., Orrington-Myers, J., Broman, M. & Malik, A. B. De novo ICAM-1 synthesis in the mouse lung: model of assessment of protein expression in lungs. *Am. J. Physiol. Lung Cell. Mol. Physiol.* **291**, L496-501 (2006).

565. Salzer, W. L. & McCall, C. E. Primed stimulation of isolated perfused rabbit lung by endotoxin and platelet activating factor induces enhanced production of thromboxane and lung injury. *J. Clin. Invest.* **85**, 1135–1143 (1990).

566. Joucher, F., Mazmanian, G. M. & German-Fattal, M. Endothelial cell early activation induced by allogeneic lymphocytes in isolated perfused mouse lung. *Transplantation* **74**, 1461–1469 (2002).

567. Lu, Y.-T. T. *et al.* Time course of lung ischemia-reperfusion-induced ICAM-1 expression and its role in ischemia-reperfusion lung injury. *J. Appl. Physiol.* **93**, 620–628 (2002).

568. Held, H. D. & Uhlig, S. Mechanisms of endotoxin-induced airway and pulmonary vascular hyperreactivity in mice. *Am. J. Respir. Crit. Care Med.* (2000) doi:10.1164/ajrccm.162.4.9912079.

569. Xie, R. *et al.* Microparticles in red cell concentrates prime polymorphonuclear neutrophils and cause acute lung injury in a two-event mouse model. *Int. Immunopharmacol.* (2018) doi:10.1016/j.intimp.2017.11.029.

570. Mesri, M. & Altieri, D. C. Leukocyte microparticles stimulate endothelial cell cytokine release and tissue factor induction in a JNK1 signaling pathway. *J. Biol. Chem.* (1999) doi:10.1074/jbc.274.33.23111.

571. Mesri, M. & Altieri, D. C. Endothelial cell activation by leukocyte microparticles. *J. Immunol.* **161**, 4382–4387 (1998).

572. Xiang, C. *et al.* Sphingosine-1-phosphate mediates the therapeutic effects of bone marrow mesenchymal stem cell-derived microvesicles on articular cartilage defect. *Transl. Res.* **193**, 42–53 (2018).

573. Mehaffey, J. H. *et al.* Increasing circulating sphingosine-1-phosphate attenuates lung injury during ex vivo lung perfusion. *J. Thorac. Cardiovasc. Surg.* **156**, 910–917 (2018).

574. Lim, K., Sumagin, R. & Hyun, Y.-M. Extravasating Neutrophil-derived Microparticles Preserve

Vascular Barrier Function in Inflamed Tissue. *Immune Netw.* **13**, 102–6 (2013).

575. Hyun, Y. M. *et al.* Uropod elongation is a common final step in leukocyte extravasation through inflamed vessels. *J. Exp. Med.* **209**, 1349–1362 (2012).

576. Dalli, J. *et al.* Annexin 1 mediates the rapid anti-inflammatory effects of neutrophil-derived microparticles. *Blood* **112**, 2512–2519 (2008).

577. Sadallah, S., Eken, C., Martin, P. J. & Schifferli, J. A. Microparticles (Ectosomes) Shed by Stored Human Platelets Downregulate Macrophages and Modify the Development of Dendritic Cells. *J. Immunol.* **186**, 6543–6552 (2011).

578. Ceroi, A. *et al.* The anti-inflammatory effects of platelet-derived microparticles in human plasmacytoid dendritic cells involve liver X receptor activation. *Haematologica* vol. 101 e72–e76 (2016).

579. Laffont, B. *et al.* Platelet microparticles reprogram macrophage gene expression and function. *Thromb. Haemost.* **115**, 311–323 (2016).

580. Yuana, Y., Levels, J., Grootemaat, A., Sturk, A. & Nieuwland, R. Co-isolation of extracellular vesicles and high-density lipoproteins using density gradient ultracentrifugation. *J. Extracell. Vesicles* **3**, (2014).

581. Tran-Dinh, A. *et al.* HDL and endothelial protection. *British Journal of Pharmacology* vol. 169 493–511 (2013).

582. Karliner, J. S. Sphingosine kinase and sphingosine 1-phosphate in the heart: A decade of progress. *Biochim. Biophys. Acta - Mol. Cell Biol. Lipids* **1831**, 203–212 (2013).

583. Theilmeier, G. *et al.* High-density lipoproteins and their constituent, sphingosine-1-phosphate, directly protect the heart against ischemia/reperfusion injury in vivo via the S1P3 lysophospholipid receptor. *Circulation* **114**, 1403–1409 (2006).

584. Krabbe, J. *et al.* The effects of hydroxyethyl starch and gelatine on pulmonary cytokine production and oedema formation. *Sci. Rep.* **8**, 1–11 (2018).

585. Matsumoto, A. *et al.* Blood concentrations of small extracellular vesicles are determined by a balance between abundant secretion and rapid clearance. *J. Extracell. Vesicles* **9**, 1696517 (2020).

586. Exline, M. C. *et al.* Microvesicular caspase-1 mediates lymphocyte apoptosis in sepsis. *PLoS One* **9**, 1–8 (2014).

587. Sarkar, A., Mitra, S., Mehta, S., Raices, R. & Wewers, M. D. Monocyte derived microvesicles deliver a cell death message via encapsulated caspase-1. *PLoS One* **4**, e7140 (2009).

588. Tacke, F. *et al.* Immature monocytes acquire antigens from other cells in the bone marrow and present them to T cells after maturing in the periphery. *J. Exp. Med.* **203**, 583–597 (2006).

589. Ohuchi, M. *et al.* Association of the plasma platelet-derived microparticles to platelet count ratio with hospital mortality and disseminated intravascular coagulopathy in critically ill patients. *J. Atheroscler. Thromb.* **22**, 773–782 (2015).

590. Puskarich, M. A. *et al.* Phosphatidylserine expressing platelet microparticle levels at hospital presentation are decreased in sepsis non-survivors and correlate with thrombocytopenia. *Thromb. Res.* **168**, 138–144 (2018).

591. Agouni, A. *et al.* Endothelial dysfunction caused by circulating microparticles from patients with metabolic syndrome. *Am. J. Pathol.* (2008) doi:10.2353/ajpath.2008.080228.

592. Böing, A. N. *et al.* Single-step isolation of extracellular vesicles from plasma by size-exclusion chromatography. *Int. Meet. ISEV Rotterdam* **3**, 118 (2014).

593. Welton, J. L., Webber, J. P., Botos, L. A., Jones, M. & Clayton, A. Ready-made chromatography columns for extracellular vesicle isolation from plasma. *J. Extracell. Vesicles* **4**, 1–9 (2015).

594. Held, H. D., Boettcher, S., Hamann, L. & Uhlig, S. Ventilation-induced chemokine and cytokine release is associated with activation of nuclear factor-kappaB and is blocked by steroids. *Am.*

J. Respir. Crit. Care Med. (2001) doi:10.1164/ajrccm.163.3.2003001.

595. Walker, M. G. *et al.* The effect of tidal volume on systemic inflammation in acid-induced lung injury. *Respiration* **81**, 333–342 (2011).

596. Perl, M., Lomas-Neira, J., Venet, F., Chung, C.-S. S. & Ayala, A. *Pathogenesis of indirect (secondary) acute lung injury*. *Expert Review of Respiratory Medicine* vol. 5 115–126 (2011).

597. Griffiths, M. J. D. & McAuley, D. F. RAGE: A biomarker for acute lung injury. *Thorax* vol. 63 1034–1036 (2008).

598. Jabaudon, M. *et al.* Soluble receptor for advanced glycation end-products predicts impaired alveolar fluid clearance in acute respiratory distress syndrome. *Am. J. Respir. Crit. Care Med.* **192**, 191–199 (2015).

599. Uchida, T. *et al.* Receptor for advanced glycation end-products is a marker of type I cell injury in acute lung injury. *Am. J. Respir. Crit. Care Med.* **173**, 1008–1015 (2006).

600. Dahlin, K. *et al.* Identification of genes differentially expressed in rat alveolar type I cells. *Am. J. Respir. Cell Mol. Biol.* **31**, 309–316 (2004).

601. Brett, J. *et al.* Survey of the distribution of a newly characterized receptor for advanced glycation end products in tissues. *Am. J. Pathol.* **143**, 1699–1712 (1993).

602. Roviezzo, F. *et al.* Angiopoietin-2 causes inflammation in vivo by promoting vascular leakage. *J. Pharmacol. Exp. Ther.* **314**, 738–744 (2005).

603. Fiedler, U. *et al.* The Tie-2 ligand Angiopoietin-2 is stored in and rapidly released upon stimulation from endothelial cell Weibel-Palade bodies. *Blood* **103**, 4150–4156 (2004).

604. Parikh, S. M. *et al.* Excess circulating angiopoietin-2 may contribute to pulmonary vascular leak in sepsis in humans. *PLoS Med.* **3**, 356–370 (2006).

605. Van Der Flier, M. *et al.* Plasma vascular endothelial growth factor in severe sepsis. *Shock* **23**, 35–38 (2005).

606. Thurston, G. *et al.* Angiopoietin-1 protects the adult vasculature against plasma leakage. *Nat Med* **6**, 460–463 (2000).

607. Benest, A. V. *et al.* Angiopoietin-2 Is Critical for Cytokine-Induced Vascular Leakage. *PLoS One* **8**, e70459 (2013).

608. Hashimoto, T. & Pittet, J. F. Angiopoietin-2: Modulator of vascular permeability in acute lung injury? *PLoS Medicine* vol. 3 294–296 (2006).

609. Lomas-Neira, J. *et al.* Neutrophil-endothelial interactions mediate angiopoietin-2-associated pulmonary endothelial cell dysfunction in indirect acute lung injury in mice. *Am. J. Respir. Cell Mol. Biol.* **50**, 193–200 (2014).

610. Woth, G. *et al.* Activated platelet-derived microparticle numbers are elevated in patients with severe fungal (Candida albicans) sepsis. *Ann. Clin. Biochem.* **49**, 554–560 (2012).

611. Fadok, V. A., Bratton, D. L., Frasch, S. C., Warner, M. L. & Henson, P. M. *The role of phosphatidylserine in recognition of apoptotic cells by phagocytes*. http://www.stockton-press.co.uk/cdd (1998).

612. Szondy, Z., Sarang, Z., Kiss, B., Garabuczi, É. & Köröskényi, K. Anti-inflammatory mechanisms triggered by apoptotic cells during their clearance. *Frontiers in Immunology* vol. 8 909 (2017).

613. Eken, C. *et al.* Ectosomes released by polymorphonuclear neutrophils induce a MerTK-dependent anti-inflammatory pathway in macrophages. *J. Biol. Chem.* **285**, 39914–39921 (2010).

614. Eken, C., Sadallah, S., Martin, P. J., Treves, S. & Schifferli, J. A. Ectosomes of polymorphonuclear neutrophils activate multiple signaling pathways in macrophages. *Immunobiology* **218**, 382–392 (2013).

615. Gasser, O. & Schifferli, J. A. Activated polymorphonuclear neutrophils disseminate anti-

inflammatory microparticles by ectocytosis. *Blood* **104**, 2543–2548 (2004).

616. Hong, C. W. Extracellular vesicles of neutrophils. *Immune Network* vol. 18 (2018).

617. Park, S. A. & Hyun, Y. M. Neutrophil extravasation cascade: What can we learn from two-photon intravital imaging? *Immune Network* vol. 16 317–321 (2016).

618. Wei, X. *et al.* Surface Phosphatidylserine Is Responsible for the Internalization on Microvesicles Derived from Hypoxia-Induced Human Bone Marrow Mesenchymal Stem Cells into Human Endothelial Cells. *PLoS One* **11**, e0147360 (2016).

619. Pitanga, T. N. *et al.* Neutrophil-derived microparticles induce myeloperoxidase-mediated damage of vascular endothelial cells. *BMC Cell Biol.* **15**, 21 (2014).

620. Jaiswal, R. *et al.* Microparticle conferred microRNA profiles - implications in the transfer and dominance of cancer traits. *Mol. Cancer* **11**, 37 (2012).

621. Gomez, I. *et al.* Neutrophil microvesicles drive atherosclerosis by delivering miR-155 to atheroprone endothelium. *Nat. Commun.* **11**, 1–18 (2020).

622. Alexander, M. *et al.* Exosome-delivered microRNAs modulate the inflammatory response to endotoxin. *Nat. Commun.* **6**, 1–16 (2015).

623. Im, Y. *et al.* Association of plasma exosomes with severity of organ failure and mortality in patients with sepsis. *J. Cell. Mol. Med.* **24**, 9439–9445 (2020).

624. LACROIX, R. *et al.* Impact of pre-analytical parameters on the measurement of circulating microparticles: Towards standardization of protocol. *J. Thromb. Haemost.* **10**, 437–446 (2012).

625. Wu, Y., Deng, W. & Klinke, D. J. Exosomes: Improved methods to characterize their morphology, RNA content, and surface protein biomarkers. *Analyst* **140**, 6631–6642 (2015).

626. Maroto, R. *et al.* Effects of storage temperature on airway exosome integrity for diagnostic and functional analyses. *J. Extracell. Vesicles* **6**, (2017).

627. Proudfoot, A. G., McAuley, D. F., Griffiths, M. J. D. & Hind, M. Human models of acute lung injury. *DMM Dis. Model. Mech.* **4**, 145–153 (2011).